Defining the dynamic relationship between interferon-gamma and $CD8^+$ T cell dysfunction in melanoma.

By Julie Marie Mathilde Mazet



St Hugh's College, University of Oxford

The Kennedy Institute of Rheumatology, NDORMS

A thesis submitted in fulfilment of the requirements for the degree of Doctor of Philosophy in Molecular and Cellular Medicine, University of Oxford

Michaelmas Term 2022

Table of contents

Abstract ***7***

Acknowledgments ***9***

Contributions ***12***

List of abbreviations ***13***

1. General introduction ***16***

1.1 Cancer: how the immune system has changed the field **16**

1.1.1 Hallmarks of Cancer: the common features of cancer 17

1.1.2 The cancer-immunity cycle 20

1.2 IFNγ: the versatile immune cytokine with pro and anti-tumour functions **23**

1.2.1 IFNγ: an overview 24

1.2.2 IFNγ: a pleiotropic cytokine in the TME 28

1.3 $CD8^+$ T cell dysfunction in cancer: exhaustion and beyond **33**

1.3.1 $CD8^+$ T cell biology 33

1.3.2 $CD8^+$ T cell response: Acute *versus* chronic context 38

1.3.3 $CD8^+$ T cell in cancer 42

1.4 Stem-like T cells: the essential piece for long-term anti-tumour response **43**

1.4.1 Stem-like T cells: the recent discovery 43

1.4.2 Stem-like T cells: the keystone for long-term immune responses and immunotherapies efficacy 48

1.4.3 Open questions on stem-like T cells 50

1.5 Thesis rationale and objectives **52**

2. Materials and methods ***55***

2.1 Murine models **55**

2.2 Genotyping **56**

2.3 Murine cancer cell lines **59**

2.4 Tumour inductions and treatment of mice **60**

2.5 Tumour processing for imaging **60**

2.6 Tumour and lymph node processing for flow cytometry 62

2.7 Tumour processing for soluble analysis (ELISA – Legendplex) 63

2.8 Adoptive T cell transfer 63

2.9 *In vitro* T cell stimulation 66

2.10 *Ex vivo* T cell assays 67

2.11 Flow cytometry 68

2.12 FACS sorting for *ex vivo* T cell proliferation assay 72

2.13 Single-cell RNA sequencing 72

2.14 Statistical analysis 75

3. IFNγ restricts CD8⁺ T cell immune response toward murine melanoma cell line 76

3.1 IFNγ: a key player for CD8⁺ T cell function 76

3.1.1 IFNγ: a regulator for CD8⁺ T cell function 77

3.1.2 IFNγR expression landscape in CD8⁺ T cells 78

3.1.3 IFNγ response in CD8⁺ T cells 81

3.2 Characterisation of the murine model – IFNγR1KO CD8⁺ T cell mice 83

3.2.1 A murine model for IFNγR1 targeted deletion in mature CD8⁺ T cells at the endogenous level 84

3.2.2 CD8⁺ T cell specific Cre expression *in vivo* 85

3.2.3 OTI system for antigen specificity study (WT and IFNγR1KO) 88

3.2.4 Murine melanoma model: the B16F10tyr$^{-/-}$mCherryOVA cell line 89

3.3 B16F10-OVA tumours are better controlled by IFNγR1KO CD8⁺ T cells compared to control mice 91

3.3.1 Endogenous IFNγR1KO CD8⁺ T cells better control murine melanoma tumours 92

3.3.2 Tumour specific IFNγR1KO CD8⁺ T cells better control murine melanoma tumours – OTI system 94

3.3.3 Endogenous IFNγR1KO CD8⁺ T cells better control murine colon tumours 95

3.4 Discussion and conclusion 97

3.4.1 IFNγ and CD8⁺ T cell function in tumours 97

3.4.2 The ablation of IFNγR1 only in mature CD8⁺ T cells enhanced the tumour control 99

3.4.3 IFNγ triggered negative feedback loop: a general mechanism? 102

3.4.4 Conclusion 103

4. The role of IFNγ sensing for CD8⁺ T cell spatial and functional fitness 104

4.1 IFNγ sensing does not significantly affect CD8⁺ T cell effector functions 105

4.1.1 Cytokine production capabilities – *ex vivo* restimulation 106

4.1.2 Cytokine bioavailability *in vivo* 107

4.1.3 Cytolytic functions *in vivo* 109

4.2 IFNγ sensing affects CD8⁺ T cell expansion *in vivo* 112

4.2.1 Tumour infiltrating CD8⁺ T cell absolute number 112

4.2.2 Tumour infiltrating CD8⁺ T cell apoptosis level 113

4.2.3 Tumour infiltrating CD8⁺ T cell proliferation *in vivo* – OTI system 114

4.3 IFNγ sensing affects CD8⁺ T cell tumour infiltration 116

4.3.1 CD8⁺ T cell tumour localisation – imaging and quantification 117

4.3.2 IFNγ effect on CD8⁺ T cell tumour recruitment 120

4.4 Discussion and conclusion 125

4.4.1 IFNγR1KO CD8⁺ T cells are not intrinsically better effector cells 125

4.4.2 IFNγ restricts CD8⁺ T cell expansion in tumours 127

4.4.3 IFNγ is required for CD8⁺ T cell tumour homing 128

4.4.4 Conclusion 133

5. IFNγ sensing influences CD8⁺ T cells at the subset population level 134

5.1 IFNγ sensing regulates tumour-infiltrating but not CD8⁺ T cells from lymph nodes…… 134

5.1.1 Single-cell RNA sequencing analysis comparing control and IFNγR1KO CD8⁺ T cells – the setup…… 134

5.2 IFNγ sensing by CD8⁺ T cells affects their intra-tumoral proportion *in vivo* 137

5.2.1 Immune composition remodelling in tumours: control *versus* CD8-IFNγR1KO 137

5.2.2 Intra-tumoral CD8⁺ T cell population proportion *in vivo*: control *versus* CD8-IFNγR1KO. 140

5.3 IFNγ-sensing reinforces the overall CD8⁺ T cell exhaustion in tumour 143

5.3.1 Focus on the IFNγ effect on CD8⁺ T cell exhaustion 143

5.3.2 IFNγ-sensing is not sufficient to alter CD8⁺ T cell metabolism *in vivo* 145

5.3.3 Preventing IFNγ-sensing by CD8⁺ T cells decreases their exhaustion level 148

5.3.4 IFNγ-sensing does not restrict exhausted CD8⁺ T cell proliferation 150

5.4 Discussion and conclusion 152

5.4.1 IFNγ-sensing does not affect exhausted T cells in tumours 154

5.4.2 IFNγ-sensing affects T cell subset proportion 156
5.4.3 Conclusion 157

6. IFNγ sensing particularly affects the CD8⁺ stem-like T cell maintenance in tumours 158

6.1 Stem-like T cells have the greatest proliferative capacity in tumours. 158
6.1.1 Intra-tumoral stem-like T cells are better able to proliferate compared to exhausted T cells..... 159
6.1.2 Stem-like T cells are IFNγ sensitive in tumours 161

6.2 IFNγ affects stem-like T cell maintenance in tumours 162
6.2.1 Stem-like T cells are critical for IFNγR1KO CD8⁺ T cell expansion *in vivo* 163
6.2.2 Blocking IFNγ enhances the maintenance of intra-tumoral stem-like T cells *ex vivo* 165
6.2.3 IFNγ inhibits the self-renewal capacity of intra-tumoral stem-like T cells 167

6.3 Preventing IFNγ sensing enhanced CD8⁺ T cell clonality *via* enhancing the stem-like T cell pool 170

6.4 Discussion and conclusion 172
6.4.1 Intra-tumoral stem-like T cell maintenance is altered by IFNγ 172
6.4.2 How does IFNγ restrict stem-like T cell maintenance in tumours? 175
6.4.3 Conclusion 180

7. General discussion and conclusion 182

7.1 Thesis summary 183

7.2 Significance in human: IFNγ and CD8⁺ T cells in cancer patients 187

7.3 New insight in stem-like T cell biology: therapeutic potential 192

7.4 Future directions 194
7.4.1 Fundamental opened questions 194
7.4.2 Translational and therapeutic potential questions 198

List of Figures 201

List of Tables 202

References 203

Abstract

Defining the dynamic relationship between interferon-gamma and CD8$^+$ T cell dysfunction in melanoma.

By Julie M. M. Mazet

Thesis submitted in fulfilment of the requirements for the degree of Doctor of Philosophy, University of Oxford, Michaelmas Term 2022

CD8$^+$ T cells or cytotoxic T lymphocytes (CTLs) are crucial to anti-tumour responses, as they kill cancer cells. However, CD8$^+$ T cells are becoming dysfunctional over time in tumours leading to tumour escape. The concept of T cell exhaustion linking the CTL dysfunction with the upregulation of inhibitory molecules known as immune checkpoints only partly explains their dysfunction, as immunotherapies targeting immune checkpoints showed very limited success. This underlines that there is a critical need to decipher other mechanisms involved in CTL dysfunction in cancer. CTL efficacy notably relies on their interferon-gamma (IFNγ) production for cytotoxic cytokine release. IFNγ is a major immune mediator with strong anti-tumour functions but also concomitant pro-tumour effects. Because IFNγ is inherently linked to tumour immunity efficacy, it is critical to fully understand how it can also simultaneously impede it. CTLs are the main IFNγ producers in tumours but how the chronic IFNγ presence affects their anti-tumour function has not been properly assessed yet. To address whether IFNγ

sensing is directly involved in CTL dysfunction we used a mouse model where the interferon-gamma receptor (IFNγR) is specifically ablated in $CD8^+$ T cells (CD8-IFNγR1KO) rendering them unable to sense the cytokine. Depleting the IFNγR1 in $CD8^+$ T cells is sufficient to restore immunity towards B16F10 melanoma with better tumour control, although it does not substantially enhance CTL functions. The characterisation of intra-tumoral $CD8^+$ T cells revealed that IFNγ preferentially affects a particular $CD8^+$ T cell subset of precursor cells: the stem-like T cells. Indeed, stem-like T cells that do not sense IFNγ originate a greater T cell expansion through greater $CD8^+$ T cell proliferation in tumours, reducing the exhaustion level of IFNγR1KO $CD8^+$ T cells. Mechanistically, IFNγ restricts their active maintenance, preventing the steady generation of early-exhausted $CD8^+$ T cells in tumours. Besides, while control $CD8^+$ T cells are excluded from the tumour core, IFNγR1KO $CD8^+$ T cells infiltrate better the tumour core. Altogether, our data show that IFNγ drives a negative feedback loop whereby IFNγ depletes stem-like T cells in the tumour restricting the CTL anti-tumour potential. Targeting this pathway might offer an alternative strategy to enhance the efficacy and longevity of adoptive T cell therapies.

Acknowledgments

I always pictured the PhD as a high-paced marathon that requires passion, motivation, and dedication. After 4 years, I can say that this is an accurate definition although incomplete. I think achieving this journey requires additional key ingredients that I was fortunate enough to find: a permissive environment, that goes with supportive and inspiring scientific colleagues and encouraging people surrounding you.

It was a true privilege to have been given the opportunity to undertake my PhD at the Kennedy Institute of Rheumatology at the University of Oxford. It was the perfect environment to do my PhD and start my academic career. I would like to thank the Kennedy Trust for funding my DPhil and the entire Kennedy Institute ecosystem for all the opportunities and support provided throughout the years. This was such a great place to do, listen and talk about science with many talented people.

This would have never been possible without the trust of my primary supervisor Dr. Audrey Gerard and for that, I would like to express my deepest gratitude to her. She supported me for the last 4 years. I learned a lot from her both directly with her guidance and advice, and indirectly through our many scientific discussions. She created a lab atmosphere where I felt supported and guided, but I also had the freedom to bring ideas and explore hypothesises.

This leads to a special thanks to my colleagues Dr. Lion Uhl and Vivian Lau, my grad mates. Thank you for your help, support, critical reading, and your friendship. There were ups and downs and I could count on you to help me put things into perspective. I

would like to thank the other Gerard lab members past and present. In particular Dr. Ana Chiodetti for her motivational speeches and of course, Dr. Jagdish Mahale without whom the start of my PhD would have been so different. Your “It’s okay, don’t worry” will always be in my head to cool down when a lab crisis happens. Thank you for your patience and kindness.

I also want to thank my co-supervisor, Prof. Kim Midwood, for her advice throughout the PhD and also for her career advice regarding the next steps in Academia.

On a larger scale, I am grateful to have met incredible scientists and people who influenced my PhD and scientific vision: Dr. Natacha Zanin, Dr. Claire Deligne, Dr. Mathilde Pohin, Dr. Anne Chauveau, and everybody who helped me along the way either by sharing their experiences and knowledge or simply by making me feel listened when I needed it.

Next, I would like to thank all the collaborators who took part in this scientific project, thank you for your involvement.

From the personal side, first and foremost, I would like to deeply thank my wonderful spouse, Sandy, with whom I would have never achieved what I achieved throughout the years. From day 1, more than 13 years ago, she always believed in me and saw my potential. She never doubted me and I am beyond grateful for having found her and the happiest for having her by my side. Thank you for your support, love, and reminder that life has so much to offer. I can always rely on your encouraging support which was critical on some occasions, notably when the imposter syndrome knocked on the door. I am looking forward to seeing what we will accomplish together in the future.

Next, I would like to thank my parents, Martine and Claude, who taught my sister and me 3 key values: hard work, perseverance, and self-awareness. From a very young age, they always made sure that I learn new things and do the best that I can with sports and musical activities. They provided me with the best environment possible to grow up with the best education possible and the value of working hard to obtain what I envision through my dedication. They encouraged me to pursue my PhD abroad even though I know they would have preferred me to stay closer. Thank you for your continuous support, love, and trust. Finally, Aurore my little sister, I would like to thank you for your kindness and long calls and visits, we always cheer each other up even though we do not understand each other professional fields.

To finish, I would like to share one of Nelson Mandela's quotations that I always cherished since I was young: “I never lose, I either win or learn.” And I am eager to do both.

Contributions

Contributions are mentioned in figure legends throughout the thesis.

- Dr. Jagdish Mahale helped and performed experiments included in chapters 3 and 4.
- Dr. Audrey Gerard analysed the single-cell RNA and TCR Sequencing murine dataset.
- Dr. Gabriela Pirgova performed the tumour homing assay.
- Dr. Ana Victoria Lechuga-Vieco greatly helped with the *in vivo* metabolism experiments.
- Dr. Benjamin Fairfax and his team analysed the human dataset discussed in chapter 3 and in the general discussion.

List of abbreviations

ACT	Adoptive cell therapy
APC	Allophycocyanin
APCs	Antigen-presenting cells
BEC	Bioenergetic Cellular index
BV	Brilliant violet
CAFs	Cancer-associated fibroblasts
CCL	Chemokine (C-C motif) ligand
CD	Cluster of differentiation
CFSE	Carboxyfluorescein succinimidyl ester
CTLs	Cytotoxic T lymphocytes
CTV	CellTrace violet
CXCL	Chemokine (C-X-C motif) ligand
DCs	Dendritic cells
DNA	Deoxyribonucleic acid
EDTA	Ethylenediaminetetraacetic acid
FACS	Fluorescence-activated cell sorting
FAS	FAS Receptor
FAS-L	FAS Ligand
FCS	Foetal calf serum
FITC	Fluorescein isothiocyanate
GAF	Gamma-activated factors
GAS	Gamma-activated sites
GFP	Green fluorescent protein
GLUT-1	Glucose transporter 1
GSK3β	Glycogen synthase kinase-3 beta
HSC	Hematopoietic stem cells
ICAM-I	Intercellular Adhesion Molecule 1

ICB	Immune checkpoint blockade
IFN	Interferon
IFNγ	Interferon-gamma
IFNγR	Interferon-gamma receptor
IL	Interleukin
ISG	Interferon-stimulated genes
ISRE	Interferon-stimulated response elements
JAK	Janus kinase
KO	Knock-out
Lag-3	Lymphocyte Activating 3
LAMP1	Lysosomal-associated membrane protein 1
LCMV	Lymphocytic choriomeningitis virus
LDHA	Lactate Dehydrogenase A
LN(s)	Lymph nodes
MDSCs	Myeloid-derived suppressor cells
MHC	Major histocompatibility complex
NK	Natural Killer
OVA	Ovalbumin peptide
PBS	Phosphate-buffered saline
PCR	Polymerase chain reaction
PD-1	Programmed Cell Death Protein 1
PD-L1	Programmed death-ligand 1
PE	Phycoerythrin
RNA	Ribonucleic acid
scRNA-seq	Single-cell RNA sequencing
STAT	Signal transducer and activator of transcription
TAMs	Tumour-associated macrophages
Tcf1	T cell factor 1
TCR	T cell receptor
TGF-β	Transforming Growth Factor-beta

Tigit	T cell immunoreceptor with Ig and ITIM domains
TILs	Tumour infiltrating lymphocytes
Tim-3	T cell immunoglobulin domain and mucin domain 3
TLS	Tertiary lymphoid structure
TME	Tumour microenvironment
TNF	Tumour Necrosis Factor
Tregs	Regulatory T cells
WNT	Wingless-related integration site
WT	Wild type

1. General introduction

1.1 Cancer: how the immune system has changed the field

Cancer is defined as a large group of diseases whereby abnormal cells start to grow uncontrollably from any organs or tissues. The formed cancer cell mass known as the primary tumour will eventually overgrow to invade surrounding tissues and/or spread to further organs: this is the metastasis process. Cancer is a global health issue since it is the second cause of death worldwide[1,2] with nearly 10 million deaths in 2020 according to the World Health Organization (WHO)[3,4]. The major cause of cancer death is metastasis, when cancer cells invade multiple locations, rendering local treatments useless. There is, therefore, a critical need to develop treatments and discover predictive parameters to better treat and cure cancers.

Melanoma is a serious type of skin cancer developing from melanocytes that grow out of control. Skin cancers are the most common cancer group diagnosed yearly; melanoma accounts for 1 in 5 skin cancers. This cancer type is one of the most aggressive due to its ability to metastasise rapidly if not diagnosed and treated at an early stage. Prevention and public awareness improvement are essential, as according to an estimation by Cancer Research UK, 86% of melanoma cases could have been avoidable in 2015. Although some cases are preventable, melanoma is a major health issue as a report in 2020 predicted the melanoma incidence to rise to 50% with a 68% increase in deaths by 2040 worldwide[5].

Both basic and translational research is critical in the cancer research field to give rise to hope against the burden it represents for the patients and our society. It is vital to decipher how a tumour is initiating, growing, and spreading to create new therapeutics targeting relevant mechanisms. Cancer is a highly complex set of diseases with many forms converging on key shared features that represent the foundations of cancer research: the Hallmarks of Cancer.

1.1.1 Hallmarks of Cancer: the common features of cancer

Historically, the cancer research field focused on cancer cells themselves to study how a tumour is developing, which is called tumorigenesis. Tumorigenesis is complex and comprises multi-steps to transform normal cells into malignant cells. In 2000, a keystone review[6] proposed 6 key capabilities that cancer cells acquire during human tumour development:

- Self-sufficiency in growth signals = cancer cells are able to sustain proliferating signalling
- Insensitivity to growth-inhibitory signals = cancer cells are able to evade growth suppressors
- Evasion of programmed cell death (apoptosis) = cancer cells are able to resist cell death
- Limitless replicative potential = cancer cells are able to sustain an infinite replication
- Tissue invasion and metastasis = cancer cells are able to actively invade and metastasise
- Sustained angiogenesis = cancer cells are able to induce and access vasculature

Eleven years after this hallmark work, Hanahan and Weinberg have updated their previous review with two additional hallmarks of cancer[7]:

- Avoiding immune destruction = cancer cells are able to evade the immune system
- Deregulating cellular metabolism = cancer cells are able to tune their metabolism

Further studies revealed that the acquisition of these hallmarks was enabled by the genome instability of cancer cells and the tumour-promoting inflammation[8,9]. Within the last decades, lines of evidence have validated those hallmarks of cancer, which are summarised in **Figure 1** (a figure extracted from the last hallmarks of cancer updated in 2022[10]).

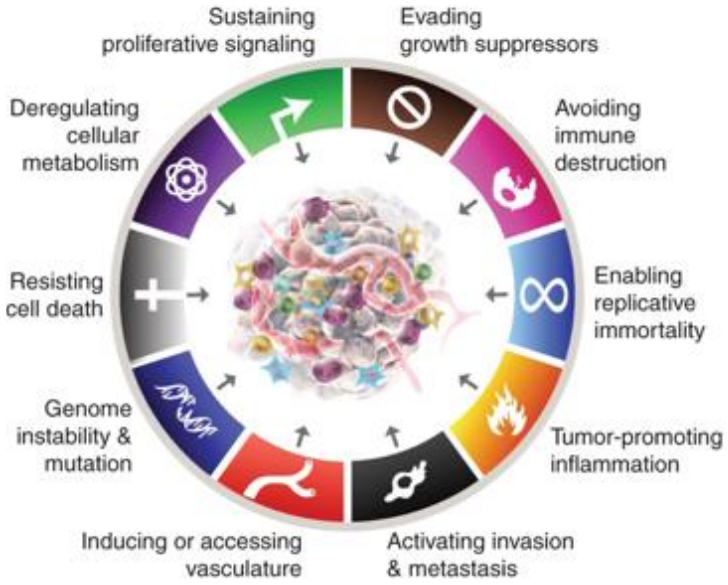


Figure 1: The Hallmarks of Cancer. The 8 key features that cancer cells acquire during cancer development are enabled by the 2 additional features: genome instability and tumour-induced inflammation. Figure extracted from the Hallmarks of Cancer: New Dimensions from Douglas Hanahan in 2022[10].

Interestingly, after focusing on the tumour cells themselves, the cancer research field has widened its investigations drawing its attention to the actors surrounding the cancer cells. Indeed, by recognising the heterogeneity of tumours, not only at the genetic level but also at the cellular, soluble and structural levels, the study of the tumour ecosystem or tumour microenvironment (TME) appeared to be critical[11,12,13]. Tumorigenesis is accompanied by the formation of a tumour bed and a profound alteration of the surrounding connective tissue and stroma, a process that culminates in the establishment of a pathological tumour microenvironment. Cancer cells can manipulate the neighbouring cells to shape their environment favouring their growth. The contribution of the TME to tumorigenesis is now well established and many research groups are aiming to decipher it and evaluate whether it can be therapeutically manipulated to better treat cancer patients[14,15,16,17,18,19,20].

The TME is extremely heterogeneous depending on the tumour type, stage, and between patients. It is generally constituted of cellular and non-cellular components, which are well described. At the cellular level, the TME is composed of non-malignant cells such as the stromal cells including endothelial cells, pericytes, adipocytes, cancer-associated fibroblasts (CAFs), and immune cells. At the molecular level, there are extracellular matrix components embedding cells and the soluble TME with signalling molecules such as cytokines, chemokines, and growth factors. Additionally, some factors such as nutrient availability, hypoxia, or environment acidity can affect the tumour cells, the immune cells, and the stromal cells and can influence the tumorigenesis[21,11,13]. Overall, the TME is a heterogeneous mass that is highly dynamic both spatially and temporally. The TME can be an obstacle to cancer treatment but also to the immune

response. The discovery of the crosstalk between cancer cells and the immune system opened a new area of research with a huge therapeutic potential as one solution to treat cancer might reside from inside the body.

1.1.2 The cancer-immunity cycle

The immune system was first seen as monitoring cells and tissues to recognise and eradicate nascent cancer cells and tumour formation, which gave birth to the concept of immunosurveillance of the immune system[22]. This concept led to adding the "ability to evade immune destruction" as a hallmark of cancer cells[7]. Years later it was proven that indeed the immune system especially $CD8^+$ T cells and interferon-gamma (IFNγ), their primary effector molecule, were able to eradicate primary tumours cells to protect against the development of carcinogen-induced tumours in a mouse model[23]. Subsequently, the study of the crosstalk between cancer cells and the immune system revealed several layers and steps of communication going both ways throughout the tumour stages. In other words, cancer cells influence the immune response and *vice versa*. In the immune TME, there are a variety of immune cells with a range of activation and differentiation statuses leading to various functions. Each cell type may also comprise several distinct subsets with different phenotypes, functions, abundance, localisation, dynamics, and lifespan for instance[24]. It is generally composed of natural killer cells (NK cells), tumour-associated macrophages (TAMs), monocytes, neutrophils, various types of dendritic cells (DCs), myeloid-derived suppressor cells (MDSCs), regulatory T cells (Tregs), $CD4^+$ T cells, and $CD8^+$ T cells or CTLs. Historically, the study of the anti-tumour response has been focused on $CD8^+$ T cells as they can specifically target

cancer cells, however, the immune system is complex and every cell type has a potential role that is now investigated. Interestingly, the fact that cancer cells are not stable genetically leads to new mutations with the creation of tumour neoantigens which allow for targeting by $CD8^+$ T cells for cancer cell eradication. This continuous deletion of cancer cells by $CD8^+$ T cells leads to a Darwinian selection process named immune editing[25,26,27]. As a result, this anti-tumour process can also trigger pro-tumour effects shaping the tumour.

This knowledge led to the description of a cancer immunity cycle that integrates the different steps required to eradicate cancer cells efficiently[28] (**Figure 2**). If the first step implies that cancer cells express neoantigens, the starting point of the immune response relies on the release and capture of tumour antigens by antigen-presenting cells (APCs) such as DCs. Subsequently, DCs process the antigens and present them to $CD8^+$ T cells by loading the processed peptides on major histocompatibility complex 1 (MHC-I) molecules[29]. This results in the priming and activation of tumour-specific $CD8^+$ T cells, allowing for differentiation and expansion into CTLs, the effector cells that can directly eliminate tumour cells following recognition by the T cell receptor (TCR)[30]. Of note, naïve $CD8^+$ T cells can reach the tumour *via* the tumour-induced vasculature, without being previously activated. These $CD8^+$ T cells can be directly activated on-site by tumour-infiltrating DCs.

Additionally, there is a great presence of macrophages in tumours, called TAMs, which represent another pool of intra-tumoral APCs for T cells, and consequently are part of the anti-tumour response[31]. However, TAMs can also be part of the pro-tumoral response, as they actively promote all aspects of the tumour development, especially

when macrophages are primed/polarised with an M2-like phenotype induced by the tumour, which is opposed to an M1-like phenotype with anti-tumour functions[32,33,34,35]. This example highlights the fact that the tumour microenvironment is highly dynamic and that a particular cell population can have both positive and negative outcomes on the tumour progression. All-in-all, all these steps are required for efficient anti-tumour response. In reality, this is more complex and hardly achieved, with disturbances at every step of this cycle.

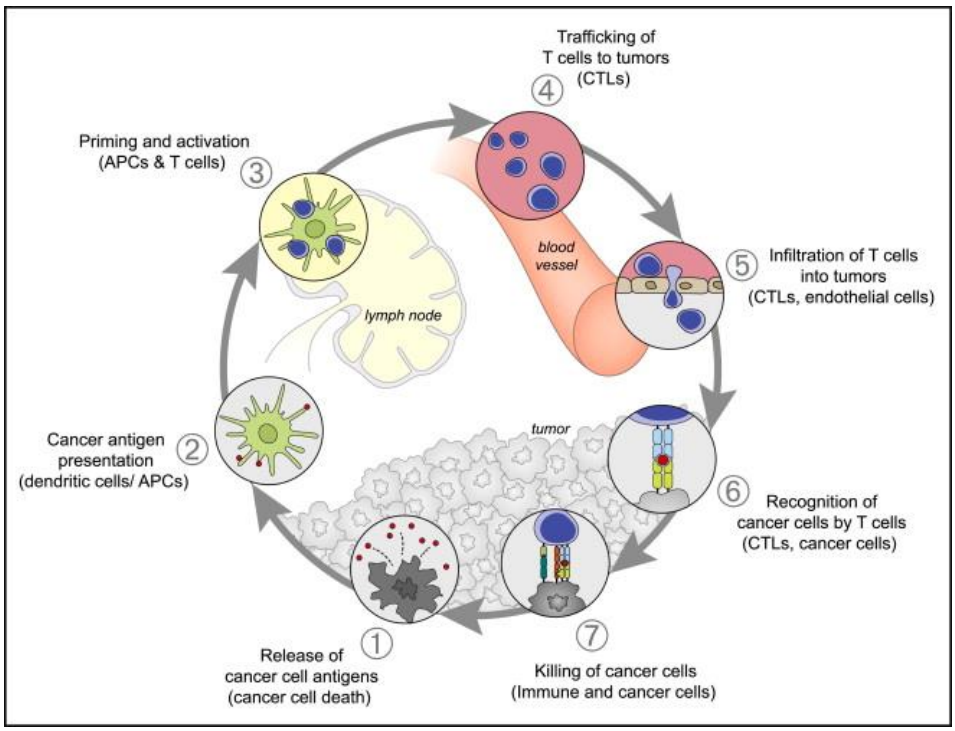


Figure 2: The cancer immunity cycle: 7 steps to eradicate cancer cells. Figure representing the different steps required to eradicate cancer cell efficiently. Starting from the release of tumour-associated antigens processed by antigen-presenting cells to specifically activate T cells. Tumour-specific T cells once primed need to traffic to the tumour, infiltrate it to kill cancer cells by direct contacts. Figure extracted from the review Oncology meets immunology: the cancer-immunity cycle from Chen *et al*[28].

Over time, with cancer immunoediting, the selection of aggressive poorly immunogenic cancer cell clones leads to the inhibition of the anti-tumour response[36]. Moreover, tumours can take advantage of immune regulatory mechanisms such as the expansion of Tregs[37,9], and the upregulation of inhibitory receptors such as programmed death-ligand 1 (PD-L1) to directly restrict CTLs function for instance[38,39,40,41,42]. Tumours can also imbalance soluble cues to favour immunosuppressive tumour microenvironment with transforming growth factor-beta (TGF-β), interleukin 10 (IL-10), or indoleamine 2,3-dioxygenase (IDO) for instance[37,43,44,45]. They can also develop resistance to anti-tumour effects such as the acquisition of IFNγ resistance[46,47,48], a critical effector molecule secreted by CTLs to destroy cancer cells[47].

In line with the role of IFNγ, the immune system is versatile and can adapt to many situations. Studying the crosstalk between cancer cells and the immune system seems a promising direction to help decipher weak points in this immunity cycle in order to restore an efficient and durable anti-tumour response.

1.2 IFNγ: the versatile immune cytokine with pro and anti-tumour functions

Efficient immune responses are crucial for health with a constant and tightly regulated balance between immunity and tolerance. Interferon-gamma, known as the immunological cytokine is the major effector of immunity in both innate and adaptive immune responses. IFNγ was first reported in 1965 by Wheelock *et al.*[49] for its anti-viral

activity, however, evidence rapidly showed pleiotropic functions of this immune regulator[50,51,52,53]. In 1993, the availability of gene knock-out (KO) mice for IFNγ or its cognate receptor (the interferon-gamma receptor: IFNγR) confirmed its critical role in clearing several infection models and in pathogenesis. Later, several studies with IFNγ insensitive cancer models (tumour cell lines or murine models) highlighted the importance of IFNγ in fighting carcinogenesis, tumour appearance, propagation, and relapse[54,55,56,46]. It strengthens the relevance of IFNγ functions in the immune innate and adaptive immunity. Moreover, it enhances the knowledge of IFNγ in immune surveillance of tumours as murine models with disrupted IFNγ pathway (IFNγRKO or STAT1 deficient – STAT1 = Signal transducer and activator of transcription 1, a downstream critical molecule for IFNγ signalling) were more susceptible to tumour progression and were not able to clear or control them[57]. Today, it seems that IFNγ triggers as much interest as precautions due to its versatile complexity of action.

1.2.1 IFNγ: an overview

Mostly secreted during immune responses by activated immune cells, IFNγ has important functions spearheading local and systemic effects, which are essential to overcome the immune threat. Indeed, IFNγ is mainly produced by activated T cells ($CD4^+$ Th1 T cells, cytotoxic T cells), NK cells, natural killer T cells (NKT cells), γδT cells but also B cells, and antigen-presenting cells, highlighting its central role in immunity[58,59,60,61].

Since its discovery, the classical IFNγ signalling pathway has been extensively studied (described in **Figure 3**). IFNγ is composed of two polypeptides anti-parallelly bound to form a symmetrical homodimer mature molecule[62,63]. Complementarily, the interferon-

gamma receptor is also made of two high-affinity IFNγ-binding subunits called IFNγR1, and two signal-transducing subunits called IFNγR2[64]. It is admitted that IFNγR1 is expressed in excess in nucleated cell types and that IFNγR2 is more tightly regulated. As such, IFNγR2 is the limiting factor controlling IFNγR signalling[65,50,66,64]. Both IFNγR1 and IFNγR2 can recruit Janus Kinase 1 (JAK1) and JAK2 respectively through their binding/recruitment sites, to trigger phosphorylation and therefore downstream signalling cascade[66,67]. Of note, whether the IFNγR heterotetramer (IFNγR1 and IFNγR2 homodimer subunits) is pre-assembled or whether IFNγR2 subunits are rapidly recruited after IFNγ binding on IFNγR1 is still debated[66,68,69,70]. After IFNγ binding at the cell surface, IFNγR undergoes conformation changes allowing transphosphorylation and activation of JAK1 and JAK2 following the phosphorylation of the IFNγR1 on their tyrosine residues Tyr440[71,72,73]. The latter creates a binding site triggering the recruitment and the activation through the phosphorylation of STAT1 dimers on their C-terminal tyrosine Tyr701[66,74,75,76]. Activated dimers of phosphorylated-STAT1 reported as gamma-activated factors (GAF) are then able to translocate to the nucleus and bind gamma-activated site (GAS) elements that are found in promoter regions of targeted genes: the interferon-stimulated genes (ISGs)[51,77,78] see **Figure 3**.

ISGs define any genes induced by interferon stimulation including type I Interferon (IFN), type II IFN (IFNγ), and type III IFN[79,80,81]. Mostly relying on the JAK/STAT signalling pathway, there is redundant ISGs expression induction within the IFN family[82,83], however, IFNγ is a very specific interferon with a significant number of specific genes induced being not redundant[84], suggesting that IFNγ cannot be compensated by other IFNs during immune responses. ISGs are incredibly diverse, the primary response

induced by GAF triggers among others the expression of transcription factors such as interferon regulatory factor 1 (IRF1) which then leads to secondary responses[51,66,85]. There is an amplification of the system with interferon-stimulated response elements (ISRE) that diversify and ramify the response, primed by IFNγ signalling, resulting in the induction of other signalling pathways[86]. Physiological negative feedback can also be elicited by IFNγ, preventing an overload of the system to efficiently restore homeostasis. For instance, the suppressor of cytokine signalling 1 (SOCS1) which is directly induced by IFNγ signalling, is a specific inhibitor of the classical IFNγ pathway[87]. Another example of a classical regulatory feedback loop is the IFNγ-IFNγR complex internalization for degradation or IFNγR recycling[66,69,88,89]. Of note, the latter to a lesser extent has been shown to translocate in the nucleus and transduce signal *via* a non-classical pathway[90].

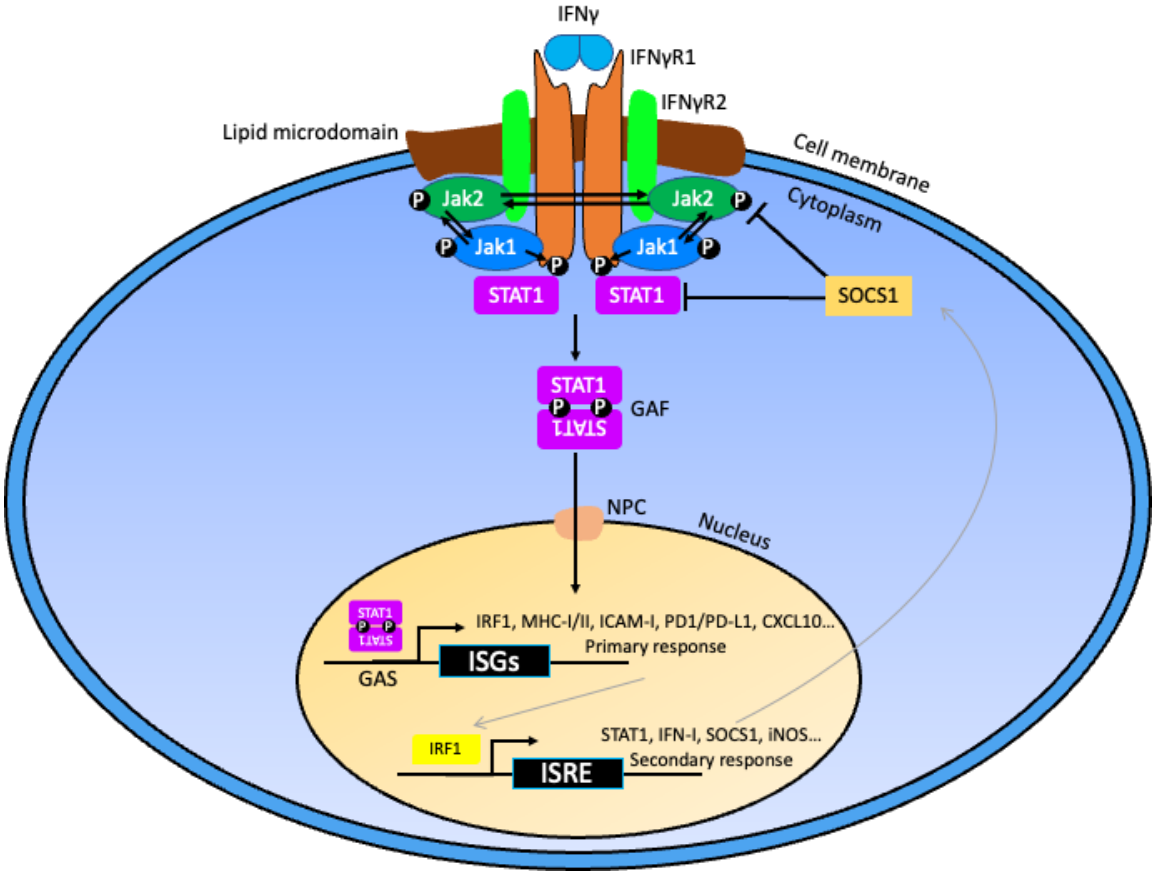


Figure 3: Classical pathway of IFNγ signalling. The current canonical IFNγ pathway stipulates that IFNγ mature molecule (homodimer in cyan) binds its cognate receptor (IFNγR) composed of IFNγR1 subunit (orange) and IFNγR2 subunit (light green). Upon oligomerisation, the IFNγR new conformation allows JAK2 activation through its autophosphorylation, followed by the activation of JAK1. Then, activated JAK1 creates the STAT1 binding sites by phosphorylating IFNγR1. Once recruited, homodimers of STAT1 are phosphorylated which released them from the receptor, they represent the gamma-activated factors (GAF). Next, GAF translocates to the nucleus through the nuclear pore complex (NPC) and binds to gamma-activated sites (GAS) present in promotor regions of the interferon-stimulated genes (ISGs). Some of the genes expressed during the primary response are transcription factors that triggered a second response level to IFNγ signalling, such as the interferon regulatory factor 1 (IRF1) which leads to interferon-stimulated response elements (ISRE) expression. This cycle can enhance signalling (more STAT1 availability for instance) but also restricts the system amplification (with SOCS1 for instance). SOCS1 = Suppressor of cytokine signalling 1; MHC-I/II = Major histocompatibility complex class I and II; ICAM-I = Intercellular adhesion molecule-1; PD-1= Programmed cell death 1; PD-L1 = Programmed death-ligand 1; IFN-I = type I interferons; iNOS = inducible nitric oxide synthase.

The complexity of the ISGs and ISRE network leading to various biological responses explains partly the IFNγ pleiotropic properties. The ISGs and their related numerous biological functions have been well reviewed by Schroder *et al*[66].

Overall, in a physiological context when the immune response is efficient and complete as during acute infections, IFNγ primes and recruits relevant immune cell populations to clear the pathogen, orientates a Th1-type response, induces a pro-inflammatory environment, and induces an anti-viral/microbial state along with cytostatic and cell death for infected cells[79,91]. However, it is becoming clear that IFNγ also has immune inhibitory effects which are essential for getting back to homeostasis in physiological contexts but can act in favour of the disease progression in case of auto-immune and chronic diseases such as cancer[59,92].

1.2.2 IFNγ: a pleiotropic cytokine in the TME

IFNγ is a critical player in every immune response. It is well established that IFNγ is essential for the cytotoxic functions of CTLs and NK cells, leading to cytotoxic and cytostatic effects on target cells. It also induces the upregulation of MHC-I and MHC-II molecules essential for antigen recognition, and upregulation of immune-modulatory molecules such as programmed cell death protein 1 (PD-1), PD-L1, cytokine, and chemokine axis for instance[59,66,93,94]. IFNγ has pro-inflammatory functions that have potent anti-tumour functions (**Figure 4** – left panel). With this knowledge, IFNγ was seen as having great therapeutic potential in the past. The first therapeutic strategy was the administration of recombinant IFNγ which was doable after its cloning from cDNA (complementary DNA) in 1982[95]. IFNγ-based therapies were expected to trigger IFNγ-

dependent anti-tumoral functions[96]. Multiple clinical trials have been performed to test the efficiency of recombinant IFNγ in treating various cancers and other diseases[97]. Failures, mixed results, or even worse outcomes with terrible side effects in patients, leading to premature trial ends[97], suggested that IFNγ also had pro-tumor functions favouring tumour escape. For example, in ovarian cancer patients, mixed results were obtained after recombinant IFNγ administration. It improved overall response rates and anti-tumour response in subcutaneous or intraperitoneal injection conditions (local delivery)[97], while it had negative effects leading to ending phase III clinical trials when delivered systemically[98]. This underlines that the range of IFNγ functions also depends on its dose, duration, and localisation which are critical parameters to consider for optimal therapeutic responses[99]. Other therapeutic failures taught us that IFNγ can trigger immune response resistance with cancer cell unresponsiveness due to long and continuous exposure for instance[100]. Overall, those strategies aimed to act at a systemic level, targeting inflammatory symptoms or directly cancer cells for instance. However, these disappointing results suggest that IFNγ also has concomitant pro-tumour functions that need to be investigated and studied in parallel to the anti-tumour functions.

As representative examples of IFNγ dual type of functions in a cancer context, IFNγ can induce leukocyte trafficking which can be seen as an anti-tumour function, however, IFNγ can also enhance the immune inhibitory microenvironment by the upregulation of inhibitory molecules (PD-L1/2) and the stimulation of immunosuppressive cells[94,101] (Tregs, MDSCs, TAMs, CAFs, etc.) (see **Figure 4** – right panel). Secondly, although IFNγ has been shown to be anti-angiogenic which restricts the tumour growth[102], IFNγ can

also upregulate FAS-Ligand (FAS-L) expression notably on endothelial cells[89] which induces CTLs death leading to the immune escape of the tumour. In addition, when IFNγ normal production is disturbed such as in auto-immune diseases[103], the IFNγ exposure often exacerbates the pathogenesis by triggering specific cell death, chronic inflammation, tissue damage, or immune resistance[103,54]. Those examples also underline the fact that the global effect of IFNγ depends on spatiotemporal parameters such as duration and localisation of IFNγ secretion. In other words, the biological effect of IFNγ relies on its bioavailability, which cell populations are present to respond to it, and the stage of the disease (early phase, effector phase, chronic context, etc.). Overall, the immunomodulatory effect of IFNγ should be locally and timely controlled to prevent pathogenesis and its progression. This knowledge made IFNγ a promising single targetable candidate for numerous disease treatments. However, it seems very difficult to anticipate and control its function due to its pleiotropic actions.

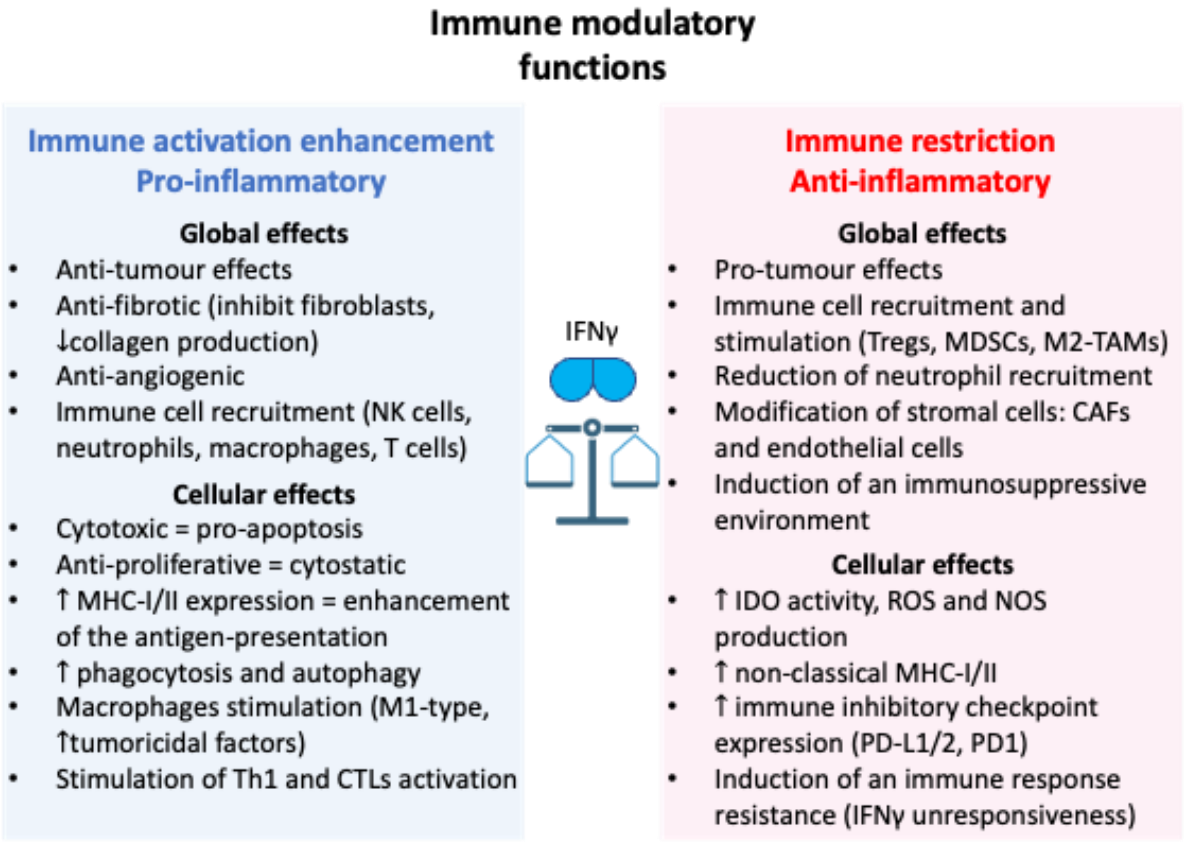


Figure 4: Overview of the opposite effects of IFNγ in tumours. On the left panel, are the pro-inflammatory effects. On the right panel, are the immune inhibitory effects. The overall IFNγ effects depend on the balance between its versatile functions triggered by the different cell types present in the TME. Tregs = Regulatory T cells; MDSCs = Myeloid-derived suppressor cells; TAMs = Tumour-associated macrophages; CAFs = Cancer-associated fibroblasts; IDO = Indoleamine 2,3-dioxygenase; ROS = Reactive oxygen species; RNS = Reactive nitrogen species; TRAIL = TNF-related apoptosis-inducing ligand.

IFNγ is often found in tumours and can trigger many effects with opposite functions as mentioned in **Figure 4**. This pleiotropism can also be explained by the fact that every cell present in the tumour microenvironment can respond to it as they all express its cognate receptor the IFNγR. Furthermore, the different cell types have different IFNγR1

and IFNγR2 expression levels which will dictate different cellular effect[66]. It is therefore critical to investigate the IFNγ effect at the cellular level.

$CD8^+$ T cells or CTLs are the main IFNγ producers in tumours, they are therefore in direct contact with IFNγ. Additionally, IFNγ is known to be involved in the maturation of $CD8^+$ T cells during the priming and differentiation phases, highlighting its important immune-modulatory role at early stages of the response by both systemic and autocrine/paracrine mechanisms[104,105]. More recently, the concept of $CD8^+$ T cells ecosystem arise with the linked subtype populations and T cell clones regulating each other at a collective level *via* cell contact and autocrine/paracrine communications[106].

While the function of IFNγ on cancer and stromal cells has been extensively studied, how it affects immune cells is still unclear. In particular, IFNγ function on the cells that produce it in tumours such as CTLs has not been studied in detail, based on the fact that they express low levels of the IFNγR. However, our group already studied the function of IFNγ on a monoclonal population of $CD8^+$ T cells, showing that IFNγ limits the effector differentiation of $CD8^+$ T cells[107]. IFNγ, therefore, influences the balance between $CD8^+$ T cell differentiation into terminally effector cells and memory precursors in the acute infection model of *Listeria monocytogenes*. This further suggests that $CD8^+$ T cells do respond to the cytokine they produce which has not been properly investigated in tumours so far.

1.3 CD8$^+$ T cell dysfunction in cancer: exhaustion and beyond

The immune system is extremely complex and has evolved to protect the host from a plethora of threats ranging from various types of pathogens to injuries, as well as malignant self, represented by cancer cells. The immune response is composed of the innate response which is triggered very rapidly after an immune threat in a non-specific manner followed by the adaptive response which recognises specific antigens and provides long-term protection with the immune memory formation. CD8$^+$ T cells are part of the adaptive immune response as they are able to specifically recognise and respond to immunogenic antigens.

1.3.1 CD8$^+$ T cell biology

1.3.1.a CD8$^+$ T cell development

The ability of CD8$^+$ T cells to recognise immunogenic antigens is critical to adaptive immunity. CD8$^+$ T cells use a variety of cell surface receptors to sense their environment, notably their TCR to bind specific antigens. This antigen-receptor consists of variable antigen-recognition proteins which vary from cell to cell conferring the T cell clonality, in addition to invariant complexes with signalling proteins such as CD3 and CD8[108,109,110,]. Mature CD8$^+$ T cells are considered as naïve as they have not yet encountered antigens. Each naïve mature CD8$^+$ T cell harbours a unique TCR and represent a T cell clone part of the diverse T cell repertoire[111]. The production of new CD8$^+$ T cells, called lymphopoiesis, starts from the bone marrow with the generation of lymphocyte precursors before reaching the thymus for T cell development until maturation. The

general different steps occurring in T cell development are described in **Figure 5**. The multipotent hematopoietic stem-cells present in the bone marrow give rise to some lymphoid progenitor cells that will migrate to the thymus *via* the bloodstream. Once there, cells will undergo multiple steps to mature before being released in the system as mature functional T cells[112,113]. Thymocytes or developing T cells go through four double-negative stages (DN1 to DN4) where cells do not express CD4 or CD8 co-receptors yet but harbour CD44 and CD25 expression at their surface. From the DN3 stage, cells express a pre-TCR which will mature and be used for thymic selections. Cells with a functional pre-TCR will be positively selected and will proliferate and rearrange their TCR, while cells with dysfunctional or non-responsive TCRs undergo apoptosis. Then at the double-positive stage (DP), cells express both CD4 and CD8 at their cell surface and the mature TCR will replace the pre-TCR[114]. Cells are tested and negatively selected to avoid highly self-reactive T cells released in the system causing potential auto-immune diseases. Selected cells further mature into either single-positive $CD4^+$ T cells or $CD8^+$ T cells before exiting the thymus to circulate into the system. It is noteworthy that this process gradually stops in adults as the thymus involutes and turns into fatty tissue[115,116]. It, therefore, limits the generation of new T cell clones with age.

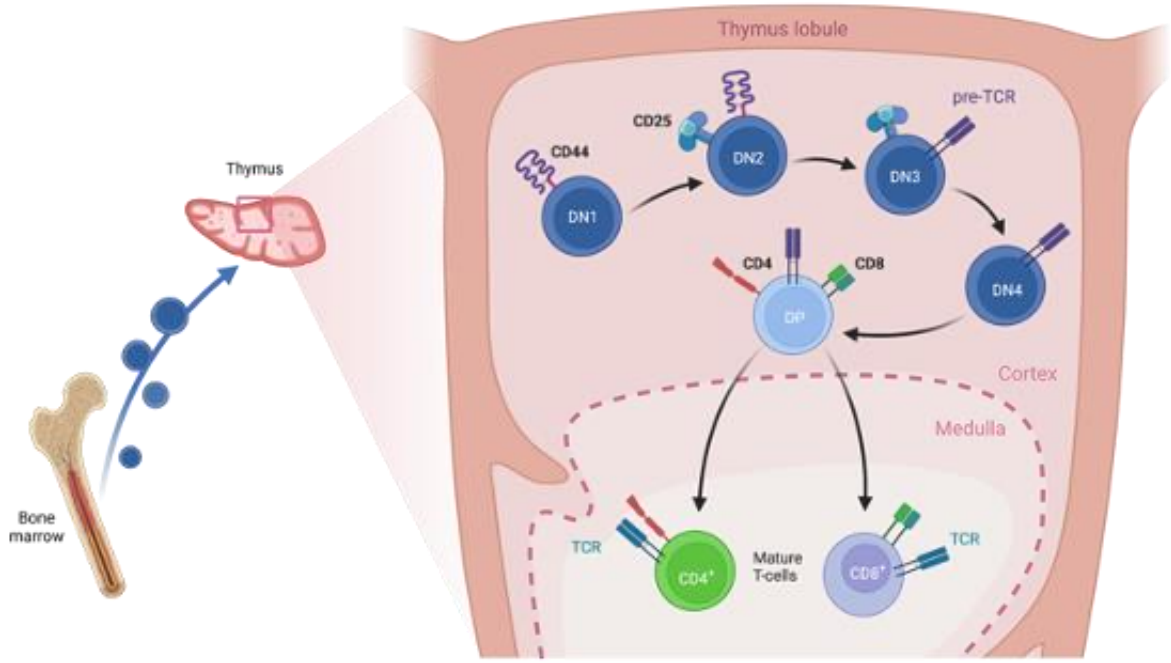


Figure 5: CD8⁺ T cell development. Lymphocyte precursors are generated from the bone marrow and reach the thymus for T cell development. Immature T cells or thymocytes underwent multiple steps. Developing T cells are called double-negative until they become double-positive before finally being single-positive either CD4⁺ or CD8⁺ T cells. The pre-TCR during the double-negative stages helps for positive selection by thymic epithelial cells in the thymus cortex until the TCR is used for negative selection by DCs in the thymus medulla. Overall, only 1-2% of the thymocytes are selected and released as naïve mature T cells in the circulation. [Created with BioRender.com].

1.3.1.b CD8⁺ T cell activation

Naïve mature CD8⁺ T cells recirculate between the peripheral blood and the lymphatics to reach and leave lymphoid tissue to patrol the body while waiting for activation. To activate an adaptive immune response, naïve CD8⁺ T cells must recognise their specific antigens processed and presented by sampling the antigen-presenting cell surface through TCR–peptide:MHC-I complexes. This mostly happens in secondary lymphoid organs such as lymph nodes, where naïve CD8⁺ T cells and mature dendritic cells are present[117].

CD8⁺ T cell activation also called CD8⁺ T cell priming, comprises 3 signals: represented in **Figure 6**.

- Signal 1: TCR activation = antigen-specific recognition *via* TCR–peptide:MHC-I on APCs
- Signal 2: Co-stimulation = interaction with co-stimulatory receptors present on APCs
- Signal 3: Cytokines = cytokines sensing which controls the type of cell differentiation

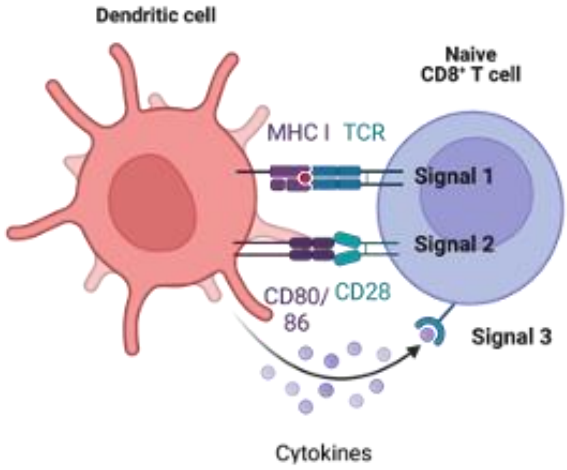


Figure 6: CD8⁺ T cell activation. CD8⁺ T cells require 3 signals for efficient priming. First, their TCR engagement by the cognate peptide presentation on MHC-I by an antigen presenting cells. Second, the engagement of co-stimulatory molecules. And third, the cytokine sensing for adequate and efficient differentiation. [Created with BioRender.com].

Signals 1 and 2, namely TCR triggering, and co-stimulation are sufficient and required for CD8⁺ T cell activation leading to cell differentiation and proliferation[118]. However, the third signal, "cytokine sensing", is critical for the complete and efficient differentiation of the required cells depending on the environment and the immune threat[119,120,121]. Additionally, a lack of cytokine sensing during CD8⁺ T cell priming showed poor CD8⁺ T cell response which fails to elicit immune memory[122,123]. Thus, the

3 signals are required to provide an optimal $CD8^+$ T cell activation and subsequent adaptive immune response. Once activated, $CD8^+$ T cells will differentiate into effector cells named cytotoxic T cells and proliferate rapidly. From the next antigen encounter, CTLs will recognise the target cells and induce cell death.

1.3.1.c CD8⁺ T cell effector function

Once activated and differentiated into cytotoxic T cells, $CD8^+$ T cell function relies on their interaction with their target cells. After antigen recognition, CTLs will use their effector molecules to kill the target cells that are either infected or cancer cells. When CTLs bind their target cells through the TCR–peptide:MHC-I complex, an immunological synapse is formed with the help of a co-receptors cluster at the cell-cell contact site with CD8 and molecules such as lymphocyte function-associated antigen 1 (LFA-1), which bind intercellular adhesion molecule 1 (ICAM-I) for instance[124,125]. The effector molecules are directly released within this immunological synapse rendering the cytotoxic function of $CD8^+$ T cells not only antigen-specific but also directly performed toward the target cells in a very precise manner[126]. Cytotoxic functions rely on the expression of several effector molecules with different effects all leading to triggering the apoptosis of target cells[127]. There are 3 main cytotoxic pathways:

- Cytolytic granules = degranulation of perforin and granzymes which are pro-proteases triggering apoptosis into the target cells
- Cytokine secretions = IFNγ and TNFα secretion directly through the immunological synapse with cytostatic and pro-apoptotic effects.
- Cell surface FAS-L expression = membrane-bound effector molecule that will activate apoptosis in FAS-expressing target cells.

Overall, the various effector molecules produced and used during the $CD8^+$ T cell effector phase allow CTLs to be very efficient in killing their targets. Interestingly, cytokine secretions can kill the target cells very locally but can also act at distance and can influence and orchestrate the immune response in the surrounding environment where the target cells are present (see **Chapter 1.2** – IFNγ and its pleiotropism in the tumour microenvironment for more details).

1.3.2 $CD8^+$ T cell response: Acute *versus* chronic context

Efficient immune responses with the $CD8^+$ T cell response are tightly regulated in size, time, and diversity to avoid overreaction leading to immunopathology or hypo-reaction with immune response failure. Indeed, the perfect efficient immune response occurs in acute infections for instance where the primary $CD8^+$ T cell response is well controlled with several steps leading to immune memory formation in case of subsequent pathogen encounters. In chronic contexts, the immune response fails to clear the pathogen or restore homeostasis leading to chronic immune activation and inflammation. $CD8^+$ T cell response in acute infection can be divided into three major phases: 1) T cell activation with cell expansion, 2) effector phase ending with the T cell population contraction, and 3) the maintenance of the memory pool over time. The antigen-specific $CD8^+$ T cells are activated from the naïve $CD8^+$ T cell pool and differentiate into effector cells with short-lived effector cells (SLECs) representing the CTLs and memory-precursor effector cells (MPECs) which will further mature and become the long-lived memory $CD8^+$ T cells (**Figure 7**). Of note, there is a variety of memory $CD8^+$ T cell subsets: central memory T cells, effector memory T cells, and tissue-

resident memory T cells. All have different levels of memory quality, location, and phenotypes and represent together the functional memory formation aimed for efficient CD8⁺ T cell response. In contrast, in chronic contexts, antigen-specific CD8⁺ T cells are activated from the naïve CD8⁺ T cell pool and differentiate into effector cells that proliferate before becoming gradually exhausted paired with the gradual loss of function (**Figure 7**).

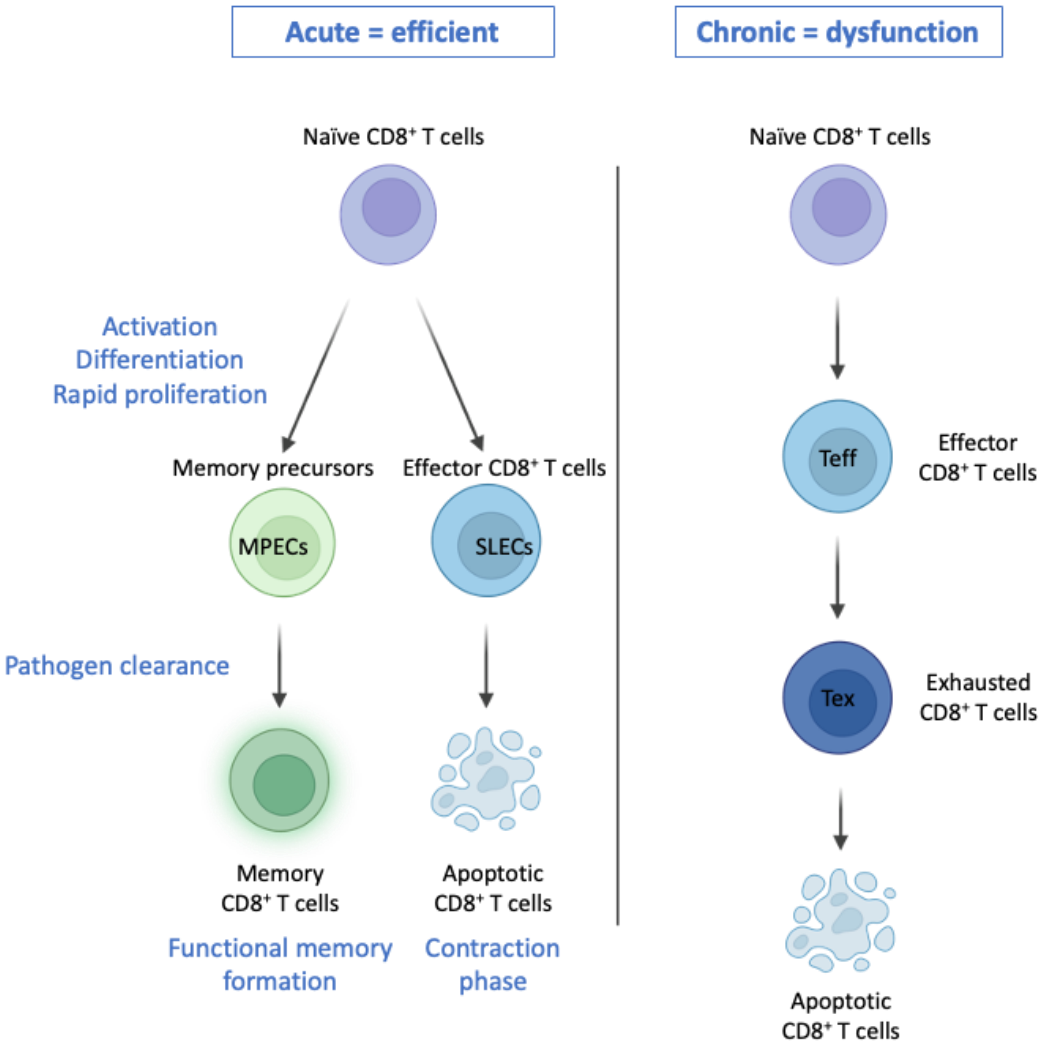


Figure 7: CD8⁺ T cell differentiation in acute *versus* chronic immune response. Naïve CD8⁺ T cells are activated and differentiate into different CD8⁺ T cell subsets depending on the context. In acute infections, cells are either becoming effector cells and will die during the contraction phase while cells differentiated into memory cells will survive to patrol the body. In contrast, in

chronic contexts, effector cells will gradually lose their function until terminal exhaustion prior to apoptosis. [Created with BioRender.com].

The kinetics of both $CD8^+$ T cell responses are quite different, which is presented in a simplified overview in **Figure 8**. In acute infections, after the establishment of the infection when the innate response takes place, the induction of the adaptive immune response starts with the antigen-specific $CD8^+$ T cells that are rapidly proliferating during the effector phase. CTLs are clearing the pathogen and will undergo the contraction phase with about 90% of those cells that will die upon the infection resolution. From here, only the specific memory cells will survive long-term to protect the host from secondary infections. In chronic conditions such as chronic infections and cancer, the immune response typically never ends, resulting in overstimulation of $CD8^+$ T cells as antigens are not cleared over time. A simplistic model suggests that the immune response induction would be similar to acute models, however, the effector phase last longer as there is no contraction phase. The amplitude of the $CD8^+$ T cell response gradually diminishes as the exhaustion and $CD8^+$ T cell dysfunction increase with some cell death. Nevertheless, it seems that there is no memory formation *per se* as the immune response is still ongoing, hence the immune response dysfunction/failure. Of note, the exhaustion pathway is still unclear whether it is a linear process as presented in **Figure 7** or whether different pathways appear simultaneously[128].

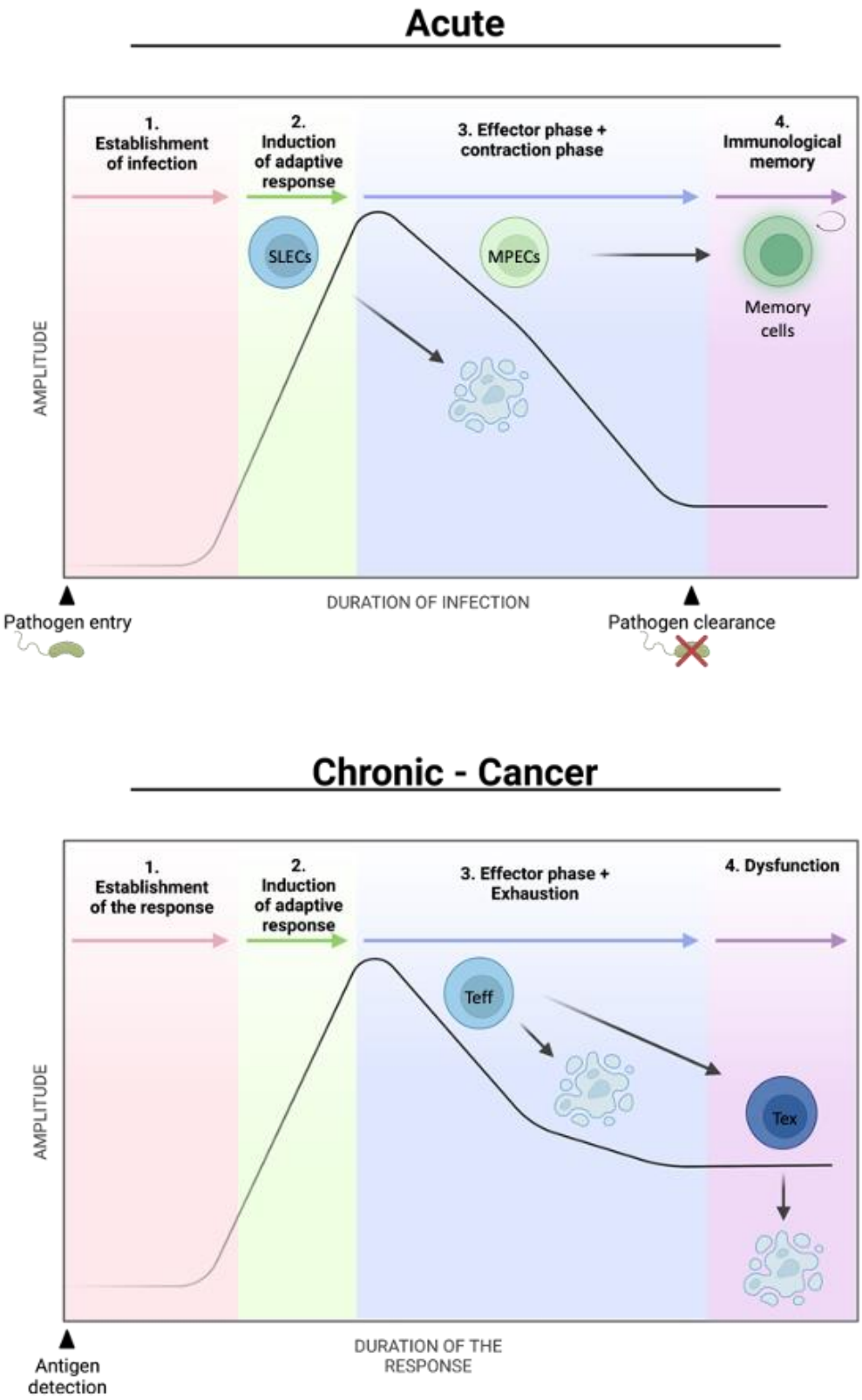


Figure 8: Course of the CD8$^+$ T cell response in acute *versus* chronic immune response. [Created with BioRender.com].

1.3.3 CD8⁺ T cells in cancer

As described in the previous section, CD8⁺ T cells are becoming dysfunctional in cancer over time, the cancer being a chronic condition. The CD8⁺ T cell dysfunction harbour different names in literature such as hypofunctional T cells, hypo-responsive T cells, anergic T cells, tolerant T cells, or exhausted T cells. Those cells are in different states showing the different flavours of T cell dysfunction with a continuum of dysfunctional states. The cancer-immunity cycle previously introduced described 7 steps for successful anti-tumour responses focusing on the role of the CTLs (**Figure 2**). However, it is hardly achieved as cancer develops and represents a deadly disease. Steps from T cell priming and activation to the killing of cancer cells harbour multiple failures, hence the CD8⁺ T cell dysfunction. The concept of exhaustion is defined by the progressive CD8⁺ T cell dysfunction linked with the upregulation of inhibitory receptors. However, it only partly explains the CD8⁺ T cell dysfunction which should not be restricted to the exhaustion process. Several therapeutic strategies have aimed to enhance every step of the cancer-immunity cycle. For example, to increase efficiently the antigen presentation to activate CD8⁺ T cells, some co-stimulatory and vaccination strategies are under clinical evaluation[28]. Then, treatment targeting blood vessels such as anti-VEGF (vascular endothelial growth factor) can influence the CD8⁺ T cell tumour trafficking. To further control and enhance the CD8⁺ T cell tumour recognition, adoptive cells transfer with chimeric antigen receptor (CAR) T cell therapy showed promising results[129]. Finally, immune checkpoint blockades (ICB) such as anti-PD-1 and anti-PD-L1 are directly targeting CD8⁺ T cell exhaustion in tumours. All those strategies have an impact on CD8⁺ T cell anti-tumour response. Some showed important success in

particular cancer types, nevertheless, there are numerous challenges to overcome in solid tumours. ICB with anti-PD-1 and anti-PD-L1 in monotherapy only harboured a response rate between 13% to 38% in human patients depending on the tumour type[28]. This first confirms that $CD8^+$ T cell dysfunction in cancer cannot be reduced to exhaustion and that targeting $CD8^+$ T cell biology is a great therapeutic strategy with high potential to unlock. There is a lot to investigate and decipher to efficiently improve the inevitable $CD8^+$ T cell dysfunction in cancer, namely the molecular mechanisms involved in the $CD8^+$ T cell response for long-term effects in cancer patients. Recently, a paper described a particular $CD8^+$ T cell subset present in chronic infections, which represents a key player in the positive response to ICB: the stem-like T cells[130]. This opens a new perspective to better understand how ICB are working and how to improve them in the future.

1.4 Stem-like T cells: the essential piece for long-term anti-tumour response

1.4.1 Stem-like T cells: the recent discovery

Stem-like T cells were first described in 2016 by Im *et al.* by identifying a $CD8^+$ T cell subset that was responsible for the proliferative response to PD-1 blockade (anti-PD-L1 treatment)[130]. In this study, researchers used the lymphocytic choriomeningitis virus (LCMV), a chronic infection model, to study the mechanisms that regulate T cell

exhaustion to improve immunotherapies in mice. By focusing on virus-specific $CD8^+$ T cells using the tetramer technology[131], they identified this new $CD8^+$ T cell subset which was exclusively generated in chronically infected mice, where antigen persistence was present as opposed to acute infections. They described a quiescent population with a slow self-renewal rate that resided in lymphoid tissues thanks to a specific set of chemokine receptors rendering them responsive to CXCL13 and CCL19/21[132]. In addition to maintaining their pool by self-renewal, stem-like T cells have a great proliferative capacity upon stimulation *via* their differentiation into early exhausted cells with effector functions[133]. This discovery led to redefining the $CD8^+$ T cell differentiation pathway during chronic immune responses. As summarised in **Figure 8**, in chronic contexts such as chronic infections, inflammation, cancer, or auto-immunity, immune responses are dysfunctional. Indeed, they are not efficient enough to clear the pathogen or restore homeostasis in tissue, therefore not able to contract the immune response and obtain an efficient immune memory as in acute infections (see **Chapter 1.3**). Here, naïve $CD8^+$ T cells are differentiating into effector cells upon activation and follow the exhaustion path with a range of exhaustion levels until they reached the terminally exhausted stage before dying (**Figure 9** – left panel). The novelty here on the right panel is that stem-like T cells are generated very early during the immune response from the naïve cell pool, but stay quiescent[134]. The generation of those cells could be an adaptation of the immune system when chronic antigen stimulation with decreased co-stimulation is persistent in the system. Stem-like T cells are long-lived they can therefore support the immune response over time by acting as resource or precursor cells. Once re-stimulated they would rapidly undergo differentiation and give rise to early

exhausted T cells with effector functions. The exhaustion path appeared to stay similar beyond this stage. However, this new cell population highlights the fact that cells are versatile and there is a great plasticity and numerous stages within the continuum of differentiation. It is not yet clear whether both paths are happening in a linear fashion or whether stem-like T cells are always generated and then disappeared[128].

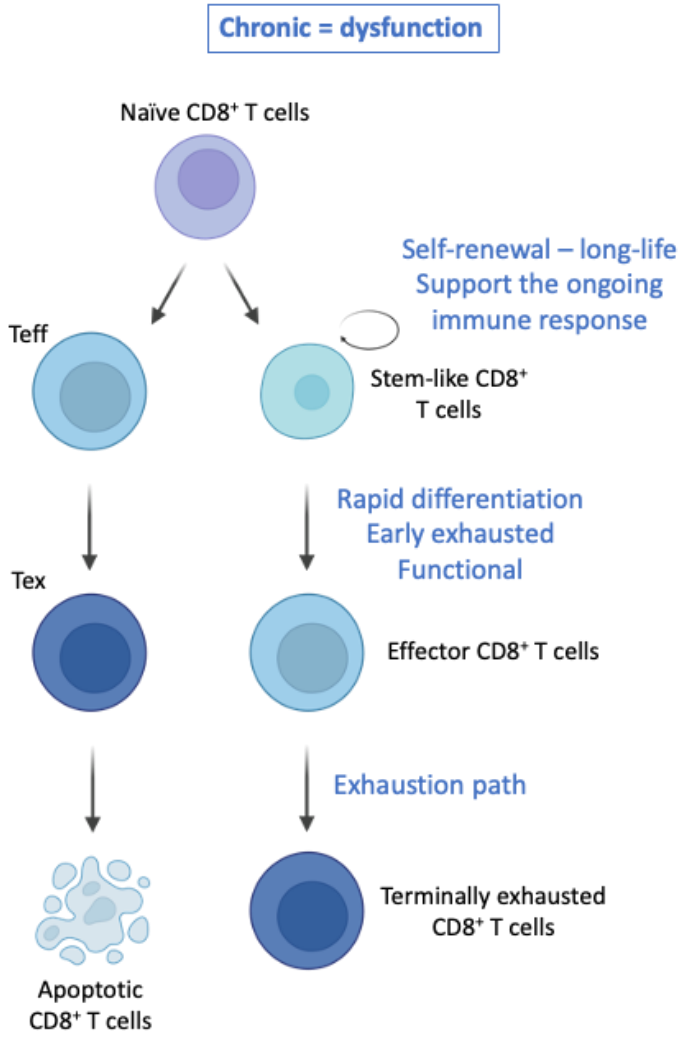


Figure 9: A simplistic revised model of CD8⁺ T cell differentiation in chronic contexts. Antigen-specific naïve CD8⁺ T cells are activated and differentiate into effector cells and follow the exhaustion path. Recently it has been shown that some naïve CD8⁺ T cells become stem-like T cells with memory-like and stemness potential to self-renew and concomitantly give rise to effector cells during an ongoing chronic immune response. [Created with BioRender.com].

Naïve $CD8^+$ T cells are found in lymphoid organs (such as lymph nodes and spleen) and in the circulation[135]. They have a high proliferation and differentiation capacity upon activation and have a long persistence and survival rate[136,137]. Naïve $CD8^+$ T cells do not have cytotoxic functions. While they phenotypically express T cell factor 1 (Tcf1), they do not express PD-1[138,139]. Conversely, stem-like T cells have been activated, and therefore upregulate PD-1. Furthermore, as stem-like T cells are antigen-experienced they are part of the ongoing antigen-specific immune response. Although their biology is not yet deciphered, they maintain the Tcf1 expression, a transcription factor key to their stemness[140,141]. They have been described as expressing co-stimulatory molecules and chemokines receptors, but not effector molecules (such as granzyme B) nor inhibitory receptors apart from PD-1. Effector T cells or early-exhausted T cells downregulate Tcf1 expression, upregulate exhaustion markers (e.g. T cell immunoglobulin domain and mucin domain 3 – Tim-3, lymphocyte activating 3 – Lag-3, T cell immunoreceptor with Ig and ITIM domains – Tigit), actively proliferate, and have effector functions[142]. Finally, terminally exhausted T cells are mostly found at the site of the immune response, harbouring high expression of exhaustion markers while lacking co-stimulatory molecules expression, and losing their effector functions[128]. Interestingly, exhausted T cells were described as ineffective and innert[143], however, if depleted during chronic infections, the virus load significantly increases suggesting that exhausted T cells are not effective enough to clear the pathogen but have a role in keeping it controlled over time[144]. The main expression features of the different cell types are listed in **Figure 10**. Of note, this list is not meant to be exhaustive but to

highlight some key markers found in the literature so far to distinguish the different cell populations.

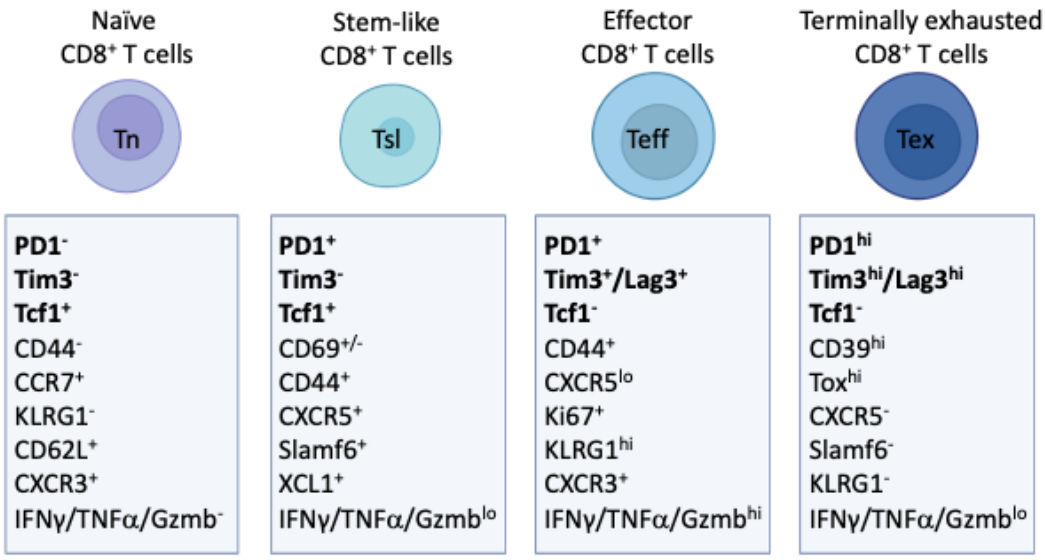


Figure 10: Main cellular markers to distinguish CD8⁺ T cell populations. Main references used[145,146,130,128,147,148]. [Created with BioRender.com].

Stem-like T cells are mainly defined as $CD8^+PD\text{-}1^+Tcf1^+$ T cells in the literature. Following this discovery, stem-like T cells were then described in many other chronic pathologies both in mice and humans. Similar observations were found in LCMV models[149,150,151,152,153,154,132,155,156], human immunodeficiency virus (HIV)[149,151,157,158], hepatitis C virus (HCV)[150], and later on in human cancers, such as in lung cancer[159,160,161], in melanoma[162,163,164] , and in kidney cancer[165]. Recently, stem-like $CD8^+$ T cells have also been associated with auto-immune diseases, such as type I diabetes[166]. Overall, they became an intense area of research as they opened new perspectives to 1) better understand the exhaustion mechanisms and functions in chronic contexts, and 2) improve immunotherapy efficacy. Of note, stem-like T cells were also described under

other names in the literature as they were recently discovered: “precursor exhausted T cells – Tpex”[167,168], or “early-precursor T cells”[142], or “progenitor exhausted T cells”[147,128], or “exhausted-stem-TILs”[140] for instance. In my thesis, I refer to these cells as stem-like T cells.

1.4.2 Stem-like T cells: the keystone for long-term immune responses and immunotherapies efficacy

$CD8^+$ T cells with memory-like, stemness-like phenotypes were described before 2016[169,145,170], however, the first stem-like T cell definition was inherently linked to their critical role in the response to immunotherapy especially anti-PD-L1 treatment in the chronic LCMV model[130]. Since this breakthrough discovery, researchers aimed to decipher stem-like T cell biology and to understand their role in sustaining immune responses as it could also help predict immune checkpoint blockade response in patients and improve the use of the therapeutics arsenal both in chronic infections and cancer. One limiting factor in $CD8^+$ T cell anti-tumour response is the fact that all adult individuals have a restricted pool of naïve cells with a certain level of TCR clonal diversity that tends to decrease with age[171,172,173]. Once the antigen-specific and relevant $CD8^+$ T cells are activated they would rapidly differentiate into effector cells that would eventually become exhausted and non-functional in a chronic context (**Figure 9** – left panel). The naïve cell pool is not replenishable, therefore once selected and activated cells cannot be replaced over time which leads to the immune response collapse. If the tumour is not generating new tumour antigens, for instance, the $CD8^+$ T cell anti-tumour response reaches its limits. However, the discovery of stem-like T cells changes this

dynamic. Indeed, stem-like T cells are differentiating from naïve cells very early on in the $CD8^+$ T cell path[134]. Therefore, the antigen-specific $CD8^+$ T cells would keep a pool of resource cells by self-renewing throughout the immune response (**Figure 9** – right panel). By maintaining a certain level of the immune response, stem-like T cells are originating virus control for instance. Even if it is not enough to clear the pathogen, it is sufficient to maintain an ongoing immune response with functional early-exhausted cells regularly generated.

ICB such as anti-PD-1 and anti-PD-L1 is aiming to reinvigorate $CD8^+$ T cell response that became dysfunctional over time in tumours. The mechanism by which it is working is not fully understood. Indeed, only a small fraction of patients respond positively to ICB, however, the majority of patients failed to trigger a long-term immune response, or acquire resistance to ICB[174,175,176,128,177,178,179]. Further investigations into such therapy are essential to enhance their efficacy and enhance the number of responding patients. $CD8^+$ T cells reaching the terminally exhausted state cannot be reinvigorated by anti-PD-1 treatment for instance as they have reached an irreversible epigenetic state[180,181]. But anti-PD-1/anti-PD-L1 can enhance temporarily the function of less exhausted T cells until they reach the terminal exhaustion state. On the other hand, anti-PD-1/anti-PD-L1 directly targets stem-like T cells as they express PD-1. It increased their self-renewal property and their proliferation into more differentiated cells. Consequently, it demonstrates that PD-1 blockade can work by increasing stem-like proliferation and by enhancing effector function at the tumour site. As stem-like T cells are persisting long-term in the system, they and their progeny are better able to control tumour growth than exhausted T cells alone. Consistent with this mechanism, melanoma patients with

a greater stem-like T cell proportion in tumours prior to treatment harbour a longer response to immune checkpoint blockade[164]. Similarly, the increased presence of stem-like T cells in melanoma lesions has a predictive value to ICB treatment in patients[162]. Murine studies demonstrated that the ablation of stem-like T cells in tumours restricted the response to therapeutic vaccination in a murine melanoma model[163]. Overall, the presence of stem-like T cells in the system better explained the mechanism by which immunotherapies targeting the PD-1 pathway are working[182]. However, it opens numerous questions and will require further studies and patients to identify whether stem-like T cells are only a predictive parameter to ICB success or whether this knowledge can be manipulated to enhance cancer treatment in general.

1.4.3 Open questions on stem-like T cells

Recent studies on stem-like T cells are bringing new insights into understanding $CD8^+$ T cell immune response in chronic contexts such as cancer. The presence of stem-like T cells seems to correlate with a greater or longer immune response at least, therefore from there, the next challenges would aim to understand how to enhance their presence in tumours, and how to maintain their presence over time, but also assess whether their greater presence can have negative effects on the long term. The immune system is well regulated and integrates a balance between negative and positive regulators along the immune responses. The amplification of this mechanism might need to be tightly investigated since anti-tumour effects can also be accompanied by pro-tumour effects or a break in the tolerance leading to auto-immune events for instance. Therefore, the sweet spot needs to be found if it exists.

Additionally, the stem-like T cell biology and regulation remain to decipher. Interestingly, studies reported them in tumour-draining lymph nodes[161] and within tumours[163,165,183]. This suggests that they are able to migrate or differentiate in different environments in addition to being able to survive on-site. It is noteworthy, that those cells are mostly named stem-like T cells in lymphoid organs and some studies are naming these cells T precursor exhausted cells (Tpex) once they reach the tumour. A recent study taking advantage of the Kaede photoconvertible mice described stem-like T cells trafficking between tumours and lymphoid tissue in MC-38 colon tumours[184].

An important question to investigate is how stem-like T cells are maintained and regulated in tumours. Some studies point to specific niches or structures within tumours such as tertiary lymphoid structures[185] or in niches with a higher density of antigen-presenting cells[165] for instance. Stem-like T cells have been shown to express XCL1[186,130] which can attract and recruit class 1 dendritic cells (cDC1)[187] known as the best cross-presenting APCs, ideal for $CD8^+$ T cells[188,189,186]. Finally, a very recent study correlates the presence of stem-like T cells in tumours with HEVs (high endothelial venules) structures[190]. In terms of intrinsic regulation, a lot remains to decipher however two very recent studies described the implication of IL-10[191] and TGF-β[155] in stem-like T cell regulation in tumours. This suggests that stem-like T cells are sensitive to their environment which will require in-depth investigation to understand their preferential cues for cell maintenance. To conclude, the relevance of stem-like T cells in anti-tumour immunity is very convincing but their regulation is not understood and requires attention as it could lead to critical advances in cancer treatment.

1.5 Thesis rationale and objectives

Cancer and notably melanoma tumours are difficult to treat once metastatic. Tumours can actively escape the immune system[192] through several means implying the induction of an immunosuppressive tumour microenvironment[193]. Immunotherapies such as immune checkpoint blockades with anti-PD-1 and anti-PD-L1 strategies enjoyed remarkable success in clinics[194,195,196,197,198]. This attests to the undoubtedly critical role of $CD8^+$ T cells in anti-tumour responses, as ICB are targeting exhaustion pathways restricting $CD8^+$ T cell biology. However, only a small minority of patients are responding and even fewer harbour complete therapeutic responses to ICB with long-term effects[196,38,197]. There is therefore an important need to decipher how to improve the $CD8^+$ T cell anti-tumour immune response durably.

Efficient effector $CD8^+$ T cells are required for effective anti-tumour response. They need to infiltrate the tumours, recognise the tumour cells, and kill cancer cells through efficient effector functions while sustaining the response for a long period of time. In chronic contexts, $CD8^+$ T cells have been shown to progressively become dysfunctional. The concept of exhaustion only partly explains their dysfunction as ICB does not resolve their dysfunction, especially once the cells have reached the terminally exhausted state. Therefore, other parameters are involved in the $CD8^+$ T cell dysfunction in tumours that remain to decipher.

Anti-tumour response relies on $CD8^+$ T cells and their secretion of IFNγ, an important immune mediator[57,199]. Indeed, IFNγ directly restricts tumour progression *via* several mechanisms: it has cytostatic effects[200], cytotoxic effects[199], inhibits angiogenesis[102],

and can recruit and activate anti-tumour immune cells[199]. However, IFNγ is a very pleiotropic cytokine that also harbour pro-tumour functions[201] with tumour growth promotion[202], the recruitment of immunosuppressive immune cells[46], and the upregulation of immune inhibitory molecule such as PD-L1[203]. Therefore, IFNγ is simultaneously essential for $CD8^+$ T cell anti-tumour response but can also impede the anti-tumour response. It is important to study the different cellular effects of IFNγ as it is very often present in the tumour microenvironment. How the chronic presence of IFNγ can affect the $CD8^+$ T cell effector function and differentiation has not been addressed in tumours yet.

In this study, I aimed to directly assess the IFNγ effects on $CD8^+$ T cells in a melanoma tumour context. To reach that goal, I have created a mouse model where mature $CD8^+$ T cells do not express the binding part of the IFNγ receptor (IFNγR1KO), they are therefore unable to sense the IFNγ present in the tumour microenvironment.

To formally investigate the IFNγ effect on $CD8^+$ T cells in tumours, I pursued the following research approach:

1- Does IFNγ-sensing by $CD8^+$ T cells affect their anti-tumour response?
    - Establishment and validation of the model: specific deletion of IFNγR1 in mature $CD8^+$ T cells in mice subsequently challenged with a murine melanoma B16F10 cell line [**Chapter 3**].
2- Does IFNγ-sensing by $CD8^+$ T cells affect their function and localisation in tumours?

- Formal $CD8^+$ T cell fitness assessment comparing IFNγR1KO $CD8^+$ T cells *versus* control $CD8^+$ T cells in tumours [**Chapter 4**].

3- Does IFNγ-sensing by $CD8^+$ T cells affect a particular $CD8^+$ T cell subset in tumours?

- Single-cell RNA sequencing data guided the investigations toward the stem-like T cells that were particularly sensitive to IFNγ in tumours [**Chapters 5** and **6**]

Altogether, the results presented in this thesis provide evidence that IFNγ directly affects $CD8^+$ T cells, restricting their anti-tumour response independently of exhaustion checkpoint. Indeed, the ablation of IFNγR1 specifically in $CD8^+$ T cells improves tumour control in our murine melanoma model. Intra-tumoral IFNγR1KO $CD8^+$ T cells harbour a greater expansion and enhanced tumour infiltration. Surprisingly, in the general $CD8^+$ T cell population, IFNγ does not affect their fitness and function. IFNγ preferentially affects stem-like T cells by limiting their active maintenance, which reduces their pool size in tumours. As a result, the stem-like T cell clonal diversity is reduced in tumours. Consequently, the fewer stem-like T cells in tumours, the fewer *de novo* $CD8^+$ T cell differentiation occurs over time leading to an overall more exhausted $CD8^+$ T cell population. This provides the first evidence that IFNγ triggers a negative feedback loop to limit $CD8^+$ T cell anti-tumour immunity by restricting stem-like T cell longevity. This offers new insight into stem-like T cell biology which represents a great opportunity to enhance their potential in tumours and potentially improve adoptive T cell transfer therapies.

2. Materials and methods

2.1 Murine models

C57BL/6J wild-type (WT) mice from 6 to 10 weeks old were purchased from Charles River (JAX number – 000664) and housed for 1 to 2 weeks before experiments. CD8a-Cre (The Jackson Laboratory – 008766) were crossed with Rosa-floxSTOPflox-Tomato (The Jackson Laboratory – 007908) and flox-IFNγR1-flox (The Jackson Laboratory – 025394) to generate IFNγR1KO-CD8 mice by specifically depleting IFNγR1 only in mature $CD8^+$ T cells. To generate IFNγR1KO-OTI, $IFN\gamma R1^{-/-}$ mice (The Jackson Laboratory – 003288) were crossed with OTI mice (The Jackson Laboratory – 003831). They were selected to either express the green fluorescent protein (GFP) or congenic markers (CD45.1, CD45.2). Tcf1/7-GFP reporter mice (The Jackson Laboratory – 030909) were also used as recipients for several experiments. Mice were bred and housed under specific pathogen-free (SPF) conditions in the in-house Biological Services Unit at the Kennedy Institute of Rheumatology, University of Oxford. All experiments involving mice were conducted in agreement with the United Kingdom Animal Scientific Procedures Act of 1986 and performed in accordance with approved experimental procedures by the Home Office and the Local Ethics Reviews Committee (University of Oxford) under UK project license (PPL and PIL).

2.2 Genotyping

The genotyping of CD8-IFNγR1KO mice was performed using polymerase chain reaction (PCR) on extracted DNA obtained from ear clips.

- DNA extraction: Once the mice were weaned, ear clips were harvested and lysed using 75μL of lysis buffer (made of 50mM NaOH and 0.5M EDTA (Ethylenediaminetetraacetic acid – Santa Cruz – sc-286969) in ddH_20) for 30 minutes at 95°C. Lysed samples were then placed on ice before adding 75μL of neutralising buffer (made of Tris-HCl in ddH_2O) to stop the reaction.
- PCR: the PCR was performed for each transgene for every mouse following the JAX protocol explained hereafter.

Volume for 1 sample (μL)	**CD8-Cre**	**IFNγR1$^{flox/flox}$**	**tdTomato**	**IFNγR1$^{-/-}$**
2X MyTaq Red mix (meridian Bioscience – BIO-25044)	10	10	10	10
1uL of each primer (100μM)	1 (x4 primers)	1 (x2 primers)	1 (x4 primers)	1 (x4 primers)
RNAse/DNAse free water	2	4	2	2
Extracted DNA sample	4	4	4	4
Total volume (μL)	20	20	20	20

Table 1: Reaction mix used for genotyping mice by PCR.

Transgenes	Primer sequences (5' → 3')
CD8-Cre	CAA TGG AAG GAA GTC GTG GT
	TGG GAT TTA CAG GGC ATA CTG
	CAC ACA TGC AAG TCT AAA TCA GG
IFNγR1$^{flox/flox}$	TTG TTT GAT CCA TTC TTT AAA TTG
	GCT TCT TTG AAG GGC TGG A
tdTomato	AAG GGA GCT GCA GTG GAG TA
	CCG AAA ATC TGT GGG AAG TC
	GGC ATT AAA GCA GCG TAT CC
	CTG TTC CTG TAC GGC ATG G
IFNγR1$^{-/-}$	CTC GTG CTT TAC GGT ATC GC
	TCG CTT TCC AGC TGA TGT ACT
	CCA CCT CAG CAC TGT CTT CA

Table 2: Primer sequences used for mice genotyping.

Steps	Cycling conditions
1	94.0°C
2	94.0°C
3	65.0°C
4	68.0°C
5	Repeat steps 2-4 for 10 cycles (Touchdown)
6	94.0°C
7	60.0°C
8	72.0°C
9	Repeat steps 6-8 for 28 cycles
10	72.0°C
11	10.0°C – hold

Table 3: PCR cycling conditions used for genotyping mice.

- Gel separation: PCR products were then put on ice before being separated using a 2% agarose gel prepared with agarose (Invitrogen – 16500-500) dissolved in TAE buffer (made with 40mM Tris-Acetate and 1mM EDTA), and SYBR^{TM} safe DNA gel stain diluted at 1/10 000 (Invitrogen – S33102) was added. DNA Loading dye 6X (Thermo scientific – RD611) was added to every PCR product before

loading the gel and GeneRuler 1kb plus DNA ladder (Thermo scientific – SM1331) was used. The gel was run at 120V until separation.

- Result visualisation: bands were visualised using the G: Box machine (Syngene). The expected results are listed in **Table 4**.

	CD8-Cre	**IFNγR1$^{flox/flox}$**	**tdTomato**	**IFNγR1$^{-/-}$**
Transgene	198 bp	360 bp	196 bp	200 bp
Heterozygote	198 bp and 341 bp	360 bp and 310 bp	196 bp and 297 bp	200 bp and 429 bp
Wild type	341 bp	310 bp	297 bp	429 bp

Table 4: Expected results for genotyping by PCR.

The genotyping of OTI mice was both made by PCR for the IFNγR1$^{-/-}$ transgene (see above) and by blood for the transgenic TCR. When weaned, the mice underwent tail bleeding to harvest blood directly added to 100µL of 0.5M of EDTA. Cells were washed with red blood cells lysis buffer twice (made of 155 mM NH_4Cl, 12 mM $NaHCO_3$, and 0.1 mM EDTA in ddH_2O) to lyse erythrocytes. Cells were then stained for 20 minutes at 4°C using antibodies listed in **Table 5** diluted in FACS buffer (made with 2% FCS (foetal calf serum – Sigma – F9665-500ml), 5mM EDTA, and 0.01% sodium azide in phosphate-buffered saline (PBS) (Gibco – 20012-068)). Cells were washed with FACS buffer and resuspended in 1% paraformaldehyde (PFA – prepared from Paraformaldehyde 16% solution Thermo Fisher Scientific – 43368) solution in PBS to run them on a BD LSR II machine.

Marker	Conjugate	Clone	Dilution	Reference
CD8a	PerCP/Cy5.5	53-6.7	1/400	Biolegend – 100734
TCR Vb5.1,5.2	APC	MR9-4	1/400	Biolegend – 139506
CD45.1	PE/Cy7	A20	1/400	Biolegend – 110730
CD45.2	PE	104	1/400	Biolegend – 109808
Chanel left free	GFP			

Table 5: List of antibodies used for genotyping mice by blood.

2.3 Murine cancer cell lines

The B16F10-mCherry-OVA-Tyr$^{-/-}$ (B16F10-OVA) murine melanoma cell line was kindly provided by Dr. Edward Roberts from the Beatson Institute (Glasgow, UK). This cell line was specifically modified to not express melanin (Tyrosinase$^{-/-}$) but to express mCherry for imaging purposes. In addition, the cell line expresses the Ovalbumin peptide (OVA) which allows us to use antigen-specific CD8^{+} T cells, the OTI. The MC-38 cell line is a murine colon cancer cell line (derived from C57BL6 murine colon adenocarcinoma cells). B16F10-OVA and MC-38 cells were cultured in Dulbecco's Modified Eagle's Medium (Sigma – D6429) supplemented with 10% FCS, 0.5μM of beta-mercaptoethanol (Gibco – 31350-10), and Penicillin/Streptomycin (Gibco – 10378-016) at 37°C in 5% CO2. Cells were split when reaching 90% confluency by using Trypsin (Sigma – T3924) for 5 minutes at 37°C in 5% CO2 to detach the cells.

2.4 Tumour induction and treatment of mice

B16F10-OVA and MC-38 cells used were between passages 3 to 12 and 60 to 70% of confluency for tumour inductions. Between 2.10^5 to 5.10^5 cells were resuspended in PBS with 25% of Matrigel (Corning – 354262) for better engraftment. Host mice are anaesthetised using Isoflurane (IsoFlo^R – Zoetis) and their flank was shaved before subcutaneous injection. Tumours were palpable after 5 to 7 days post-injection. Mice were monitored, tumours were measured using a calliper, and the [(Length*Width*Width)/2] formula was used to obtain the tumour volume in mm^3.

2.5 Tumour processing for imaging

B16F10-OVA tumours were harvested at different time points from day 8 to day 20 post-engraftment and immersed in a freshly made fixative solution (3.75mL of 0.2M L-Lysine (Sigma – L5751-100G), 3.75mL of phosphate buffer, 21mg of sodium m-periodate (Thermo Scientific – 7790-28-5) well mixed before adding 2.5mL of PFA 4% made in water from powder and 20µL of NaOH 12N) overnight under gentle agitation at 4°C protected from light. Tumours were then rinsed twice with phosphate buffer and incubated in 30% sucrose (Sigma – S9378) diluted in phosphate buffer for a minimum of 6 hours at 4°C without agitation but protected from light. Fixed tumours were then embedded in O.C.T compound (CellPath – KMA-0100-00A) and frozen down using pure methanol and dry ice. Frozen tumours were kept at -80°C and sectioned with a cryostat

(Leica – CM1900UV) to obtain 10μm cryosections harvested on slides (SuperFrost Plus – VWR – 631-0108). Cryosections were brought to room temperature and a hydrophobic Pap-Pen (Sigma-Aldrich – Z672548-1EA) was used to circle the sections. Tumour cryosections were washed with PBS to remove the remaining O.C.T and rehydrated in PBS for 10 minutes before being blocked with the blocking solution. Blocking solutions were made freshly depending on the antibody panel used. They were prepared in a wash buffer containing 2% FCS, 0.1% of Triton (X100 Sigma – T9284), and 0.01% sodium azide diluted in PBS. Specific species sera were added according to the species of secondary antibodies or primary antibodies if used directly, in addition to Fc block (anti-CD16/32). Cryosections were blocked for a minimum of 4 hours at room temperature and protected from light. Sections have then incubated either overnight at 4°C or 4 hours at room temperature with primary antibodies mix made freshly in the adequate blocking solution and spun at 13500rpm for 15 minutes at 4°C. Slides were washed 4 times with wash buffer and stained for 4 hours at room temperature with the secondary antibody mix previously made in the adequate blocking solution and spun at 13500rpm for 15 minutes at 4°C. Finally, sections were washed 4 times with wash buffer and incubated in DAPI (4',6-diamidino-2-phenylindole – Sigma – D9542) for 15 minutes at room temperature. After a round of final washes, sections were mounted with Fluoromount G (SouthernBiotech – 0100-01) using cover glass (Menzel-Glaser – VWR – 630-2869). Images were taken on the Zeiss LSM880 confocal microscope and analysed on the Imaris (Bitplane – version 9.6) software.

Products	Species – Conjugate	Clone	Concentration – Dilution	Reference
Anti-mouse CD8a	Rabbit – AF647	EPR21769	1/200	Abcam – ab237365
Anti-CD31	Rat – AF647	MEC13-3	1/200	Biolegend – 102516
Anti-collagen IV	Rabbit	Polyclonal	1/200	Abcam – ab19808
Anti-rabbit	Donkey – AF647	Polyclonal	1/400	Biolegend – 406414
Anti-rabbit	Donkey – FITC	Polyclonal	1/400	Biolegend – 406403
Donkey serum	-	-	10%	Sigma – D9663
Rat serum	-	-	10%	Invitrogen – 10710C
Anti-mouse CD16/32	-	93	1/200	Biolegend – 101302

Table 6: List of antibodies and reagents used for imaging.

2.6 Tumour and lymph node processing for flow cytometry

At the required time point, tumours and draining lymph nodes (LNs) were harvested in complete R10 [RPMI (Gibco – 21870-076) supplemented with 10% FCS, Penicillin/Streptomycin, and 0.5μM of beta-mercaptoethanol]. Tumours were measured and weighed before being processed. LNs were directly smashed through a 70μm cell strainer to obtain a single-cell suspension in PBS. Tumours were dilacerated using scalpels to obtain small tumours pieces in complete R10. Tumour pieces were then spun at 900rpm for 5 minutes and resuspended in an enzymatic digestion mix prepared in R5 (as R10 but with only 5% of FCS) containing Liberase TL at 1mg/mL (Roche – 5401020001) and DNase I at 10μg/mL (Roche – 4716728001). After 30 minutes incubated at 37°C in 5% CO2, tumour pieces were smashed through a 70μm cell strainer to obtain a single cell suspension. Cells were either undergoing Ficoll (Ficoll-paque Premium, Cytiva) to obtain live immune cells or directly used for further experiments.

Total LNs cell suspension and between 2 to 3.10^6 tumour cell suspension were plated in a 96-well plate V-shape for further staining for flow cytometry.

2.7 Tumour processing for soluble analysis (ELISA – Legendplex)

As indicated above, tumours were dilacerated in R10 media. Tumour pieces were spun at 900rpm for 5 minutes and supernatants "1" were saved. After the enzymatic digestion step, samples were spun again and supernatants "2" were saved. To obtain samples recapitulating the soluble tumour microenvironment, supernatant "1" and supernatant "2" were merged and filtered through a 0.45μm filter to obtain a cell-free sample that can be frozen and kept at -20°C. To assess the supernatant composition, samples were run neat (no further dilution) with an enzyme-linked immunosorbent assay (ELISA) against IFNγ (Invitrogen – 88-7314-88) and a Legendplex inflammation kit detecting 13 cytokines and chemokines (Biolegend – 740446).

2.8 Adoptive T cell transfer

General – OTI T cell isolation

Lymph nodes were harvested from 6 to 12 weeks old OTI WT and OTI IFNγR1KO naïve mice. $CD8^+$ T cells were separated through negative selection using the MojoSort™ $CD8^+$

T cell isolation kit (Biolegend – 480035). Collected organs were smashed onto a 70μm cell strainer to obtain a single-cell suspension in an isolation buffer (made of 1X PBS (Gibco – 20012-068) supplemented with 2% FCS (Sigma – F9665-500ML) and 10mM EDTA (Santa Cruz – sc-286969)). Cells were counted and resuspended at 10^8 cells/mL before being incubated with the biotin-antibody cocktail at a 10-fold dilution (with 10μL for 100μL of cells) for 15 minutes on ice. Then magnetic nanobeads were added at a 10-fold dilution and cells were incubated for another 15 minutes on ice. Following incubation, 2mL of isolation buffer was added and the cell suspension was transferred to a 5mL sterile collection tube. The latter was placed into the MojoSort™ magnets (Biolegend – 480019) for 5 minutes at room temperature. The supernatant containing negatively selected $CD8^+$ T cells was then collected and resuspended in 1X PBS. When indicated, cells were labelled with 5μM CellTrace Violet (Invitrogen – C34571A) for 15 minutes at 37°C. Mice were adoptively transferred with $2x10^6$ OTI in sterile PBS by intravenous injections between 5 and 7 days after B16F10-OVA cell engraftment when the tumour was palpable depending on the experiment.

Adoptive T cell transfer – Tracing experiment

For cell tracing experiments, isolated OTI cells both WT and IFNγR1KO were *in vitro* treated to induce stem-like T cells or exhausted T cells. To obtain stem-like T cells, 2.10^6 OTI/mL were incubated for 24 hours at 37°C with 5% CO2 in complete R10 [RPMI 1640 media containing 10% FCS, 0.5μM beta-mercaptoethanol, and Penicillin/Streptomycin] supplemented with 10IU/ml of IL-2, 100ng/mL of N4 peptide (N4 = OVA peptide SIINFEKL of amino acids 257-264) and 7μM of TWS119 (Merck – SML1271). This method is based on Gattinoni *et al.*'s paper[204]. To obtain *in vitro* induced exhausted T cells, 500 000

OTI/mL were plated in R10 containing 1% hepes buffer (Gibco – 15630-049), 5ng/mL IL-15 (Peprotech – 210-15-10UG), 5ng/mL IL-7 (Peprotech – 217-17-10UG), and 10ng/mL of N4 peptide. Cells were incubated at 37°C with 5% CO2 and 10ng/mL of N4 peptide was added daily for 5 days. This method is based on Zhao *et al.*'s paper[205]. Cells were split with fresh media when confluent and underwent ficoll (Ficoll-paque Premium, Cytiva) prior *in vivo* injection. Mice were adoptively transferred with $2x10^6$ OTI mix WT and IFNγR1KO at a 1:1 ratio resuspended in sterile PBS by intravenous injections 6 days after B16F10-OVA cell engraftment.

Adoptive T cell transfer – Homing experiment

To obtain effector $CD8^+$ T cells, tissue-culture plates were coated using 5μg/mL solution of anti-CD3 (Biolegend – 100302) for 2 hours at 37°C. Wells were washed with PBS before plating the cells. Naïve WT and naïve IFNγR1KO OTI were resuspended in R10 supplemented with 2μg/mL of anti-CD28 (Biolegend – 102102) and plated separately on the previously coated plates. Cells were incubated at 37°C with 5% CO2 for 7 days. After 2 days of culture, 5IU/mL of IL-2 was added with fresh media. After 7 days, activated cells were labelled with CellTrace Violet (Invitrogen – C34557) before mixing the WT and the IFNγR1KO OTI cells at a 1:1 ratio in PBS. A total of 30.10^6 cells (15.10^6 of each cell type) were injected intravenously into tumour-bearing mice, 10 days after B16F10-OVA tumour engraftment. The endpoint was 24 hours later with organs harvesting prior to being processed for flow cytometry.

Adoptive T cell transfer – *in vivo* cytotoxic assay

WT and IFNγR1KO OTI isolated cells were separately transferred into tumour-bearing mice between 5 and 7 days after B16F10-OVA cell engraftment when tumours were

palpable. 7 days after the OTI transfer, mice were injected with a 1:1 ratio of OVA-targetable and non-targetable cells (Mock). To do so, splenocytes from naïve WT mice were isolated and split into two equal pools. Targetable cells were loaded with N4-SIINFEKL peptide (1μg/mL) and further labelled with a high concentration of Carboxyfluorescein succinimidyl ester (CFSE – 2μM – Invitrogen – C34554). Non-targetable cells were not loaded but labelled with a low concentration of CFSE (0.2μM). Peptide loading was performed in R10 at 37°C for 1 hour. Cell labelling was done in PBS for 15 minutes at 37°C. After cell preparation, cells were washed with PBS and pooled together, ready for intravenous injections. After 24 hours spleens were harvested and processed for flow cytometry analysis. The percentage of target cell lysis was analysed which represents the cytotoxicity using the formula: [1-(Rcontrol – Rimmune)]*100, where R is given by the expression of $\%CFSE^{low}/\%CFSE^{hi}$ cells. Control mice harboured tumours but no OTI were transferred.

2.9 *In vitro* T cell stimulation

OTI activation using BMDCs – CD69 experiment

Naïve WT and IFNγR1KO OTI were isolated and stimulated *in vitro* by co-culturing them with bone marrow-derived dendritic cells (BMDCs) loaded with cognate peptides at 10ng/mL of N4, T4, or V4 with different activation strength[206]. Peptides were kindly provided by Dietmar Zehn from (TU Munich). Cells were incubated overnight at 37°C in

5% CO2. After 24 hours cells were harvested and processed for flow cytometry. OTI activation was quantified by CD69 expression.

WNT (Wingless-related integration site) pathway analysis *in vitro*

Naïve OTI $CD8^+$ T cells were isolated as previously described. Depending on the experiment, naïve cells were pre-treated with 100ng/mL of recombinant IFNγ (Biolegend – 575306) or not for 16 hours at 37°C, before being incubated at 37°C for 6 hours in R10 only or R10 supplemented with 3.5μM of TWS119 or 400ng/mL of WNT3a (Peprotech – 315-20). During this incubation, some cells were plated on anti-CD3 coated wells and supplemented with 2μg/ml of anti-CD28 for TCR activation with or without recombinant IFNγ. Cells were then harvested and stained for flow cytometry.

2.10 *Ex vivo* T cell assays

Re-stimulation – cytokine production experiment

For endogenous tumour-infiltrating $CD8^+$ T cells, tumours from control and CD8-IFNγR1KO mice were harvested 10 to 12 days after B16F10-OVA tumour engraftment. For OTI cells, tumours from OTI-bearing mice were harvested 5 to 7 days after the OTI transfer. Tumours were processed as above. Single-cell suspensions were ficolled and plated in 96-well V-bottom plates. Cells were incubated for 6 hours at 37°C in the presence or absence of the OVA N4 peptide (at 1μg/mL). Brefeldin A (BFA, 10μg/mL, Santa Cruz – SC-200861) was added after 30 minutes of re-stimulation. After 6 hours cells were harvested and processed for flow cytometry. In one set of experiments, cells

were stained for intracellular cytokines, and in another set of experiments, cells were stained with surface lysosomal-associated membrane protein 1 (LAMP1) to assess degranulation.

Ex vivo T cell self-renewal assessment – Proliferation assay

Tumour-infiltrating immune cells were isolated from B16F10-OVA tumour-bearing WT mice at day 12 post-engraftment and enriched using ficoll. Cells were labelled with 2μM of CFSE. Between 2.10^5 to 2.10^6 cells were resuspended in R10 supplemented with 2μg/mL of anti-CD28 (Biolegend – 37.51) and with or without blocking IFNγ antibody (BioXcell XMG1.2 at 10μg/mL) or recombinant mouse IFNγ (at 100ng/mL). Cells were then plated at a similar density in 96-well flat-bottom or 12-well plates previously coated with 2μg/mL of anti-CD3 (Biolegend – 145-2C11) in PBS for 2 hours at 37°C. Cells were incubated at 37°C and were fed every 2 days with fresh media according to the different conditions. At the desired time points cells were harvested and processed for flow cytometry.

2.11 Flow cytometry

Single-cell suspensions from tumours, LNs, or *in vitro* cell cultures were plated accordingly in 96-well V-bottom plates for a total volume of 100μL. For consistency, 2 to 3.10^6 cells were plated for staining depending on experiments. When necessary 50 000 counting beads (polybead polystyrene black dyed microspheres – Polyscience – 24293) were added in every well for further cell counting by flow cytometry. Cells were washed

with PBS and incubated with the live-dead staining (Zombie-NIR (Biolegend – 423105), Fixable Viability Dye eFluor® 780 (Invitrogen – 65-0865-14), or Live/dead-Aqua (ThermoScientific – L34966)) at 1/1500 with Fc-block at 1/200 (Biolegend – 101302) for 30 minutes at 4°C. Cells were then washed before being incubated with fluorochrome-conjugated antibodies against extracellular markers (see **Table 7**) prepared in FACS buffer (2% FCS, 2mM EDTA, and 0.01% sodium azide in PBS) for 30 minutes at 4°C. If not otherwise stipulated, cells were fixed either in 4% paraformaldehyde made in PBS for 15 minutes at room temperature or using the Cytofix/Cytoperm kit (BD Biosciences – 554714) for 30 minutes at 4°C. For metabolic experiments, single-cell suspensions from tumours were incubated in complete R10 at 37°C with either 30nM of NAO (Nonyl Acridine Orange – Invitrogen – A1372) for 10 minutes or with 100nM of MitoTrackers (Deep Red – Invitrogen – M22426, and Green – Invitrogen – M7514) for 30 minutes before the extracellular staining. Note, cells were stained for extracellular markers as explained above, and then kept alive (not fixed) before running them by flow cytometry. For intracellular staining, cells were permeabilized after fixation, using either pure cold methanol (Fisher Chemicals) for 10 minutes at 4°C (especially for Tcf1/7, cleaved-caspase 3, and beta-catenin stain), or the Cytofix/Cytoperm kit (especially for intracellular cytokines detection). Cells were then washed with either FACS buffer or perm buffer from the kit. Intracellular staining steps were then different depending on the experiment using fluorochrome-conjugated antibodies listed in **Table 7**. For metabolic markers, cells were incubated for 20 minutes at room temperature with antibodies prepared in Cytoperm buffer. For tcf1/7, cleaved-caspase 3, and beta-catenin stain, cells were incubated for 1 hour at room temperature with antibodies prepared in

FACS buffer. And finally, for intracellular cytokine detection, cells were incubated for 45 minutes at room temperature with appropriate antibodies prepared in Cytoperm buffer. Flow cytometer voltages were calibrated using stained and unstained cells in addition to compensation beads. Bead compensation controls were prepared using UltraComp eBeads (Invitrogen – 01-2222-42) for antibodies and ArC reactive beads (Invitrogen – A10346) for live dead dyes. Flow cytometry data was recorded on BD-LSR-II or BD-LSR Fortessa X-20 using the DIVA software. Data analysis was performed using FlowJo™ software (v.10 – FlowJo LLC).

Marker	Conjugate	Clone	Dilution	Type	Reference
CD8a	PerCP/Cy5.5	53-6.7	1/200	Extracellular	Biolegend – 100734
CD8a	BV711	53-6.7	1/200	Extracellular	Biolegend – 100747
CD8a	BV605	53-6.7	1/200	Extracellular	Biolegend – 100744
CD45	BV785	30-F11	1/200	Extracellular	Biolegend – 103149
CD45	BV650	30-F11	1/200	Extracellular	Biolegend – 103151
CD44	A700	IM7	1/200	Extracellular	Biolegend – 103025
CD44	A647	IM7	1/200	Extracellular	Biolegend – 103017
CD44	BV785	IM7	1/200	Extracellular	Biolegend – 103041
CD69	PE	H1.2F3	1/200	Extracellular	Biolegend – 104507
F4/80	APC	BM8	1/200	Extracellular	Biolegend – 123115
CD3	PE/Cy7	1782	1/200	Extracellular	Biolegend – 100220
CD3	PerCP/Cy5.5	1782	1/200	Extracellular	Biolegend – 100218
NK1.1	BV605	PK136	1/200	Extracellular	Biolegend – 108739
CD19	A488	6D5	1/200	Extracellular	Biolegend – 115524
CD19	PerCP/Cy5.5	6D5	1/200	Extracellular	Biolegend – 152406
CD4	BV421	RM4-5	1/200	Extracellular	Biolegend – 100543
CD11b	BV421	M1/70	1/200	Extracellular	Biolegend – 101235
CD11c	BV605	N418	1/200	Extracellular	Biolegend – 117333
Ly6C	PE/Cy7	HK1.4	1/200	Extracellular	Biolegend – 128018
Ly6G	FITC	1A8	1/200	Extracellular	Biolegend – 127606
MHC-II	A700	M5/114.15.2	1/200	Extracellular	Biolegend – 107622
CD45.1	BV421	A20	1/200	Extracellular	Biolegend – 110731

CD45.2	FITC	104	1/200	Extracellular	Biolegend – 109805
LAMP1 (CD107a)	A700	1D4B	1/200	Extracellular	Biolegend – 121627
PD-1 (CD279)	BV421	29F.1A12	1/200	Extracellular	Biolegend – 135217
PD-1 (CD279)	APC	29F.1A12	1/200	Extracellular	Biolegend – 135209
PD-1 (CD279)	FITC	29F.1A12	1/200	Extracellular	Biolegend – 135213
PD-1 (CD279)	BV605	29F.1A12	1/200	Extracellular	Biolegend – 135219
LAG-3 (CD223)	PE/Cy7	C9B7W	1/200	Extracellular	Biolegend – 125225
LAG-3 (CD223)	BV785	C9B7W	1/200	Extracellular	Biolegend – 125219
TIM-3	APC	RMT3-23	1/200	Extracellular	Biolegend – 119705
TIGIT	BV421	1G9	1/200	Extracellular	Biolegend – 142111
CD31	PE/Cy7	390	1/200	Extracellular	eBioscience – 250311
CD105	PB	MJ7/18	1/200	Extracellular	Biolegend – 120412
IFNγ	BV421	XMG1.2	1/100	Intracellular	Biolegend – 505829
TNFα	APC	MP6-XT22	1/100	Intracellular	Biolegend – 506307
GLUT-1	A405	EPR3915	1/100	Intracellular	Abcam – ab210438
GLUT-1	A647	polyclonal	1/100	Intracellular	Novus Biol – NB110-3911
ATPb	A488	3D5	1/100	Intracellular	Abcam – 14730
GADPH	A647	14C10	1/100	Intracellular	Cell Signalling – 3907S
LDHA	NIR	E9	1/50	Intracellular	SCBT – sc-137243
Cleaved-caspase 3	A647	C92-605	1/100	Intracellular	BD Bioscience – 560626
Tcf1/7	A488	C63D9	1/100	Intracellular	Cell Signalling – 6444S
Tcf1/7	A647	C63D9	1/100	Intracellular	Cell Signalling – 6709S
Beta-catenin	E660	15B8	1/100	Intracellular	Invitrogen – 50-2567-42
Granzyme B	PE/Cy7	QA16A02	1/200	Intracellular	Biolegend - 372214
Perforin	APC	eBioOMAK-D	1/200	Intracellular	eBioscience – 17-9392-80
Chanel left free for (depending on experiment)	mCherry, GFP, CTV (Pacific Blue)				

Table 7: List of antibodies used for flow cytometry.

2.12 FACS sorting for *ex vivo* T cell proliferation assay

To specifically assess the proliferation potential of stem-like T cells and exhausted T cells separately, we used Tcf1-GFP reporter mice to sort the wanted cell types. B16F10-OVA tumours were induced in Tcf1-GFP reporter mice and tumours were harvested on day 12 and processed as described above. Tumour-infiltrated $CD8^+$ T cells were enriched using a CD45 (TIL) Microbeads enrichment kit (Miltenyi Biotech – 130-110-618) and stained prior to cell sorting. Stem-like T cells were sorted from live $CD8^+PD\text{-}1^+$ T cells using ($Tcf1/7^+$) GFP^+ and $LAG\text{-}3^-$ strategy, while exhausted T cells were sorted from $CD8^+PD\text{-}1^+$ T cells using the ($Tcf1/7^-$) GFP^- and $LAG\text{-}3^+$ strategy. Cells were kept separated and labelled with 5μM of CellTrace Violet dye for 15 minutes at 37°C. Stem-like T cells and exhausted T cells were resuspended separately in R10 supplemented with 2μg/ml soluble anti-CD28 with or without blocking IFNγ antibody at 10μg/mL and plated in a 96-well U-bottom plate previously coated with 2μg/ml of anti-CD3. Cells were processed for flow cytometry after 4 days of culture to assess their proliferation rate.

2.13 Single-cell RNA sequencing

<u>Cell sorting for single-cell sequencing and library preparation</u>

All cells from B16F10-OVA tumours grown in 3 controls and 3 CD8-IFNγR1KO mice were stained with extracellular markers for flow cytometry as described above, stopping

before the fixation step. Cells were then sorted based on CD45, CD3, CD8, and Tomato expression using a FACSAria™ II (BD). Approximately 20,000 cells per sample were loaded onto the 10X Genomics Chromium Controller (Chip K). Gene expression, feature barcoding, and TCR sequencing libraries were prepared using the 10x Genomics Single Cell 5' Reagent Kits v2 (Dual Index) following the manufacturer user guide (CG000330 Rev B). The final libraries were diluted to ~10nM for storage. The 10nM library was denatured and further diluted prior to loading on the NovaSeq6000 sequencing platform (Illumina, v1.5 chemistry, 28bp/98bp paired-end for gene expression and feature barcoding, 150bp paired-end for TCR libraries).

Mouse scRNA-sequencing (scRNA-seq) and analysis

Sequence reads were mapped using CellRanger multi (version 6.0.0) with the 10x mouse reference transcriptome (version 2020-A). Datasets were analysed using Seurat version 4.0.5[207]. Samples were merged on a single Seurat object. We filtered out cells having less than 200 and more than 6,000 detected genes, cells in which mitochondrial protein-coding genes represented more than 3% of UMI (unique molecular identifier) and that had more than 20% of large gene content. Cells were then further filtered based on the expression of Cd2, Cd8a, and Cd8b1. Samples were normalized with the standard workflow (NormalizeData, FindVariableFeature, ScaleData), and variations associated with mitochondrial and ribosomal UMI percentage and cell cycle were regressed out. Principal components were calculated using the top 3,000 variable features. These genes were used as input for principal component analysis (PCA), and significant PCs (n=15) were identified using Seurat (“JackStraw” test and “Elbowplot”). Samples were then integrated with Harmony[208]. Clustering was performed with the Louvain algorithm

(n=15 PCs, resolution=0.4). Significant differentially expressed genes between clusters were identified using the "FindAllMarkers" function, Wilcoxon test, and selecting markers expressed in at least 25% of cells. This step revealed macrophage contamination in one cluster, which was filtered out and data was re-processed. The UMAP projection was computed using significant PCs ("RunUMAP" function, Seurat). Significant differentially expressed genes between genotypes within clusters were identified using the "FindMarkers" function, Wilcoxon test, and selecting markers expressed in at least 25% of cells. Pathway analysis was performed with Fast gene set enrichment analysis (fgsea), using the Gene Ontology or the Reactome pathway repositories. Gene signatures were computed manually and analysed using the packages Vision[209] and UCell which calculate module enrichment scores using Mann-Whitney U statistic[210]. Cell cycle score was calculated using the Seurat function "CellCycleScoring". A Cell Cycle score was assigned for each cell based on the expression of G2/M and S phase markers. Cells expressing neither were labelled as in G1 phase. Single-cell trajectory analysis was inferred using the Monocle 3 software[211].

Mouse TCR sequencing analysis

Paired chain TCR sequences were obtained through targeted amplification of full-length V(D)J segments during library preparation. Sequence assembly and clonotype calling was done through cellranger's immune profiling pipeline (cellranger multi). TCR profiling on filtered contig annotations was done using R package scRepertoire version 1.1.4[212]. Only cells for which both TCRa and TCRb could be identified were used. Clone calling was done for each sample set independently before integration in the Seurat object.

2.14 Statistical analysis

Statistical analysis is mentioned in figure legends throughout the thesis. Comparisons between 2 conditions or 2 groups were analysed with unpaired or paired t-tests when required. Comparisons between more than 2 groups were analysed with one-way or two-way ANOVA or with its non-parametric equivalent the mixed effect when values were missing. Survival data has been analysed with the Wilcoxon test. Tumour growth curves over time were analysed with two-way ANOVA. Statistics were done using GraphPad Prism 9 software unless specified. Data are presented as mean ± standard error of the mean (SEM). Analysis of the difference between the proportion of cells in clusters between two scRNA-seq samples was analysed with the R package "scProportionTest", which uses a permutation test to calculate the p-value for each cluster/cell state, and a confidence interval for the magnitude difference. Data were considered statistically significant when $P < 0.05$. ns = non-significant, * = $P < 0.05$, ** = $P < 0.001$, *** = $P < 0.0002$ and **** = $P < 0.0001$.

3. IFNγ restricts CD8$^+$ T cell immune response toward murine melanoma cell line

The role of interferon-gamma secreted by CD8$^+$ T cells during the effector phase is well-described[213,214], especially during infections. Besides, most of the studies trying to decipher the regulatory role of IFNγ in tumours focused on stromal and cancer cells[215]. Therefore, little is known about the direct effect of IFNγ on the mature CD8$^+$ T cells themselves. This chapter will focus on what is known about the relationship between IFNγ and CD8$^+$ T cells, before describing the development and validation of a new mouse model allowing me to properly study the effect of IFNγ on mature CD8$^+$ T cells *in vivo* in the context of melanoma.

3.1 IFNγ: a key player for CD8$^+$ T cell function

IFNγ is the major effector of immunity in both innate and adaptive immune responses. As introduced in **Chapter 1.2**, IFNγ was first reported in 1965 by Wheelock *et al.*[49] for its anti-viral activity, however, evidence rapidly showed pleiotropic functions of this immune regulator[50,51,52,53]. Predominantly secreted during immune responses by activated immune cells, IFNγ is known as the effector cytokine for cytotoxic cells including NK cells and CTLs. IFNγ has important functions spearheading local and systemic effects, which are essential to overcome immune threats. The following section

will focus on the relationship between IFNγ and the CD8⁺ T cells, one of the main producing cells, especially in tumours[92].

3.1.1 IFNγ: a regulator for CD8⁺ T cell function

CD8⁺ T cells or cytotoxic T lymphocytes are critical during immune responses to either clear infected cells or kill cancer cells, in part by secreting cytokines including IFNγ[213,214] (see **Chapter 1.3** for more details). Its secretion contributes to the cytotoxic function of CD8⁺ T cells both directly, with cytostatic, anti-proliferative, and pro-apoptotic effects, and indirectly by, for instance, upregulating the MHC-I expression on target cells[216]. Additionally, CD8⁺ T cells have been shown to communicate with each other through cytokines to calibrate and regulate the response at the population level [described in this review[217]]. IFNγ has been shown to be involved during the early phase of CD8⁺ T cell activation and differentiation leading to controversial findings. In some studies, IFNγ signalling in CD8⁺ T cells was reported as promoting the expansion of activated CD8⁺ T cells[218,219], while others showed the opposite effect with IFNγ being a limiting factor of T cell expansion[220]. Similar discrepancies were also found regarding the role of IFNγ in the formation of CD8⁺ T cell memory[221,222,17,18,19,226,227]. IFNγ has also been reported to play a role in the regulation of CD8⁺ T cell clonality and immunodominance in the context of *Listeria monocytogenes* infection[220,228,229]. As a pro-inflammatory cytokine, IFNγ was shown to exert various functions on cells. Interestingly, several studies point out that IFNγ produced by the CD8⁺ T cells themselves can act in an autocrine manner to modulate their own activity, such as their motility and cytotoxicity[230,92]. In that situation, a key parameter to take into account are the kinetics of IFNγ secretion, notably by the

$CD8^+$ T cells themselves. $CD8^+$ T cells are secreting a high quantity of IFNγ during the effector phase toward target cells, but also very early on within a 24-hour time window following activation when cells are clustering through homotypic T cell-T cell synapses, which influences their differentiation and therefore the T cell response[107]. This early source of IFNγ was also reported after bacterial lipopolysaccharides (LPS) immunisation in mice, secreted by memory-like $CD8^+$ T cells in the spleen and lymph node[231]. Overall, IFNγ has very pleiotropic functions, even when looking at one particular cell type. Depending on the context, including the experimental model, the kinetics, the quantity, and other environmental parameters, IFNγ may trigger opposite effects on cells[215]. IFNγ is critical for $CD8^+$ T cell effector functions. But how mature $CD8^+$ T cells are affected by the chronic presence of IFNγ in the tumour microenvironment has not been investigated so far.

3.1.2 IFNγR expression landscape in $CD8^+$ T cells

The IFNγR is composed of 2 subunits, IFNγR1 and IFNγR2, which are differently regulated. IFNγR1 is the high-affinity binding part of the receptor while IFNγR2 is subsequently recruited and critical for downstream signalling through JAK/STAT pathways (**Figure 11A** and **Chapter 1.2**). As mentioned previously IFNγR1 is usually constitutively expressed and in excess, whilst IFNγR2 is limiting and more tightly regulated, thus helping to dictate the cellular effect of IFNγ[232,233,50,234]. To investigate the IFNγ effect on $CD8^+$ T cells, I first assessed the IFNγR expression pattern both in mice and humans. I used a publicly available murine dataset (ImmGen – Gene Skyline; Antigen-specific $CD8^+$ T cells were isolated from naïve and *Listeria monocytogenes* infected

mice), to quantify the level of transcriptional expression of both IFNγR chains in naïve and effector $CD8^+$ T cells. This analysis revealed that naïve $CD8^+$ T cells express higher levels of IFNγR1 compared to IFNγR2. Upon activation and differentiation into effector $CD8^+$ T cells, IFNγR1 is significantly upregulated while IFNγR2 is drastically downregulated but not abrogated (**Figure 11B**). Levels of expression in effector cells were then stabilised over time. Interestingly, it seems that the IFNγR1 upregulation correlates with the IFNγ expression while IFNγR2 follows the opposite pattern (**Figure 11B**). This suggests that during the effector phase, $CD8^+$ T cells are protecting themselves by downregulating the signalling part of the receptor (IFNγR2) to limit IFNγ signalling. Following this analysis, we assessed IFNγR expression in human $CD8^+$ T cells. To do so, we collaborated with Benjamin Fairfax to reanalyse their dataset on circulating $CD8^+$ T cells from metastatic melanoma patients published in 2021[235]. Similarly, as in mice, effector $CD8^+$ T cells express higher levels of IFNγR1 and lower amounts of IFNγR2 compared to naïve $CD8^+$ T cells (**Figure 11C**). Altogether, the differential expression landscape of IFNγR1 and IFNγR2 in naïve *versus* effector $CD8^+$ T cells suggests that IFNγ may trigger a negative feedback loop on its own producers, both in mice and humans.

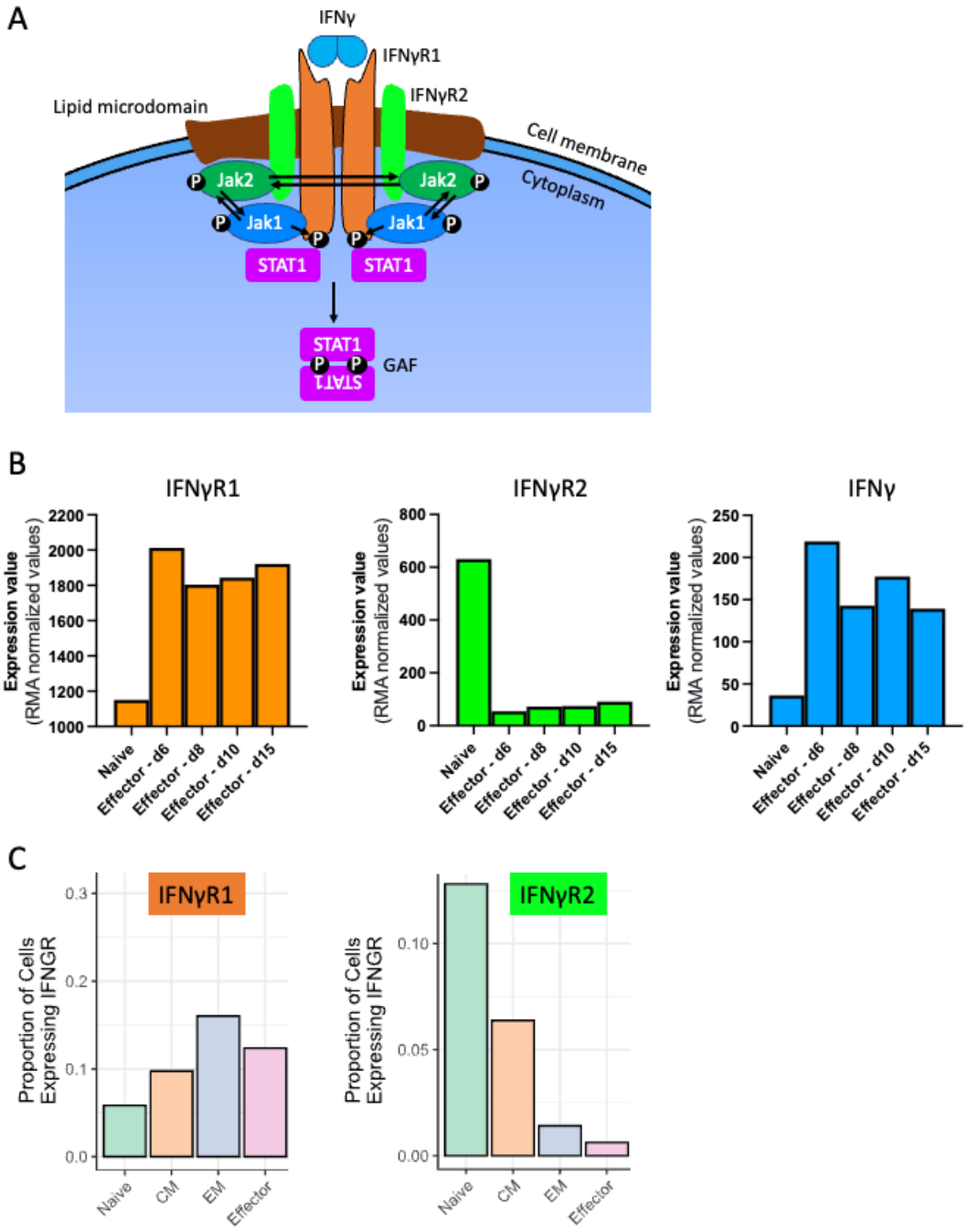


Figure 11: IFNγR expression landscape in CD8⁺ T cells both in mice and humans at the transcriptional level. A- Representation of the IFNγR structure. **B-** IFNγR1, IFNγR2, and IFNγ transcriptional expression values were extracted from the ImmGen Microarrays publicly available database. CD8⁺ T cells from 6-week-old OTI mice were sorted before or 6 to 15 days after *Listeria monocytogenes* infection for microarray sequencing by Adam Best (from Goldrath Lab – University of California, San Diego). Data are from 3 samples. Expression values were normalized by Robust Microarray Averaging (RMA). **C-** IFNγR1 and IFNγR2 transcriptional expression from circulating CD8⁺ T cells obtained from metastatic melanoma patients (Human data from Benjamin Fairfax – University of Oxford[236]).

Full IFNγR1 knock-out (IFNγR1KO) mice have been used in the past to study IFNγ biology in physiological systems[237,238]. Mice were developing normally, but they harboured profound defects in their immune responses upon challenges, especially against intracellular pathogens. $CD8^+$ T cells from those mice were capable of cytotoxic functions *in vitro*[239], and, notably, they were less prone to become exhausted in a chronic infection model[240]. Other studies showed that $CD8^+$ T cell function appears unaffected in many contexts such as in auto-immune[241,242,243,244,245], infectious[246,247,248,239], and graft-rejection models[249,250]. Few studies looked at the effect of IFNγR2 disruption in mice to assess its biological functions for IFNγ signalling[251]. Inhibiting IFNγ signalling in $CD8^+$ T cells prevents the upregulation of MHC-I after exogenous IFNγ treatment but did not alter their function. Overexpression of IFNγR2 in $CD8^+$ T cells to increase their responsiveness to IFNγ showed no effect on their development, activation, or proliferation but limited their cytotoxic activity by an unknown mechanism unrelated to IFNγ secretion[239,252]. Of note, those studies were done at the organism level and over long time periods. More precise studies would be beneficial to properly assess the IFNγ signalling effect on particular cell types or particular cell differentiation stages. Overall, both chains of IFNγR are differentially regulated and exert different functions in cells. However, their conserved expression pattern in $CD8^+$ T cells between mice and humans suggests an important regulatory role.

3.1.3 IFNγ response in $CD8^+$ T cells

The dynamic IFNγR expression pattern and changes upon differentiation of $CD8^+$ T cells suggest that $CD8^+$ T cell subsets will be differentially affected/regulated by IFNγ.

Given the pleiotropism of IFNγ and its context-dependent secretion by $CD8^+$ T cells[253], I hypothesised that the IFNγ effect will depend on the experimental design. This has led to disparate findings in the past, showing the importance of the model of study.

In infection models, for instance, previous studies obtained opposite results while investigating the effect of IFNγ on $CD8^+$ T cell expansion and memory formation. Some studies stipulated that IFNγ is needed and critical for $CD8^+$ T cell expansion, regulation of the $CD8^+$ T cell population size, and its memory formation[218,254,255], while others demonstrated that IFNγ was not necessary for $CD8^+$ T cell regulation[221,225]. The latter was also shown in a vaccine-like immunisation model[19].

In cancer models, several studies demonstrated that $CD8^+$ T cells respond to IFNγ. IFNγ signalling in $CD8^+$ T cells triggered the up-regulation of IL-2R, granzyme, and the transcription factor T-bet, important factors for $CD8^+$ T cell maturation in effector T cells[215]. But it is important to note that the majority of those studies were performed using monoclonal $CD8^+$ T cell population with transgenic mice, therefore leaving the direct function of IFNγ on endogenous populations unexplored. In more recent studies using RNA-sequencing strategies in cancer, IFNγ responsive genes in addition to T-inflamed gene expression profile were presented as predictive of immunotherapy clinical benefit for advanced melanoma and non-small cell lung cancer patients (undergoing anti-PD-1 treatment)[256]. Analysing the tumour microenvironment by bulk-RNA-sequencing further showed the relevance of studying IFNγ responsive gene expression as a predictive parameter for enhancing immune responses through immunotherapies[257,258,259]. However, to assess the effect of IFNγ on $CD8^+$ T cells, single-cell RNA-sequencing or bulk RNA-sequencing focusing on $CD8^+$ T cells is required. Several

studies did so, but they did not study CD8$^+$ T cell biology in depth. Gene ontology enrichment analysis in CD8$^+$ T cells isolated from patients with oral squamous cell carcinoma showed an IFNγ signature in several tumour-infiltrating CD8$^+$ T cell clusters[260]. Analysis of tumour microenvironments at the transcriptional level revealed that melanoma patients with high expression of IFNγ related genes in CD8$^+$ T cells have a better prognosis and survival[261]. This further demonstrates that CD8$^+$ T cells do respond to IFNγ, although this analysis was not solely performed on CD8$^+$ T cells. Finally, scRNA-seq on circulating CD8$^+$ T cells from metastatic melanoma patients revealed that IFNγ-responsive genes were upregulated after immune checkpoint blockade treatment[236]. Altogether, this underlines that mature CD8$^+$ T cells are sensitive to IFNγ and do respond to it in tumours. However, the outcome of IFNγ signalling on CD8$^+$ T cell responses within the dynamic tumour microenvironment remains to be deciphered in more detail.

3.2 Characterisation of the murine model – IFNγR1KO CD8$^+$ T cell mice

In order to investigate the specific effect of IFNγ on CD8$^+$ T cells, I created two mouse models where IFNγR1 is specifically depleted in mature CD8$^+$ T cells, either at the endogenous level or in transgenic OVA-specific CD8$^+$ T cells (OTI mice). IFNγR1KO CD8$^+$ T cells do not express the binding part of the IFNγR and are therefore insensitive to IFNγ. In this section, I will describe the validation of the murine models.

3.2.1 A murine model for IFNγR1 targeted deletion in mature CD8$^+$ T cells at the endogenous level

To specifically deplete IFNγR1 in CD8$^+$ T cells while avoiding off-target depletion in other cell types, we used a Cre recombinase system reported by Maekawa *et al.*, which is only expressed in mature CD8$^+$ T cells[262]. The *CD8a*-Cre mice (The Jackson Laboratory – 008766) have the Cre recombinase expression driven by the E8I CD8 enhancer which is only active in peripheral mature CD8$^+$ T cells. The full E8I transgene comprises the E8I enhancer fragment of 1.6-kilobase inserted in front of the *Cd8a* promoter, as well as the Cre encoding cDNA that also includes an internal ribosomal entry site (IRES)-GFP-poly(A) cassette, which was introduced after the *Cd8a* promoter sequence. However, in the purchased mice, we did not detect any GFP signal (data not shown). Of note, the Cre activity is only observed in peripheral CD8$^+$ T cells that are CD8α$^+$CD8β$^+$ αβT cells and CD8α$^+$CD8β$^-$ αβT cells, but not in CD4$^+$CD8α$^-$CD8β$^-$ αβT cells[262]. I crossed this *CD8a*-Cre transgenic mouse with an IFNγR1-floxed mouse (The Jackson Laboratory – 025394) to obtain CD8-IFNγR1KO mice. As there was no internal control for the Cre recombinase expression, I further crossed the mice with Rosa26-tdTomato reporter mice (The Jackson Laboratory – 007908) which have a loxP-flanked STOP cassette preventing the transcription of the red fluorescent protein variant tdTomato (**Figure 12**). In those mice, the Cre expression leads to permanent expression of tdTomato from the constitutively active *Rosa26* promoter[263]. As a result, IFNγR1KO CD8$^+$ T cells can be distinguished by tdTomato expression.

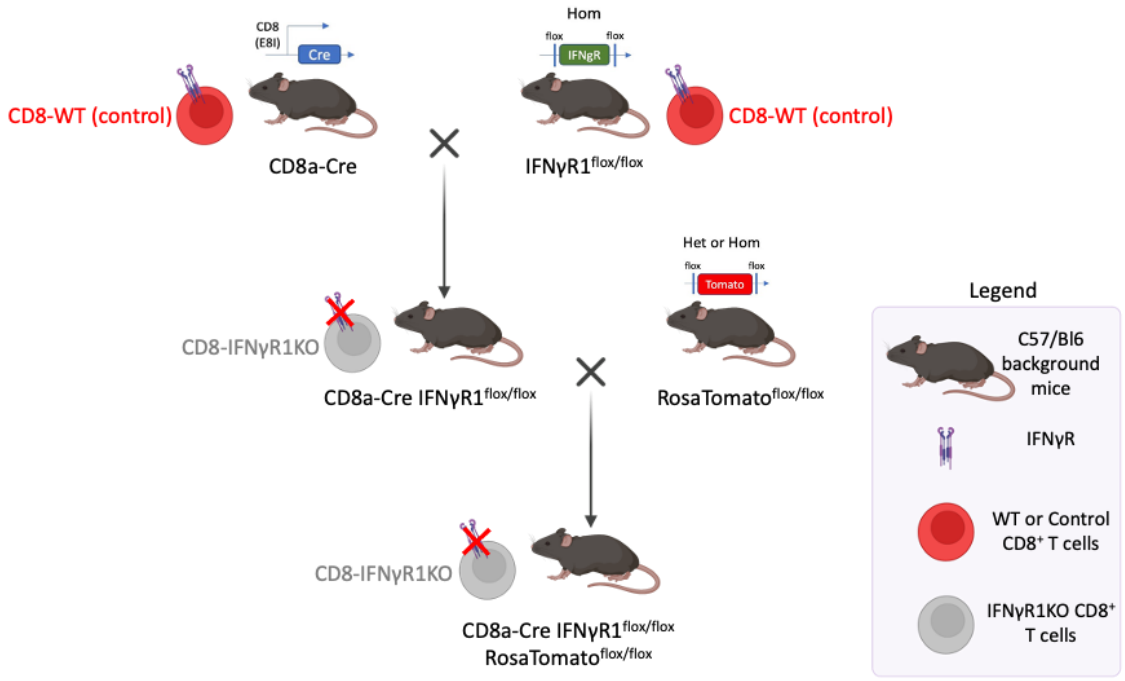


Figure 12: Crossing strategies to generate CD8-IFNγR1KO mouse model at the endogenous level. CD8a-Cre (E8I) mice are crossed with IFNγR1$^{flox/flox}$ mice to generate mice where IFNγR1 is specifically knock-out in mature CD8^{+} T cells. Subsequent crossings with floxSTOPflox-rosatdTomato mice were performed to add an internal control of the Cre expression. CD8a-Cre or IFNγR1$^{flox/flox}$ only were used in experiments as WT or Control mice (in red) while CD8-IFNγR1KO tomato positive or negative for some experiments were used (in grey). [Created with BioRender.com].

3.2.2 CD8^{+} T cell specific Cre expression *in vivo*.

To validate the penetrance of Cre expression, I assessed tdTomato expression as a readout of Cre specificity *in vivo*. To do so, I isolated spleens from tumour-bearing mice after 12 days of B16F10-OVA tumour induction and assessed tdTomato expression across the different immune cell populations and subsets by flow cytometry (**Figure 13A**). I first gated on single cells and then total live cells before gating on either CD45^{+} cells or CD8^{+} cells (**Figure 13B**). From there I gated on the different immune cell

populations and subtypes and assessed tdTomato signal intensity (**Figure 13C**). Overall, our data shows the successful and specific Cre expression only in mature $CD8^+$ T cells leading to CD8-IFNγR1KO mice. We did not detect any off-target expression in other cell types. In parallel, we formally confirmed the effective specific deletion of IFNγR1 only in mature $CD8^+$ T cells by assessing the IFNγR1 expression by flow cytometry (experiments performed by Dr. Lion Uhl in the lab – data not shown).

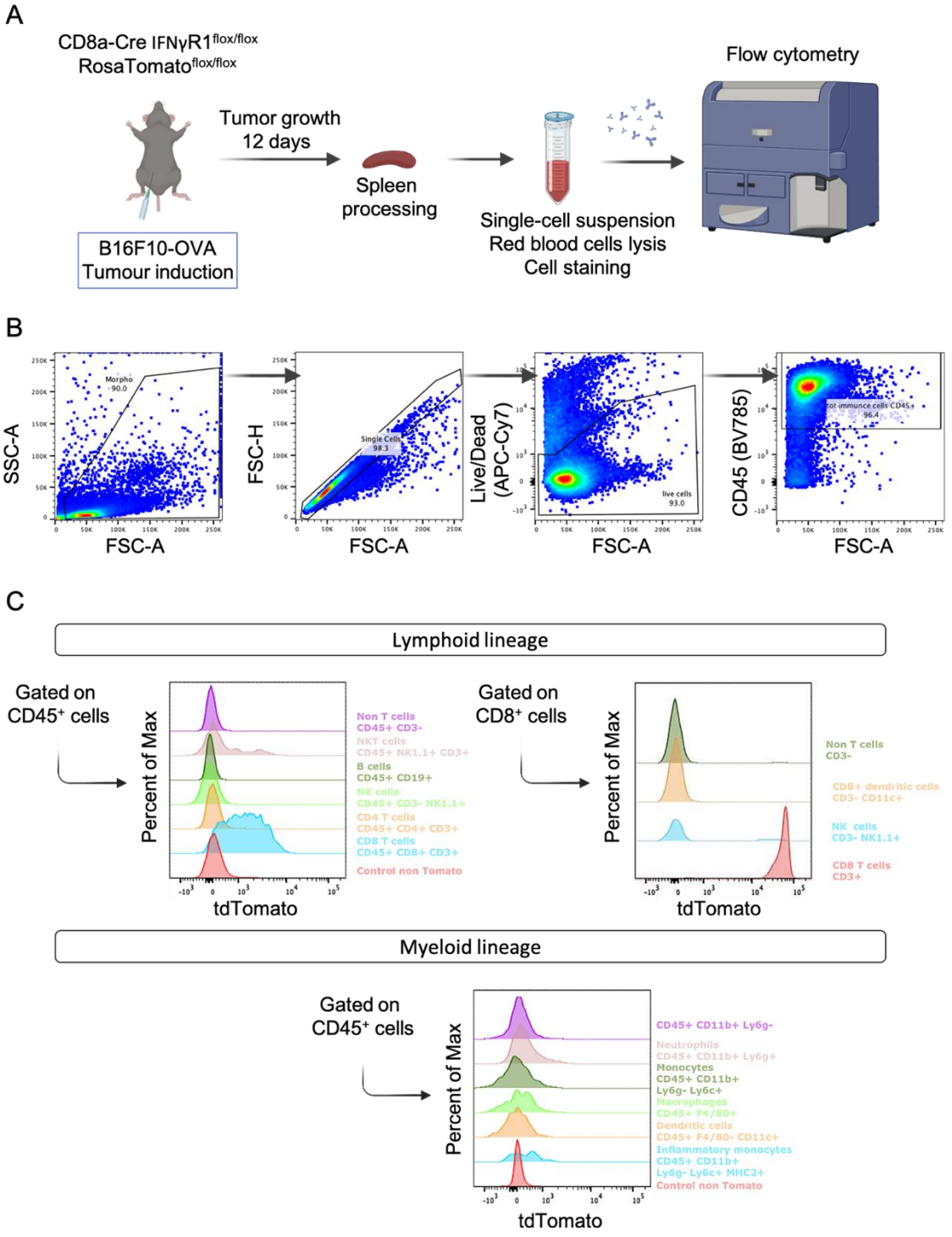


Figure 13: Validation of the CD8-IFNγR1KO mouse model *in vivo*. A- Workflow for the immune phenotyping. Spleens from B16F10-OVA tumour-bearing mice after 12 days were harvested and processed for flow cytometry. **B-** Representative gating strategy to focus on total live CD45$^+$ cells. **C-** Representative histograms showing the relative expression of tdTomato across immune cell types as a readout of *CD8a*-Cre expression knocking out the IFNγR1. [Created with BioRender.com].

3.2.3 OTI system for antigen specificity study (WT and IFNγR1KO)

The OTI and OVA system is well established and offers a great tool to study antigen-specific $CD8^+$ T cells in many contexts[264,265,266,267,268,269, and many other publications]. Ovalbumin was one of the first proteins to be purified and used widely for immunological study[270]. This glycoprotein of 45kDa is the major protein found in avian egg white. It belongs to the SERPIN (SERine Protease Inhibitor) family; however, it does not have inhibitor activity but rather acts as an amino acid source for the development of chicken embryos and eggshell mineralisation[271,272]. Historically, OVA was essential for immunology research and was used to develop our current knowledge of antibody specificity and protein interactions for instance[273,274,275,276,277]. The generation of OVA-specific $CD8^+$ T cells required the creation of TCR transgenic mice with a monoclonal repertoire targeting the OVA peptide SIINFEKL of amino acids 257-264 (also referred to as N4)[278] in the context of H-$2K^b$ (MHC-I restricted). N4-specific $CD8^+$ T cells or OTI cells harbour a transgenic TCR composed of α-chain variable region 2 ($V_\alpha 2$) and β-chain variable region 5 ($V_\beta 5$), which are inherited *via* a single transgene. OTI cells were extensively used in T cell research, notably to study thymic selection[279], tolerance and autoimmunity[264], and T cell response in vaccination or various infection models[280,265,266]; but also to study $CD8^+$ T cell behaviour *in vivo* such as migration in tissue[281,282,283]. In my case, I took advantage of this system to create OTI that do not express IFNγR1 (IFNγR1KO-OTI) by crossing WT OTI (The Jackson Laboratory – 003831), which were either expressing the GFP protein or congenic markers (CD45.1 and CD45.2 heterozygous or homozygous) with IFNγR1KO mice (The Jackson Laboratory – 003288) **Figure 14**. When required I harvested lymph

nodes and processed them to isolate CD8⁺ T cells for further experiments (see **Chapter 2** – Material and methods).

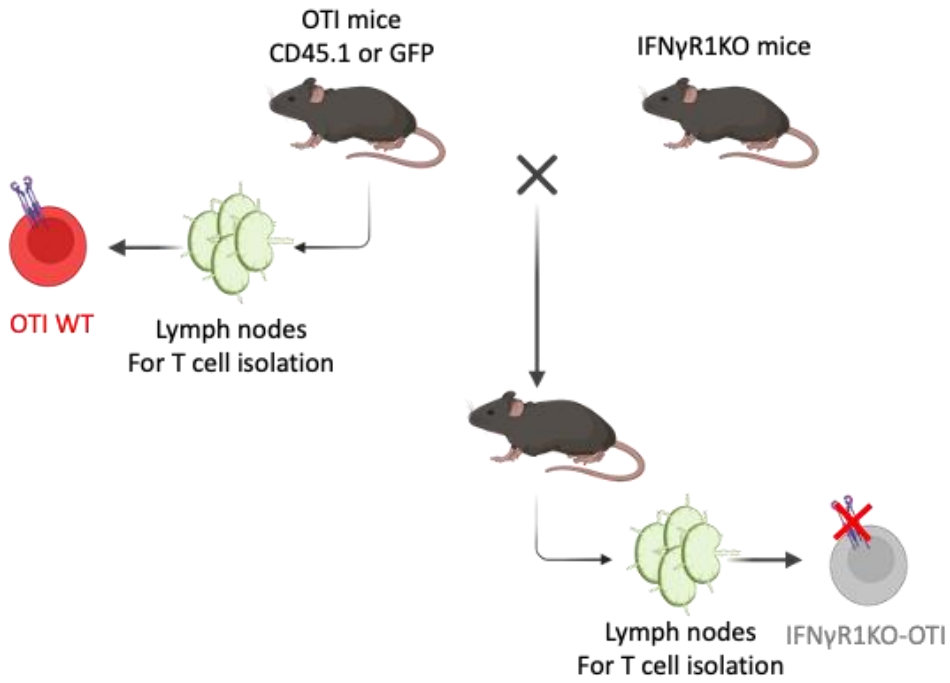


Figure 14: Crossing strategies to generate IFNγR1KO-OTI mice to obtain WT and IFNγR1KO OTI cells. WT OTI mice either GFP⁺ or with congenic markers (CD45.1) were crossed with full IFNγR1KO mice to generate IFNγR1KO-OTI. After lymph nodes isolation and CD8⁺ T cell selection, WT OTI (in red) and IFNγR1KO-OTI cells (in grey) were used for experiments. [Created with BioRender.com].

3.2.4 Murine melanoma model: the B16F10tyr$^{-/-}$mCherryOVA cell line

To study the CD8⁺ T cell anti-tumour response in our mouse models, I used a well-described tumour model: the B16F10 murine melanoma cell line. The B16F10 murine melanoma cell line was generated using its parental cell line the B16, after 10 passages *in vivo*. B16 tumour cells obtained from a spontaneous melanoma tumour in C57BL/6 mice were injected in other WT mice to trigger fresh tumours. Cells from this newly

induced tumour were then collected and cultured before being re-injected into fresh host mice. This process was done 10 times serially to obtain the B16F10 cell line[284]. This cell line is well-known and extensively used to study solid tumours and metastasis in mice[285,286,287]. B16F10 cells are adherent, epithelial-like, and can be injected intradermally, subcutaneously, or intravenously *in vivo* in C57BL/6 mice depending on the type of studies. They trigger aggressive tumours *in vivo*, are poorly immunogenic, and thus ideal models to study how to improve immune responses against solid tumours[288]. As intradermal B16F10 injections lead to necrotic and sometimes ulcerative tumours[289], and intravenous injections are only suited to study tumour homing and metastasis[290,291], we chose to inject the cell line subcutaneously as a preferred route of tumour induction. I used a B16F10 cell line engineered to ablate the tyrosinase expression leading to melanin-free cells and expressing the fluorescent mCherry protein for imaging purposes. In addition, the cell line expressed the OVA peptide, which allows us to use OTI cells to study the tumour-specific $CD8^+$ T cell immune response. Our B16F10-$Tyr^{-/-}$-mcherry-OVA (B16F10-OVA) cells were subcutaneously injected into the flank of host mice either WT, control, or CD8-IFNγR1KO depending on the experiment (**Figure 15**). After 5 to 6 days, tumours were palpable and were measured every 2 days for growth curves. OTI cells were injected to study anti-tumour specific $CD8^+$ T cell behaviour *in vivo*. Mice were either culled and tumours processed at indicated time points (usually day 12 post-engraftment) or kept until the human endpoint was reached.

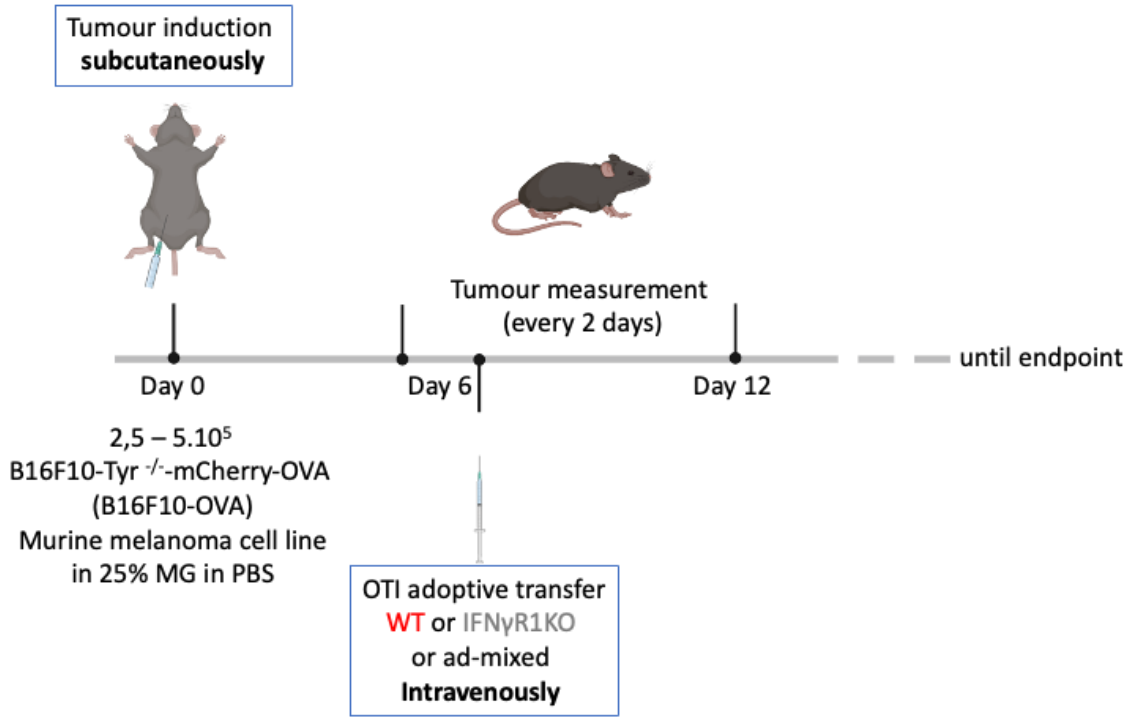


Figure 15: Workflow to obtain murine melanoma tumours to study CD8⁺ T cell response. Between 250 000 and 500 000 B16F10-OVA cells were prepared in PBS containing 25% of matrigel (MG) and were subcutaneously injected in host mice to induce tumours. To study CD8 anti-tumour response at the endogenous level, control and CD8-IFNγR1KO mice were injected and tumours were processed at day 12. To study tumour-specific CD8⁺ T cell responses, OTI cells (either WT or IFNγR1KO) were intravenously injected after 6 days of tumour induction. In both cases, tumours were left growing until the endpoint and measured every two days to obtain tumour growth curves [Created with BioRender.com].

3.3 B16F10-OVA tumours are better controlled by IFNγR1KO CD8⁺ T cells compared to control mice

To investigate the function of IFNγ on CD8⁺ T cell anti-tumour responses, we assessed B16F10-OVA tumour control in CD8-IFNγR1KO or control mice over time, both at the

endogenous level and by studying the antigen-specific response of TCR transgenic OTI T cells.

3.3.1 Endogenous IFNγR1KO CD8$^+$ T cells better control murine melanoma tumours

To assess whether IFNγ sensing affects the efficacy of the CD8$^+$ T cell anti-tumour response at the endogenous level, we engrafted control and IFNγR1KO CD8$^+$ T cell mice (CD8-IFNγRKO) with our B16F10-OVA cell line and followed the tumour growth over time as described in **Figure 15** (upper panel, no adoptive transfer). Inhibition of IFNγ sensing by CD8$^+$ T cells increased the overall survival of the tumour-bearing mice (**Figure 16A**). CD8-IFNγR1KO mice were more potent in controlling B16F10-OVA tumours over time (**Figure 16B**). They are better at controlling tumour size on average (**Figure 16B**), but also in terms of tumour rate with 50% of tumours being controlled in CD8-IFNγR1KO mice compared to 20% in control mice (**Figure 16C**). Furthermore, when tumours were harvested after 12 to 15 days, CD8-IFNγR1KO have a significantly decreased tumour weight compared to control mice (**Figure 16D**). Altogether, this showed that inhibition of IFNγ sensing by CD8$^+$ T cells restores anti-tumour immunity against murine melanoma without the need for external treatments such as immune checkpoint blockade.

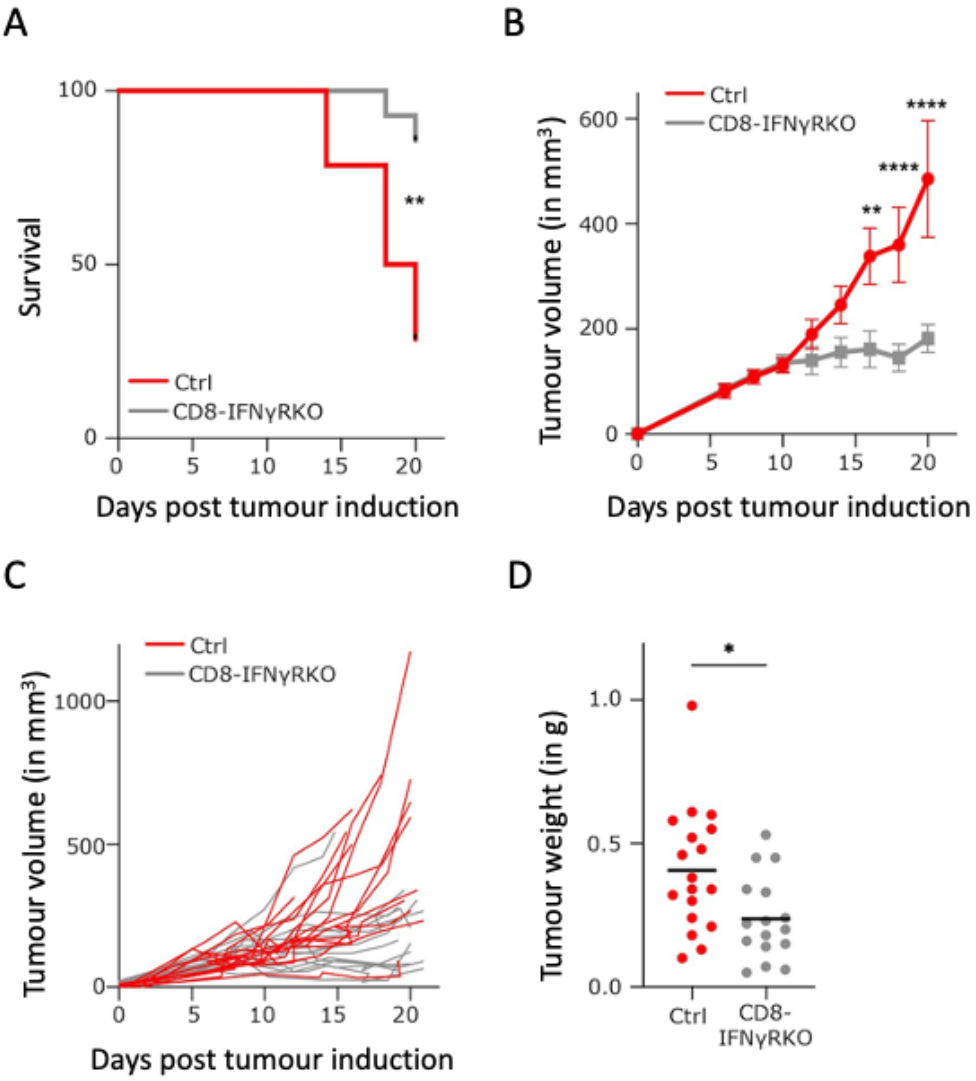


Figure 16: IFNγ sensing by CD8⁺ T cells restricts anti-tumour immunity in mice. (A-D) CD8-IFNγR1KO (in grey) and control mice (in red) were engrafted with B16F10-OVA melanoma tumours and followed over time. **A-** The graph shows mouse survival over time (n= 12 for Control and n=13 for CD8-IFNγR1KO). Data is from 3 independent experiments. Survival curves statistical comparison was performed using the Gehan-Breslow-Wilcoxon test on GraphPad Prism. **B-** The graph shows the average tumour volume over time (n= 12 for Control and n=13 for CD8-IFNγR1KO). Data is from 3 independent experiments. Data represent mean + standard error of the mean (SEM). The growth curves over time were analysed with two-way ANOVA on GraphPad Prism. **C-** The graph shows the tumour volume of individual mice over time (n= 12 for Control and n=13 for CD8-IFNγR1KO). Data is from 3 independent experiments. **D-** The graph shows tumour weight between days 12 and day 15 after tumour engraftment (n=18 for control and n=16 for CD8-IFNγR1KO). Data is from 3 independent experiments. The comparison between the 2 groups was analysed using an unpaired t-test on GraphPad Prism. * = $P < 0.05$, ** = $P < 0.002$, **** = $P<0.0001$. Experiments were jointly performed with Jagdish Mahale.

3.3.2 Tumour specific IFNγR1KO CD8$^+$ T cells better control murine melanoma tumours – OTI system

To further investigate the IFNγ effect on CD8$^+$ T cells we assessed whether IFNγ would affect similarly a particular tumour-specific CD8$^+$ T cell population. To do so, I took advantage of TCR transgenic OTI T cells (described in **Figure 14**), and the fact that our tumour cell line expresses their cognate antigen OVA (described in **Figure 15**). The efficacy of adoptive cell therapy (ACT), used to treat cancer patients with their own T cells, is limited, especially in solid tumours. Given our findings at the endogenous level (**Figure 16**), we sought to assess whether IFNγ sensing by tumour-specific CD8$^+$ T cells could also restrict their anti-tumour potential. To test this, I induced B16F10-OVA tumours in WT mice and adoptively transferred either WT or IFNγR1KO naïve OTI CD8$^+$ T cells when tumours were palpable (see **Figure 15** – lower panel), and monitored the mice over time. The transfer of IFNγR1KO OTI cells significantly increased mouse survival (**Figure 17A**). Overall, by transferring IFNγR1KO OTI, tumour growth was reduced compared to the transfer of WT OTI (**Figure 17B**). As shown at the endogenous level, the presence of IFNγR1KO CD8$^+$ T cells not only decreased the overall tumour size but also improved the tumour control rate (**Figure 17B**). When harvested at a specific time point (day 12 post-tumour engraftment), mice with IFNγR1KO OTI harbour smaller tumours than WT OTI transferred mice (**Figure 17C**). This line of evidence demonstrates that IFNγ sensing by transferred tumour-specific CD8$^+$ T cells restricts their anti-tumour response.

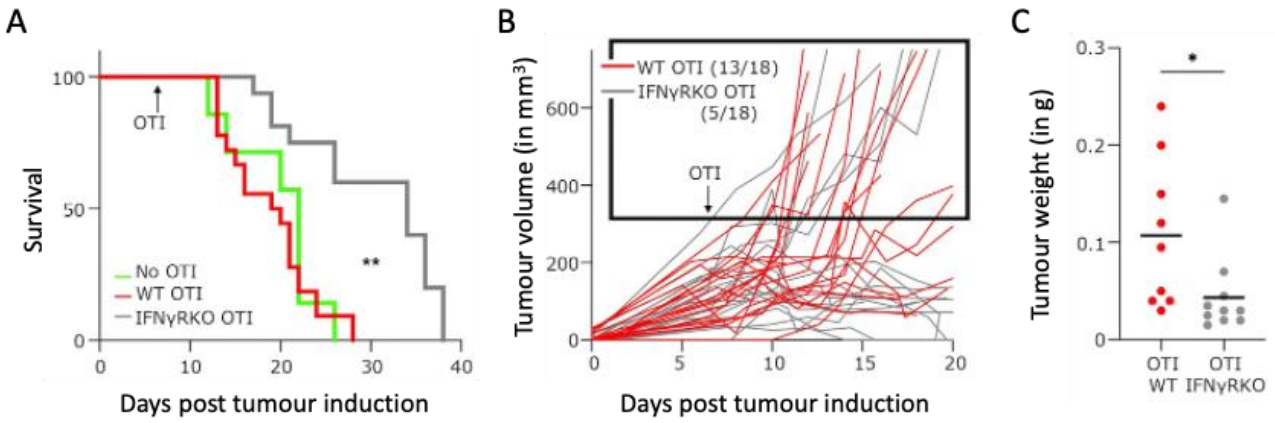


Figure 17: IFNγR1 ablation in tumour-specific CD8⁺ T cells improves tumour control in an adoptive T cell transfer model. (A-C) WT mice were engrafted with B16F10-OVA tumours and either transferred with WT (in red) or IFNγR1KO (in grey) OTI cells or not transferred (in green for **Figure 17A**) after 6 days when tumours were palpable. **A-** The graph shows mouse survival over time (n=7 control, n=17 WT and n=18 IFNγR1KO). Data is from 3 independent experiments. Survival curves statistical comparison was performed using the Gehan-Breslow-Wilcoxon test on GraphPad Prism. **B-** The graph shows the tumour volume of adoptively transferred individual mice over time (n=18 WT and n=18 IFNγR1KO). Black square highlight tumours that show increased tumour growth after OTI transfer, with a volume of at least 300 mm^3. The numbers represent the frequency of tumours with enhanced growth out of the total mice enrolled. Data is from 3 independent experiments. **C-** The graph shows the average tumour weight at day 7 post-OTI transfer (n=9 WT and n=10 IFNγR1KO). Data is from 2 independent experiments. The comparison between the 2 groups was analysed using an unpaired t-test on GraphPad Prism. * = $P < 0.05$, ** = $P < 0.002$. Experiments were jointly performed with Jagdish Mahale.

3.3.3 Endogenous IFNγR1KO CD8⁺ T cells better control murine colon tumours

To reinforce the phenotype and assess whether the better tumour control observed was not B16F10 specific, we used another syngeneic transplantable murine cancer model: the MC-38 colon cancer cell line. Historically isolated from a colon tumour in a C57Bl/6 mouse induced by long-term exposure to the DMH carcinogen (1,2-dimethylhydrazine dihydrochloride)[292], the MC-38 is a murine colon adenocarcinoma

adherent cell line. As the B16F10 model, it can be subcutaneously injected to induce tumours. It differs from the B16F10 as it is more immunogenic with a favourable response to immunotherapies (anti-PD-1, anti-PD-L1, and anti-CTLA4) suggesting a better immune response in this model[293,294]. Following the same experimental design, we subcutaneously injected MC-38 cells in control and CD8-IFNγR1KO mice and monitored the mice over time. We observed an overall enhanced tumour control when $CD8^+$ T cells were IFNγR1KO compared to control $CD8^+$ T cells (**Figure 18A**). Individual curves (**Figure 18B**) show that the phenotype observed with the B16F10-OVA was recapitulated with the MC-38 model. This suggests that IFNγ restricts anti-tumour $CD8^+$ T cell responses in a general mechanism that is not model-dependant.

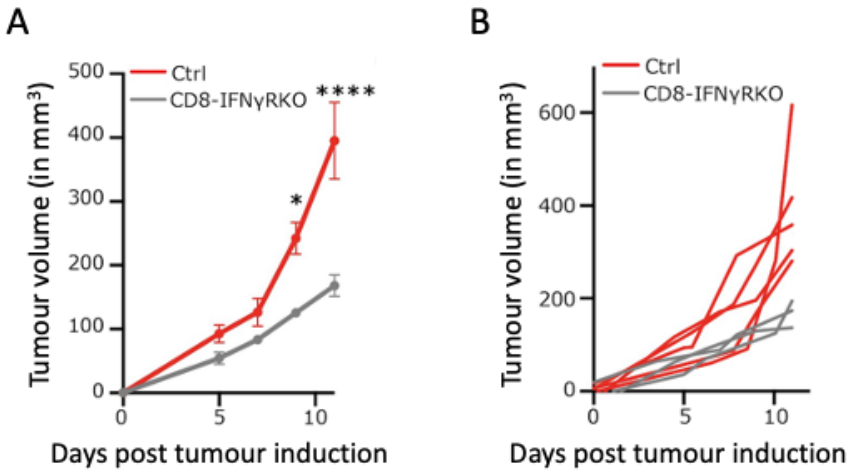


Figure 18: IFNγ sensing by $CD8^+$ T cells restricts anti-tumour immunity in MC-38 murine colon cancer. (A-B) Control (in red) and CD8-IFNγR1KO (in grey) mice were engrafted with MC-38 tumours and monitored over time. **A-** The graph shows the average tumour volume over time (n=5 per group). **B-** The graph shows the tumour volume of individual mice over time (n=5 per group). Data represent mean + standard error of the mean (SEM). The growth curves over time were analysed with two-way ANOVA on GraphPad Prism. * = $P < 0.05$, ****= $P < 0.0001$. Experiments were performed by Jagdish Mahale.

3.4 Discussion and conclusion

This chapter interrogated the relationship between IFNγ and CD8$^+$ T cells in several contexts. In this study, I investigated the direct effect of the loss of IFNγ sensitivity in mature CD8$^+$ T cells during anti-tumour responses.

3.4.1 IFNγ and CD8$^+$ T cell function in tumours

The earlier described contrasting findings reported in the literature regarding the function of IFNγ on CD8$^+$ T cells underline the fact that IFNγ secretion and IFNγ responsiveness in CD8$^+$ T cells is dynamically regulated. However, most of the investigations were made in acute infections or with a single stimulation where the CD8$^+$ T cell response is more timely controlled than in a chronic context such as chronic infection or cancer. As introduced in **chapter 1.3**, general CD8$^+$ T cell responses are composed of 3 main phases: activation with T cell expansion, the effector phase followed by the contraction phase, and finally the immune memory formation. According to the different studies, CD8$^+$ T cells can be affected by IFNγ during the activation phase and the contraction phase, as well as during memory formation, while being insensitive to IFNγ when they are secreting it during the effector phase. Furthermore, the IFNγR expression profile suggests that naïve cells are more responsive to IFNγ during the activation or priming phase of the response. Downregulation of the IFNγR2 chain by early activated CD8$^+$ T is likely making them less responsive to IFNγ for a certain period[295]. Additionally, IFNγ-producing cytotoxic T cells have been shown to not upregulate IFNγ-inducible genes *in vitro*[252], which could serve again a protective

function. However, in the past, IFNγR2 was not detected in $CD8^+$ T cells mostly due to technical limitations. Hence, it was concluded that activated $CD8^+$ T cells were not responsive at all to IFNγ. We now know that IFNγR2 is detectable at the transcriptional level in activated cells but at very low levels compared to IFNγR1, suggesting that activated $CD8^+$ T cells may still be sensitive to IFNγ if IFNγR mRNAs are translated, even though signalling may significantly be reduced in cells. In more recent human studies with RNA sequencing, IFNγ-responsive genes were detected in the general $CD8^+$ T cell population, especially in tumoral contexts. This further suggests that in a chronic context such as in cancer, IFNγ would be present throughout the $CD8^+$ T cell response and therefore can affect $CD8^+$ T cells at different stages of differentiation. It is therefore critical to study the IFNγ effect on the different $CD8^+$ T cell subsets. Another key parameter to consider in the context of cancer is $CD8^+$ T cell localisation. Indeed, in most immune responses $CD8^+$ T cells are activated and primed mainly in secondary lymphoid organs such as draining lymph nodes, where antigen-presenting cells are located[214,296,297]. At that stage, there should be no IFNγ in the T cell environment. However, once activated, cells will egress and reach the tumours where IFNγ is already present. In contrast, in some acute infection models, such as *Listeria monocytogenes*, the nearest secondary lymphoid organ site to activate naïve $CD8^+$ T cells is the white pulp of the spleen whilst the infection site is the spleen as well[298,299,300]. The spatial organisation is very important when primary tumours are established, tumour-associated vasculature is present, and naïve $CD8^+$ T cells will be recruited and activated on-site over time in addition to early activated $CD8^+$ T cells being re-stimulated[301]. Hence, the activation will be different within the tumour microenvironment with a

variety of surrounding cells and soluble cues, notably IFNγ compared to the activation in the draining lymph node. In order to correctly assess the IFNγ effect on the $CD8^+$ T cell response, specific deletion of IFNγR expression is required. In tumours, it is challenging to synchronise endogenous immune responses as it is a chronic, versatile and dynamic environment. Therefore, studying the different $CD8^+$ T cell subsets and differentiation stages will be crucial to better understanding the function of IFNγ on $CD8^+$ T cells.

3.4.2 The ablation of IFNγR1 only in mature $CD8^+$ T cells enhanced the tumour control

As shown in this chapter, we created a mouse model to specifically knock out the IFNγR1 in mature $CD8^+$ T cells making them insensitive to IFNγ. Indeed, by ablating the binding part of the receptor, $CD8^+$ T cells cannot sense IFNγ. Inducing syngeneic tumours in those mice using subcutaneous cancer cell lines, improved tumour control and overall survival over time compared to WT mice. Those results demonstrated that IFNγ restricts the $CD8^+$ T cell anti-tumour response. I used the B16F10 murine melanoma model as it is well suited to study $CD8^+$ T cell dysfunction. To date, it has been shown to be unresponsive to modern immunotherapy approaches, and thus $CD8^+$ T cell dysfunction cannot be explained by terminal exhaustion. Other murine melanoma models are currently available such as xenograft transplantation models, syngeneic transplantation models, genetically modified models, ultraviolet radiation, and chemically induced models (detailed in those reviews[302,303]). But syngeneic models are the most suited to study the anti-tumour immune response in immunocompetent mice without host rejection. The B16F10 cell line is also commonly used, notably to study poorly

immunogenic tumours as it has low genetic diversity[304,305]. In our case, by adding the OVA peptide, we enhance its immunogenicity, making the abundance of antigen not a limiting factor. Nonetheless, this approach only recovers the lack of neo-antigen or low mutational burden but does not affect the "excluded" phenotype, characterised by a low immune infiltration in tumour nest of B16F10 tumours[306] (see **Figure 28** in the next Chapter). Additionally, by using the MC-38 cell line we proved that the phenotype observed was not restricted to the B16F10 model. Recapitulating the better tumour control in two different models suggests that the IFNγ effect on the $CD8^+$ T cell anti-tumour response might be a general regulating mechanism.

Furthermore, we specifically depleted the IFNγR1 chain in $CD8^+$ T cells to prevent IFNγ binding, and not the signalling component, IFNγR2. Our rationale was that preventing the binding of the cytokine will completely prevent IFNγ signalling in $CD8^+$ T cells. Thus, cells will become IFNγ-insensitive. Another, more technical, reason was that at that time, only $IFN\gamma R1^{floxed}$ mice were available to purchase. However, recently some labs created and characterized $IFN\gamma R2^{floxed}$ mice[307,308,309]. It would be very interesting to assess whether CD8-IFNγR2KO and CD8-IFNγR1/2 double KO mice would give rise to the same phenotype. It is reasonable to assume that CD8-IFNγR2KO mice should phenocopy the results obtained in the CD8-IFNγR1KO model, given that IFNγR signalling should be disabled in both models. However, it is conceivable that with IFNγR1 still expressed, $CD8^+$ T cells may still bind the cytokine in a more or less stable way, leading to several effects without downstream signalling. For instance, it could be an unconventional way of cytokine presentation towards neighbouring cells, similarly to the "catch and release" model shown in cancer cells[310]; or, alternatively, binding of IFNγ may mechanistically

change the CD8$^+$ T cell surface topology following receptor oligomerisation which may possibly influence the plasticity of the cell membrane, and, thus, cell migration[311]. Finally, such cytokine sensing by external binding may also act as a "stop signal" for cells to stay at the inflammatory effector site without triggering downstream signalling. I can furthermore hypothesise that IFNγ bound to IFNγR1 could still signal either through the recruitment of an unknown subunit or another cytokine receptor chain as it has been previously shown for several interleukin receptors sharing subunits (for example the IL-2R is composed of 3 chains among which 2 are shared with IL-5R, or IL-4R, IL-7R, IL-9R[312,313]). Of note, once bound to IFNγR1, IFNγ may possibly trigger non-canonical pathways through endocytosis pathways while IFNγR2 remains at the cell surface[314,315]. Transphosphorylation with IFNγR2 was shown to lead to STAT1 recruitment, which is required for its activation. However, STAT1 may also be activated through other pathways such as type 1 interferon. STAT1 may also not need to be present for the endocytosis of the IFNγR complex[316,317]. Overall, testing whether the ablation of IFNγR2 recapitulates the better anti-tumour response observed by deleting IFNγR1 would help to answer some of these open questions.

Finally, in this study, we did not use immunotherapies. Firstly, we chose the B16F10 model to assess CD8$^+$ T cell dysfunction, which is not driven by exhaustion pathways targetable with immunotherapy. Secondly, as we improved tumour control bypassing the need for further treatment, we focused on deciphering the mechanisms behind this enhanced anti-tumour response. However, it could be an interesting experimental design to treat the mice with immunotherapies after tumour relapse following primary

control and compare whether the IFNγ sensitivity in $CD8^+$ T cells affects their response to immunotherapies.

3.4.3 IFNγ triggered negative feedback loop: a general mechanism?

In this chapter, I demonstrated that $CD8^+$ T cells respond to IFNγ and that by preventing IFNγ sensing, the anti-tumour response is enhanced and results in better tumour control. This demonstrates that IFNγ triggers a negative feedback loop in $CD8^+$ T cells. Notably, the IFNγR expression pattern suggests that naïve $CD8^+$ T cells can sense IFNγ and that upon activation $CD8^+$ T cells restrict their responsiveness against IFNγ signalling by downregulating the IFNγR2. However, the upregulation of IFNγR1 suggests that $CD8^+$ T cells are still capable of binding hence sensing IFNγ. This dual regulation of the expression of these distinct IFNγR chains suggests a regulatory role possibly contributing to immune tolerance. There are plenty of regulatory physiological mechanisms in the immune system to uphold the delicate balance between effective immune response and immune tolerance. In addition, the IFNγR expression pattern in resting/naïve *versus* activated NK cells harbour a similar pattern as observed in $CD8^+$ T cells (**Figure 19** – assessed using ImmGen database) with a much higher expression level of IFNγR1 and a very low level of IFNγR2. This further suggests that a negative feedback loop could be a general mechanism for how IFNγ-producing cells tune their responsiveness to IFNγ. NK cells are the innate counterpart of $CD8^+$ T cells, both are cytotoxic cells but NK cells do not rely on antigen recognition for the selection of their targets[318]. Their response and kinetics are different with NK cells being mobilised more quickly than $CD8^+$ T cells. However, both are using IFNγ secretion for their effector

functions. In the future, it could be interesting to assess whether the IFNγ negative feedback loop is a fundamental general mechanism by specifically deleting IFNγR1 in NK cells prior to tumour engraftment and following the anti-tumour response over time.

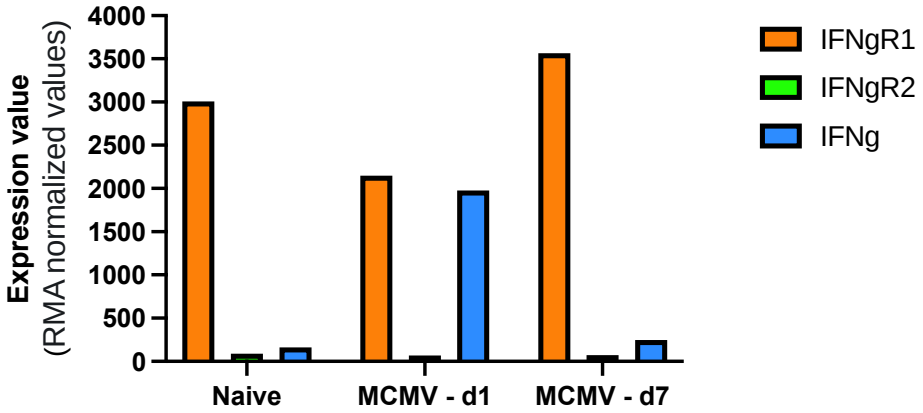


Figure 19: IFNγR and IFNγ expression landscape in NK cells at the transcriptional level. IFNγR1, IFNγR2, and IFNγ transcriptional expression values were extracted from the ImmGen Microarrays publicly available database. Splenic natural killer cells were sorted from 6-week-old C57BL/6 mice (using $CD3^{-}NK1.1^{+}$ strategy) before or day 1 and day 7 post-murine cytomegalovirus infection (MCMV) for microarray sequencing by Joe Sun (from Lanier Lab – University of California, San Francisco). Data are from 3 samples. Expression values were normalized by Robust Microarray Averaging (RMA).

3.4.4 Conclusion

In summary, preventing IFNγ sensing by $CD8^{+}$ T cells restore anti-tumour immunity in murine melanoma model without needing external immunotherapies. I discussed the limitations of the model but the strong phenotype suggests that it is suitable to study this potential fundamental mechanism. The loss of IFNγ responsiveness in $CD8^{+}$ T cells enhanced their tumour control both at endogenous and antigen-specific levels. In the following chapters, I will be investigating through which mechanism this better tumour control is achieved.

4. The role of IFNγ sensing for CD8$^+$ T cell spatial and functional fitness

In this chapter, I am investigating the mechanism by which the expression of IFNγR1 on CD8$^+$ T cells impacts their functions leading to tumour progression. In the previous chapter, we demonstrated that IFNγR1KO CD8$^+$ T cells were better at controlling B16F10-OVA tumours. Here, I am assessing whether enhanced effector functions and efficient tumour infiltration could contribute to the better tumour control observed. To do so, I used the endogenous and antigen-specific CD8$^+$ T cells previously described (see **Chapter 3**). The general workflow is presented in **Figure 20**. In one set of experiments, B16F10-OVA cells were engrafted in control and CD8-IFNγR1KO mice to study the CD8$^+$ T cell immune response at the endogenous level (upper panel). In another set of experiments, B16F10-OVA were engrafted in WT recipient mice and OTI cells WT or IFNγR1KO were injected intravenously between day 5 and day 7 post-tumour engraftment to study antigen-specific CD8$^+$ T cells (lower panel). For both sets of experiments, tumours were harvested usually on day 12 post-tumour engraftment, as it is at this particular time point that differences were first observed (**Figure 16B** in **Chapter 3**). Tumours were then processed in different ways depending on the subsequent applications. For imaging purposes, tumours were directly fixed and frozen before being cryosectioned for further tissue staining. Slides were imaged on a confocal microscope (see **Chapter 2** – Material and methods and **Figure 28** for more details). For molecular and cellular analysis, tumours were first mechanistically dilacerated and then digested

enzymatically. Supernatants were collected, filtered, and used as a milieu recapitulating the soluble tumour microenvironment. Tumour pieces were smashed to obtain a single cell suspension ready for further *ex vivo* assays or direct staining for flow cytometry.

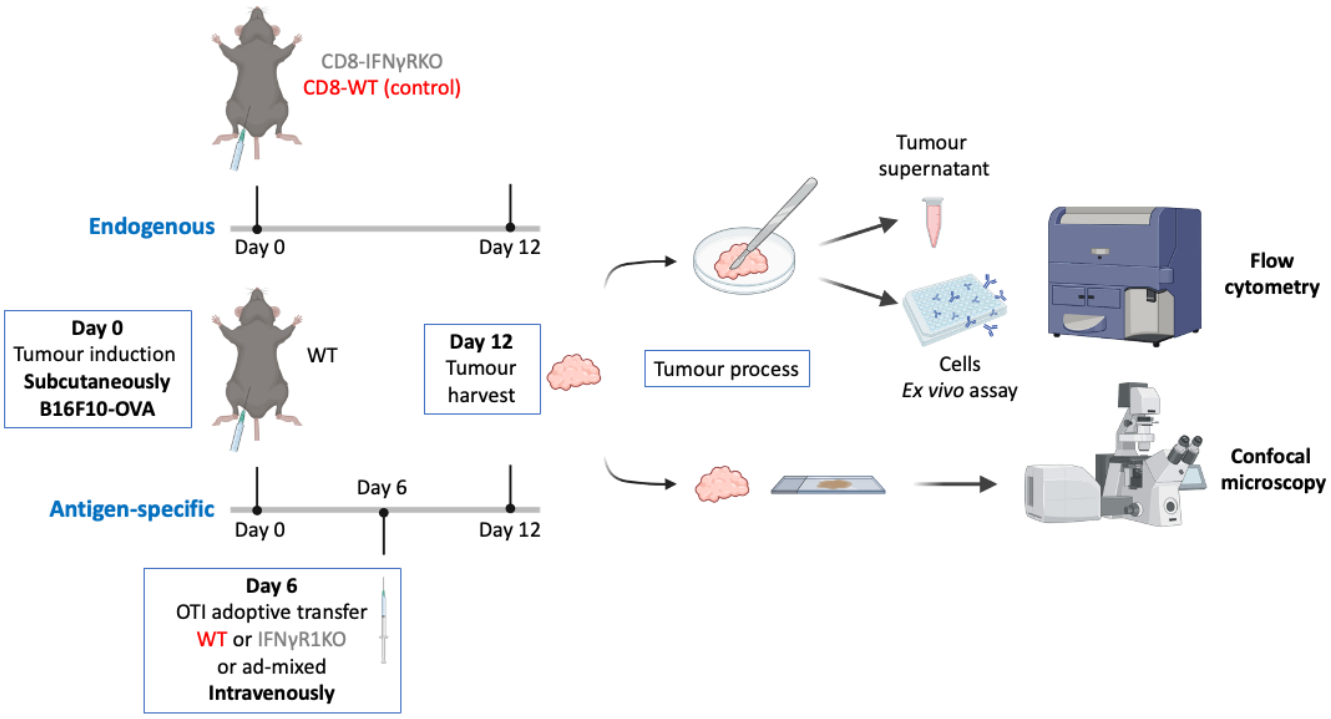


Figure 20: General workflow to investigate tumour-infiltrating CD8⁺ T cell fitness. [Created with BioRender.com].

4.1 IFNγ sensing does not significantly affect CD8⁺ T cell effector functions

To investigate by which mechanism IFNγ-sensing by CD8⁺ T cells restricted tumour control, I first assessed whether IFNγR1KO CD8⁺ T cells exhibit enhanced effector

functions compared to control CD8$^+$ T cells. In this section, I assessed tumour-infiltrating CD8$^+$ T cell cytokine production, cytolytic degranulation, and cytotoxic functions *in vivo* or *ex vivo*.

4.1.1 Cytokine production capabilities – *ex vivo* restimulation

CD8$^+$ T cell effector functions rely on their capacity to produce and secrete pro-inflammatory cytokines such as IFNγ and TNFα[319] toward target cells. First, I assessed the cytokine production potential of endogenous tumour-infiltrating CD8$^+$ T cells by restimulating them *ex vivo* with the OVA peptide in the presence of brefeldin A for 6 hours. Brefeldin A co-incubation prevents cytokine secretion and therefore leads to cytokine accumulation in cells. Cytokine detection was performed by intracellular staining and analysed by flow cytometry. Although slightly more IFNγR1KO CD8$^+$ T cells produced IFNγ and/or TNFα, the difference was not statistically significant (**Figure 21A**). This suggests that IFNγ-sensing by CD8$^+$ T cells does not significantly affect their cytokine production. Similarly, I interrogated the cytokine production potential of tumour-infiltrating antigen-specific CD8$^+$ T cells with the OTI cells. A greater percentage of transferred IFNγR1KO OTI T cells produced IFNγ, but not TNFα, nor both cytokines together when restimulated under the same *ex vivo* conditions (**Figure 21B**). Altogether this suggests that tumour-infiltrating IFNγR1KO CD8$^+$ T cells do not display an enhanced capacity to produce cytokines compared to control CD8$^+$ T cells.

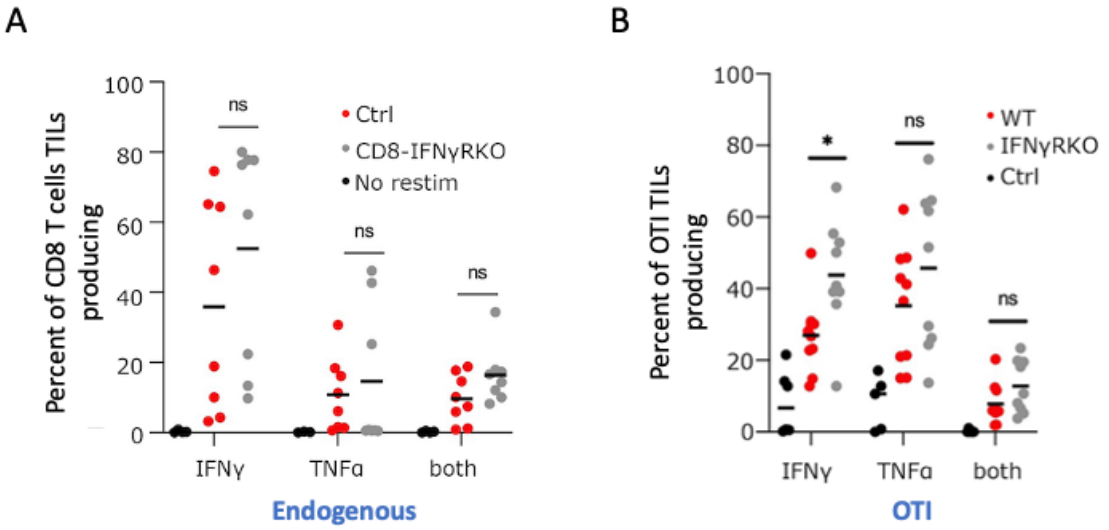


Figure 21: Tumour-infiltrating CD8⁺ T cell cytokine production potential assessed by *ex vivo* re-stimulation. A- B16F10-OVA tumours were harvested between days 12 and 15 from control or CD8-IFNγR1KO mice. Tumour-infiltrating lymphocytes (TILs) were restimulated *in vitro* with 1μg N4-OVA peptide for 6 hours in presence of Brefeldin A or not restimulated. Cytokine production by CD8⁺ T cells was analysed by flow cytometry. The graph shows the quantification of IFNγ and TNFα producing cells. Data is from 2 experiments (n=8 per group). **B-** WT mice bearing B16F10-OVA tumours were transferred with Control (red) and IFNγR1KO (grey) OTI T cells. Tumours were harvested on days 5 to 7 after OTI transfer. Cells were restimulated *in vitro* with 1μg OVA peptide or not (Ctrl) for 6 hours in presence of Brefeldin A. Cytokine production by OTI cells was analysed by flow cytometry. The graph shows the quantification of IFNγ and TNFα production by OTI WT (red, n=10), OTI IFNγRKO (grey, n=9), and not stimulated OTI (black, n=6). Data is from 3 experiments. The comparison between more than 2 groups was analysed using two-way ANOVA on GraphPad Prism. * = $P < 0.05$, ns = not significant. Experiments were jointly performed with Jagdish Mahale.

4.1.2 Cytokine bioavailability *in vivo*

IFNγ production by CD8⁺ T cells is not significantly affected by the IFNγ sensitivity status of cells. However, the lack of IFNγR1 expression on CD8⁺ T cells might affect the IFNγ uptake from the tumour microenvironment resulting in changing the IFNγ bioavailability for the surrounding cells. To assess the IFNγ bioavailability in the soluble

tumour milieu, I harvested tumour supernatants from either CD8-IFNγR1KO or control tumour-bearing mice at day 12 (see **Figure 20** upper panel). Similar quantities of IFNγ were detected in the soluble tumour microenvironment from control and CD8-IFNγR1KO tumours (**Figure 22A**). This suggests that the lack of IFNγR1 on $CD8^+$ T cells is not sufficient to change the IFNγ bioavailability or that the IFNγ secretion/uptake is compensating to reach the same IFNγ levels in tumours. Following the reasoning that both $CD8^+$ T cells and IFNγ are part of a sophisticated immune response network, I hypothesised that the IFNγ insensitivity in $CD8^+$ T cells could also result in indirect effects, such as a change in other soluble cues secretion in the tumour microenvironment. Thus, I further assessed the soluble compartment in the tumour microenvironment by screening other inflammatory cytokines. Overall, there were no significant differences in IL-23 (pro-inflammatory), IL-1a (pro-inflammatory), IFNγ (pro-inflammatory), TNFα (pro-inflammatory), MCP1 (= CCL2, chemokine chemoattractant), and IL-6 (pro-inflammatory), presence in the tumour microenvironment from control and CD8-IFNγR1KO mice (**Figure 22B**). In addition, IL-12p70 (pro-inflammatory), IL-10 (anti-inflammatory), IL-27 (both pro and anti-inflammatory), IL-17A (pro-inflammatory), IFN-β (pro-inflammatory), and GM-CSF (cytokine-like factor, pro-inflammatory) were not detected (data not shown). We can reasonably conclude that IFNγ sensing by $CD8^+$ T cells does not substantially imbalance the soluble tumour microenvironment.

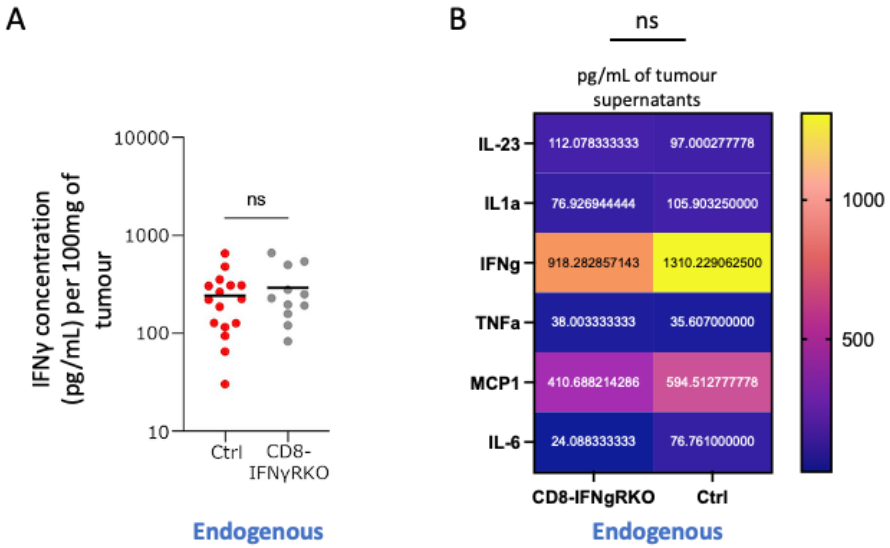


Figure 22: IFNγR1 ablation in CD8⁺ T cells does not affect the cytokine bioavailability in the tumour microenvironment. (A-B) Control and CD8-IFNγR1KO mice were engrafted with B16F10-OVA. Tumours were harvested 12 to 15 days post-engraftment, and cytokines were quantified in the tumour supernatant by ELISA for IFNγ (**A**), and LegendPlex for other inflammatory cytokines represented by a heatmap (**B**). Data are from 2 independent experiments (n=16 for Control and n=11 for CD8-IFNγR1KO). The comparison between the 2 groups was analysed using an unpaired t-test on GraphPad Prism. ns = not significant.

4.1.3 Cytolytic functions *in vivo*

To assess the cytotoxic capacity of tumour-infiltrating CD8⁺ T cells, I investigated the surface expression of LAMP1, a marker of degranulation[320]. At the endogenous level, IFNγR1KO CD8⁺ T cells do not harbour a significant increase in degranulation as shown in **Figure 23A**. In addition, cells do not express more granzyme B and perforin, two critical effector molecules[321,322,323] (**Figure 23B**). This further shows that IFNγ sensing does not affect CD8⁺ T cell degranulation *in vivo* at the endogenous level. I confirmed these results using our transgenic antigen-specific CD8⁺ T cells. Indeed, tumour-infiltrating OTI cells either WT or IFNγR1KO harboured the same percent of cells that

had degranulated after *ex vivo* re-stimulation (**Figure 23C**). To further confirm that cytotoxicity was not affected by IFNγ-sensing, we performed *in vivo* cytotoxic assays. WT mice were engrafted with B16F10-OVA tumours and were adoptively transferred with either WT or IFNγR1KO OTI. After 5 days, CFSE labelled splenocytes were transferred into the mice: $CFSE^{high}$ cells were previously pulsed with OVA peptide rendering them targetable, while $CFSE^{low}$ cells were not targetable by OTI as they do not present OVA. 24 hours later, the percentage of target cells lysis was assessed to evaluate the cytotoxic function of OTI cells *in vivo*. IFNγR1KO $CD8^+$ T cells do not have enhanced killing function *in vivo* (**Figure 23D-E**). This overall suggested that increased tumour control in CD8-IFNγR1KO mice was not primarily due to increased $CD8^+$ T cell effector functions.

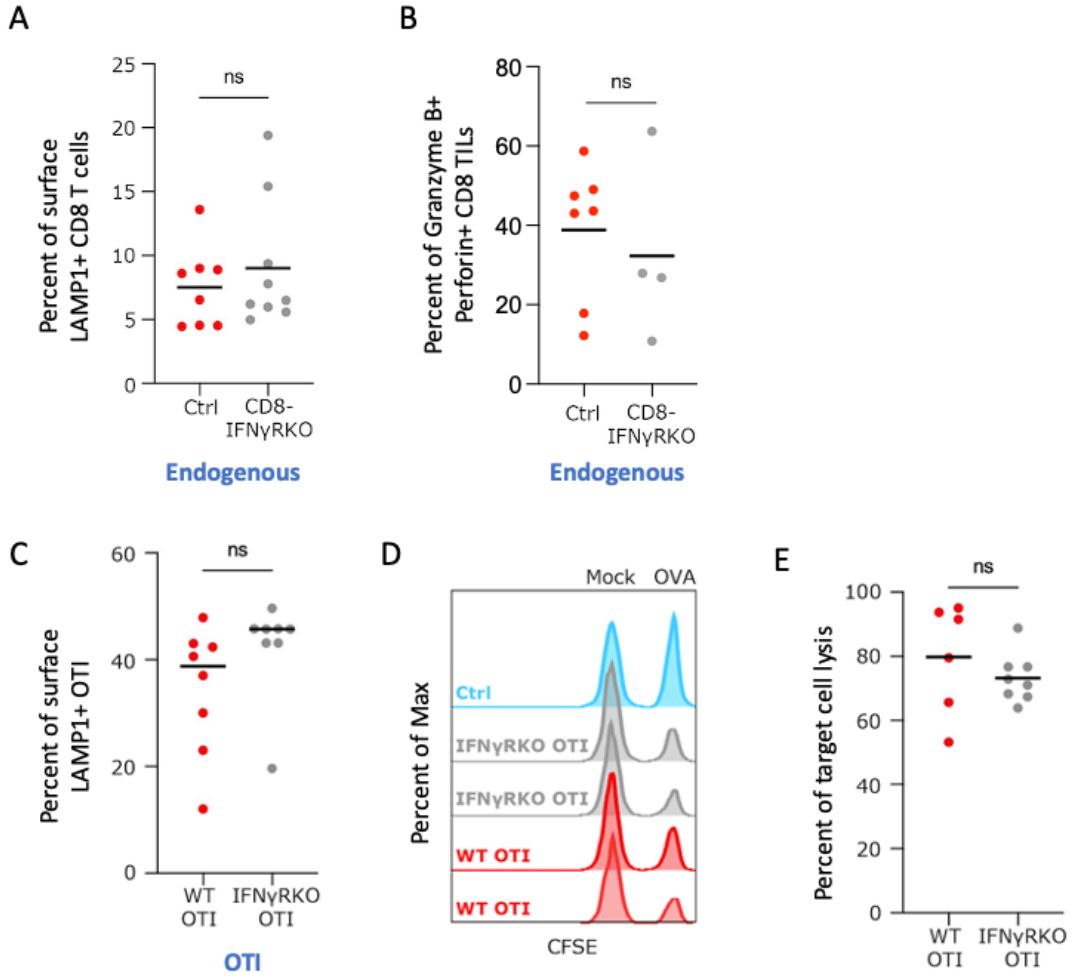


Figure 23: IFNγR1 ablation in CD8⁺ T cells does not affect their cytotoxic functions. (**A-B**) B16F10-OVA tumours were harvested between days 12 and 15 from control or CD8-IFNγR1KO mice. **A-** Cells were restimulated *in vitro* with 1µg OVA peptide for 6 hours in presence of Brefeldin A. The graph shows the quantification of surface LAMP1 staining. Data is from 2 experiments (n=8 for Control and n=9 for CD8-IFNγRKO). The comparison between the 2 paired groups was analysed using a paired t-test on GraphPad Prism. **B-** Cells were directly used and intracellularly stained for granzyme B and perforin (n=7 for Control and n=4 for CD8-IFNγRKO). (**C-E**) Tumour-specific CD8⁺ T cell cytotoxic functions were assessed both *ex vivo* and *in vivo*. **C-** WT mice bearing B16F10-OVA were transferred with Control (red) and IFNγR1KO (grey) OTI T cells. Tumours were harvested on days 5 to 7 after OTI transfer. LAMP1 expression on OTI cells was measured by flow cytometry after restimulation (n=8 per group). (**D-E**) WT mice bearing B16F10-OVA were transferred with Control (red) and IFNγR1KO (grey) OTI T cells. Mice were injected with CFSE labelled splenocytes (targets) pulsed with OVA ($CFSE^{high}$) or not ($CFSE^{low}$, Mock) 5 days after OTI transfer. After 24h, the percent of target lysis in the spleen was analysed by flow cytometry. **D-** Representative histogram of CFSE labelled targets after 24h. **E-** Graph shows quantification of cell lysis. Data is from 2 experiments (n=6 WT, n=8 KO). Unless stipulated, the comparison between the 2 groups was analysed using an unpaired t-test on

GraphPad Prism. ns = not significant. Some experiments were jointly performed with Jagdish Mahale.

4.2 IFNγ sensing affects CD8$^+$ T cell expansion *in vivo*

As IFNγR1KO CD8$^+$ T cells do not have enhanced effector functions compared to normal CD8$^+$ T cells, we investigated whether their expansion and abundance in the tumour could influence the better tumour control observed. This section investigates the CD8$^+$ T cell expansion *in vivo*.

4.2.1 Tumour infiltrating CD8$^+$ T cell absolute number

The previous section demonstrated that IFNγR1KO CD8$^+$ T cells were not significantly more functional than WT CD8$^+$ T cells. However, greater intra-tumoral abundance would likely result in increased killing of cancer cells and therefore improved overall tumour control. By assessing the absolute number of CD8$^+$ T cells in tumours, I demonstrated that IFNγR1KO CD8$^+$ T cells were found in greater numbers in tumours compared to control CD8$^+$ T cells at the endogenous level (**Figure 24A**). Furthermore, this increased number of IFNγR1KO CD8$^+$ T cells was independent of tumour volume (**Figure 24B**). A greater CD8$^+$ T cell population size can result from several concomitant mechanisms which I will explore in the next sections.

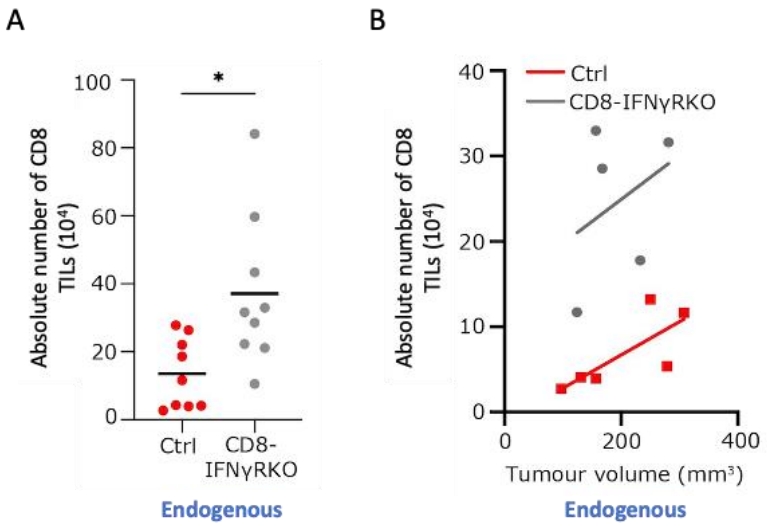


Figure 24: IFNγ sensing restricts the CD8⁺ T cell absolute number in B16F10-OVA tumours. (**A-B**) B16F10-OVA tumours were harvested between days 12 and 15, and cells were stained for CD3, CD8, and CD45 after ficoll to analyse the total number of CD8⁺ T cells per tumour (**A**, n=9 per group) and the number of CD8⁺ T cells according to the tumour volume (**B**, n=6 Control and n=5 CD8-IFNγRKO). The comparison between the 2 groups was analysed using an unpaired t-test on GraphPad Prism. * = P < 0.05.

4.2.2 Tumour infiltrating CD8⁺ T cell apoptosis level

Because IFNγR1KO CD8⁺ T cells were found in greater numbers in tumours, I wondered whether it was due to a better survival leading to a lower apoptosis rate. To investigate this, I assessed the level of active caspase 3 (or cleaved caspase 3), as a readout of apoptosis level. Indeed, caspase 3 has been shown to play a central role in apoptosis[324]. At the endogenous level, I did not observe any difference in cleaved caspase 3 levels (**Figure 25**), suggesting that the greater expansion of IFNγR1KO CD8⁺ T cells is not primarily due to decreased apoptosis compared to control CD8⁺ T cells in tumours.

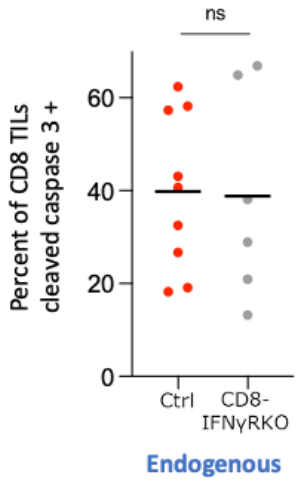


Figure 25: IFNγ sensitivity does not affect CD8⁺ T cell apoptosis level. B16F10-OVA tumours were harvested at day 12 post-engraftment and processed for flow cytometry. Cleaved caspase 3 was used as an apoptosis level readout. Data is from 2 independent experiments. The comparison between the 2 groups was analysed using an unpaired t-test on GraphPad Prism. ns = not significant.

4.2.3 Tumour infiltrating CD8⁺ T cell proliferation *in vivo* – OTI system

The second critical parameter involved in defining a cell population size is the proliferation rate. To assess the CD8⁺ T cell proliferation *in vivo*, I used naïve WT and IFNγR1KO tumour-specific CD8⁺ T cells that I co-transferred at a 1-to-1 ratio in WT tumour-bearing mice, as described in **Figure 26A**. After 5 days, we assessed the ratio of IFNγR1KO/WT OTI in tumours and in their draining lymph nodes. IFNγR1KO CD8⁺ T cells outcompeted their WT counterpart both in LN and tumours (**Figure 26B**). This demonstrated that IFNγR1KO CD8⁺ T cells expanded more than the WT *in vivo*.

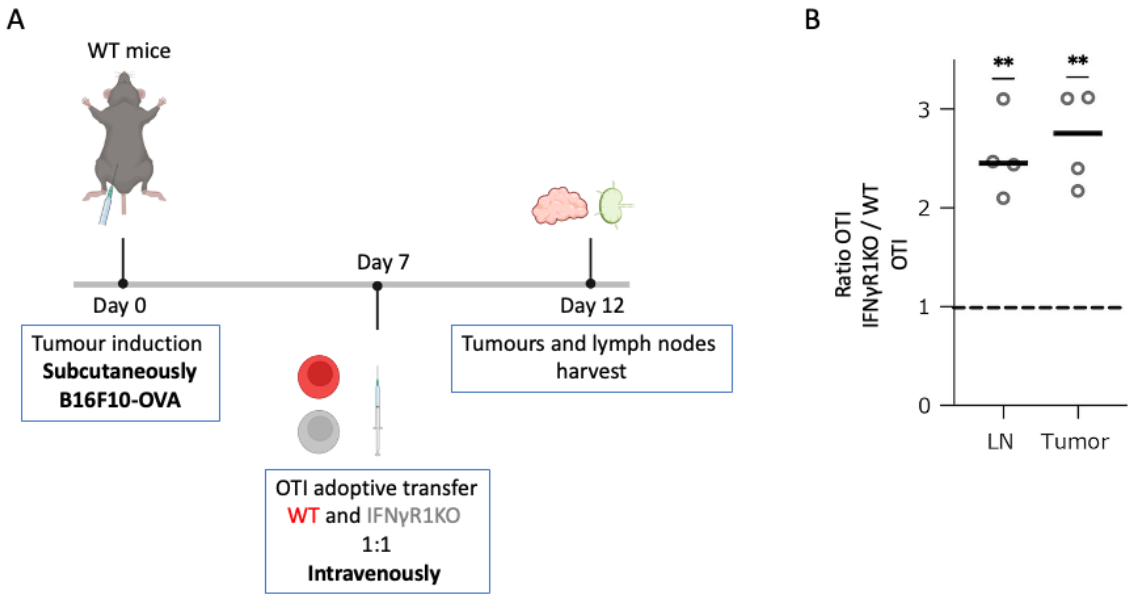


Figure 26: IFNγ restricts tumour-specific CD8⁺ T cell proliferation in tumours. A- Experimental design to assess OTI proliferation *in vivo*. **B-** Tumours and draining lymph nodes were harvested 5 to 7 days after OTI transfer, and cell suspensions were analysed by flow cytometry. The graph shows the ratio between the number of IFNγR1KO and WT OTI cells in lymph nodes (LN) and Tumours. Data are representative of 2 independent experiments. The comparison between the 2 groups within the same organ was analysed using a paired t-test on GraphPad Prism. ** = P < 0.002. [Created with BioRender.com]. Experiments were jointly performed with Jagdish Mahale.

To further confirm that IFNγ solely affects the proliferation and not cell activation, we performed an *in vitro* assay to evaluate the differences in activation between WT and IFNγR1KO OTI. WT and IFNγR1KO naïve OTI cells were primed with dendritic cells presenting different altered OVA peptides (N4, T4, and V4 with decreasing OTI affinity[206]), and evaluate their priming potential by assessing CD69 up-regulation, a marker of early activation[325]. Overall, we confirmed that IFNγR1KO OTI and WT OTI did not get differentially activated during priming **Figure 27**. We, therefore, confirmed that the increased proliferation observed in IFNγR1KO CD8⁺ T cells was not primarily due to more efficient cell priming.

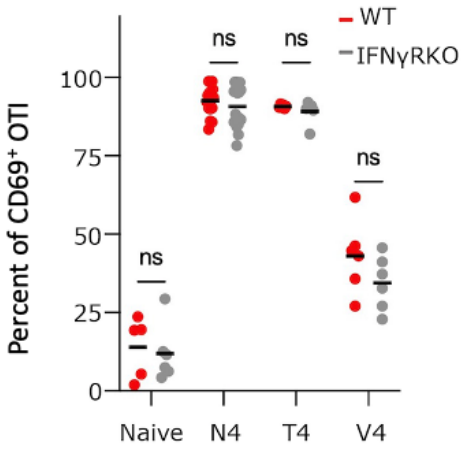


Figure 27: IFNγ sensing does not affect CD8⁺ T cell priming. WT and IFNγR1KO OTI were stimulated *in vitro* with BMDCs loaded with N4, T4, or V4 peptides. After 24h, OTI activation was quantified by CD69 expression using flow cytometry. The graph shows the percentage of CD69⁺ expressing OTI cells. Data is from 2 independent experiments. The comparison between more than 2 groups was analysed using two-way ANOVA on GraphPad Prism. ns = not significant. Experiments were performed by Jagdish Mahale.

4.3 IFNγ sensing affects CD8⁺ T cell tumour infiltration

While CD8-IFNγR1KO mice display increased CD8⁺ T cell intra-tumoral expansion (**Figure 24A-B**), this is often not sufficient to predict tumour immunity. Indeed, their localisation within the tumour microenvironment is also vitally important[326]. In recent studies, tumours have been classified based on several parameters such as their immune infiltration features. Thus, intra-tumoral T cell localisation has a major impact on tumour control[327]. Tumours can be divided into "cold", "hot", and "excluded" phenotypes[328,329,21]. In "cold" tumours (also referred to as "ignored" or "not-inflamed" in the literature), there is almost no immune infiltrate observed. Conversely, "hot" (also referred to as "inflamed") tumours display abundant tumour-infiltrating T lymphocytes

with inflammation and immune activation. Finally, in "excluded" tumours, there are immune cells within the tumour microenvironment, however, they are segregated and excluded from the core of the tumour[328,21,329,330]. Immune exclusion is correlated with poor clinical outcomes after immunotherapies in epithelial tumours such as in melanoma[331,332,21,333]. And B16F10 murine tumours have been reported with an excluded phenotype[334]. In our model, IFNγ sensing by $CD8^+$ T cells restricts their expansion *in vivo*, therefore IFNγR1KO $CD8^+$ T cells are found in greater numbers in tumours. If numbers can be the key, the $CD8^+$ T cell localisation in the tumour microenvironment is critical. Indeed, having more cells does not necessarily lead to better tumour core infiltration, and might not be sufficient to enhance tumour control.

In this section, I determined $CD8^+$ T cell localisation in the tumour microenvironment and investigated whether IFNγ affects $CD8^+$ T cell tumour infiltration through several means.

4.3.1 $CD8^+$ T cell tumour localisation – imaging and quantification

To assess the tumour localisation of $CD8^+$ T cells, I engrafted B16F10-OVA tumours in control and CD8-IFNγR1KO mice. Tumours were harvested after 12 to 15 days and processed as described in **Figure 28A**. Tumour cryosections were stained with antibodies against CD8a to visualise $CD8^+$ T cells (in green) and incubated with DAPI to see nuclei (in blue) while cancer cells express mCherry (in red). Tile scans were performed to examine $CD8^+$ T cell localisation throughout the tumour. Once obtained, I determined the $CD8^+$ T cell localisation and whether the cells were in stromal areas defined as $mCherry^-DAPI^+$ (blue spots) or properly infiltrating the tumour core defined as

mCherry^{+}DAPI^{+} (pink spots) **Figure 28B**. IFNγR1KO CD8^{+} T cells were observed at the tumour margin similarly to control CD8^{+} T cells. However, they were also greater found in the tumour nest while control CD8^{+} T cells remained mostly excluded **Figure 28C**. In line with these observations, tumours from control mice had an excluded phenotype, with most CD8^{+} T cells being localised at the margin or trapped within the stromal network, and only 30% were present in the tumour core. By contrast, IFNγR1KO CD8^{+} T cells were more infiltrated, with approximately 50% of CD8^{+} T cells in direct proximity to tumour cells (**Figure 28D**), suggestive of a hot phenotype. My data demonstrate that IFNγR1 ablation in CD8^{+} T cells improved their expansion and tumour infiltrating capabilities.

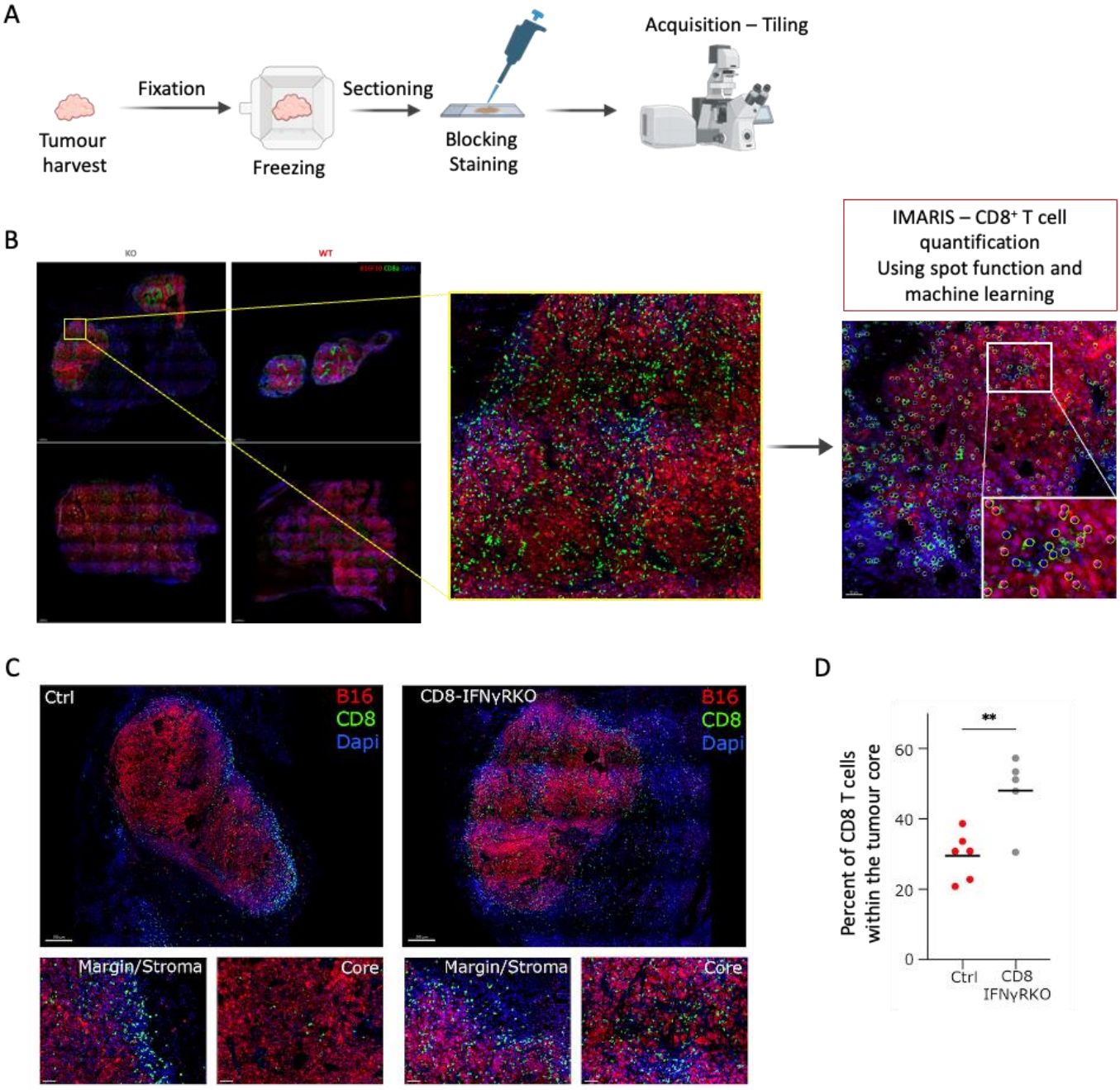


Figure 28: CD8⁺ T cell tumour localisation *in vivo*. A- B16F10-OVA tumours were harvested and fixed before freezing. Cryosections were stained to visualise CD8⁺ T cells. The acquisition was performed on a confocal microscope to image the entire tumours using tile functions. **B-** Methods used to quantify CD8⁺ T cell localisation. Tile scans from entire tumours either control or CD8-IFNγR1KO were obtained. Cancer cells are in red (mCherry⁺), CD8⁺ T cells are in green (CD8⁺) and nuclei are in blue (DAPI⁺). The Imaris software was used to quantify CD8⁺ T cells. The spot function determined CD8⁺ T cells and machine learning was used to specify whether the cell was in stromal areas (blue spots) or properly infiltrating the tumour core (pink spots). (**C-D**) Control and CD8-IFNγR1KO mice were engrafted with B16F10-OVA tumours. Tumours were harvested after 12 to 15 days and CD8⁺ T cell localisation was analysed by microscopy. The tumour core was defined as mCherry⁺DAPI⁺ regions. The stroma network and tumour margin

were defined as mCherry^{-}DAPI^{+} regions. **C-** Representative images of whole tumour sections from control (left panels) and CD8-IFNγR1KO (right panels) mice (n=6 control and n=5 CD8-IFNγR1KO). Scales bars represent 300μm for the upper images and 50μm for the lower images. **D-** Quantification of the proportion of CD8^{+} T cells present in the core of tumours from control (red) and CD8-IFNγR1KO (grey) mice. The comparison between the 2 groups was analysed using an unpaired t-test on GraphPad Prism. ** = P < 0.002 [Created with BioRender.com].

4.3.2 IFNγ effect on CD8^{+} T cell tumour recruitment

A better CD8^{+} T cell tumour infiltration can result from several mechanisms. Firstly, efficient tumour recruitment *via* tumour homing could explain the increased intra-tumoral presence of IFNγR1KO CD8^{+} T cells. T cell tumour homing results from a sophisticated molecular network, with cytokines and chemokine axes. Inflammatory chemokines are responsible for T cell recruitment to peripheral tissues for immune responses, this phenomenon is known as chemotaxis. In melanoma, better tumour-infiltrating T cells rate has been shown to correlate with the presence of CCL2, CCL3, CCL4, CCL5, CXCL9, and CXCL10 in human[335,336]. However, in our model, CCL2 levels were similar between control and CD8-IFNγR1KO tumours, with no significant differences in the soluble tumour microenvironment (**Figure 22B**). As dissecting molecular axes can be fastidious, we first evaluated whether IFNγ sensing by CD8^{+} T cells could affect their tumour homing *per se*. To test this, we *in vitro* activated OVA-specific CD8^{+} T cells. Effector WT OTI and IFNγR1KO OTI were ad-mixed at a 1-to-1 ratio and co-transferred in WT B16F10-OVA tumour-bearing recipient mice as explained in **Figure 29A**. 24 hours later, we assessed their recruitment by comparing the latter ratio in different organs: tumours, tumour-draining lymph nodes, spleens, and peripheral blood. Surprisingly, we

found that IFNγR1KO OTI had a strong defect in homing to tumours *in vivo* (**Figure 29B**). This suggests that IFNγ-sensing is required for efficient CD8⁺ T cell tumours homing in this model. Importantly, it highlighted the fact that increased tumour-infiltrating CD8⁺ T cell expansion and infiltration in CD8-IFNγR1KO mice could not be explained by increased tumour homing/recruitment. This also suggests that the mechanism by which IFNγR1KO CD8⁺ T cells expand in tumours is dominant and most likely happens within tumours as it compensates for the lack of tumour homing.

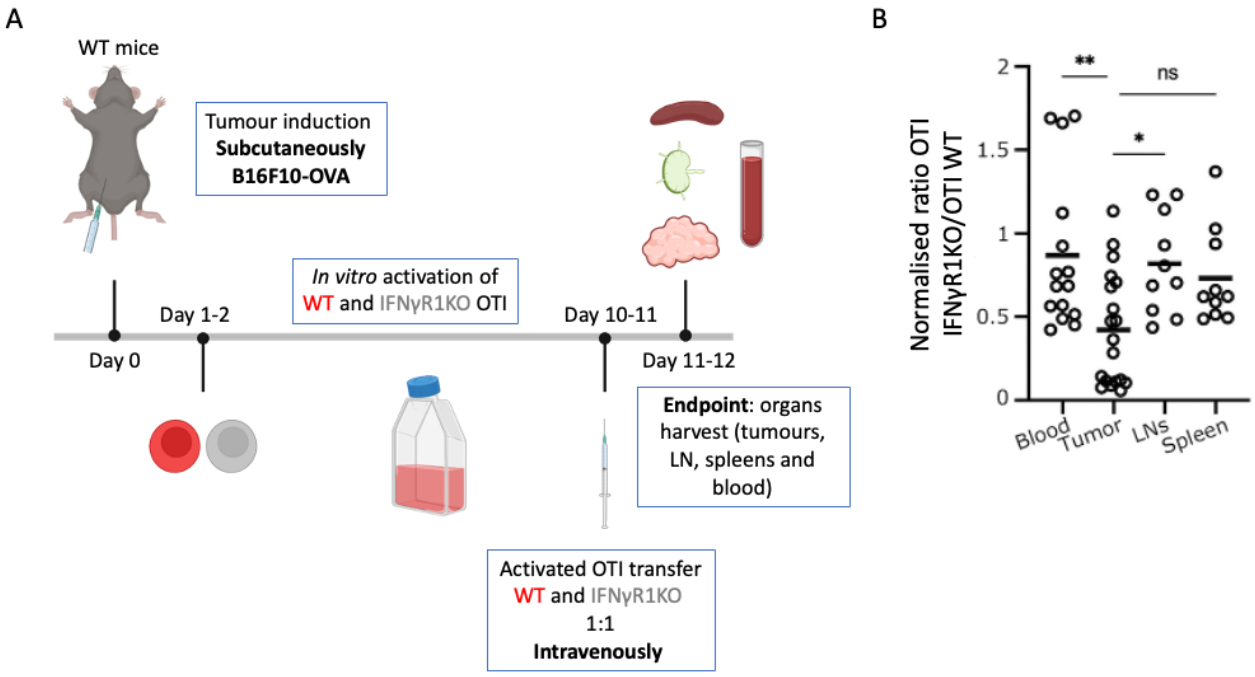


Figure 29: IFNγ sensing is required for effector CD8⁺ T cell tumour homing. A- Schematic workflow to assess tumour homing capability of effector tumour-specific CD8⁺ T cells *in vivo*. **B-** *In vitro* activated WT and IFNγR1KO OTI were ad-mixed and injected in B16F10-OVA tumour-bearing mice. After 24 hours, the ratio between IFNγR1KO and WT OTI was assessed in tumours, lymph nodes (LNs), spleens, and blood by flow cytometry. Data is from 2 independent experiments (n = 15 for blood, n=19 for tumours, n= 10 for LNs, and n= 10 for spleens). The comparison between more than 2 groups was analysed using one-way ANOVA on GraphPad Prism. ns = not significant, * = P < 0.05, ** = P <0.005. Experiments were performed by Gabriela Pirgova. [Created with BioRender.com].

Secondly, efficient tumour infiltration can be achieved with efficient CD8$^+$ T cell migration properties. In addition to tumour recruitment from the circulation or from LN, T cell migration properties are important to invade tumours to reach target cells[328,337,338,339]. IFNγ has been shown to greatly influence CD8$^+$ T cell migration both directly and indirectly[340,230,341,342,199,343]. It modifies their migration in tissues, for instance, in an IFNγ-deprived environment, CD8$^+$ T cells were found less motile, suggesting that IFNγ indeed enhances their motility[230]. In addition, IFNγ upregulates MHC-I on target cells and antigen-presenting cells which deeply influences their priming and binding to target cells. IFNγ also upregulates critical molecules for T cell migration such as adhesion molecules and integrins[92,344,345] but also involves potent CD8$^+$ T cells chemoattractants such as CXCL10[346,347,348]. Those examples are not exhaustive and IFNγ is again pleiotropic. Thus, I assessed the intrinsic migratory properties of WT *versus* IFNγR1KO OTI through *in vitro* activation and subsequent plating on fibronectin or ICAM-I-coated plates. Time-lapse imaging of CD8$^+$ T cell migration over time did not reveal significant differential patterns between WT and IFNγR1KO OTI (data inconclusive). Although *in vivo* data revealed defects in tumour homing by IFNγR1KO CD8$^+$ T cells (**Figure 29B**), my *in vitro* setup likely fails to recapitulate the complex tissue-specific features within the tumour microenvironment. As a result, future experiments may require *in situ* imaging to best visualize the movement of CD8$^+$ T cells within the tumour as opposed to *ex vivo* methods.

Thirdly, tumour invasion by CD8$^+$ T cells is greatly influenced by external cues. As previously mentioned, cell interactions and integrins can influence CD8$^+$ T cell migration therefore tumour invasion. On top of that, some physical barriers are at play in the

tumour microenvironment, such as the extracellular matrix protein network[349,350,] or the tumour vasculature[330,351,352].

$CD8^+$ T cells predominantly enter tumours *via* tumour-induced vasculature. Therefore, $CD8^+$ T cells interact with endothelial cells which can affect their biology, function, and tumour infiltration[353,354,355,356]. In line with this, I sought to investigate the endothelium phenotype in our model and whether that could influence the $CD8^+$ T cell differential localisation between control and CD8-IFNγR1KO tumours. Blood vessels were found throughout the tumour mass and were not segregated at the tumour margin both in control and CD8-IFNγR1KO mice (**Figure 30A**). This suggested that the localisation of IFNγR1KO $CD8^+$ T cells towards the tumour core was not due to a differential location of blood vessels. I further evaluated the endothelium quantity by looking at the proportion of endothelial cells out of total live cells from tumours by flow cytometry. Overall, there were no differences in the endothelium proportion between control and CD8-IFNγR1KO tumours (**Figure 30B**). However, the endothelium quality assessment revealed that endothelial cells in CD8-IFNγR1KO tumours expressed higher levels of CD105, a marker of active proliferation in endothelial cells[357] (**Figure 30C**). This suggests a more dynamic and permissive endothelium in CD8-IFNγR1KO; however, it is difficult to conclude whether it affects the $CD8^+$ T cell localisation in tumours, especially with the defect in tumour homing demonstrated previously (**Figure 29B**). Altogether, this indicates that the greater IFNγR1KO $CD8^+$ T cell abundance and infiltration in tumours is achieved by *in situ* proliferation rather than better survival, potent recruitment, or retention in tumours.

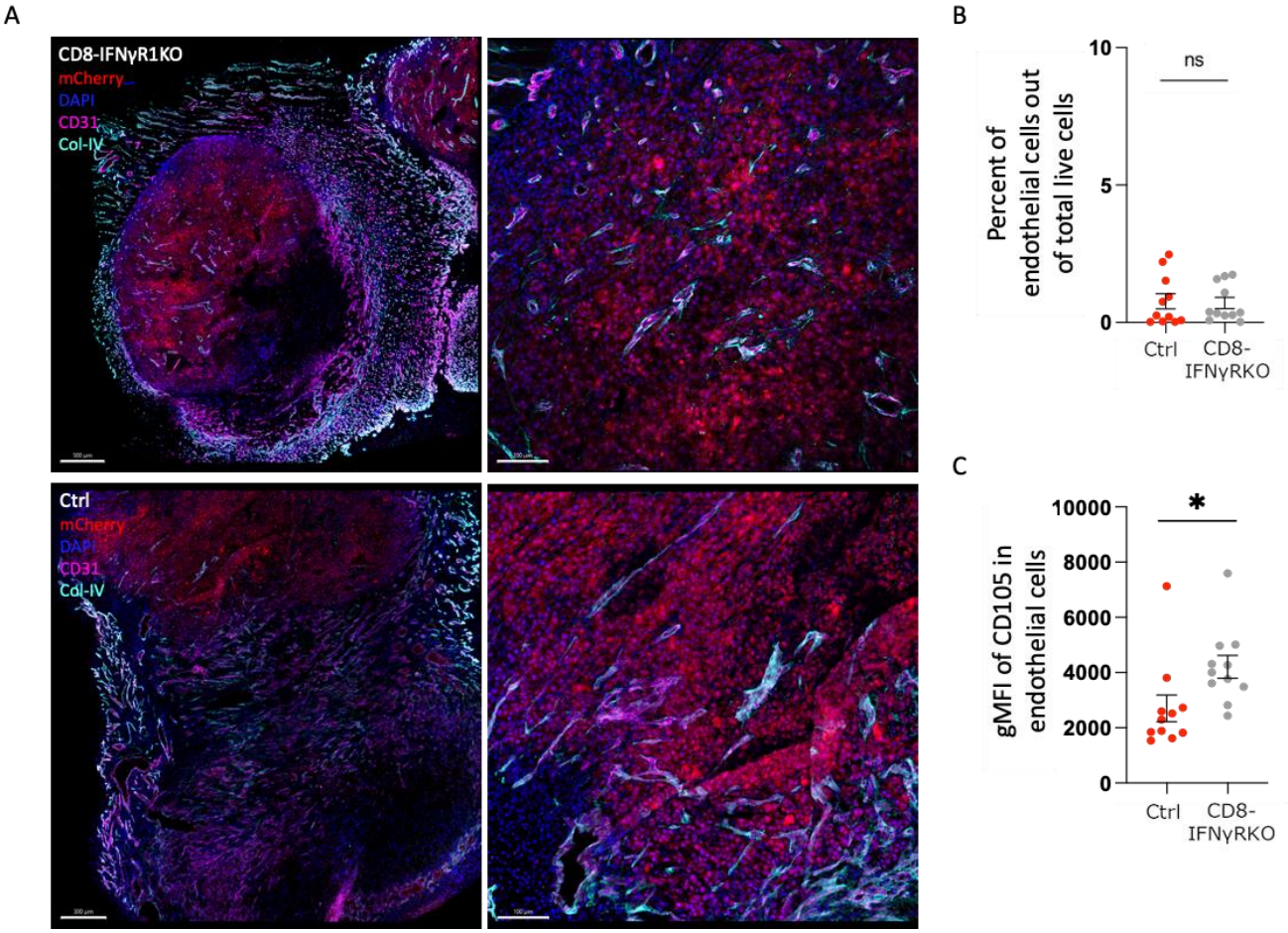


Figure 30: Tumour-associated endothelium assessment in control *versus* CD8-IFNγR1KO mice. (**A-C**) B16F10-OVA tumours were engrafted in control and CD8-IFNγR1KO mice. **A-** Representative images of tumours stained with antibodies against CD31 to visualise endothelial cells (in magenta) and collagen IV (in cyan). Cancer cell express mCherry (in red) and DAPI represent nuclei (in dark blue). Scale bars on the upper panel (CD8-IFNγR1KO) represent 500µm and 100µm respectively from left to right. Scale bars on the lower panel (control) represent 300µm and 100µm respectively from left to right. (**B-C**) Tumours were harvested after 12 days and processed for flow cytometry. Data is from 2 independent experiments. **B-** The graph shows the proportion of endothelial cells out of total live cells. **C-** The graph represents the level of CD105 expression in endothelial cells. The comparison between the 2 groups was analysed using an unpaired t-test on GraphPad Prism. ns = not significant, * = $P < 0.05$.

4.4 Discussion and conclusion

Results presented in this chapter demonstrate that IFNγR1 ablation in CD8$^+$ T cells does not substantially enhance intrinsic functional properties but increases overall CD8$^+$ T cell expansion and tumour infiltration despite inhibiting their tumour homing.

4.4.1 IFNγR1KO CD8$^+$ T cells are not intrinsically better effector cells

IFNγ sensing by CD8$^+$ T cells restricts their anti-tumour response. Indeed, IFNγR1KO CD8$^+$ T cells are better at controlling B16F10-OVA tumours *in vivo* which is not caused by enhanced effector functions. IFNγ sensing by CD8$^+$ T cells does not significantly affect their effector function both at the endogenous and the antigen-specific level. Of note, IFNγR1KO CD8$^+$ T cells appeared to be slightly better cytokine producers than control cells, and it was significantly the case for IFNγ production in our antigen-specific OTI system. If overall it is only a trend, I could still speculate that this slight increase could result from a particular small CD8$^+$ T cell population with more efficient effector functions. In those experimental setups, cells were re-stimulated to properly assess their capacity in producing cytokines. Those *ex vivo* experiments tested the intrinsic capacity of cells to produce cytokines, but it does not necessarily correlate with that cells produce *in vivo*. To properly investigate that, *in vivo* assessment would have been relevant with the injection of Brefeldin A 6 hours prior to tumour harvest for instance[358,359]. Nevertheless, by examining the cytokine level *in vivo* in the soluble tumour microenvironment I demonstrated that the cytokine bioavailability was not different between control and CD8-IFNγR1KO mice. This suggests that the lack of IFNγ-sensitivity

by $CD8^+$ T cells is not sufficient to change the IFNγ level *in vivo*. I concluded that cytokine secretion was not the key effector function leading to enhanced tumour control observed in CD8-IFNγR1KO mice. Similarly, IFNγ-sensing by $CD8^+$ T cells did not affect their cytotoxic functions, as assessed by *ex vivo* degranulation and *in vivo* cytotoxicity assay. To further my investigation, I also attempted to assess the surface LAMP1 expression *in vivo* by directly injecting antibodies intravenously in combination with brefeldin A prior to killing the mice. However, this was technically challenging and was not consistent. Another interesting parameter that would have been relevant to assess was the level of FAS-L expression in $CD8^+$ T cells. Indeed, they can use FAS-L – FAS interaction to trigger cell death in target cells[360,361]. Interestingly, $CD8^+$ T cells also express FAS, which could in return be a way to inhibit anti-tumour $CD8^+$ T cell response by the tumour microenvironment[362,363,364]. However, the fact that I did not see enhanced cytotoxicity *in vivo* highlights the fact that better effector functions, regardless of the precise mechanism, could not explain better tumour control observed. Regarding the cytotoxic assay, I sought of reproducing it *in vitro* to formally assess the intrinsic killing capability of $CD8^+$ T cells either IFNγR1KO or WT. But the fact that we did not find any differences *in vivo* suggests that it was not relevant to investigate this *in vitro* as we demonstrated that it does not occur in tumours and therefore would not explain the better tumour control exerted by IFNγR1KO $CD8^+$ T cells. Overall, IFNγ does not affect $CD8^+$ T cell effector functions *in vivo*.

4.4.2 IFNγ restricts CD8$^+$ T cell expansion in tumours

The cell population size in a particular organ, here a tumour, is the result of several mechanisms: cell recruitment, cell proliferation on site, cell death, and cell retention. IFNγ-sensing by CD8$^+$ T cells restricts their expansion in tumours. But this was not due to apoptosis as I detected a similar level of engaged apoptosis with cleaved-caspase 3 expression between IFNγR1KO and control CD8$^+$ T cells. Other techniques would have been relevant here, especially to investigate other types of cell death such as necrosis for instance. Nevertheless, the greater cell number would not be only explained by cell death as there are no differences in apoptosis and tumours were rarely necrotic (data not shown). But it would have been interesting to investigate the localisation of apoptotic cells in the two conditions by imaging, as IFNγR1KO and WT CD8$^+$ T cells were found in different localisation. The same cell death rate but happening preferentially in different areas could partially explain the different localisation patterns. In line with this, we intended to look at the survival potential of cells by assessing the Bcl2 (B-cell lymphoma 2) level of expression in CD8$^+$ T cells[365]. Results were not conclusive as it was technically challenging to detect any Bcl2 expression in cells by flow cytometry (data not shown). However, the single-cell RNA sequencing technique would be ideal to evaluate survival and cell death pathways in our model. We next sought to investigate CD8$^+$ T cell proliferation *in vivo*. Indeed, we attempted different experimental designs to assess the proliferation rate, such as staining of Ki67 an intracellular proliferation marker[366], and bromodeoxyuridine (BrdU) incorporation to follow cells that underwent proliferation[367] (data not shown), but the most relevant and convincing experiments were proliferation assays directly performed *in vivo*. Indeed, we used naïve tumour-specific OTI CD8$^+$ T cells

WT and IFNγR1KO co-transferred in the same host. This experimental design bypasses tumour microenvironment bias as cells were co-injected, therefore evolving within the same environment. In addition, our data demonstrated that IFNγ restricts $CD8^+$ T cell proliferation which was not due to more potent cell activation. Finally, to get further insight into mechanisms at play on the tumour site, we then investigated cell recruitment and localisation within tumours.

4.4.3 IFNγ is required for $CD8^+$ T cell tumour homing

The final critical parameter to study $CD8^+$ T cell expansion in tumours was to take into account tumour recruitment and retention. In this section, I am going to discuss the different parameters involved and some that I particularly investigated. $CD8^+$ T cell tumour recruitment is undoubtedly critical for anti-tumour responses[368,369,370,371,372]. Studies dissecting efficient tumour recruitment detailed several criteria involved: such as efficient $CD8^+$ T cell migration, tumour homing, cytokine and chemokine axis, and the presence of entry routes with vasculature with a permissive tumour microenvironment for example[373,374,375,376,377,356 among others]. Investigating cell migration in itself is not that straightforward as it results from a combination of numerous processes. In this review, several types of migration are described showing how much the environment as well as cell-intrinsic features influence the cell migration pattern[378]. I intended to use a simplistic approach by *in vitro* assessing $CD8^+$ T cell migration but it was not conclusive. Probably because it would have been required to screen a plethora of parameters to find the best condition possible recapitulating to a certain level the tumour environment, such as 3D migration settings, soluble cues, cell density, *etc.*

Consequently, the most accurate way to explore $CD8^+$ T cell differential migration patterns would have been to use multi-photon intravital imaging to follow cells directly migrating within tissues[282]. Even so, the fact that some control and IFNγR1KO $CD8^+$ T cells were found infiltrating the tumour core suggests that both $CD8^+$ T cells are able to migrate to a certain extent in our model. In regards to tumour homing, here again, it implies multiple parameters. To address this in a relevant manner, we *in vitro* activated tumour-specific $CD8^+$ T cells WT and IFNγR1KO to differentiate them into effector cells before co-injecting them at a 1-to-1 ratio into tumour-bearing mice. By evaluating the latter ratio 24 hours later we demonstrated that IFNγ is required for tumour homing. With reference to some published studies, this is not *per se* unexpected[379,92], but respecting the fact that IFNγR1KO $CD8^+$ T cells are greatly expanded in tumours this was surprising. Utterly, the defect in tumour homing suggests that the IFNγR1KO $CD8^+$ T cells greater expand within tumours rather than being more recruited from the circulation. Along with the tumour homing process, soluble cues are also essential for $CD8^+$ T cell tumour infiltration[380]. Cytokines and chemokines have been extensively studied and represent major networks supporting efficient immune responses[335,336,381,382]. Interestingly, key $CD8^+$ T cell attracting chemokines are IFNγ-inducible such as CXCL9 and CXCL10 creating an amplification loop to recruit more $CD8^+$ T cells on-site[335,383,347]. They would have been ideal candidates to assess their bioavailability between control and CD8-IFNγR1KO tumours at the endogenous level. However, the defect in tumour homing was demonstrated within the same hosts highlighting the fact that soluble cues were not the dominant factor influencing $CD8^+$ T cell infiltration in the model. In parallel, I did not perform an exhaustive cytokine and chemokine screening but evaluated a mix

of inflammatory cytokines that did not reveal any imbalance in the soluble players tested.

As IFNγ is required for $CD8^+$ T cell tumour homing, I hypothesised that IFNγ could also restrict their tumour core infiltration. Indeed, sensing IFNγ can attract $CD8^+$ T cells to the inflammatory site where NK cells are already there and secrete IFNγ for instance. But once arrived at the tumour, IFNγ concentration would most likely increase, and $CD8^+$ T cells would integrate IFNγ signalling. This could act as a "stop signal" stipulating they have reached the effector site, therefore would change their migration pattern and stop their further invasion. IFNγ insensitive or IFNγR1KO $CD8^+$ T cells would still be recruited to tumours by alternative attracting pathways but without the IFNγ-negative feedback loop, they could continue their progression into tumours, therefore infiltrating the tumour nest. To investigate this, I could optimise *in vitro* migration assays using WT-activated $CD8^+$ T cells. Treating the cells with a high enough concentration of IFNγ could in theory change their migration pattern. This is a reductive approach especially because IFNγ is so pleiotropic that it would have a lot of indirect effects *in vivo* that cannot be recapitulated *in vitro*. Alternatively, imaging IFNγ in tissue could give us a clue whether this hypothesis occurs *in vivo*. This is again technically challenging with the caveat that $CD8^+$ T cells also produce IFNγ themselves. It would be difficult to distinguish IFNγ secretion alone, but I could stain for NK cells and IFNγ at different time points to see $CD8^+$ T cell preferential arrival and whether WT $CD8^+$ T cells stay in IFNγ-rich areas compared to IFNγR1KO $CD8^+$ T cells for instance. Altogether, it is very hard to integrate every parameter but our functional assay suggests that IFNγ restricting effect on $CD8^+$ T

cell anti-tumour response takes place within tumours as IFNγR1KO CD8$^+$ T cells better infiltrate the tumour core compared to control CD8$^+$ T cells.

I then investigated whether the tumour-associated vasculature could play a role in their differential localisation. Regardless of their IFNγ sensitivity status, CD8$^+$ T cells could theoretically enter tumours similarly in both conditions at least in terms of localisation. Indeed, blood vessels were found at the tumour margin and within the tumour core both in control and CD8-IFNγR1KO conditions. The injections of anti-CD8 conjugated antibodies *in vivo* at different time points prior to tumour harvesting could help us delineate the preferred route of tumour entrance between control or IFNγR1KO CD8$^+$ T cells. However, tumour vasculature is documented as being aberrant, fragile, leaky, and with immunosuppressive properties[330,384,385]. The endothelium plays a pivotal role in CD8$^+$ T cell tumour infiltration, indeed, they are relying on them to extravasate and as they are interreacting, endothelial cells can influence CD8$^+$ T cell biology[352]. For example, the upregulation of FAS-L on endothelial cells can kill CD8$^+$ T cells that express FAS directly at the tumour entrance[386,387]. Endothelial cells can also upregulate inhibitory receptors that can alleviate CD8$^+$ T cell anti-tumour response such as PD-L1[388,389] and Tim-3[390,391]. In our model, I found similar endothelial cells proportion suggesting no massive differences in tumour vasculature distribution. However, in CD8-IFNγR1KO tumours, endothelial cells relatively expressed more CD105 compared to control tumours, illustrating a more proliferating endothelium[392,357]. Interestingly, ongoing proliferative endothelium sometimes with the presence of high endothelial venules, suggests increased vasculature leading to potentially greater CD8$^+$ T cell recruitment and on the contrary, studies demonstrated that increased presence of CD8$^+$

T cells leads to proliferating endothelium[393,394,395,396,397]. It is therefore nearly impossible to decide which of those caused the other. CD105 is also part of the hypoxia response element suggesting that CD8-IFNγR1KO tumours might contain more hypoxic regions[398,399]. The level of hypoxia is another parameter that can influence $CD8^+$ T cell localisation, migration pattern, and biology within the tumour microenvironment.

Finally, $CD8^+$ T cell tumour retention is also resulting from a plethora of parameters: changes in chemokine and chemokine receptor pairing, level and variety of integrins and selectins expressed, interactions with other immune cells such as tumour-associated macrophages, or stromal cells such as fibroblasts, and extracellular matrix proteins network for instance. The best way to formally investigate $CD8^+$ T cell tumour retention would be to photoconvert tumour-infiltrating $CD8^+$ T cells and trace them over time to assess whether they stay in tumours or recirculate in the system[400,401,402].

As IFNγ and $CD8^+$ T cells are central in many aspects of the immune response, we kept in mind that IFNγ insensitivity of $CD8^+$ T cells could also lead to indirect effects, such as changes in the tumour microenvironment, in the end, affecting their infiltration. Again, the tumour microenvironment is so diverse that it would be very challenging to be exhaustive with covering every aspect. Most of those open questions can be screened by scRNA sequencing data by looking at relevant cellular pathways in $CD8^+$ T cells with in-depth analysis for instance. Furthermore, as we did not see obvious differences between control and IFNγR1KO $CD8^+$ T cells at the endogenous level, scRNA sequencing could help us investigate the different $CD8^+$ T cell subsets and relevant pathways in cells.

4.4.4 Conclusion

Data presented in this chapter demonstrated that IFNγ-sensing by $CD8^+$ T cells limits anti-tumour immunity, $CD8^+$ T cell expansion, and localisation to the core of the tumour while enhancing $CD8^+$ T cell tumour homing. As it was difficult to delineate significant differences at the $CD8^+$ T cell population level, we next investigated the different tumour immune microenvironment, notably the different $CD8^+$ T cell subsets in tumours using single-cell RNA sequencing to elucidate the relevant parameters induced by IFNγ-sensing that limits $CD8^+$ T cell-dependent anti-tumour immunity.

5. IFNγ sensing influences CD8$^+$ T cells at the subset population level

This chapter investigates how IFNγ affects the different CD8$^+$ T cell subsets present in tumours and whether it influences the immune tumour microenvironment in general. Single-cell RNA sequencing data helped to gain further insights into the role of IFNγ on CD8$^+$ T cells in a tumour context. Findings were also assessed functionally with *in vivo* experiments.

5.1 IFNγ sensing regulates tumour-infiltrating but not CD8$^+$ T cells from lymph nodes

This section investigates the overall difference between control and IFNγR1KO CD8$^+$ T cells from tumour-draining lymph nodes and tumours. We first used scRNA-seq data to identify CD8$^+$ T cell clusters regardless of their IFNγ sensitivity status before assessing the impact of IFNγ on CD8$^+$ T cells by comparing control and IFNγR1KO CD8$^+$ T cells in the next section.

5.1.1 Single-cell RNA sequencing analysis comparing control and IFNγR1KO CD8$^+$ T cells – the setup

In the previous chapter, I demonstrated that IFNγ does not significantly affect CD8$^+$ T cell function in tumours. However, I investigated CD8$^+$ T cells at the population level. To

go further, scRNA-seq was suited to assess the role of IFNγ on CD8⁺ T cell anti-tumour response at the single-cell level as significant functional differences were not detected at the endogenous level *in vivo*. ScRNA-seq data would allow us to look at different CD8⁺ T cell sub-populations in-depth which will then guide me to some extent. The experimental design followed is depicted in **Figure 31A**. Control and CD8-IFNγR1KO mice were engrafted with B16F10-OVA tumours. After 12 days, tumours and their draining lymph nodes were harvested. I processed tumours and LN and prepared them for CD8⁺ T cell sorting following the gating strategy detailed in **Figure 31B**. Sorted CD8⁺ T cells were then subjected to single-cell RNA sequencing.

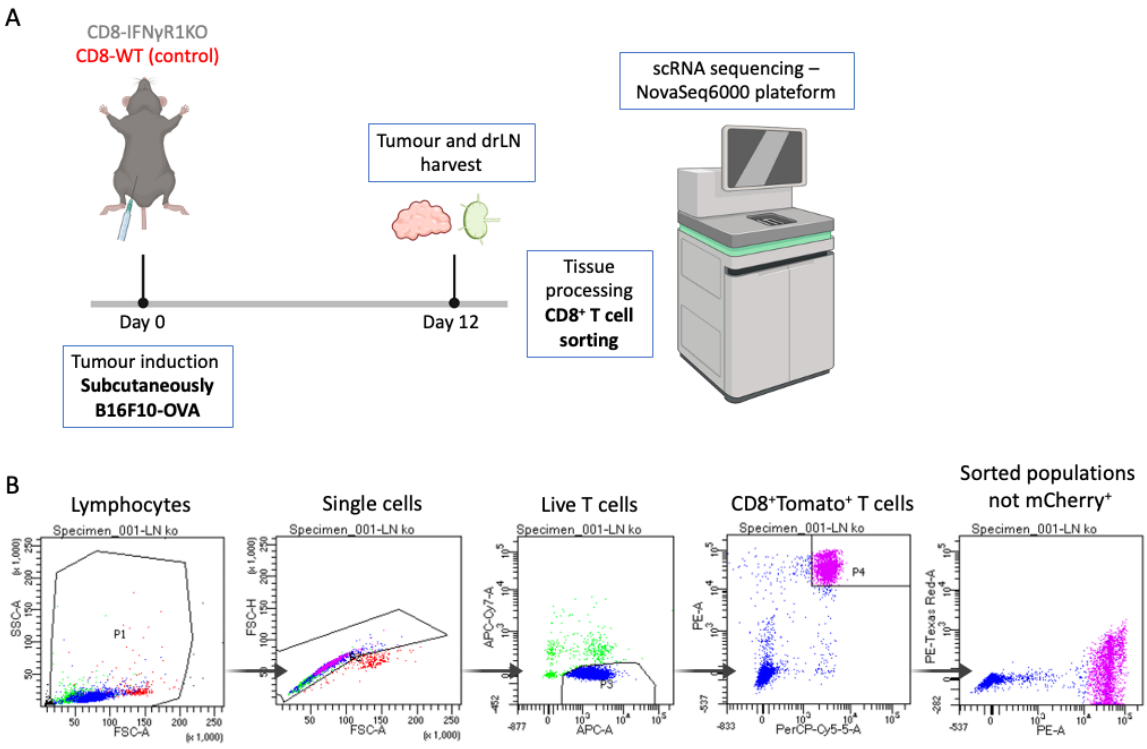


Figure 31: Sorting of CD8⁺ T cells from tumours and draining lymph nodes prior to single-cell RNA sequencing. Control (n=3) and CD8-IFNγR1KO (n=3) mice were engrafted with B16F10-OVA tumours. CD45⁺CD3⁺CD8⁺Tomato⁺ cells were sorted from tumours and draining lymph nodes (drLN) and subjected to scRNA-sequencing analysis. **A-** Workflow to isolate CD8⁺ T cells from B16F10-OVA tumours and their draining lymph nodes. **B-** Gating strategy for CD8⁺ T cell sort. [Created with BioRender.com]

Firstly, to investigate whether IFNγ would affect CD8⁺ T cells in tumour-draining lymph nodes or directly at the tumour site, differential gene expression analysis between control and IFNγR1KO CD8⁺ T cells isolated from draining lymph nodes and tumours was performed. Cells from LN and tumours formed distinct clusters (**Figure 32A**). Interestingly, there was only a few differentially expressed transcript detectable in LN, suggesting that IFNγ does not have a potent effect on CD8⁺ T cells in LN in our model (**Figure 32B**). Differential gene expressions were observed in CD8⁺ T cells isolated from tumours (**Figure 32C**). We therefore focused our analysis on tumour samples. Additionally, this further suggests that the better anti-tumour response in CD8-IFNγR1KO mice solely happens at the tumour site.

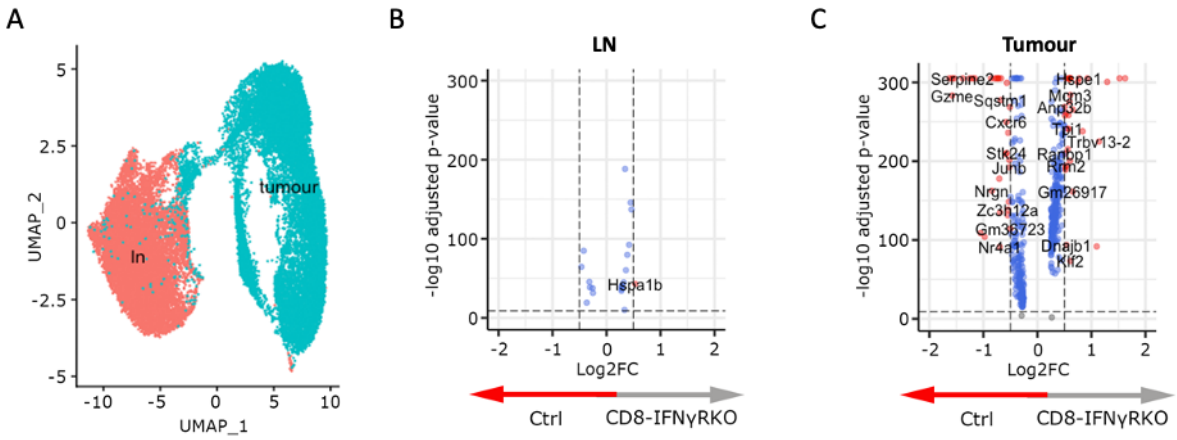


Figure 32: CD8⁺ T cell unbiased characterisation in lymph nodes and tumours from control and CD8-IFNγR1KO mice by scRNA-seq. Control (n=3) and CD8-IFNγR1KO (n=3) mice were engrafted with B16F10-OVA tumours. CD45⁺CD3⁺CD8⁺Tomato⁺ cells were sorted from tumours and draining lymph nodes and subjected to scRNA-seq analysis. **A-** UMAP embeddings of merged scRNA-seq profiles from tumour and lymph node (ln) CD8⁺ T cells. (**B-C**) Volcano plot representing differentially expressed genes between control and CD8-IFNγR1KO CD8⁺ T cells from LN (**B**) and tumour (**C**). Blue dots: genes with an adjusted p value<0.05; Red dots: genes with log2 (fold-change) value >0.5 or <-05 and an adjusted p value<0.05. ScRNA-seq analysis was performed by Audrey Gerard.

5.2 IFNγ sensing by CD8$^+$ T cells affects their intra-tumoral proportion *in vivo*

In the previous section, the scRNA-seq revealed that IFNγ affects CD8$^+$ T cells that are at the site of the tumour. In parallel, as IFNγ and CD8$^+$ T cells are critical and central in anti-tumour responses, I first wanted to assess whether IFNγ-insensitivity in CD8$^+$ T cells could lead to changes in the general immune tumour microenvironment. I then focused on the different intra-tumoral CD8$^+$ T cell subsets defined by the scRNA-seq.

5.2.1 Immune composition remodelling in tumours: control *versus* CD8-IFNγR1KO

As IFNγR1KO CD8$^+$ T cells were found in greater numbers in tumours, most likely due to their increased proliferative capacity, I investigated whether only CD8$^+$ T cells were affected or whether indirect effects triggered could lead to immune landscape remodelling which can also influence the CD8$^+$ T cell tumour localisation. To do so, I further characterised the tumour immune landscape and looked at the relative proportion of immune cells in CD8-IFNγR1KO *versus* control mice. I designed two flow cytometry panels to characterise the lymphoid (**Figure 33A**) and myeloid compartment (**Figure 33B**). I looked at the main immune cell populations with the cell marker combinations used listed in (**Table 8**).

Cell population	markers	Panel
Total immune cells	live > CD45+	Both
T cells	CD3+	Lymphoid
B cells	CD19+ CD3-	
CD8+ T cells	CD3+ CD8+	
CD4+ T cells	CD3+ CD4+	
Tregs	CD3+ CD4+ FoxP3+	
NK cells	CD19- CD3- NK1.1+	
NKT cells	CD3+ NK1.1+	
Lymphoid cells	DUMP = CD3+ and CD19+	Myeloid
Neutrophils	CD11b+ Ly6G+	
Monocytes	CD11b+ Ly6C+ MHC-II-	
Inflamatory monocytes	CD11b+ Ly6C+ MHC-II+	
Macrophages	CD11b+ Ly6C- MHC-II+ F4/80+	
TAM1	CD11b+ Ly6C- MHC-II+ F4/80+CD11c-	
TAM2	CD11b+ Ly6C- MHC-II+ F4/80+CD11c+	
Dendritic cells	CD11b+ MHC-II+ CD11c+	

Table 8: Marker combinations used to phenotype immune cell populations in tumours.

Overall, I did not find any significant differences in immune cell population proportions between CD8-IFNγR1KO and control tumours at day 12 (**Figure 34**). Apart from T cells and particularly $CD8^+$ T cells, there were no interesting trends of immune cell population modulation both from lymphoid and myeloid compartments. From this snapshot, it is difficult to speculate any immune landscape remodelling, however, in this particular set of experiments, tumours were from similar sizes between IFNγR1KO and control mice (data not shown). Furthermore, it was done at a particular time point and does not reflect the dynamic immune microenvironment. As I did not pinpoint any significant trends, I decided to not investigate further in that direction, but focus on $CD8^+$ T cell subsets.

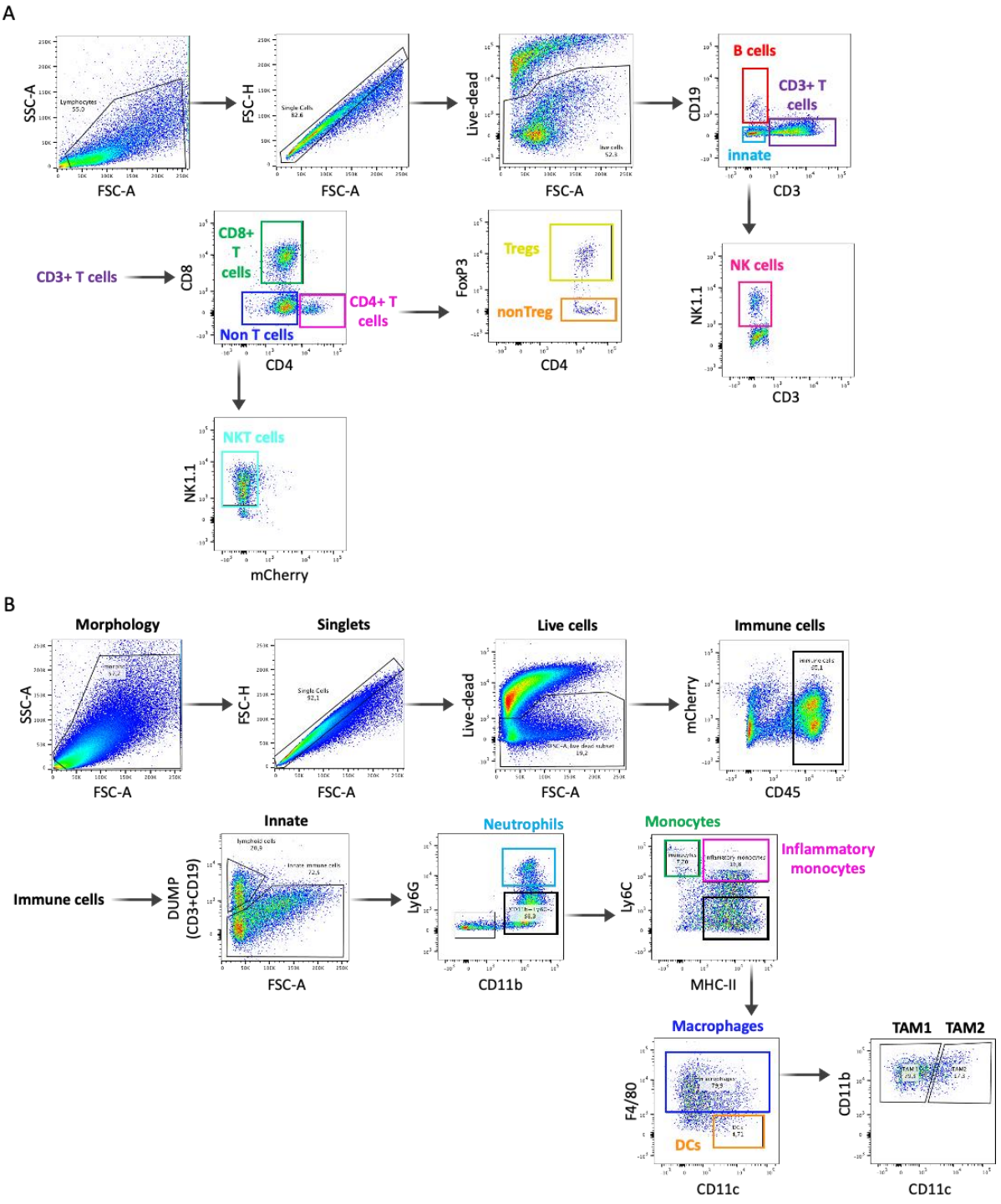


Figure 33: Flow cytometry gating strategy to assess immune composition remodelling within B16F10-OVA tumours. A- Panel focusing on lymphoid cells. **B-** Panel focusing on myeloid cells.

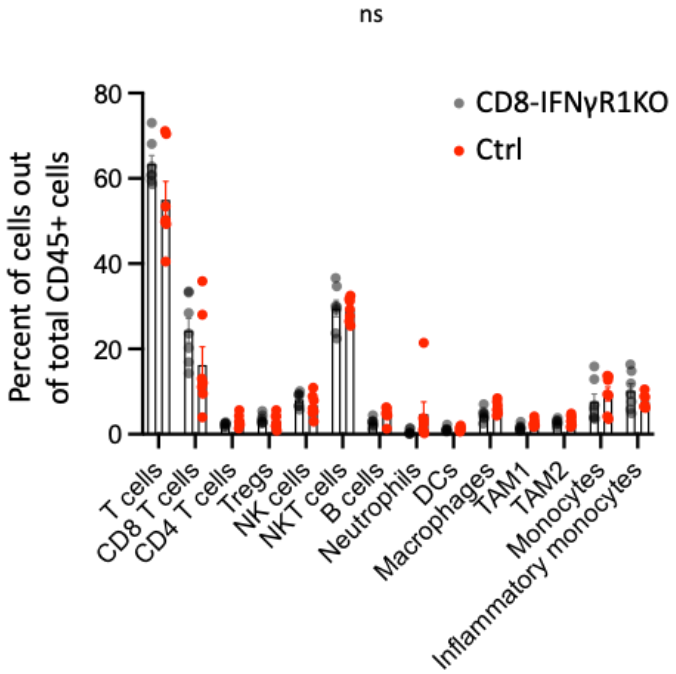


Figure 34: Immune composition proportion from B16F10-OVA tumours in control *versus* CD8-IFNγR1KO mice. B16F10-OVA tumours were harvested on day 12 and processed for flow cytometry staining (n=7 per group). Immune cell populations were assessed following the gating strategy detailed in **Figure 33**. The comparison between more than 2 groups was analysed using two-way ANOVA on GraphPad Prism. ns = not significant.

5.2.2 Intra-tumoral CD8⁺ T cell population proportion *in vivo*: control *versus* CD8-IFNγR1KO

In order to compare intra-tumoral control *versus* IFNγR1KO CD8⁺ T cells, unsupervised hierarchical clustering was used to determine CD8⁺ T cell cluster populations. As a result, 3 main cell states were used in the following analysis: stem-like T cells, exhausted T cells, and bystander-like, as shown in **Figure 35A**. Additionally, relevant gene signatures were then applied to confirm the nature of the clusters **Figure 35B**. The stem-like T cell cluster has a strong stem-like gene signature and was defined

using relevant markers (including Tcf1/7, Il-7r, Ccr7), the exhausted cluster contains the range of exhausted cells, and the bystander-like cluster was defined as it has no TCR signature but harbour some activation markers. To assess whether IFNγ sensitivity can broadly affect $CD8^+$ T cell subset proportions in tumours, the frequency of the different cell states was calculated. Tumour-infiltrating IFNγR1KO $CD8^+$ T cells contain more cells that belong to the stem-like cell state compared to control cells (**Figure 35C**). This suggests that IFNγ-sensing may particularly affect stem-like T cells in tumours. In parallel, there were no significant differences in cell proportion regarding the exhausted and bystander-like clusters in the scRNA-seq data (**Figure 35C**). To further confirm the increased stem-like T cell frequency in CD8-IFNγR1KO tumours, I assessed their presence in tumours by flow cytometry using the marker combination $CD8^+PD\text{-}1^+Tcf1^+$. Consistently, the tumour-infiltrating IFNγR1KO $CD8^+$ T cell population contains a higher proportion of stem-like T cells compared to control $CD8^+$ T cells (**Figure 35D**). In conclusion, IFNγR1 ablation in $CD8^+$ T cells induced the accumulation of intra-tumoral stem-like T cells.

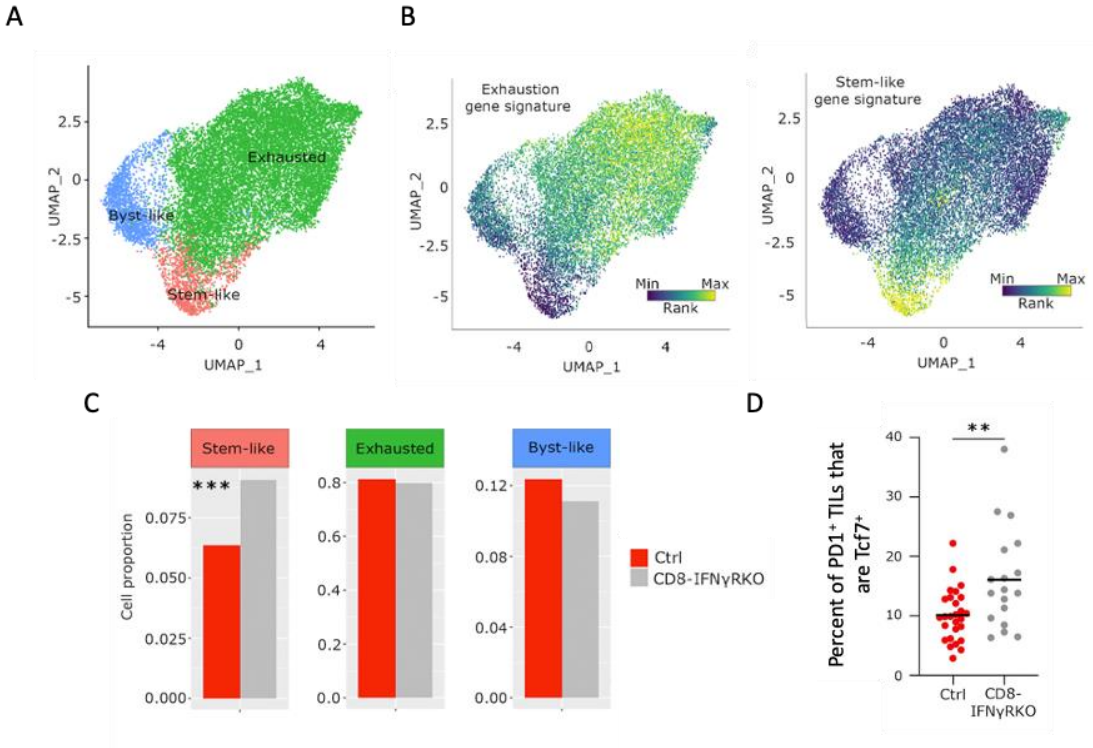


Figure 35: IFNγ sensing affects CD8⁺ T cell clusters proportion. Control and CD8-IFNγR1KO mice were engrafted with B16F10-OVA tumours. (**A-C**) $CD45^+CD3^+CD8^+Tomato^+$ cells were sorted from tumours and subjected to scRNA-seq analysis. **A-** Graph-based clustering (n = 15706 total) of the assembled cell states according to the signatures identified. **B-** UMAP visualization of $CD8^+$ T cell terminal exhaustion signature and $CD8^+$ T cell stem-like signature. **C-** The bar plots show the percentages of $CD8^+$ T cells from Control (red) and CD8-IFNγR1KO (grey) mice that were found in each cell state. ScRNA-seq analysis was performed by Audrey Gerard. Analysis of the difference between the proportion of cells in clusters between two scRNA-seq samples was analyzed with the R package "scProportionTest", which uses a permutation test to calculate the p-value for each cluster/cell state, and a confidence interval for the magnitude difference. **D-** Tumours were harvested 10-12 days post-tumour engraftment and cell suspensions were stained for CD45, CD3, PD-1, and Tcf1/7 and subjected to flow cytometry. The graph shows the percentage of $Tcf1/7^+$ $PD\text{-}1^+$ $CD8^+$ T cells in tumours from Control (red) and CD8-IFNγR1KO (grey) mice (n=27 for Ctrl; n=18 for CD8-IFNγRKO). The comparison between the 2 groups was analysed using an unpaired t-test on GraphPad Prism. Data are from 4 independent experiments. ** = $P < 0.002$, *** = $P < 0.001$.

5.3 IFNγ-sensing reinforces the overall CD8$^+$ T cell exhaustion in tumour

This section focuses on the CD8$^+$ T cell exhausted population as they are: 1) the most abundant in tumours and 2) they contain the effector cells. In **Chapter 3**, I determined that IFNγR1 deletion in CD8$^+$ T cells did not significantly affect their cytotoxic functions. With the use of scRNA-seq data, I aimed to further characterise the function of IFNγ-sensing by exhausted T cells and unbiasedly assess the impact of IFNγ sensing in CD8$^+$ T cells during anti-tumour response.

5.3.1 Focus on the IFNγ effect on CD8$^+$ T cell exhaustion

To directly investigate whether IFNγ affects exhaustion, differential pathways analysis was performed comparing exhausted CD8$^+$ T cells from control and CD8-IFNγR1KO tumours. As expected, we observed the downregulation of IFNγ-response and JAK-STAT signalling pathways in IFNγR1KO exhausted T cells. Interestingly, pathways related to apoptosis, chemokine, and cytokine cell signalling were downregulated in IFNγR1KO exhausted T cells (**Figure 36**). Most enriched pathways in IFNγR1KO exhausted CD8$^+$ T cells were related to metabolism (**Figures 36A** and **36B**). Pathways related to oxidative phosphorylation, fatty acid metabolism, and glycolysis were significantly upregulated in tumour-infiltrating exhausted IFNγR1KO CD8$^+$ T cells compared to control cells. This suggests that the cells are more metabolically active.

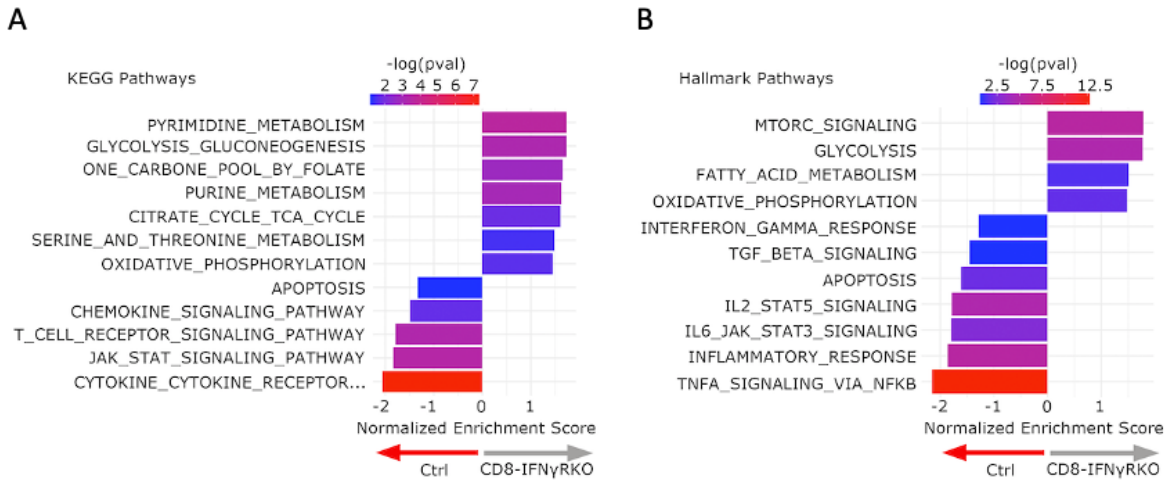


Figure 36: Differential pathways analysis in exhausted CD8⁺ T cells from control and CD8-IFNγR1KO tumours. (**A-B**) Control (n=3) and CD8-IFNγR1KO (n=3) mice were engrafted with B16F10-OVA tumours. CD45⁺CD3⁺CD8⁺Tomato⁺ cells were sorted from tumours and subjected to scRNA-seq analysis. Bar plots show the NES of chosen KEGG (**A**) and Hallmark (**B**) pathways up- and down-regulated in CD8-IFNγR1KO *vs* control Exhausted TILs. Bars are coloured by adjusted p-values. ScRNA-seq analysis was performed by Audrey Gerard.

Glycolysis and oxidative phosphorylation (oxphos) are the two main metabolism pathways providing energy for cells[403,404]. Further analysis showed that both glycolysis and oxphos gene signatures were mainly observed in the exhausted cell state (**Figure 37A**), but not in the stem-like cluster which is consistent with the fact that stem-like T cells are mainly quiescent[148]. Comparison between control and IFNγR1KO exhausted CD8⁺ T cells, revealed that IFNγR1KO tumour-infiltrating CD8⁺ T cells displayed increased glycolysis (**Figure 37B**) and oxphos scoring (**Figure 37C**). As glycolysis and oxphos are differentially regulated, this suggests that IFNγR1KO CD8⁺ T cells are potentially more capable of adaptation *in vivo* with those increased pathways at the transcriptional level.

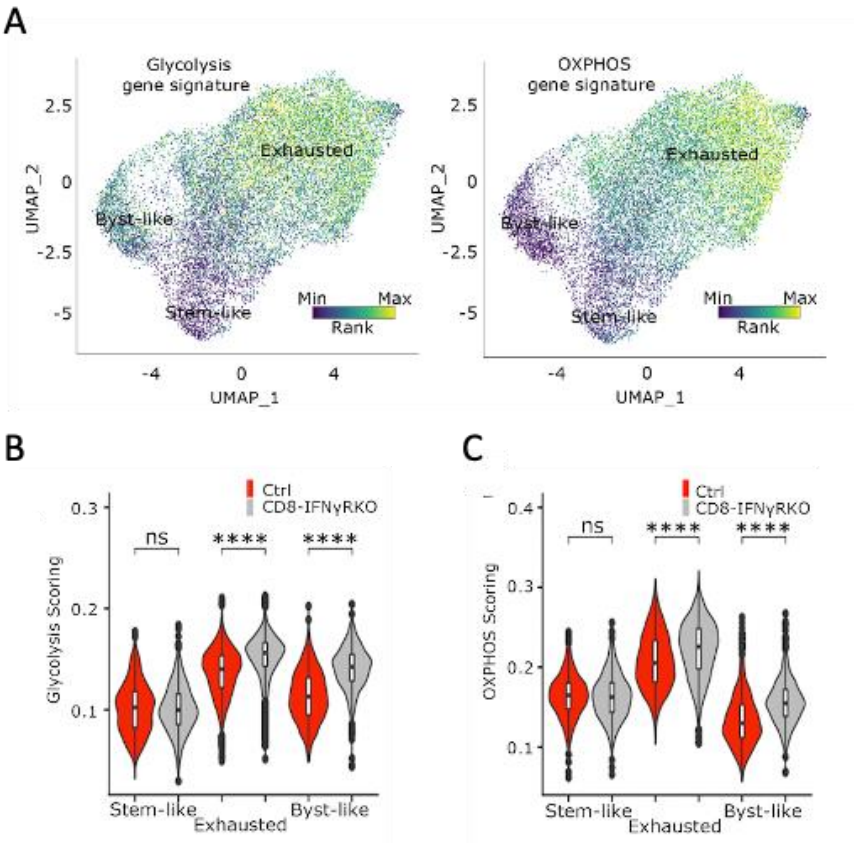


Figure 37: IFNγ-sensing influences the metabolic status of exhausted CD8⁺ T cells at the transcriptional level. (**A-C**) Control (n=3) and CD8-IFNγR1KO (n=3) mice were engrafted with B16F10-OVA tumours. CD45⁺CD3⁺CD8⁺Tomato⁺ cells were sorted from tumours and subjected to scRNA-seq analysis. **A-** UMAP visualization of Glycolysis gene signature (left) and OXPHOS gene signature (right). **B-** Violin plots show Glycolysis scoring of Control (red) and CD8-IFNγR1KO (grey) mice within each cell state. **C-** Violin plots show Oxphos scoring of Control (red) and CD8-IFNγR1KO (grey) mice within each cell state. ns = not significant, **** = P < 0.0001. ScRNA-seq analysis was performed by Audrey Gerard.

5.3.2 IFNγ-sensing is not sufficient to alter CD8⁺ T cell metabolism *in vivo*

Increased metabolism-related transcripts could reflect truly increased metabolism, or rather indicate indirect consequences of activation or environmental adaptation. Based on the scRNA-seq data, I next examined the metabolic status of exhausted CD8⁺ T cells *ex vivo* from control and CD8-IFNγR1KO tumours. B16F10-OVA tumours were

harvested after 12 days in control and CD8-IFNγR1KO mice, processed, and cells were stained to assess their mitochondrial functions by flow cytometry (**Figure 38**). Exhausted $CD8^+$ T cells (gated as live $CD8^+$LAG-3^+ T cells) from tumours either control or IFNγR1KO harbour similar mitochondrial bioenergetics as shown by the relative uptake of mitochondrial dyes[405,406] (**Figure 38A** and **38B**). To get a better insight into cell metabolism occurring *in vivo*, we assessed the bioenergetic cellular (BEC) index which measures the dependence on respiratory capacity over glycolysis rate[407]. The quantification of the BEC index calculated by the ratio between β-F1-ATPase (ATPB) and GAPDH revealed no difference between $CD8^+$ T cells from control or CD8-IFNγR1KO tumours (**Figure 38C**). Similarly, $CD8^+$ T cells harboured similar glucose transporter 1 (GLUT-1)-dependent glycolysis regardless of their IFNγ-sensitivity (**Figure 38D**), suggesting similar ATP production levels through GLUT-1-dependent aerobic and anaerobic glycolysis. As there are hypoxic regions in the tumour microenvironment[408], this could naturally lead to an increase in anaerobic glycolysis with the upregulation of lactate dehydrogenase A (LDHA) expression in cells as an adaptation mechanism. IFNγR1KO exhausted $CD8^+$ T cells displayed a lower level of LDHA expression (**Figure 38E**), even though it is not significant, this suggests that IFNγR1KO $CD8^+$ T cells relied less on anaerobic glycolysis. Overall, this *ex vivo* data demonstrated that the general metabolism pathways increased at the transcriptional level observed in IFNγR1KO $CD8^+$ T cells is not recapitulated *in vivo*, therefore suggesting environmental adaptation rather than an intrinsic enhanced metabolism capacity.

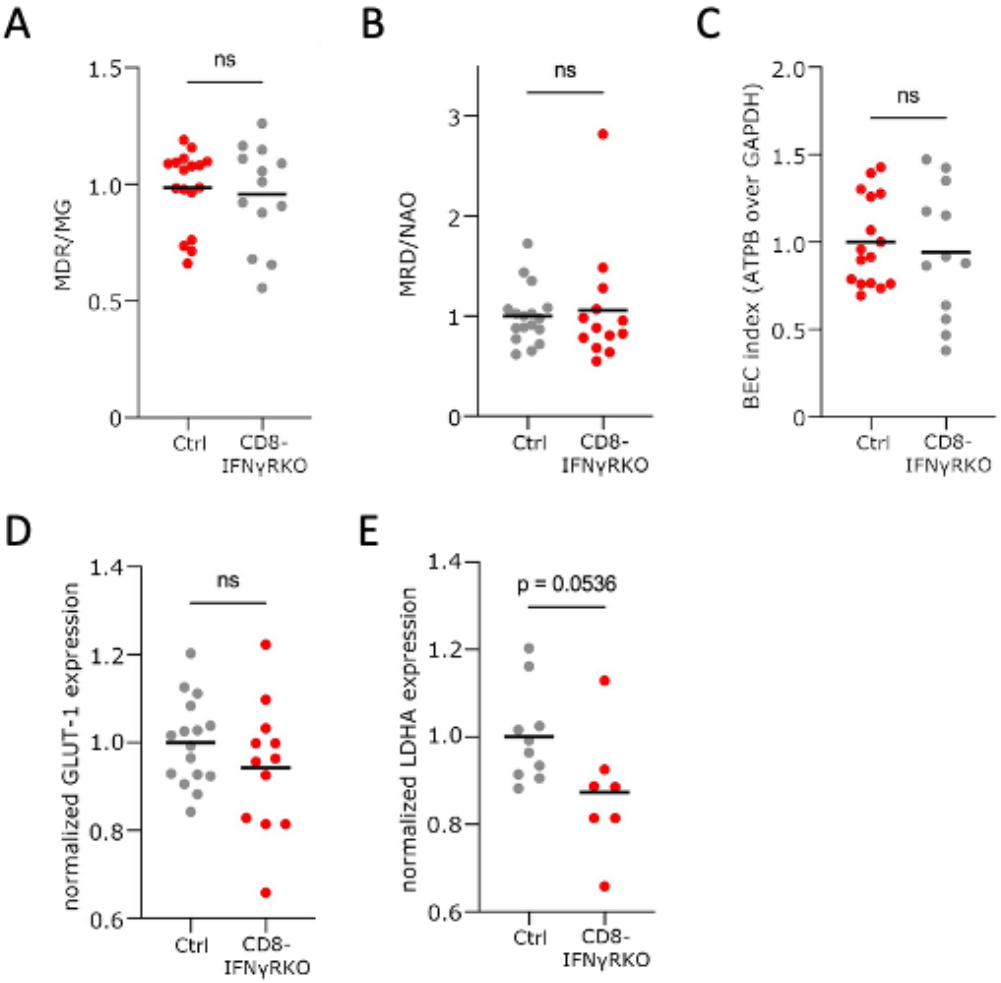


Figure 38: IFNγ-sensing does not influence the metabolic status of exhausted CD8⁺ T cells *in vivo*. (**A-E**) Control and CD8-IFNγR1KO mice were engrafted with B16F10-OVA, tumour-infiltrating lymphocytes were isolated after 12 days, and the metabolic status of exhausted T cells (PD-1⁺ LAG-3⁺) was analysed by flow cytometry. Data is from 3 independent experiments (Control n=16 and CD8- IFNγR1KO n=12). **A-** Graph shows the ratio between MitoTracker Deep red (mitochondrial membrane potential-related uptake) and MitoTracker green (mitochondrial mass). **B-** Graph shows mitochondrial function per mitochondrial mass using a mitochondrial membrane potential-dependent dye (MDR, MitoTracker deep red) over the uptake of a mitochondrial mass uptake dye (NAO, Nonyl Acridine Orange). Data is from 3 independent experiments (Control n=17 and CD8-IFNγR1KO n=13). **C-** Graph shows the BEC index representing the Oxphos to glycolysis rate *ex vivo*. BEC was quantified by measuring the ratio between ATPB expression and GADPH (Glyceraldehyde-3-phosphate Dehydrogenase) expression. **D-** Graph shows the overall glycolysis rate using the protein level expression of GLUT-1. Data is from 3 independent experiments (Control n=16 and CD8-IFNγR1KO n=12). **E-** Graph representing the anaerobic glycolysis level using LDHA expression as a readout. The comparison between the 2 groups was analysed using an unpaired t-test on GraphPad Prism. Data is from 2 independent experiments. (Control n=10 and CD8-IFNγR1KO n=7). ns = not significant. Experiments were jointly performed with Ana Victoria Lechuga-Vieco.

5.3.3 Preventing IFNγ-sensing by CD8$^+$ T cells decreases their exhaustion level

T cell exhaustion is often defined as a continuum of CD8$^+$ T cell states ending in a terminally exhausted state together with non-reversible cell dysfunction[409]. Therefore, there are degrees of exhaustion and (dys)functional states. In addition, as exhausted CD8$^+$ T cells have been shown to become defective in mitochondrial metabolism over time[410], the increased oxphos signature found in IFNγR1KO CD8$^+$ T cells could also indirectly reflect a lesser level of exhaustion compared to control cells in our model. To confirm the impact of IFNγ on T cell exhaustion, I performed multidimensional flow cytometry on tumour-infiltrating CD8$^+$ T cells to evaluate the expression of multiple exhaustion markers at the protein level. To do so, following the same experimental setup as before, B16F10-OVA tumours from control and CD8-IFNγR1KO mice were processed at day 12 post-engraftment. By focussing on CD8$^+$PD-1$^+$ T cells, I then looked at different exhaustion markers. A subpopulation of exhausted T cells harbouring low to intermediate inhibitory receptors (circled in **Figure 39A**) was found in tumours. Indeed, CD8$^+$PD-1^{int}Tim-3^{int} T cells (**Figure 39B**), CD8$^+$PD-1^{int}Lag-3^{int} T cells (**Figure 39C**), and CD8$^+$PD-1^{int}Tigit^{int} T cells (**Figure 39D**) were found in greater proportion when CD8$^+$ T cells could not sense IFNγ. This suggests that preventing IFNγ-sensing by CD8$^+$ T cells reduces their level of exhaustion in tumours, with a higher proportion of newly generated less exhausted T cells.

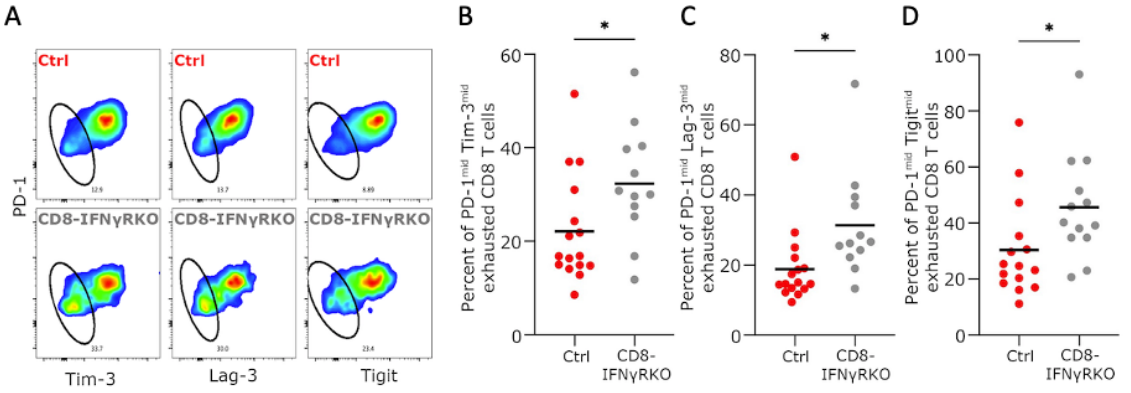


Figure 39: IFNγ-sensing reinforces CD8⁺ T cell exhaustion *in vivo*. Control and CD8-IFNγR1KO mice were engrafted with B16F10-OVA and TILs were isolated after 12 days. Exhaustion status was analysed by flow cytometry using the indicated markers. Data is from 2 independent experiments. **A-** Representative flow cytometry plots. Gate highlights a population with intermediate expression (mid) of PD-1, Tim-3, Lag-3, and Tigit. (**B-D**) Graphs show the percentage of exhausted CD8⁺ T cells with intermediate expression of both PD-1 and Tim-3 (**B**; Control n=16 and CD8-IFNγRKO n=12), Lag-3 (**C**; Control n=16 and CD8-IFNγRKO n=12) and Tigit (**D**; Control n=15 and CD8-IFNγRKO n=13). The comparison between the 2 groups was analysed using an unpaired t-test on GraphPad Prism. * = $P < 0.05$.

In order to evaluate the level of exhaustion at the transcriptional level, we compared the average expression of a variety of exhaustion receptors between control and IFNγR1KO CD8⁺ T cells. In tumours, IFNγR1KO CD8⁺ T cells consistently lower express multiple exhaustion markers compared to control cells, regardless of the cell cluster they belonged to (**Figure 40A**). This further confirms that IFNγ-sensing by CD8⁺ T cells increases the overall exhaustion level in tumours, also transcriptionally. When focused on the exhausted cell cluster, differential gene expression demonstrated a slight but highly significant decrease of exhaustion markers in IFNγR1KO CD8⁺ T cells compared to control cells, confirming the previous results (**Figure 40B**).

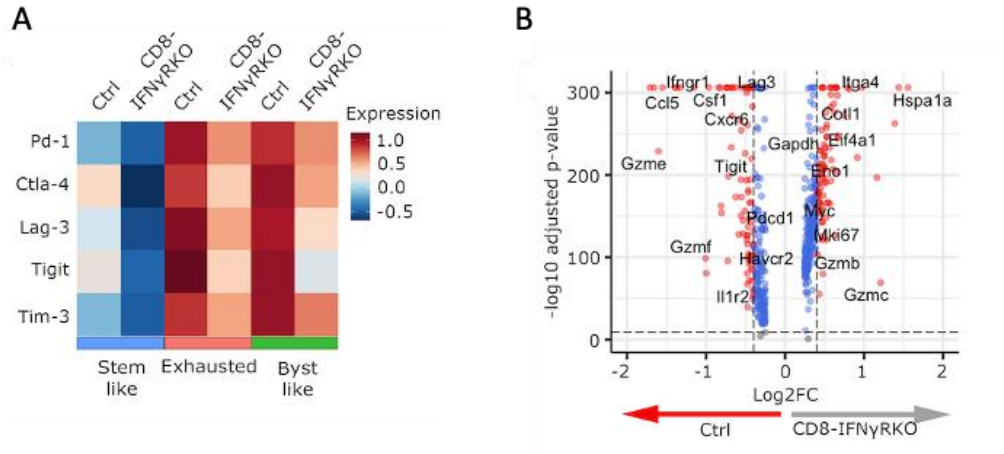


Figure 40: IFNγ-sensing reinforces CD8⁺ T cell exhaustion at the transcription level. Control (n=3) and CD8-IFNγR1KO (n=3) mice were engrafted with B16F10-OVA tumours. CD45⁺CD3⁺CD8⁺Tomato⁺ cells were sorted from tumours and subjected to scRNA-seq analysis. **A-** Heatmap shows the relative average expression of selected exhaustion markers in control and CD8-IFNγR1KO CD8⁺ T cells over the different cell states. **B-** Volcano plot representing differentially expressed genes between control and CD8-IFNγR1KO CD8⁺ T cells in Exhausted T state. Blue dots: genes with an adjusted p value<0.05; Red dots: genes with log2 (fold-change) value >0.5 or <-05 and an adjusted p value<0.05. Total variables = 543. ScRNA-seq analysis was performed by Audrey Gerard.

5.3.4 IFNγ-sensing does not restrict exhausted CD8⁺ T cell proliferation

Finally, as we described in **Chapter 4** an increased expansion of IFNγR1KO CD8⁺ T cells in tumours, I next sought to investigate whether IFNγ affected cell cycle, first using the scRNA-seq dataset, as IFNγ is known to induce cell cycle arrest[314]. We first quantified the proportion of control and IFNγR1KO CD8⁺ T cells in the different cell cycle phases based on the transcriptomic data. The G1 phase of the cell cycle is the first stage of the so-called interphase (i.e. cells will make a decision of either dividing or putting a stop to further proliferation), while G2/M and S phases are more advanced in the cell cycle therefore cells are actively proliferating[411]. The quantification of the cell proportion in

each cell cycle phase indicated that IFNγR1KO CD8$^+$ T cells were more proliferating than control CD8$^+$ T cells (**Figure 41**). Cell scoring revealed that 61% of tumour-infiltrating IFNγR1KO CD8$^+$ T cells were in G2/M and S phases compared to 38.9% in control mice suggesting an increased proliferation. This is consistent with previous results obtained through the *in vivo* expansion assay using the OTI system (see **Figure 26** in Chapter 4).

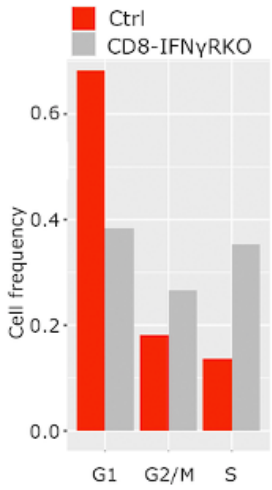


Figure 41: IFNγ-sensing restricts CD8$^+$ T cell proliferation at the transcriptional level. Control (n=3) and CD8-IFNγR1KO (n=3) mice were engrafted with B16F10-OVA tumours. CD45$^+$CD3$^+$CD8$^+$Tomato$^+$ cells were sorted from tumours and subjected to scRNA-seq analysis. The bar plots show the percentages of CD8$^+$ T cells from Control (red) and CD8-IFNγR1KO (grey) mice in G1, G2/M, or G1 phase of the cell cycle. ScRNA-seq analysis was performed by Audrey Gerard.

Previous studies stipulated that exhausted T cells gradually lost proliferative capacity[412,413,414,415]. The increased proportion of cycling T cells in CD8-IFNγR1KO mice might suggest that IFNγ inhibits the proliferation of exhausted T cells. To explore this hypothesis, I investigated exhausted CD8$^+$ T cell proliferation *ex vivo*. I sorted WT-exhausted CD8$^+$ T cells as CD8$^+$PD-1$^+$LAG-3$^+$Tcf1$^-$ T cells from B16F10-OVA tumours on day 12. Cells were then loaded with a proliferation dye and restimulated *ex vivo* with

anti-CD3 and anti-CD28 antibodies in the presence of blocking IFNγ or not for 4 days (**Figure 42A**). Overall, less than 50% of the cells had divided in 4 days. Surprisingly, exhausted T cell proliferation was not rescued by anti-IFNγ treatment (**Figure 42B**). These results suggest that IFNγ did not directly inhibit exhausted T cell proliferation.

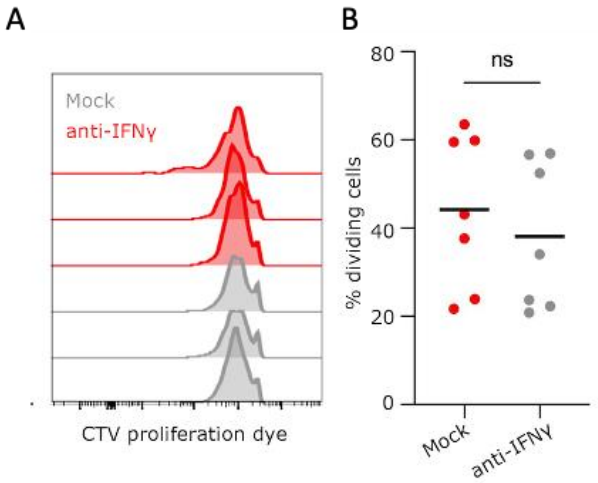


Figure 42: IFNγ-sensing does not affect exhausted CD8⁺ T cell proliferation *ex vivo*. (**A-B**) Tumour-infiltrating exhausted CD8⁺ T cells were sorted from B16F10-OVA tumours 12 days post-engraftment, labelled with CellTrace Violet dye (CTV), and restimulated with anti-CD3 and anti-CD28 antibodies, in the presence (red) or absence (grey) of anti-IFNγ. Proliferation was assessed after 4 days of culture. **A-** Histogram showing representative examples of dye dilution. **B-** Graph shows the percentage of exhausted T cells that divided after 4 days of culture *ex vivo* with or without anti-IFNγ. The comparison between the 2 groups was analysed using an unpaired t-test on GraphPad Prism. ns = not significant.

5.4 Discussion and conclusion

This chapter first showed that IFNγ sensing by CD8⁺ T cells does not affect the overall tumour immune cells microenvironment in terms of proportions. It then took advantage of scRNA-seq data to further investigate the IFNγ effect on mature CD8⁺ T cells in the

cancer context. The first step was to investigate whether IFNγ would influence $CD8^+$ T cells from the tumour draining lymph node or directly at the tumour. Interestingly, there were no differentially expressed genes in cells isolated from draining lymph nodes, suggesting that IFNγ-sensing does not play a critical role in cells in this localisation. As not all cells isolated from lymph nodes would have been sequenced, the majority of the cells included in the scRNA-seq analysis are most likely naïve and non-tumour specific T cells. Furthermore, even if naïve $CD8^+$ T cells express higher levels of IFNγR rendering them more sensitive to IFNγ than activated $CD8^+$ T cells, in theory, IFNγ is not expected to be found in lymph nodes, especially in a non-metastatic stage of the model. Therefore, preventing IFNγ signalling would not have any effect as the cytokine is not present in the control situation. Conversely, in tumour-infiltrating $CD8^+$ T cells, there were differentially expressed genes highlighting that IFNγ sensing affects $CD8^+$ T cells in tumours. In addition, all the cells isolated from tumours and sequenced were all expressing activation and exhaustion markers to some extent, highlighting a sufficient level of activation which can be due to direct TCR activation therefore cells are most likely tumour specific, or indirectly through soluble cues present in the tumour microenvironment. Nonetheless, there was little diversity between the different $CD8^+$ T cell subsets in tumours. We further described 3 main cell states that we used to compare control to IFNγR1KO $CD8^+$ T cells. Overall, scRNA-seq data confirmed some of my previous *in vivo* findings such as the exhaustion level and the enhanced proliferation in CD8-IFNγR1KO tumours. It also guided me to further investigate stem-like T cells and T cell metabolism, two important parameters in anti-tumour immune response.

5.4.1 IFNγ-sensing does not affect exhausted T cells in tumours

IFNγ is known to induce apoptosis and cell cycle arrest[199]. It is therefore often assumed that IFNγ would directly inhibit $CD8^+$ T cell cytokinesis or lead to cell death. But control activated T cells were barely responsive to IFNγ as they downregulate the signalling IFNγR2 chain upon activation (**Figure 11B** and **11C** in **Chapter 3**). This has also been shown in the *Listeria monocytogenes* infection model and in human $CD8^+$ T cells[416,417]. As IFNγ does not kill cytotoxic T cells but is very pleiotropic, it is important to further study its effect on exhausted T cells in tumours. scRNA-seq first pointed out that some metabolic pathways were differentially regulated when $CD8^+$ T cells could sense IFNγ or not. However, *ex vivo* experiments did not recapitulate those differences which can be explained by the fact that mRNA expression does not necessarily correlate with protein expression levels. Alternatively, it might also suggest that IFNγR1KO $CD8^+$ T cells are more suited to adapt themselves to environmental stress than WT $CD8^+$ T cells, as they have the relevant mRNAs readily available for translation. To assess the effect of IFNγ sensing on intra-tumoral $CD8^+$ T cell metabolic status, I focused on exhausted T cells ($CD8^+$LAG-3^+ T cells) isolated from B16F10-OVA tumours on day 12. With the use of different mitochondrial dyes, we first assessed mitochondrial bioenergetics. MitoTracker green (MG) is showing the total mitochondrial mass while MitoTracker Deep Red (MDR) uptake is dependent on the mitochondria membrane potential therefore their functions. Hence, the ratio between MDR and MG gives an indication of the mitochondrial activity per mitochondrial mass[406]. IFNγ-sensing by $CD8^+$ T cells did not change this ratio, however, as MG can also stain reactive-oxygen species (ROS) in mitochondria[418] and compete with MDR for the uptake we decided to confirm the

results by using another dye, NAO whose uptake does not depend on mitochondrial membrane potential but labels cardiolipin present in mitochondrial membranes[419]. Results were recapitulated, confirming that IFNγ does not affect exhausted $CD8^+$ T cell relative mitochondrial metabolic activity normalised by total mitochondrial mass in tumours. Another way to assess mitochondrial activity was to look at the BEC index. However, again, no differences were found between control and IFNγR1KO exhausted $CD8^+$ T cells in tumours. In addition, IFNγR1 ablation in exhausted $CD8^+$ T cells does not change the GLUT-1-dependent glycolysis rate in the tumour-infiltrating cells. Other more advanced techniques exist to investigate cell metabolism statuses such as Seahorse[420] and SCENITH method[421]. Nevertheless, the data collected here suggest that cells were not that metabolically different, stipulating that metabolic changes would not be an intrinsic different feature nor a driven mechanism in the better anti-tumour response observed in CD8-IFNγR1KO mice.

Interestingly, the slight decrease of LDHA expression in IFNγR1KO $CD8^+$ T cells suggests that they are less dependent on anaerobic glycolysis. Even though it was not significant, it suggests that hypoxia levels may be different between control and IFNγR1KO $CD8^+$ T cells. In the previous chapter, I described $CD8^+$ T cells tumour infiltration (**Figure 28** in **Chapter 4**). IFNγR1KO $CD8^+$ T cells were invading the tumour nest, suggesting that they would be in a more hypoxic environment as the tumour core was previously described as oxygen-deprived[422,408]. Those two results seemed contradictory at first. However, tumours were observed to be vascularised throughout tumour sections in both conditions (**Figure 30** in **Chapter 4**). It would have been interesting to use hypoxia probes to formally assess whether IFNγR1KO $CD8^+$ T cells were

indeed located in less hypoxic regions than control cells or whether they are just better suited and resistant to hypoxic conditions *in vivo*. This could also lead to assessing whether IFNγ sensing influences hypoxic response in intra-tumoral $CD8^+$ T cells.

Following these findings, I then investigated the level of exhaustion in tumours, which revealed a greater population of intermediate exhausted T cells in CD8-IFNγR1KO mice compared to control mice. Thus, scRNA-seq data confirmed that cells were quite similar, but that IFNγ sensing increased the expression level of the different exhaustion markers in $CD8^+$ T cells. I hypothesised that IFNγ-sensing would not *per se* change the exhaustion trajectory but could rather fasten it or prevent the new generation of less exhausted T cells and therefore would increase the overall exhaustion level at the $CD8^+$ T cell population scale. The increased presence of intermediate exhausted T cells with effector phenotype in the CD8-IFNγR1KO tumours cannot be explained by enhanced tumour homing (see **Figure 29** in **Chapter 4**). Moreover, I showed that blocking IFNγ does not enhance their proliferation *ex vivo*. Altogether this suggests that the increased presence of less exhausted cells may result from on-site $CD8^+$ T cell differentiation which is restricted by IFNγ.

5.4.2 IFNγ-sensing affects T cell subset proportion

In **Chapter 4**, I described that IFNγ restricts overall $CD8^+$ T cell tumour expansion. Here, scRNA-seq data and *in vivo* experiments revealed that IFNγ reduces the presence of stem-like T cells in tumours. In addition, *ex vivo* proliferation assays proved that the proliferative capacity of $CD8^+$ T cells is not derived from exhausted T cells as blocking IFNγ did not enhance their proliferation after restimulation. This discovery suggests that

in the IFNγR1KO condition, more stem-like T cells could potentially lead to more intermediate exhausted T cells in tumours over time, which may explain the lower exhaustion level at the whole IFNγR1KO $CD8^+$ T cell population level. Literature showed that stem-like T cells are critical for anti-tumour responses and responses to immunotherapies (see **Chapter 1.4**). IFNγ-sensing may affect their biology in tumours and thus this particular cell population will be targeted as well by preventing IFNγ-sensing in every $CD8^+$ T cell. In the next chapter, I further investigated the relevance of IFNγ signalling by stem-like T cells for their biology in tumours.

5.4.3 Conclusion

This chapter investigated the effect of IFNγ on the different $CD8^+$ T cell populations. The better control of B16F10-OVA tumours in CD8-IFNγR1KO mice is solely due to mechanisms occurring in tumours. Exhausted $CD8^+$ T cells did not seem particularly impacted by IFNγ-sensing, however, the greater presence of stem-like T cells when cells are IFNγ-insensitive suggests that they are playing a critical role in efficient tumour control. Altogether, our data demonstrate that IFNγ sensing by $CD8^+$ T cells leads to a widespread defect in proliferation which I hypothesise could originate from stem-like T cells.

6. IFNγ sensing particularly affects the CD8$^+$ stem-like T cell maintenance in tumours

Stem-like T cells are important for long-term T cell immune responses, hence their critical role in the success of immunotherapies in cancer patients[148,423,424] (see **Chapter 1.4**). However, a lot of their biology remains unknown. This chapter focuses on the IFNγ effect on stem-like T cells and whether their enhanced presence in B16F10-OVA tumours is directly due to their non-responsiveness to IFNγ. In the previous chapter, I identify a greater proportion of stem-like T cells in tumours from CD8-IFNγR1KO mice. Here, I further investigated their proliferation potential and how IFNγ may affect their maintenance. Then, I tested whether IFNγ impacts their maintenance directly in tumours and their implication in CD8$^+$ T cell population expansion *in vivo* using the OTI system. Finally, I investigated a potential cellular mechanism that could have explained the sustained stemness of the cells when insensitive to IFNγ.

6.1 Stem-like T cells have the greatest proliferative capacity in tumours.

In the previous chapters, I highlighted that IFNγR1KO CD8$^+$ T cells were better expanded in tumours mainly through cell proliferation. Further investigations revealed that the increased proliferation was not initiated by exhausted CD8$^+$ T cells. In addition,

I observed a greater presence of stem-like T cells in CD8-IFNγR1KO tumours compared to control tumours. This section investigates the proliferation capacity and IFNγ sensitivity of stem-like T cells present in B16F10-OVA tumours.

6.1.1 Intra-tumoral stem-like T cells are better able to proliferate compared to exhausted T cells

Following the previous results, I hypothesised that the greater T cell population expansion found in CD8-IFNγR1KO tumours could result from the higher stem-like T cell proportion observed (see **Figures 35C** and **35D** in **Chapter 5**). Indeed, stem-like T cells have been shown to self-renew and give rise to more differentiated effector $CD8^+$ T cells in tumours, they are therefore a potential pool of progenitors for early exhausted T cells in tumours[425,424,148,165,161]. Moreover, stem-like T cells have been described as having a greater proliferative capacity compared to exhausted T cells[165]. To properly compare tumour-infiltrating stem-like T cells and exhausted T cell proliferative potential, I sorted stem-like and exhausted T cells from B16F10-OVA tumours grown in WT mice following the experimental design depicted in **Figures 43A** and **43B**. Cells were loaded with CTV dye, restimulated, and kept in culture for 4 days before assessing their proliferation by dye dilution. As previously described[164,165], stem-like $CD8^+$ T cells have enhanced proliferative capacity compared to exhausted $CD8^+$ T cells (**Figures 43C, 43D,** and **43E**). Correspondingly, almost 100% of intra-tumoral stem-like T cells divided within 4 days while only half of the exhausted T cells proliferated (**Figure 43D**). In addition, 35% of stem-like T cells had completely diluted the proliferation dye, as opposed to 5% for exhausted T cells (**Figure 43E**). Those results confirm that intra-tumoral stem-like T cells

are the subset with the highest proliferative capacity. The fact that there was an increased pool of those precursor cells in CD8-IFNγR1KO tumours suggests that IFNγ may preferentially target stem-like T cells in tumours and their newly differentiated progeny.

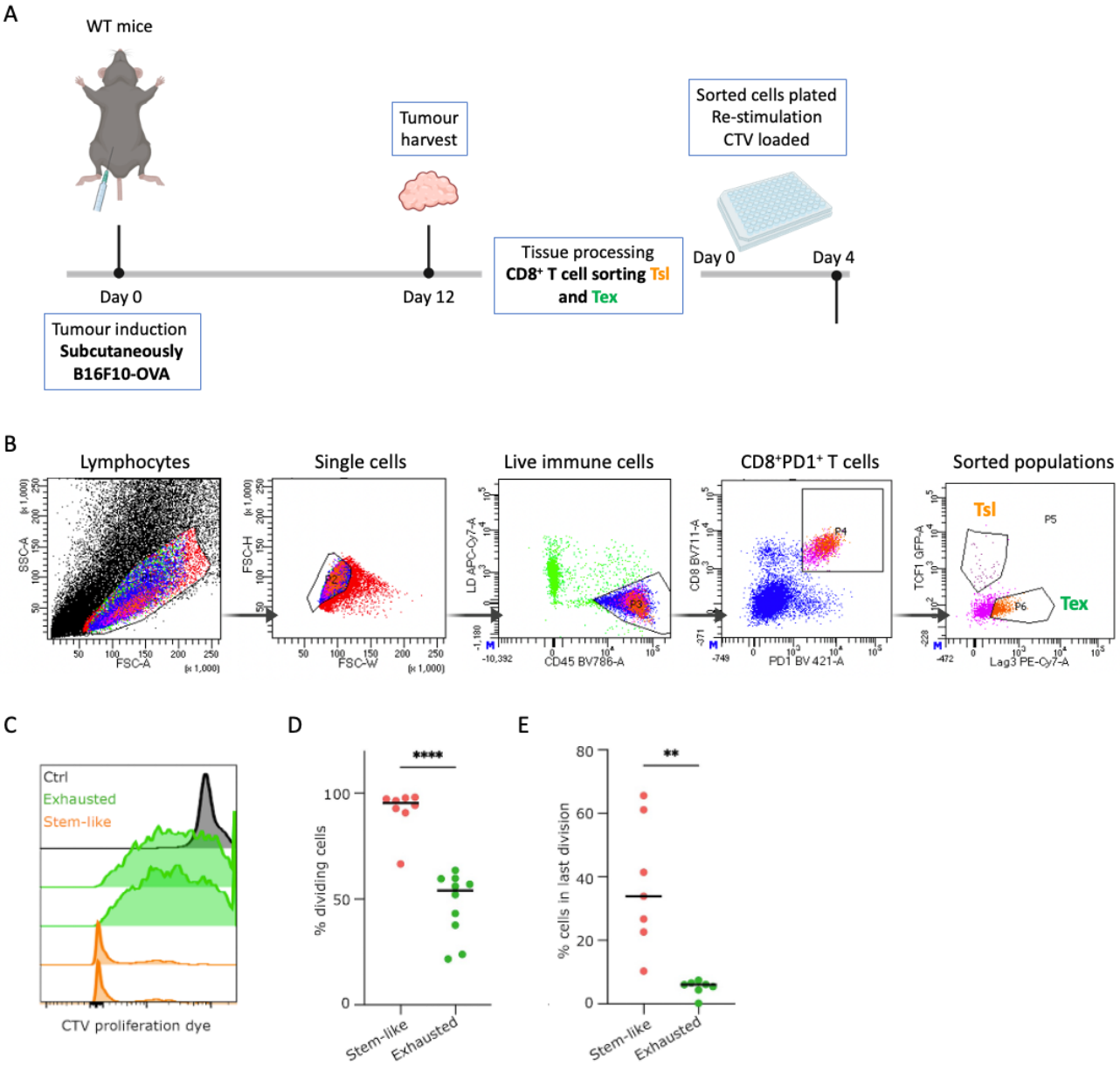


Figure 43: Proliferative capacity of tumour-infiltrating CD8⁺ T cells is initiated by stem-like T cells not exhausted T cells. (**A-E**) Tumour-infiltrating stem-like T cells (orange) and exhausted T cells (green) were sorted from B16F10-OVA tumours bearing WT mice, 12 days post-

engraftment. Cells were labelled with CellTrace violet dye (CTV) and restimulated with anti-CD3 and anti-CD28 antibodies. Proliferation was assessed after 4 days of culture. **A-** Experimental workflow. **B-** Gating strategy used to sort stem-like T cells (Tsl) and exhausted T cells (Tex) from tumours. **C-** Histogram showing representative examples of dye dilution. Control represents cells loaded with the CTV at day 0. **D-** Graph showing the percentage of dividing cells. **E-** Graph shows the percentage of cells that completely diluted the dye. The comparison between the 2 groups was analysed using an unpaired t-test on GraphPad Prism. ** = P < 0.002, **** = P<0.0001. [Created with BioRender.com].

6.1.2 Stem-like T cells are IFNγ sensitive in tumours

As stem-like T cells were more abundant in tumours when $CD8^+$ T cells are IFNγR1KO, I hypothesised that they might be depleted because of the presence of IFNγ in the tumour microenvironment. To support this, we investigated the IFNγ-sensitivity of stem-like T cells in tumours, focusing on the control cells with full IFNγR expression. The stem-like T cell cluster in the scRNA-seq data demonstrated that stem-like T cells displayed higher IFNγR expression compared to all other intra-tumoral $CD8^+$ T cell subsets (**Figure 44A**). This suggests that this particular $CD8^+$ T cell subset is more sensitive to IFNγ compared to the others. Indeed, it resulted in enhanced responsiveness to IFNγ in tumours, as exemplified by increased expression of multiple IFNγ-responsive genes (**Figure 44B**). This is proof of concept that stem-like T cells may have an enhanced sensitivity to IFNγ and that IFNγR1 depletion could particularly affect stem-like T cells in tumours.

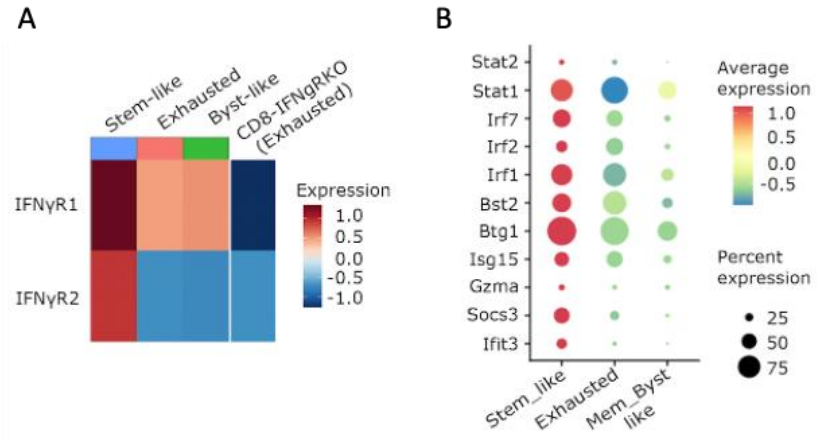


Figure 44: Stem-like T cells are IFNγ sensitive in tumours. (**A-B**) Control mice were engrafted with B16F10-OVA tumours. $CD45^{+}CD3^{+}CD8^{+}Tomato^{+}$ cells were sorted from tumours and subjected to scRNA-seq analysis. **A-** Heatmap of control tumour-infiltrating $CD8^{+}$ T cells shows the relative average expression of IFNγR1 and IFNγR2 in the different cell states in control mice. The average expression of IFNγR1 and IFNγR2 in CD8-IFNγR1KO cells from the exhausted state was used as a control for negative IFNγR1 expression. **B-** The dot plot shows the relative average expression and percent of cells expressing transcripts implicated in IFNγ signalling and response within the different cell states. ScRNA-seq analysis was performed by Audrey Gerard.

6.2 IFNγ affects stem-like T cell maintenance in tumours

The previous section highlighted that intra-tumoral stem-like T cells are sensitive and respond to IFNγ in addition to having a high proliferative capacity compared to exhausted T cells. In this section, I sought to investigate the effect of preventing IFNγ-sensing by stem-like T cells in tumours, and its implication in the observed expansion of IFNγR1KO $CD8^{+}$ T cells.

6.2.1 Stem-like T cells are critical for IFNγR1KO CD8$^+$ T cell expansion *in vivo*

To further confirm that increased CD8$^+$ T cell expansion in CD8-IFNγR1KO tumours was caused by the enhanced presence of stem-like T cells rather than exhausted T cells, I set up a lineage cell-tracing experiment *in vivo*. To do so, I generated *in vitro* stem-like tumour-specific OTI T cells and exhausted tumour-specific OTI T cells in both WT and IFNγR1KO following previously published protocols[47,48] (**Figure 45A**). Stem-like or exhausted WT and IFNγR1KO OTI T cells were ad-mixed at a 1-to-1 ratio and co-transferred in B16F10-OVA tumour-bearing WT mice. The ratio of intra-tumoral IFNγR1KO OTI to WT was then analysed 6 days later. On the day of injection, stem-like-induced T cells expressed Tcf1 stemness marker and upregulated PD-1 expression upon activation while exhausted-induced T cells expressed exhaustion markers including PD-1, Tigit, and Lag-3. Both WT and IFNγR1KO OTI were similarly activated as shown in **Figure 45B**. Five times more WT than IFNγR1KO exhausted T cells were found in tumours (**Figure 45C**) which was consistent with the IFNγR1KO CD8$^+$ T cell defect in tumour homing (**Figure 29** in **Chapter 4**). More importantly, IFNγR1KO stem-like T cells had the potential to recover this tumour homing defect, with almost half of the tumours harbouring more IFNγR1KO OTI than WT OTI originated from stem-like T cells (**Figure 45C**). This further demonstrates that preventing IFNγ sensing by stem-like CD8$^+$ T cells originates an enhanced proliferation of tumour-specific T cells in tumours.

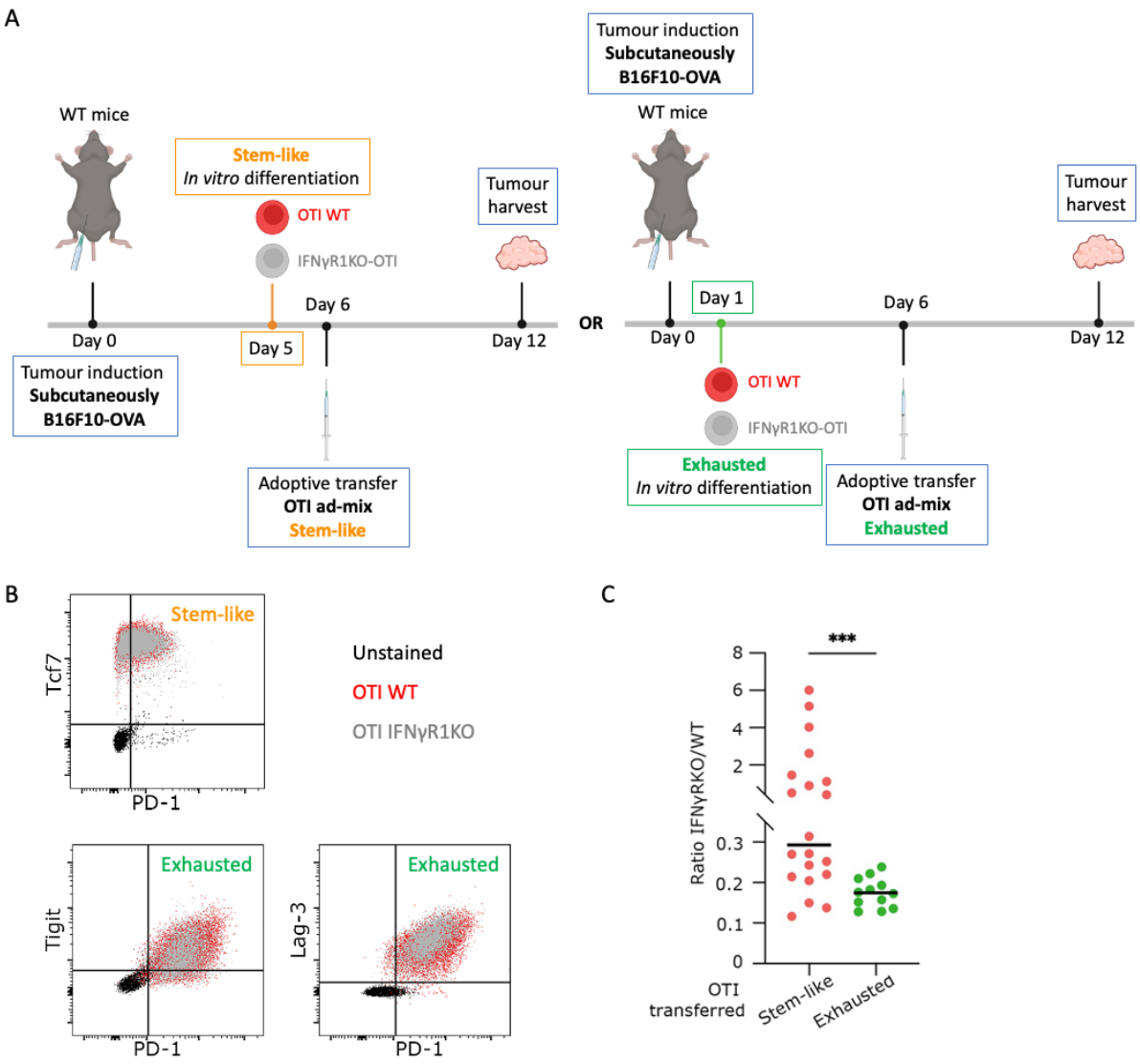


Figure 45: Stem-like T cell proliferation supports the greater IFNγR1KO CD8⁺ T cell expansion in tumours. (**A-C**) Competitive cell tracing experiment. Stem-like and exhausted CD8⁺ T cells were generated *in vitro* using WT and IFNγR1KO OTI. Differentiated OTI cells WT and IFNγR1KO from each cell state were ad-mixed at a 1:1 ratio and injected intravenously into B16F10-OVA tumour-bearing WT mice. Data is from 3 independent experiments. **A-** Experimental workflow. **B-** Flow cytometry plots showing the expression of selected exhaustion markers and Tcf1/7 of *in vitro* differentiated WT and IFNγR1KO OTI before transfer. The Mock represents unstained OTI T cells. **C-** Graph shows the ratio between IFNγR1KO and WT OTI from stem-like (orange) or exhausted (green) conditions in tumours 6 days after transfer. The comparison between the 2 groups was analysed using a non-parametric Mann-Whitney test on GraphPad Prism. *** = P < 0.001. [Created with BioRender.com].

6.2.2 Blocking IFNγ enhances the maintenance of intra-tumoral stem-like T cells *ex vivo*

To gain further insights into the direct effect of IFNγ on stem-like T cells, I isolated tumour-infiltrating immune cells from B16F10-OVA tumours grown in WT mice. Cells were then loaded with CFSE dye and restimulated with anti-CD3 and anti-CD28 antibodies in different conditions to properly assess the IFNγ effect on the stem-like T cell proliferation, proportion against other $CD8^+$ T cells, and maintenance *ex vivo* after 4 or 5, and 7 days of culture. The experimental design followed is depicted in **Figure 46A**. Firstly, by looking at the CFSE dye dilution within the stem-like population ($CD8^+PD\text{-}1^+Tcf1^+$ cells) I could confirm that those cells were able to divide while maintaining some level of Tcf1 expression, thereby harbouring self-renewal capacity over multiple division cycles (**Figure 46B**). I then quantified the percentage of dividing cells that expressed Tcf1 as a read-out of stem-like T cells following their restimulation in the presence or absence of recombinant IFNγ or blocking IFNγ antibodies. Anti-IFNγ treatment increased the proportion of stem-like T cells over other $CD8^+$ T cells compared to the control condition (Mock) or cells treated with recombinant IFNγ (**Figure 46C**). This suggests an increased presence of stem-like T cells when IFNγ is reduced or deprived in the environment. To validate the hypothesis that blocking IFNγ resulted in an accumulation of stem-like T cells rather than a decrease of other cells, I analysed the actual cell number of stem-like T cells over time and normalised them by the stem-like T cell number present at day 0. Blocking IFNγ increased the retention and/or decreased the disappearance of stem-like T cells compared to the other conditions (**Figure 46D**). Furthermore, the analysis of the cell division by looking at the dye dilution demonstrated that the increased presence of

stem-like T cells when blocking IFNγ was potently due to better active maintenance rather than retention in a quiescent cell state as more than 80% of stem-like T cells proliferated when treated with anti-IFNγ (**Figure 46E**). This line of evidence suggested that IFNγ blocking resulted in the accumulation of stem-like T cells that are self-renewing.

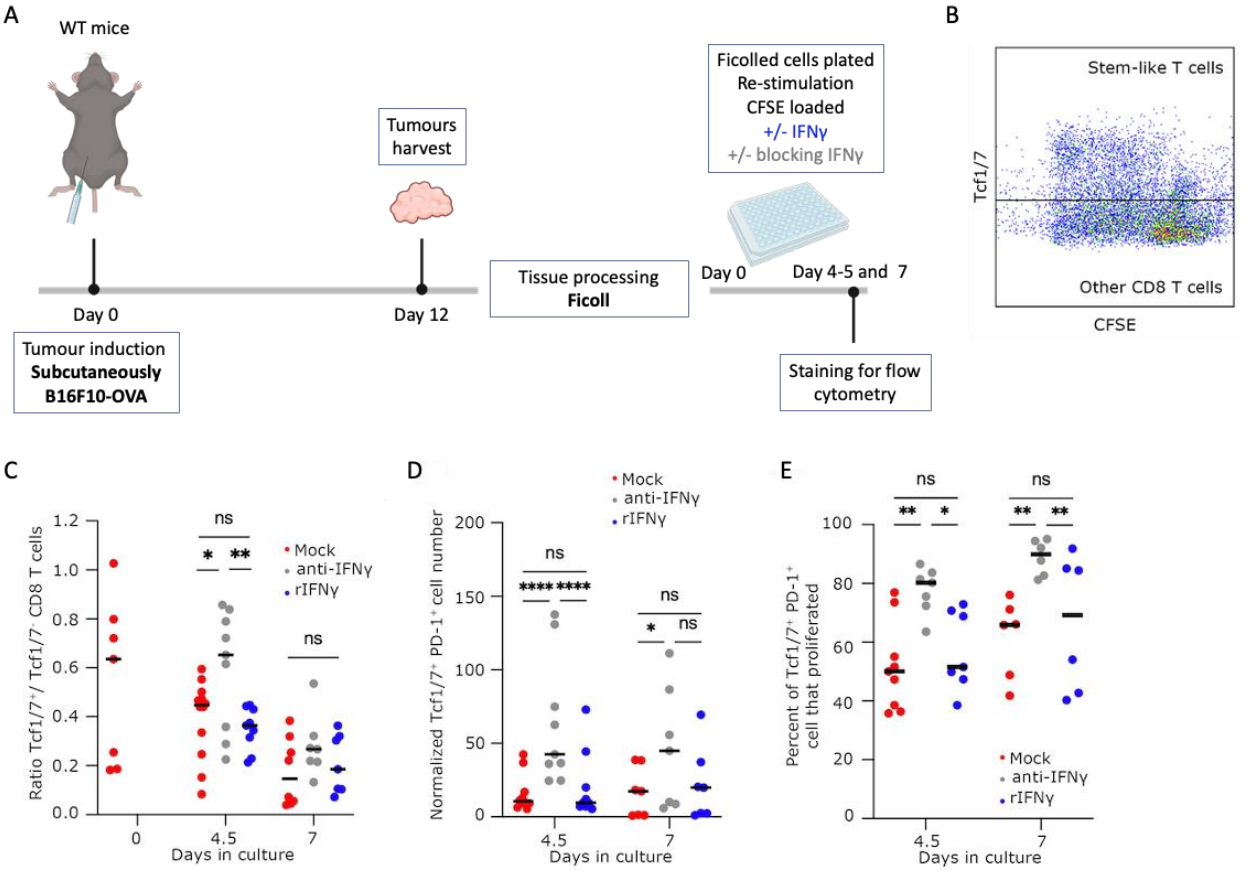


Figure 46: Blocking IFNγ increases the maintenance of tumour-infiltrating stem-like T cells *ex vivo*. B16F10-OVA tumours were engrafted in WT mice. Total live immune cells were isolated from tumours after 12 days and were restimulated *ex vivo* with anti-CD3 and anti-CD28 antibodies in the presence of blocking IFNγ antibody, recombinant IFNγ, or media only (Mock). Cells were labelled with CFSE at day 0, stained for CD8, Tcf1/7, and PD-1 at the indicated time points, and analysed by flow cytometry. Data are from 3 independent experiments (n=5 mice per experiment). Each dot is one well of immune cells pooled from multiple mice. **A-** Experimental workflow. **B-** Representative flow cytometry dot plot showing CFSE dilution against Tcf1/7 expression 4 days after *ex vivo* culture in presence of anti-IFNγ blocking antibody. **C-** Graph showing the Tcf1/7^{+} by Tcf1/7^{-} CD8^{+} T cell ratio over time. **D-** Graph showing the

absolute number of Tcf1/7^{+} PD-1^{+} stem-like T cells over time normalized to the number of stem-like T cells at day 0. **E-** Graph showing the percentage of stem-like T cells that divided, as assessed by proliferation dye dilution. The comparison between more than 2 groups was analysed using two-way ANOVA on GraphPad Prism. ns = not significant, * = P < 0.05, ** = P < 0.002, **** = P<0.0001. [Created with BioRender.com].

6.2.3 IFNγ inhibits the self-renewal capacity of intra-tumoral stem-like T cells

As mentioned previously, IFNγ is known to induce cell death[21]. Here, I further assessed whether IFNγ could induce apoptosis of tumour-infiltrating CD8^{+} T cells by using cleaved caspase 3 as a readout of engaged apoptosis. IFNγR1 deletion in CD8^{+} T cells did not affect the percentage of apoptotic cells both in stem-like T cells and exhausted T cells (**Figure 47A**), which was consistent with our previous findings demonstrating no differences at the general CD8^{+} T cell population level in tumours (**Figure 25** in **Chapter 4**). Further experiments confirmed those results when blocking IFNγ had no effect on apoptosis on *in vitro* activated OTI stem-like T cells (**Figure 47B**). Overall, this further demonstrates that the IFNγ effect on stem-like T cells is not due to increased cell apoptosis.

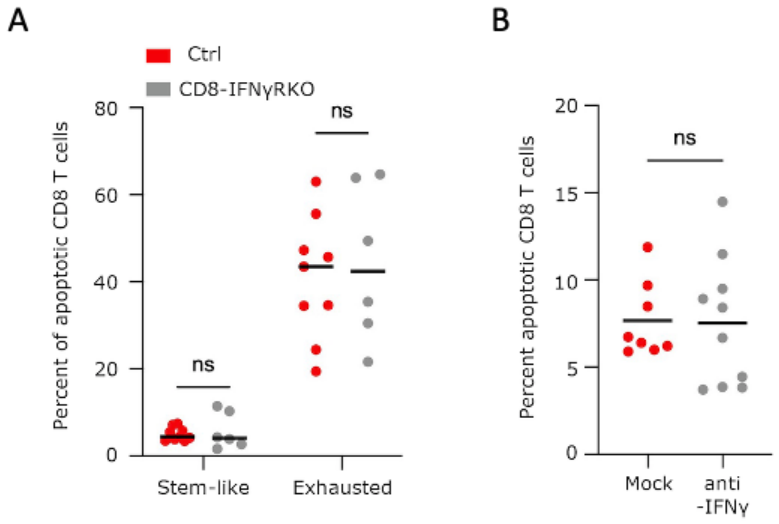


Figure 47: IFNγ-sensing does not increase CD8⁺ T cell death. A- Control (n=9, red) and CD8-IFNγR1KO (n=6, grey) mice were engrafted with B16F10-OVA tumours. Tumours were harvested 12 days after engraftment and cells were stained with antibodies against CD8, PD-1, Tcf1, and cleaved Caspase 3. The graph shows the percentage of stem-like or exhausted CD8⁺ T cells that were positive for cleaved Caspase 3. Data are from 2 independent experiments. **B-** Naïve CD8⁺ T cells from lymph nodes were stimulated with anti-CD3 and anti-CD28 in the presence of IL-2. When indicated, cells were treated with anti-IFNγ. After 4 to 5 days, cells were harvested and stained for CD45, CD8, Tcf1, PD-1, and cleaved caspase 3. The graph shows the percentage of apoptotic CD8⁺ T cells, as defined by cleaved caspase 3 staining (n=8 for Mock and n=10 for anti-IFNγ, data is from 2 independent experiments). The comparison between the 2 groups was analysed using an unpaired t-test on GraphPad Prism. ns = not significant.

Finally, to formally assess whether IFNγ inhibits the maintenance of stem-like T cells in tumours, I co-transferred *in vitro* generated WT and IFNγR1KO stem-like OTI T cells into B16F10-OVA tumour-bearing WT mice following the same experimental design detailed in **Figure 45A**. After 6 days, I quantified the percentage of OTI cells that retained Tcf1 expression as a readout of their stem-like state in tumours. IFNγR1KO OTI had a greater ability to retain their stemness in tumours (**Figure 48A**), demonstrating that IFNγ-sensing by stem-like T cells alters or decreases their stem-like phenotype

maintenance in tumours. Similarly, IFNγR1KO OTI isolated from the tumour-draining lymph nodes better maintained the expression of the Tcf1 stemness marker compared to WT OTI. Consistently, when stem-like T cells were sorted from B16F10-OVA tumours and restimulated *ex vivo*, the presence of blocking-IFNγ antibodies increased their maintenance over time (**Figure 48C**). Altogether this demonstrated that preventing IFNγ-sensing in stem-like T cells increased their maintenance *ex vivo* and within tumours which was not due to less apoptosis but rather a greater proliferation and self-renewal capacity therefore active maintenance.

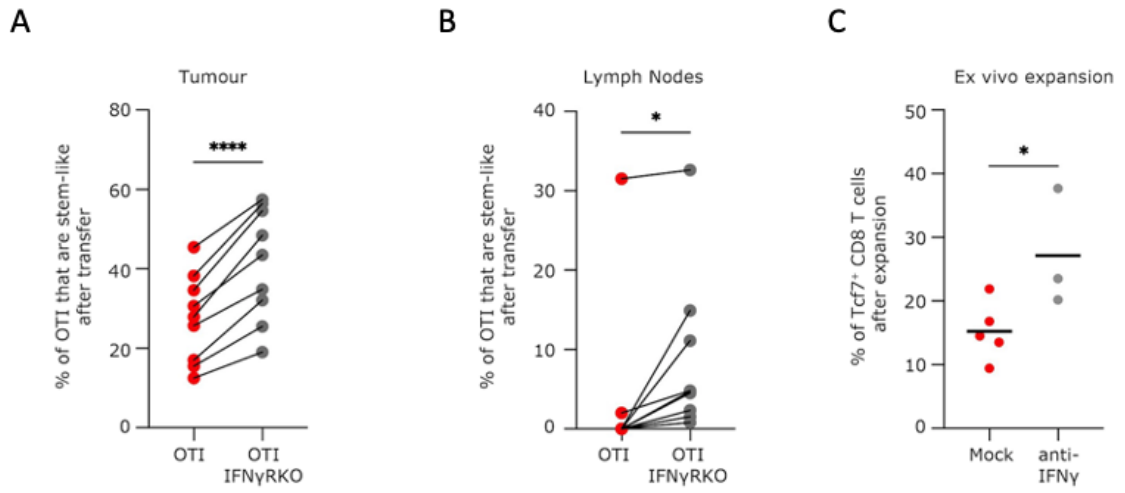


Figure 48: IFNγ sensing in intra-tumoral stem-like CD8⁺ T cells impairs their maintenance. (**A-B**) The graph shows the percentage of OTI that retained Tcf1/7 expression in tumours (**A**) and in draining lymph nodes (**B**) after 6 days. Lines link control and IFNγR1KO OTI from the same mouse. The comparison between the 2 paired groups was analysed using a paired t-test on GraphPad Prism. **C-** *Ex vivo* assessment of stemness maintenance in tumour-sorted stem-like T cells. Tumour-infiltrating stem-like T cells were sorted and restimulated with anti-CD3 and anti-CD28 antibodies in the presence or absence of IFNγ blocking antibodies. The graph shows the percentage of cells that retained expression of Tcf1/7, assessed by flow cytometry. Data is from 3 independent experiments. The comparison between the 2 groups was analysed using an unpaired t-test on GraphPad Prism. * = $P < 0.05$, **** = $P < 0.0001$.

6.3 Preventing IFNγ sensing enhanced CD8$^+$ T cell clonality *via* enhancing the stem-like T cell pool

In recent studies, stem-like T cells have been shown to be continuously depleted at the tumour site[161,426]. Here we brought new insight into their biology by showing that IFNγ-sensing affects their maintenance in tumours. Their continuous depletion might result in the reduction of their intra-tumoral clonal diversity, therefore, limiting the entire CD8$^+$ T cell breadth of the response in tumours. Indeed, we reasoned that the increased accumulation of stem-like T cells in CD8-IFNγR1KO tumours could lead to more diverse precursor cells generating more exhausted T cell diversity at the endogenous level. This would therefore sustain a more diverse anti-tumour response directly at the tumour site. To explore the clonal landscape of intra-tumoral CD8$^+$ T cells, we performed single-cell TCR sequencing in parallel to the scRNA-seq data from the control and IFNγR1KO CD8$^+$ T cells isolated (see **Figure 31** in **Chapter 5**). The analysis of the top 20 clones revealed a high degree of overlap between stem-like T cells and the other cell state clusters for both control and IFNγR1KO intra-tumoral CD8$^+$ T cells (**Figure 49A**). This demonstrated that indeed, exhausted T cells are differentiating from stem-like T cells as they share the same TCRs. Surprisingly, the stem-like clonotype also overlaps with the bystander-like cells. However, only 15% of clonotypes were recovered in the latter, plus they have a low TCR score suggesting that they either lost their TCR reactivity or are true bystanders (data not shown). Regarding the clonal diversity, we found that IFNγR1KO stem-like T cells have a higher relative abundance of rare clones which implies that they are more diverse overall (**Figure 49B**). Related to this, the

accumulation of low-abundance clones in stem-like T cells is recapitulated into the exhausted cluster. To conclude, IFNγR1 ablation in CD8$^+$ T cells increases the clonal diversity *via* the accumulation of stem-like T cells in tumours. This further confirms that IFNγ-sensing by tumour-infiltrating CD8$^+$ T cells inhibits stem-like T cell maintenance leading to less diversity in the overall CD8$^+$ T cell anti-tumour response. Moreover, it highlights the fact that stem-like T cells are at the origin of exhausted T cell responses.

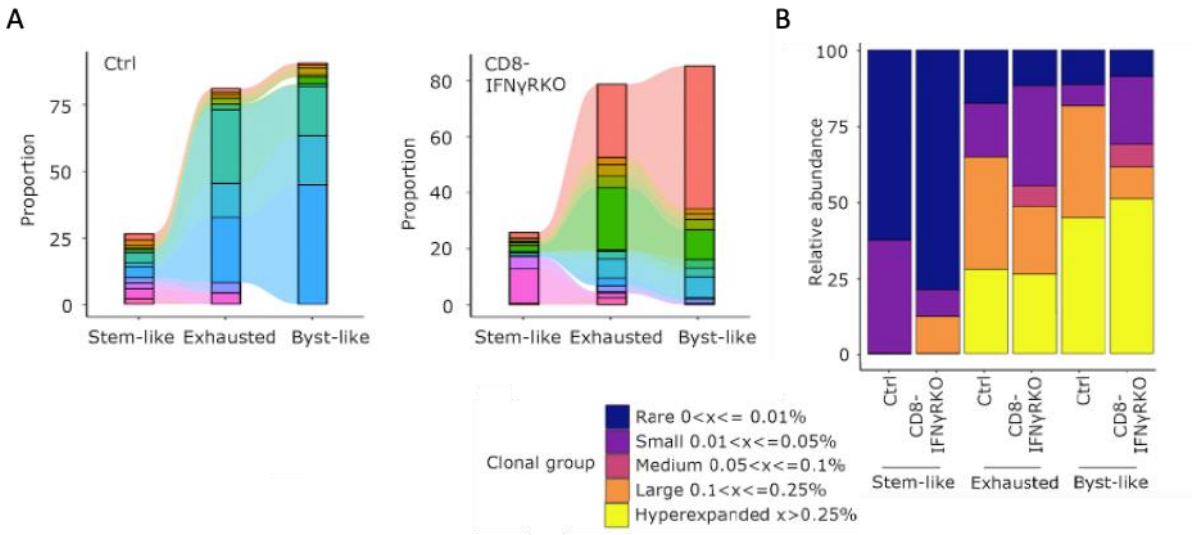


Figure 49: IFNγ sensing by CD8$^+$ T cells in tumours alters their TCR clonality. (**A-B**) CD45$^+$CD3$^+$CD8$^+$Tomato$^+$ cells were sorted from tumours and subjected to scRNA-seq and scTCR-seq analysis. **A-** The relative frequency of the top 20 clones and their distribution throughout the cell states were analysed within Control and CD8-IFNγR1KO mice. Each colour corresponds to a different clone. **B-** Relative TCR clonal abundance by cell state and genotype. Clonotype abundance (as the frequency of total repertoire per cell state per genotype) is defined as: Rare = 0<X<=0.01%; Small = 0.01<X<=0.05%; Medium = 0.005<X<=0.1%; Large 0.1<X<=0.25%; Hyperexpanded 0.25< X <=1%. ScRNA-Seq and scTCR-Seq analyses were performed by Audrey Gerard.

6.4 Discussion and conclusion

This chapter interrogated the effect of IFNγ on stem-like T cells. Following previous results characterising their greater presence in B16F10-OVA tumours when they are insensitive to IFNγ, I further questioned the mechanism behind this accumulation as it might be the key parameter for the better anti-tumour immune response observed in our model.

6.4.1 Intra-tumoral stem-like T cell maintenance is altered by IFNγ

Here I showed that stem-like T cells were sensitive to IFNγ and actually respond to it in B16F10-OVA tumours (**Figure 44**). Then, I demonstrated that intra-tumoral stem-like T cells have a greater proliferative capacity than exhausted T cells *per se* (**Figure 43**). Moreover, in the previous chapter, I demonstrated that IFNγ does not affect exhausted T cell proliferation (see **Figure 42** in **Chapter 5**). Altogether this suggests that stem-like T cells might be at the origin of greater $CD8^+$ T cell expansion in our model. Indeed, experiments using *in vitro*-induced stem-like T cells revealed that when there are IFNγR1KO stem-like T cells in the system, they will overcome the defect in tumour homing and most likely trigger the enhanced $CD8^+$ T cell expansion directly in tumours (**Figure 45**). Therefore, IFNγ affects stem-like T cells which could influence the overall $CD8^+$ T cell expansion at the population level. In this set of experiments, only half of the mice had a greater expansion of tumour-infiltrating IFNγR1KO OTI T cells compared to WT OTI when injected with stem-like induced cells. It would have been interesting to further assess the kinetic of the IFNγR1KO OTI tumour replenishment, and whether

harvesting at a later time point would have led to the IFNγR1KO $CD8^+$ T cell tumour homing defect recovery in every mouse for example. Interestingly, when focusing on the stem-like T cells, IFNγR1KO stem-like induced OTI cells maintained longer their Tcf1 expression, therefore harbouring a greater proportion of stem-like T cells in tumours compared to WT cells after 6 days (**Figure 48**). This suggests that indeed IFNγ-sensing negatively affects stem-like T cell maintenance in tumours.

I also sought to formally assess the self-renewal capacity of the cells to examine whether stem-like T cells stayed quiescent or self-renew therefore proliferate resulting in active maintenance. First of all, I isolated live immune cells from WT tumours, loaded them with a dye, and restimulated them *ex vivo* with exogenous IFNγ or blocking IFNγ. Detecting stem-like T cells ($CD8^+PD\text{-}1^+Tcf1^+$ cells) with diluted dye confirmed that they were able to divide and self-renew (**Figure 46B**). Blocking IFNγ increased the stem-like T cell proportion and retention while dividing therefore by proper self-renewal suggesting an active stem-like T cell maintenance (**Figure 46**). Interestingly, adding a high concentration of exogenous IFNγ did not affect the cells as compared to the mock situation (control with media only). This suggests that the IFNγ produced in the milieu is already saturating therefore adding IFNγ in excess at least did not further affect stem-like T cells. To go further into the direct IFNγ effect on stem-like T cells I decided to reproduce the same *ex vivo* proliferation assay but on pure stem-like T cells to evaluate whether it is an intrinsic and direct IFNγ mechanism on those cells. To do so, I needed to sort stem-like T cells from tumours. However, this came with challenges. First of all, stem-like T cells are rare in tumours, representing only 10% of all infiltrating $CD8^+$ T cells at day 12 post-engraftment (see **Figure 35** in **Chapter 5**). As a result, it would be critical

to evaluate their intra-tumoral presence over time to 1) reveal a particular time point where their number might be higher and 2) to decipher whether IFNγ sensing reduces their pool from the early immune response when cells reach tumours or whether it gradually diminishes the pool *in vivo*. In addition to their rarity in tumours, the use of the transcription factor Tcf1 expression to distinguish them was a limiting factor. It requires an intra-nuclear stain that technically restricted my flow cytometry panel size as not every fluorophore can handle nuclear permeabilization. Plus, in order to formally investigate their behaviour *ex vivo* I needed to sort them which was impossible using intracellular staining. Alternatively, some published papers suggested using a surface marker as a surrogate of stemness such as Ly108/SLAMF6 as it is supposed to be highly co-expressed with Tcf1[164,427]. However, the Ly108 stain was not as clean as the Tcf1 one, therefore $CD8^+PD\text{-}1^+Ly108^+$ were not fully recapitulating the $CD8^+PD\text{-}1^+Tcf1^+$ cells (data not shown) suggesting that using Ly108 as a surrogate was not accurate in our model. This could also suggest that there are potentially stem-like T cell subsets that can be defined using different markers and probably chemokine receptors as well. To tackle this, I used the commercially available Tcf1-reporter mouse. This mouse line expresses the GFP fluorescent protein from the Tcf7 locus, however, a significant caveat was that it also contains *loxP* sites which would result in a conditional mutation therefore deletion of the Tcf1 expression if I further cross the mouse with a Cre-positive mouse line. All-in-all this meant that this great tool would only be used as WT recipients but I will not have IFNγR1KO $CD8^+$ T cells with Tcf1-GFP-reporter. Thanks to those Tcf1-GFP reporter mice, WT stem-like T cells were sorted and used for *ex vivo* experiments using blocking IFNγ.

Inhibiting IFNγ increased the percentage of proliferating stem-like T cells, which further demonstrates that IFNγ directly restricts stem-like T cell expansion in tumours (**Figure 48C**). Of note, in this experiment intra-tumoral stem-like T cells encountered IFNγ before being isolated and treated *ex vivo*, suggesting that the IFNγ effect might be reversible on those cells. On another hand, it could also suggest that in tumours, some stem-like T cells might be in specific niches where surrounding cells can uptake IFNγ, therefore, protecting the stem-like phenotype to some extent. By isolating them and disrupting their microenvironment but treating the cells with blocking-IFNγ antibodies *ex vivo*, it could recreate this aspect of the niche and increase their maintenance. Indeed, in the tumour microenvironment not only tumour cells but macrophages and dendritic cells for instance express high levels of IFNγR, therefore, will have potentially a greater IFNγ uptake than $CD8^+$ T cells[428,199]. In line with this, some studies investigated such niches both in tumours and draining-lymph nodes suggesting that indeed stem-like T cell biology depends on their surrounding environment both at the cellular and soluble level[165,148,184,161]. However, to formally assess whether WT stem-like T cells would appear in those niches while IFNγR1KO stem-like T cells would be found throughout tumours, I would require another Tcf1-reporter mouse to create IFNγR1KO-CD8-Tcf1-reporter mice to properly image them in tumours.

6.4.2 How does IFNγ restrict stem-like T cell maintenance in tumours?

IFNγ restricts the stem-like T cell overall maintenance in tumours. To investigate the mechanism supporting this, I first evaluated whether IFNγ could induce cell death of stem-like T cells, therefore, reducing the pool *in vivo*. There was no difference in

apoptosis levels between control and IFNγR1KO stem-like T cells in tumours and treating *in vitro*-activated cells with blocking-IFNγ did not affect their apoptosis level (**Figure 47**). Therefore, IFNγ does not increase stem-like T cell apoptosis. Moreover, I demonstrated that blocking IFNγ increased the stem-like T cell pool size and their proliferation (**Figure 46**). This highlights that IFNγ inhibits stem-like self-renewal by inhibiting cell division. In this case, stem-like T cell division can result in two cell types: stem-like T cells after self-renewal or more differentiated cells leading to early exhausted T cells after differentiation. In addition, several studies described the model of asymmetric division in stem cells from various tissues but also in T cells[429,148,430,431,432,433]. Following this reasoning stem-like T cells can in theory choose between 3 paths described in **Figure 50**: one stem-like $CD8^+$ T cell could either self-renew and give rise to two identical daughter cells (middle panel), differentiate and give rise to two early exhausted T cells (right panel) or undergo an asymmetric division and give rise to one identical stem-like T cell and one early exhausted T cells (left panel). In our model, stem-like T cells were dividing as they diluted the dye while maintaining the stemness as they kept Tcf1 expression. This suggests that they either performed asymmetric division or at least some cells were only self-renewing. In our scTCRseq data, stem-like T cells are sharing TCRs with the exhausted T cells (**Figure 49**). This suggests that again asymmetric divisions are occurring or it could also result from subsequent self-renewal and then full differentiation for example. Here we can speculate that IFNγ may influence the cell division choice of stem-like T cells toward differentiation into effector cells for instance or prevent asymmetric divisions to happen which could lead to the overall decrease of the stem-like T cell pool. In future directions, it would be interesting to study the cell division of stem-like $CD8^+$ T

cells and whether IFNγ could preferentially induce or force stem-like T cells to differentiate or inhibit asymmetric division for instance at the single-cell level. A recent study revealed that IL-10R signalling promotes stem-like T cell maintenance, indeed, blocking IL-10R impairs their maintenance and increased the overall $CD8^+$ T cell exhaustion in a chronic lymphocytic leukaemia model[191]. This is relatively expected as IFNγ (pro-inflammatory) and IL-10 (anti-inflammatory) are two pleiotropic cytokines with some opposite effects. Another recent study described the detrimental role of TGF-β on tumour-draining lymph node stem-like T cells that are critical for efficient tumour vaccination *in vivo*[434]. Altogether this suggests that stem-like T cell maintenance is most likely dependent on external cues which points out again specific niches *in vivo* that can protect or provide pro-stemness cues.

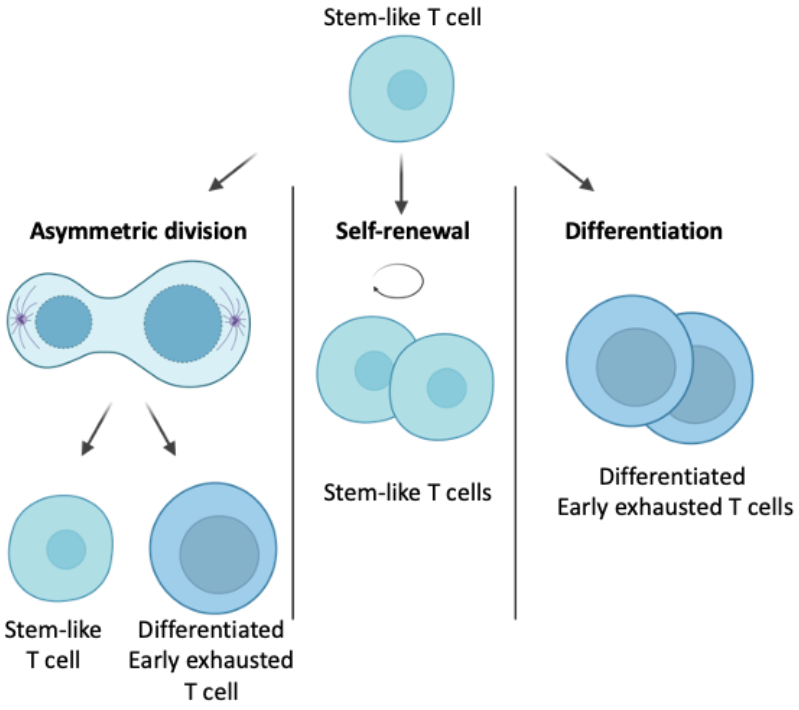


Figure 50: Stem-like T cell division decision tree. Three theoretical paths for stem-like T cell division and hence proliferation. [Created with BioRender.com].

In other studies, IFNγ has also been shown to regulate stemness in other cell types. Indeed, IFNγ has a strong impact on cells from bone marrow during inflammation, especially on hematopoietic stem cells (HSCs). It, for instance, directly impairs the self-renewal property of HSCs but also stimulates the differentiation into monocytes while inhibiting the differentiation into erythrocytes, eosinophils, neutrophils, and B cells during hematopoiesis[435]. Interestingly, short-term IFNγ signalling favours HSC proliferation whereas long-term IFNγ stimulation induces HSC differentiation by impairing their self-renewal capacity[436]. Again, IFNγ is very pleiotropic and can affect HSCs homeostasis directly by signalling or by modifying the surrounding niche of those cells. IFNγ effect depends on its production that needs to be timely (duration) and quantitatively (concentration) examined. Indeed, here I described different IFNγ outcomes depending on the duration of the signal. Another example highlighting the IFNγ dose-dependent effect of IFNγ is looking at cancer stem cells. Indeed, IFNγ has dose-dependent effects on cancer stem cells leading to different effects. For example, a low dose of IFNγ can potentiate the quiescence of cancer stem cells in melanoma and breast cancer[437] while high doses of IFNγ inhibit the self-renewal capacity and induces apoptosis of cancer stem cells from a colon cancer cell line which expresses a higher level of IFNγR[438]. Overall stem cell maintenance requires niches to enable their self-renewal property. Stem cells are sensitive to a variety of cues rendering them able to differentiate into the most needed cell types according to the changing environment. IFNγ plays an important role in this dynamic network as it is secreted during inflammation and cancer[439].

In terms of cell mechanism, T cell stemness has been shown to be promoted by the β-catenin pathway[440]. Therefore, I investigated whether IFNγ interferes with the WNT/β-catenin pathway in $CD8^+$ T cells which could result in the inhibition of the self-renewal function of stem-like T cells. This came with challenges, I tested several conditions by changing concentrations, and durations, using naïve or activated $CD8^+$ T cells, adding IFNγ, or blocking IFNγ before or after T cell activation. Surprisingly, the upregulation of β-catenin was only observed following TCR stimulation in $CD8^+$ T cells, as previously described[441], but not increased by its direct ligand WNT or an agonist triggering the pathway (glycogen synthase kinase-3 beta – GSK3β inhibitor – the TWS119)[442] (**Figure 51A**). This was surprising that the former ligand does not increase the β-catenin expression. However, the TCR-induced β-catenin was reduced by recombinant IFNγ treatment (**Figure 51B**). This suggests that IFNγ might inhibit the intrinsic capacity of T cells to maintain stemness *via* β-catenin accumulation following T cell activation[443]. Therefore, favouring effector differentiation over stemness. Interestingly, this was no longer observed when stem-like T cells were generated in the presence of the GSK3β inhibitor a potent activator of the WNT/β-catenin pathway[442]. This suggests that blocking IFNγ does not increase stemness through this pathway[444]. Altogether it shows that IFNγ presence upon T cell activation reduces the stemness potential of $CD8^+$ T cells by limiting the TCR-induced β-catenin upregulation and blocking IFNγ enhanced the stem-like T cells pool potentially through another cellular pathway. To further investigate the cellular effect of IFNγ on stem-like T cells would require more functional assays.

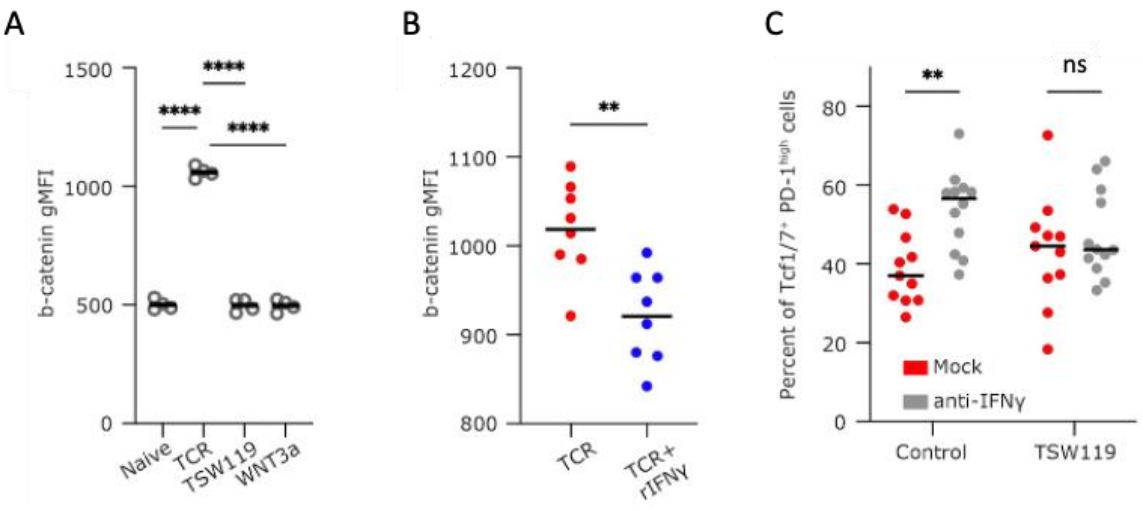


Figure 51: Relationship between IFNγ-sensing and WNT/β-catenin pathway in CD8⁺ T cells. A- Naïve CD8⁺ T cells from lymph nodes were treated with anti-CD3 and anti-CD28 (TCR), the GSK3β inhibitor TWS119, or the WNT agonist WNT3a for 6 hours. β-catenin expression was assessed by flow cytometry. Data is from 2 independent experiments (n=4). The comparison between more than 2 groups was analysed using one-way ANOVA on GraphPad Prism. **** = P<0.0001. **B-** Naïve CD8⁺ T cells from Lymph nodes were pre-treated with IFNγ when indicated for 16 hours before being stimulated with anti-CD3 and anti-CD28 (TCR) for 6 hours. β-catenin expression was assessed by flow cytometry. Data is from 2 independent experiments (n=8). The comparison between the 2 groups was analysed using an unpaired t-test on GraphPad Prism. ** = P<0.001. **C-** Naïve CD8⁺ T cells from lymph nodes were stimulated with anti-CD3 and anti-CD28 antibodies in the presence of IL-2. When indicated, cells were further treated with blocking-IFNγ (anti-IFNγ) and the glycogen synthase kinase 3 beta (GSK3β) inhibitor TWS119. After 4 to 5 days in culture, cells were harvested and stained for CD45, CD8, Tcf1, and PD-1. The graph shows the percentage of Tcf1⁺PD-1^{high} stem-like T cells following re-stimulation in the presence (grey) or absence (red) of anti-IFNγ (n=11 from 3 experiments). The comparison between the groups was analysed using Mixed-effects model on GraphPad Prism. ns = not significant, ** = P<0.001.

6.4.3 Conclusion

In recent studies, stem-like T cells have been described as a keystone in the efficacy of immunotherapies against cancer. Their continuous depletion in tumours[194,196] remains to be fully understood to improve cancer treatment. Here we brought new insight into their biology by showing that IFNγ-sensing affects their active maintenance

in tumours. IFNγ preferentially targets stem-like T cells which will lead to consequences in the exhausted T cell population therefore the entire immune response. Overall, we demonstrated that IFNγ signalling in intra-tumoral stem-like $CD8^+$ T cells inhibits their self-renewal potential, therefore, reducing the stem-like T cells pool and the immune response diversity in tumours.

7. General discussion and conclusion

CTLs are vital to eradicate cancer cells, however, they are becoming dysfunctional in chronic contexts. Indeed, numerous immunosuppressive factors are restricting their immunity cycle hence their effector functions in tumours. Consequently, this $CD8^+$ T cell dysfunction led to tumour tolerance and represents an important obstacle for successful immunotherapies against tumours[445,446]. It is therefore critical to formally investigate mechanisms behind this dysfunction and whether some are targetable to enhance the anti-tumour response. Indeed, ICB appeared as a very promising new way to treat cancer patients, however with the small fraction of responders, the appearance of acquired resistance, and the many side effects, nowadays ICB requires drastic improvements to reach its full potency. Efficient $CD8^+$ T cell anti-tumour responses are a dynamic process as it implies multiple critical steps. The concept of exhaustion with $CD8^+$ T cell terminal exhaustion only partly explains their dysfunction in cancer as ICB is rarely effective[181]. Recent discoveries point out that stem-like T cells are key players in immunotherapy efficacy. Ultimately ICB targets early exhausted $CD8^+$ T cells that have just reached the tumour[447] and stem-like T cells that are able to positively respond to ICB with new effector cell differentiation occurring directly at the tumour site[150,130,448,163]. The stem-like T cells are therefore essential to study and deciphering their biology, survival, and function in tumours may contribute towards improving ICB and opening new therapeutic avenues.

By investigating the specific role of the effector molecule IFNγ in $CD8^+$ T cell dysfunction in cancer, I have discovered that IFNγ plays a critical role in stem-like T cell

maintenance in tumours. This contributes to a better understanding of their regulation and especially of their active intra-tumoral maintenance. This chapter summarises the key results and presents the proposed mechanism before assessing the relevance of this work in humans. Finally, these new insights into both stem-like biology and IFNγ function in tumours bring a new opportunity for rethinking therapeutics design.

7.1 Thesis summary

To formally investigate the role of IFNγ on $CD8^+$ T cells in a tumour context, I prevented IFNγ-sensing by specifically depleting IFNγR1 in mature $CD8^+$ T cells, which represent the main IFNγ producers in tumours. Ablating IFNγ sensing by $CD8^+$ T cells recovers their anti-tumour response against murine melanoma, thus bypassing the need for further immunotherapy. Preventing IFNγ sensing in $CD8^+$ T cells enhanced tumour control both at the endogenous and antigen-specific levels. This suggested an IFNγ-driven fundamental mechanism regulating IFNγ producers in a negative manner. Further mechanistic analyses revealed that the IFNγ-restricting effect on $CD8^+$ T cell anti-tumour response was not due to less efficient effector functions. Indeed, IFNγR1 depletion in $CD8^+$ T cells did not enhance their effector functions, including cytokine secretion, and cytotoxic killing, but enhanced their expansion and tumour infiltration. IFNγ-sensing does not affect $CD8^+$ T cell activation nor apoptosis, suggesting that the greater tumour expansion results from a greater proliferation or cell recruitment at the tumour site. Further tumour homing experiments revealed that IFNγ-sensing is critical for $CD8^+$ T cell

recruitment to the tumour. Therefore, the greater $CD8^+$ T cell expansion of IFNγR1KO $CD8^+$ T cells must result from an enhanced proliferation directly in tumours. Overall, IFNγ-sensing by $CD8^+$ T cells limits anti-tumour immunity, $CD8^+$ T cell expansion, and localisation to the core of the tumour while enhancing $CD8^+$ T cell tumour homing. Further in-depth investigations guided by scRNA-seq data revealed that IFNγ does not affect $CD8^+$ T cells in lymph nodes but indeed directly in tumours. Three main cellular clusters were defined and their proportion in tumours revealed that IFNγ preferentially targets stem-like T cells. Indeed, IFNγ-sensing limits the presence of stem-like T cells in tumours. On top of that, *in vivo* analysis showed that IFNγ also increased the overall level of $CD8^+$ T cell exhaustion, and the enhanced IFNγR1KO $CD8^+$ T cell expansion through proliferation is not due to exhausted T cell proliferation, suggesting that this increase in proliferative capacity must start before the exhausted state. With the defect in tumour homing, this suggests that the increased presence of less exhausted cells may result from on-site $CD8^+$ T cell differentiation which is restricted by IFNγ. Altogether, the better control of B16F10-OVA tumours in CD8-IFNγR1KO mice is solely due to mechanisms occurring in tumours. Exhausted $CD8^+$ T cells did not seem particularly impacted by IFNγ-sensing, however, the greater presence of stem-like T cells when cells are IFNγ-insensitive suggests that they are playing a critical role in efficient tumour control. As a matter of fact, WT stem-like T cells have higher proliferative capacity than exhausted T cells and represent a pool of precursors for early exhausted T cells with effector capabilities in tumours. In addition, WT stem-like T cells harbour a greater level of IFNγR expression suggestive of an enhanced IFNγ sensitivity compared to other $CD8^+$ T cell subsets in tumours. Therefore, IFNγR1 depletion would particularly affect intra-

tumoral stem-like T cells. Further investigations revealed that indeed IFNγ restricts stem-like T cell proliferation and their active maintenance by self-renewal. Consequently, IFNγ-sensing by tumour-infiltrating stem-like $CD8^+$ T cells decreases their pool size and their clonal diversity which leads to less diversity in the overall $CD8^+$ T cell anti-tumour response. Moreover, it highlights the fact that stem-like T cells are at the origin of exhausted T cell responses.

To summarise my findings, I propose a working model depicted in **Figure 52**. The upper side of the scheme in red represents the WT context, where $CD8^+$ T cells can sense IFNγ, as opposed to the lower panel in grey with IFNγ-insensitive $CD8^+$ T cells. In both conditions, there is a stem-like T cell pool reaching the tumours where they differentiate and coexist with effector $CD8^+$ T cells, the CTLs. As cytotoxic cells, the CTLs produce IFNγ for their effector function, releasing IFNγ in the tumour microenvironment. In the WT condition, this triggers a negative feedback loop targeting the stem-like T cells inhibiting their active maintenance. Consequently, the stem-like T cell pool decreases, and with this the differentiation of CTLs in tumours. The CTLs will then follow the exhaustion path and become dysfunctional. Overall, tumours will escape from the immune system and will overgrow. In the alternative context, when $CD8^+$ T cells do not sense IFNγ, the negative feedback loop is abrogated and the stem-like T cell pool is maintained for longer and in greater size. This leads to the *de novo* replenishment of CTLs overtime directly into tumours, thus, maintaining an ongoing anti-tumour response controlling the tumour growth.

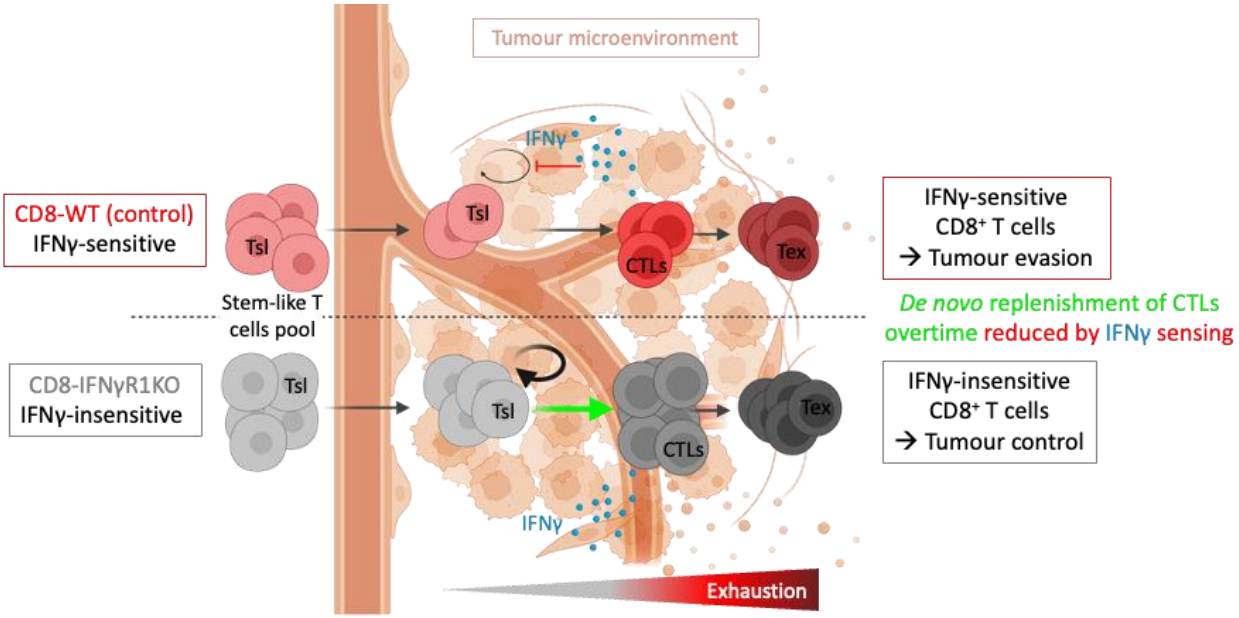


Figure 52: Proposed mechanism of IFNγ triggered negative feedback loop in tumour infiltrating CD8⁺ T cells. [Created with BioRender.com].

Altogether, we discovered that IFNγ targets stem-like T cells in tumours, which can quickly differentiate into early exhausted T cells, hence the indirect IFNγ effect on T cell exhaustion. Our data suggest that IFNγ limits both the stemness and the proliferative capacity following restimulation of stem-like T cells. If IFNγ-sensing is important for tumour homing, it then impedes the *de novo* replenishment of less exhausted T cells in the tumour core. This highlights a new dual function of IFNγ with pro- and anti-tumour functions exerted on CD8⁺ T cells. Interestingly, the increased CD8⁺ T cell tumour homing triggered by IFNγ is greatly outweighed by the restricting IFNγ effect inhibiting the intra-tumoral maintenance of stem-like T cells and their subsequent differentiation in early exhausted T cells leading to CD8⁺ T cell expansion. This study emphasises the pleiotropic effect of IFNγ and its role in the CD8⁺ T cell anti-tumour dysfunction. Uncoupling the

anti-tumour function of IFNγ from its tumour driving effects appears critical in achieving a more efficient anti-tumour response, especially in the context of immunotherapy.

7.2 Significance in human: IFNγ and CD8$^+$ T cells in cancer patients

CD8$^+$ T cells and IFNγ are critical players in anti-tumour responses both in mice and humans. This thesis demonstrated that IFNγ triggers a negative feedback loop in CD8$^+$ T cells in tumours, which restricts the overall tumour control in mice. To characterise the relevance of IFNγ sensing by CD8$^+$ T cells during cancer in humans, we collaborated with Benjamin Fairfax to re-analyse their scRNA and bulk-RNA sequencing dataset[235] on circulating CD8$^+$ T cells harvested from metastatic melanoma patients before and after ICB treatment.

We first investigated the IFNγR transcriptional level of expression in different CD8$^+$ T cell subsets from blood, in 8 patients before and after 21 days of ICB using the scRNA-seq dataset. As previously described, CD8$^+$ T cell subsets with an activated and memory phenotype upregulate IFNγR1 and downregulate IFNγR2 compared to naïve cells. Interestingly, most of the CD8$^+$ T cell subsets supposed to produce IFNγ have a similar IFNγR expression pattern (**Figure 53A** and **53B** – left panels) including MAIT (mucosal-associated invariant T) and γδ T cells which are unconventional CD8$^+$ T cells that can rapidly harbour effector functions[449,450]. As in mice, the IFNγR2 downregulation and IFNγR1 upregulation suggest that IFNγ-producing cells became less sensitive to IFNγ compared to naïve cells while still being able to sense the cytokine from the

environment. This is consistent with the IFNγ negative feedback loop described in mice, suggesting that the same mechanism could be relevant in human $CD8^+$ T cells as well. ICB did not affect the IFNγR expression across $CD8^+$ T cell subsets. However, mitotic cells which represent $CD8^+$ T cells that are proliferating have a decreased proportion of cells expressing IFNγR1 and IFNγR2 after ICB. Of note, mitotic cells are the only cell subset with very low transcriptional levels of both IFNγR chains that are not affected by ICB (**Figure 53A** and **53B** – right panels), suggesting an escape from the IFNγ-driven regulatory loop. Expressing less IFNγR can either cause a proliferative advantage for $CD8^+$ T cells or, alternatively, the reduced IFNγR expression may be a consequence of the enhanced proliferation of the $CD8^+$ T cell population. In our mouse study, not expressing IFNγR correlated with a greater $CD8^+$ T cell expansion suggesting a causative effect rather than a consequence.

In another similar study, Fairfax *et al.*[236] described that ICB-responsive melanoma patients have more large $CD8^+$ T cell clones, defined as representing over 0.5% of the blood T cell repertoire (a clone size is calculated as the number of cells having the same TCR). The greater presence of large clones was associated with a good prognosis 6 months after ICB. Here we revealed that the proportion of cells expressing IFNγR2 significantly decreased across clone size while IFNγR1 expression remains unchanged (**Figure 53C** and **53D** – left panels). And ICB further decreased the level of IFNγR2 expression in cells (**Figure 53D** – right panel). This further suggests that enhanced proliferation with large clones is 1) predictive of a more effective $CD8^+$ T cell response and 2) that it correlates with lower IFNγR2 expression. Knowing that patients with more large clones have a better clinical outcome after ICB and that large T cell clones express

less IFNγR2 we next interrogated whether IFNγR expression could have a predictive value for ICB treatment. Further characterisation of bulk-RNAseq data from circulating $CD8^+$ T cells after the first cycle of ICB treatment in metastatic melanoma patients revealed that lower IFNγR2 but not IFNγR1 expression was associated with no disease progression therefore better response to ICB (**Figure 53E**). Interestingly, the downregulation of both IFNγR chains significantly correlated with auto-immune events suggesting that IFNγ-sensing by $CD8^+$ T cells may regulate tolerance during active immune responses, therefore triggering a physiological regulatory loop in humans as well (**Figure 53F**).

Overall, this line of evidence in human $CD8^+$ T cells indicates that IFNγR expression is tightly regulated and negatively correlates with a positive response to ICB in metastatic melanoma patients. This further confirms the relevance of our study and the translational potential as IFNγ-sensing by $CD8^+$ T cells may induce a negative feedback loop impacting the anti-tumour response after ICB.

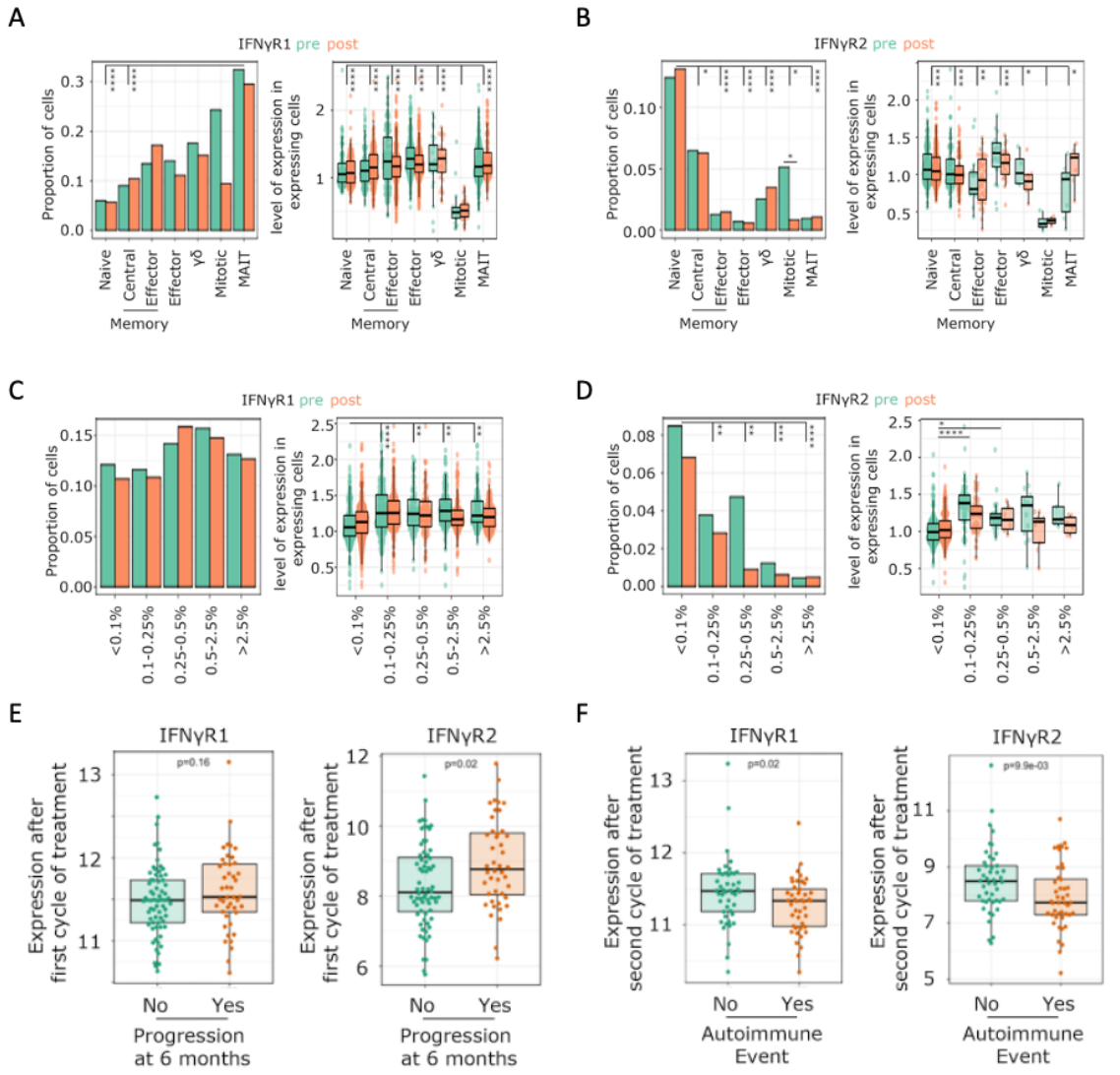


Figure 53: IFNγR transcriptional expression in circulating CD8⁺ T cells from metastatic melanoma patients undergoing ICB and correlation with disease progression. (**A-D**) scRNAseq data of peripheral CD8⁺ T cells from 8 metastatic melanoma cancer patients treated with immune checkpoint blockade from Watson *et al.*[235] was analysed for IFNγR expression. Samples were taken before (Day 0, pre) and after (Day 21, post) treatment. Patients received either pembrolizumab (anti-PD-1; 4 patients) or a combination of ipilimumab/nivolumab (anti-CTLA-4 and anti-PD-1 respectively; 4 patients). (**A-B**) The proportion of cells displaying a detectable expression of the IFNγ-receptor (left panels) and level of expression (right panels) of IFNγR1 (**A**) and IFNγR2 (**B**) in multiple T cell subsets. For (**A-B**, right panels), statistics compare Mitotic cells to other cell subsets. For (**B**, left panel), statistics compare Naive cells to other cell subsets. (**C-D**) The proportion of cells displaying a detectable expression of the receptor (left panels) and level of expression (right panels) of IFNγR1 (**C**) and IFNγR2 (**D**) according to CD8⁺ T cell clonal size. For (**C-D**, right panels), statistics compare the smallest clonal size to others. (**E-F**) Bulk-RNA seq analysis of CD8⁺ T cells from metastatic melanoma patients (n=110) 21 days after starting checkpoint blockade therapy for which clinical follow-ups were available (see Watson *et al.*[235]

for more details). For (**C**, left panel) data is non-significant. **E-** Correlation between disease progression and IFNγR1 (left panels) or IFNγR2 (right panels) expression after a first cycle of checkpoint blockade. **F-** Correlation between autoimmune event and IFNγR1 (left panels) or IFNγR2 (right panels) expression after a first cycle of checkpoint blockade. Comparisons between individuals with divergent 6-month progression and autoimmune toxicity outcomes were performed using Wilcoxon rank sum tests. Analysis performed by Benjamin Fairfax's team within a collaboration. * = P < 0.05, ** = P < 0.002, *** = P < 0.001, **** = P<0.0001.

In our murine study, we showed that IFNγR1 expression in $CD8^+$ T cells inhibits the stem-like T cell active maintenance and therefore their stemness. To investigate the relationship between IFNγR expression and the stem-like T cells or stemness potential of $CD8^+$ T cells in human tumours, we re-analysed datasets publicly available from patients with melanoma[162] and non-small cell lung cancer[451]. We revealed a negative correlation between the percentage of stem-like T cells with a detectable expression of IFNγR1 and the strength of their stem-like signature (**Figure 54**). This inverse correlation is consistent with my findings in mice where IFNγ inhibits the maintenance of stem-like T cells and thus the stemness.

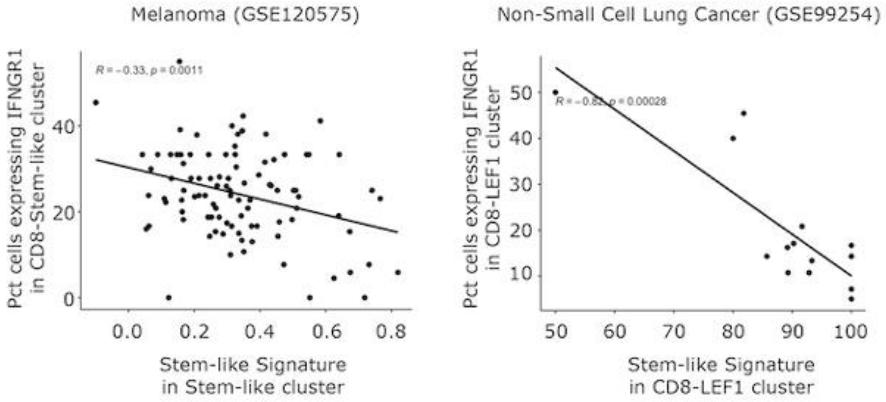


Figure 54: Correlation between IFNγR1 and stem-like signature in human tumour patients using single-cell RNA-seq. Graphs show the correlation between the percentage of IFNγR1 expressing stem-like T cells and stem-like signature scoring (R = Pearson's correlation coefficient; statistical significance was assessed using Fisher's test). Each dot represents a patient. Analysis performed by Audrey Gerard.

To conclude on the human relevance, a lower IFNγR2 expression in $CD8^+$ T cells was predictive of ICB response effectiveness and therefore of an efficient anti-tumour response. Furthermore, the lower IFNγR1 expression correlated with the cancer patient greater stem-like signature in stem-like $CD8^+$ T cells. This suggests that the IFNγ regulatory effects in mice may also occur in humans. The IFNγR transcriptional level of expression can be tested as a predictive parameter to stratify melanoma patients selected for ICB treatment. Lastly, the IFNγR expression dictating IFNγ sensitivity in $CD8^+$ T cells may offer a therapeutic potential that needs to be further investigated in mice and *in fine* humans as a means for improving adoptive cell transfer therapy for instance.

7.3 New insight in stem-like T cell biology: therapeutic potential

The recent discovery of stem-like T cells and their role in the positive response to ICB raised new questions on their regulation, biology, and function. While their generation and maintenance in LN have received significant attention[161,426,452], their presence and more importantly their disappearance in tumours is incompletely understood so far. A very recent paper described their presence in LN before their migration to tumour with TCR lineage tracing, where they rapidly differentiate into exhausted T cells[453]. The authors of this study demonstrated that stem-like T cells are primarily activated in the tumour draining LNs before migrating to the tumour to differentiate, which fits with the proposed model of my thesis. Interestingly they also showed that stem-like T cells in

tumours upregulated IFNγ-signalling and co-stimulation pathways which might drive their differentiation, which is again in agreement with the findings of my thesis.

Our work here provides new insights into stem-like T cell regulation at the tumour site whereby IFNγ-sensing induces the reduction of the stem-like T cell pool by inhibiting their active maintenance over time. This novel parameter indicates that stem-like T cell fate is notably determined by environmental cues. This knowledge can serve to test whether boosting the presence of stem-like T cells in tumours may, as speculated, improve the immune response against tumours after ICB. To do this, it will be critical to assess whether the enhanced presence of stem-like T cells in terms of number and duration indeed improves the anti-tumour response in murine models first, without triggering detrimental effects leading to auto-immune events, for instance by breaking of the immune tolerance. If this is the case, then this knowledge can be very beneficial, especially to improve current types of cellular and molecular immunotherapies. Adoptive cell therapy is a type of immunotherapy based on the isolation, selection, and amplification of immune cells, mostly $CD8^+$ T cells that will be re-injected into cancer patients to attack cancer cells. The aim can be to simply expand the selected cells or may involve genetic engineering to modify and enhance tumour recognition, for instance with CAR-T cells. As an example, tumour tissue can be surgically extracted from a metastatic patient, and $CD8^+$ T cells isolated *ex vivo*. In some patients, there will be stem-like T cells in the extracted $CD8^+$ T cell mixture. Knowing that stem-like T cells are involved in the positive response to ICB, re-injecting pure or enriched stem-like T cells mix into the patient prior to ICB treatment may represent in theory an optimised therapeutical approach. As IFNγ inhibits the stem-like T cell maintenance in tumours,

genetically preventing IFNγ-sensing in the cultured cells may enhance their survival in tumours once re-injected into the patient and may consequently last longer. Alternatively, blocking IFNγ during the *ex vivo* cell culture step may be a way to increase the stem-like T cell proportion in the re-injected $CD8^+$ T cell mix. This may have a great impact on improving immunotherapy efficacy and durability in metastatic patients or patients with inoperable tumour sites.

7.4 Future directions

In this thesis, I discussed the obtained results and several interesting future experiments or paths to investigate for follow-up studies in the discussion sections. In this chapter section, I am summarising some potential approaches that would be interesting to pursue either for answering fundamental questions or to further investigate therapeutic avenues.

7.4.1 Fundamental opened questions

Taken together, this work demonstrated an IFNγ regulatory role exerted on $CD8^+$ T cells that restrict their anti-tumour function. By specifically knocking out the IFNγR1 on mature $CD8^+$ T cells we improved tumour control of a murine melanoma model.

As previously mentioned, IFNγR1 is the high-affinity binding chain of the IFNγR, and IFNγR2 is critical for downstream signalling. Therefore, it would have been interesting to reproduce our study in a CD8-IFNγR2KO and/or a double IFNγR1-IFNγR2KO murine

model to investigate whether it would phenocopy our enhanced tumour control results. Indeed, this would help us define whether our phenotype is solely due to the prevention of IFNγ-sensing or whether it is specifically through the prevention of IFNγ-signalling. This would also give information on whether IFNγR1 harbours its own role of IFNγ-binding triggering cellular effects without signalling, therefore having an IFNγR2-independent role in $CD8^+$ T cells. Moreover, I proposed a model hypothesising that IFNγ could act as a "stop-signal" for $CD8^+$ T cell migration without integrating detrimental IFNγ signalling cellular effects. This would mean that the upregulation of IFNγR1 upon $CD8^+$ T cell activation could have mechanical effects affecting the effector $CD8^+$ T cell tumour migration as a result of the IFNγ-binding properties of IFNγR1. Comparing IFNγR1KO and IFNγR2KO $CD8^+$ T cell migration patterns in different conditions both *in vitro* and *in vivo* would substantiate this hypothesis. In line with this, two-photon microscopy experiments may have been very interesting to perform, allowing the direct assessment of whether IFNγ-sensing can affect the intra-tumoral migration and invasion of $CD8^+$ T cells in our model. Indeed, a recent paper developed a method to investigate the T cell motility in tumours and human tumour biopsies[454]. They revealed that $CD8^+$ T cell motility in tumours positively correlated with the engaged exhaustion program. As IFNγ-sensing affect the overall exhaustion level in our model, it would have been interesting to assess their motility directly in tumours.

In parallel, it is well established that the tumour core localisation of $CD8^+$ T cells is critical for efficient anti-tumour responses. By preventing IFNγ-sensing in $CD8^+$ T cells, we enhanced the $CD8^+$ T cell tumour infiltration. Apart from the increased $CD8^+$ T cell expansion and differentiation on site, I did not elucidate further this enhanced tumour

core invasion. Therefore, it would be interesting to thoroughly investigate how this different tumour localisation is achieved. Is it only a consequence of local differentiation or is it an active process where IFNγ indeed restrict their tumour infiltration? Answering this question may lead to the discovery of new factors enhancing T cell infiltration in tumours that may be of therapeutic interest. In line with this, it would be very interesting to investigate the $CD8^+$ T cell expansion and localisation over time at different time points.

On another note, the IFNγ-driven negative feedback loop described in this thesis interrogates its fundamental mechanism. In other words, does it only affect $CD8^+$ T cells or could it happen in other cell types? As $CD8^+$ T cells are the main IFNγ producers, I am wondering whether NK cells which represent the second main IFNγ-producing cell population in our model could also be affected by this IFNγ negative feedback loop. We observed that IFNγ preferentially targets stem-like T cells however this does not exclude other regulatory mechanisms on other $CD8^+$ T cell subsets. Moreover, NK cells harbour a similar IFNγR expression pattern with very high levels of IFNγR1 compared to IFNγR2. Also, IFNγR1KO-NK models may help to answer the question of whether IFNγ can affect other key IFNγ-producing cells in tumours.

Regarding stem-like T cells, this study revealed a novel biological negative regulator of their active maintenance in tumours. Multiple future experiments may be relevant to further the basic research on their biology.

Firstly, several studies speculated that they are present in particular niches within the tumour microenvironment. My findings suggest that indeed if stem-like T cells are surrounded by APCs they could in theory protect them by consuming the IFNγ present

at proximity resulting in the sustainment of their self-renewal properties. Deciphering those niches may be a key to characterise additional factors that can influence and control the stem-like T cell maintenance in tumours. In parallel, as stem-like T cells have been described in T cell zone/lymphoid structures in human tumours[165], and in proximity to HEVs in murine tumours[190], this further suggests that they might be present in tertiary lymphoid structures (TLS) hence very specific niches. TLS have been described in many human tumours and are defined as ectopic lymphoid structures present in long-lasting inflammatory conditions such as cancer[455,456]. Furthermore, they have been strongly associated with improved clinical outcomes upon immunotherapies[457,185]. Therefore, TLS could represent an entry route and provide appropriate niches for stem-like T cells in tumours. It could be interesting to investigate the relationship between stem-like T cells and TLS. Does the enhanced presence of stem-like T cells (naturally or induced) trigger the formation of TLS which are a critical advantage for ongoing anti-tumour responses? Or *vice versa*, does the presence of TLS influence the maintenance of stem-like T cells in tumours?

Secondly, I have demonstrated that IFNγ affects the proliferation and self-renewal properties of stem-like T cells. In **Chapter 6**, I discussed the potential model of stem-like T cell division (see **Figure 50**). Following this, it would be very interesting to investigate whether 1) stem-like T cells divide asymmetrically, 2) whether IFNγ may preferentially induce or force stem-like T cells to differentiate, thus inhibiting their self-renewal properties and 3) whether IFNγ may prevent the stem-like T cell asymmetric division for instance.

Thirdly, further experiments are required to properly investigate the molecular mechanism at play in the stem-like T cell restriction by IFNγ. Indeed, I assessed whether IFNγ could interfere with the WNT/β-catenin pathway as it is involved in the biology of many other stem cells. However, this does not appear to be the case, suggesting that other molecular pathways must act here, which once deciphered can potentially represent therapeutic targets.

7.4.2 Translational and therapeutic potential questions

Fundamental research and translational research are relying on each other and pursue the same end goal, improving the scientific knowledge to understand and *in fine* treat human diseases. Investigating fundamental questions very often raises translational or therapeutic opportunities.

Here I described the regulatory role of IFNγ on their own producers in melanoma tumours. For my experiments, I used the OTI system which is a great tool for fundamental research but furthermore represents a valuable tool to study adoptive cell therapy similar to ACT in humans. This work demonstrated that transferring IFNγR1KO tumour-specific $CD8^+$ T cells improved tumour control. This has therapeutic potential and could be a new parameter as an immune checkpoint for T cell-based therapies. With the CRISPR-Cas9 gene editing system, $CD8^+$ T cells can be genetically manipulated to ablate IFNγR expression for instance. This may also be applicable while generating CAR-T cells for instance. As mentioned in the previous section, ACT can in theory benefit from transferring stem-like T cells into patients. It would be very interesting to test this in mice by transferring IFNγR1KO stem-like T cells into tumour-bearing WT mice and assess

their tumour growth. Having demonstrated that blocking IFNγ increases the stem-like T cell maintenance *ex vivo* and that IFNγR1KO cells keep longer and greater their stemness *in vivo*, it would be appealing to test if it could be achieved by treating WT tumour-bearing mice with blocking-IFNγ systemically. However, this would likely trigger many side effects and would prevent the anti-tumour effects of IFNγ, which are critical for efficient immune response, with for example the $CD8^+$ T cells and other immune cells tumour homing and the CTLs effector functions by secreting IFNγ toward tumour cells. The aim of increasing stem-like T cells *in vivo* without transferring cells appears quite challenging as they seem to differentiate very early on during the immune response, therefore, aiming to increase their recruitment, survival, and self-renewal to the tumours appears more feasible than enhancing their primary differentiation as many aspects of this approach remain to be understood.

In this work, I mainly used one murine melanoma model. Further experiments would be relevant to reproduce these findings using other murine cell lines, for instance, models with different characteristics such as different levels of immunogenicity, or even different tumour models which are more physiological, such as genetic models with spontaneous tumours. Following those studies, it would be very relevant to investigate this mechanism in metastatic models as nowadays cancer patients are mostly dying from metastasis, rarely from primary tumours.

Finally, to further expand the findings of this study, it would be interesting to treat the tumour-bearing mice with immunotherapies after tumour relapse following primary control and compare whether the IFNγ sensitivity in $CD8^+$ T cells affects their response to immunotherapies.

Overall, this study brings a new piece of knowledge regarding stem-like T cell biology which improves our understanding and may hopefully have an impact on improving current immunotherapies, or even help in designing novel cancer therapies.

List of Figures

Figure 1: The Hallmarks of Cancer. 18
Figure 2: The cancer immunity cycle: 7 steps to eradicate cancer cells. 22
Figure 3: Classical pathway of IFNγ signalling. 27
Figure 4: Overview of the opposite effects of IFNγ in tumours. 31
Figure 5: $CD8^+$ T cell development. 35
Figure 6: $CD8^+$ T cell activation. 36
Figure 7: $CD8^+$ T cell differentiation in acute *versus* chronic immune response. 39
Figure 8: Course of the $CD8^+$ T cell response in acute *versus* chronic immune response. 41
Figure 9: A simplistic revised model of $CD8^+$ T cell differentiation in chronic contexts. 45
Figure 10: Main cellular markers to distinguish $CD8^+$ T cell populations. 47
Figure 11: IFNγR expression landscape in $CD8^+$ T cells both in mice and humans at the transcriptional level. 80
Figure 12: Crossing strategies to generate CD8-IFNγR1KO mouse model at the endogenous level. 85
Figure 13: Validation of the CD8-IFNγR1KO mouse model *in vivo*. 87
Figure 14: Crossing strategies to generate IFNγR1KO-OTI mice to obtain WT and IFNγR1KO OTI cells. 89
Figure 15: Workflow to obtain murine melanoma tumours to study $CD8^+$ T cells response. 91
Figure 16: IFNγ sensing by $CD8^+$ T cells restricts anti-tumour immunity in mice. 93
Figure 17: IFNγR1 ablation in tumour-specific $CD8^+$ T cells improves tumour control in an adoptive T cell transfer model. 95
Figure 18: IFNγ sensing by $CD8^+$ T cells restricts anti-tumour immunity in MC-38 murine colon cancer. 96
Figure 19: IFNγR and IFNγ expression landscape in NK cells at the transcriptional level. 103
Figure 20: General workflow to investigate tumour-infiltrating $CD8^+$ T cell fitness. 105
Figure 21: Tumour-infiltrating $CD8^+$ T cell cytokine production potential assessed by *ex vivo* re-stimulation. 107
Figure 22: IFNγR1 ablation in $CD8^+$ T cells does not affect the cytokine bioavailability in the tumour microenvironment. 109
Figure 23: IFNγR1 ablation in $CD8^+$ T cells does not affect their cytotoxic functions. 111
Figure 24: IFNγ sensing restricts the $CD8^+$ T cell absolute number in B16F10-OVA tumours. 113
Figure 25: IFNγ sensitivity does not affect $CD8^+$ T cell apoptosis level. 114
Figure 26: IFNγ restricts tumour-specific $CD8^+$ T cell proliferation in tumours. 115
Figure 27: IFNγ sensing does not affect $CD8^+$ T cell priming. 116
Figure 28: $CD8^+$ T cell tumour localisation *in vivo*. 119
Figure 29: IFNγ sensing is required for effector $CD8^+$ T cell tumour homing. 121
Figure 30: Tumour-associated endothelium assessment in control *versus* CD8-IFNγR1KO mice. 124
Figure 31: Sorting of $CD8^+$ T cells from tumours and draining lymph nodes prior to single-cell RNA sequencing. 135
Figure 32: $CD8^+$ T cells unbiased characterisation in lymph nodes and tumours from control and CD8-IFNγR1KO mice by scRNA-seq. 136
Figure 33: Flow cytometry gating strategy to assess immune composition remodelling within B16F10-OVA tumours. 139
Figure 34: Immune composition proportion from B16F10-OVA tumours in control *versus* CD8-IFNγR1KO mice. 140

Figure 35: IFNγ sensing affects CD8$^+$ T cell clusters proportion. Control and CD8-IFNγR1KO mice were engrafted with B16F10-OVA tumours. 142
Figure 36: Differential pathways analysis in exhausted CD8$^+$ T cells from control and CD8-IFNγR1KO tumours. 144
Figure 37: IFNγ-sensing influences the metabolic status of exhausted CD8$^+$ T cells at the transcriptional level. 145
Figure 38: IFNγ-sensing does not influence the metabolic status of exhausted CD8$^+$ T cells *in vivo*. 147
Figure 39: IFNγ-sensing reinforces CD8$^+$ T cell exhaustion *in vivo*. 149
Figure 40: IFNγ-sensing reinforces CD8$^+$ T cell exhaustion at the transcription level. 150
Figure 41: IFNγ-sensing restricts CD8$^+$ T cell proliferation at the transcriptional level. 151
Figure 42: IFNγ-sensing does not affect exhausted CD8$^+$ T cell proliferation *ex vivo*. 152
Figure 43: Proliferative capacity of tumour-infiltrating CD8$^+$ T cells is initiated by stem-like T cells not exhausted T cells. 160
Figure 44: Stem-like T cells are IFNγ sensitive in tumours. 162
Figure 45: Stem-like T cell proliferation supports the greater IFNγR1KO CD8$^+$ T cells expansion in tumours. 164
Figure 46: Blocking IFNγ increases the maintenance of tumour-infiltrating stem-like T cells *ex vivo*. B16F10-OVA tumours were engrafted in WT mice. 166
Figure 47: IFNγ-sensing does not increase CD8$^+$ T cell death. 168
Figure 48: IFNγ sensing in intra-tumoral stem-like CD8$^+$ T cells impairs their maintenance. 169
Figure 49: IFNγ sensing by CD8$^+$ T cells in tumours alters their TCR clonality. 171
Figure 50: Stem-like T cell division decision tree. 177
Figure 51: Relationship between IFNγ-sensing and WNT/β-catenin pathway in CD8$^+$ T cells. 180
Figure 52: Proposed mechanism of IFNγ triggered negative feedback loop in tumour infiltrating CD8$^+$ T cells. 186
Figure 53: IFNγR transcriptional expression in circulating CD8$^+$ T cells from metastatic melanoma patients undergoing ICB and correlation with disease progression. 190
Figure 54: Correlation between IFNγR1 and stem-like signature in human tumour patients using single-cell RNA-seq. 191

List of Tables

Table 1: Reaction mix used for genotyping mice by PCR. 56
Table 2: Primer sequences used for mice genotyping. 57
Table 3: PCR cycling conditions used for genotyping mice. 57
Table 4: Expected results for genotyping by PCR. 58
Table 5: List of antibodies used for genotyping mice by blood. 59
Table 6: List of antibodies and reagents used for imaging. 62
Table 7: List of antibodies used for flow cytometry. 71
Table 8: Marker combinations used to phenotype immune cell populations in tumours. 138

References

1. GBD 2019 Diseases and Injuries Collaborators. Global burden of 369 diseases and injuries in 204 countries and territories, 1990-2019: a systematic analysis for the Global Burden of Disease Study 2019. *Lancet Lond. Engl.* **396**, 1204–1222 (2020).
2. Global Burden of Disease Cancer Collaboration *et al.* Global, Regional, and National Cancer Incidence, Mortality, Years of Life Lost, Years Lived With Disability, and Disability-Adjusted Life-Years for 29 Cancer Groups, 1990 to 2017: A Systematic Analysis for the Global Burden of Disease Study. *JAMA Oncol.* **5**, 1749–1768 (2019).
3. Cancer. https://www.who.int/news-room/fact-sheets/detail/cancer.
4. Sung, H. *et al.* Global Cancer Statistics 2020: GLOBOCAN Estimates of Incidence and Mortality Worldwide for 36 Cancers in 185 Countries. *CA. Cancer J. Clin.* **71**, 209–249 (2021).
5. Arnold, M. *et al.* Global Burden of Cutaneous Melanoma in 2020 and Projections to 2040. *JAMA Dermatol.* **158**, 495–503 (2022).
6. Hanahan, D. & Weinberg, R. A. The Hallmarks of Cancer. *Cell* **100**, 57–70 (2000).
7. Hanahan, D. & Weinberg, R. A. Hallmarks of Cancer: The Next Generation. *Cell* **144**, 646–674 (2011).
8. Mantovani, A., Allavena, P., Sica, A. & Balkwill, F. Cancer-related inflammation. *Nature* **454**, 436–444 (2008).
9. Greten, F. R. & Grivennikov, S. I. Inflammation and Cancer: Triggers, Mechanisms, and Consequences. *Immunity* **51**, 27–41 (2019).
10. Hanahan, D. Hallmarks of Cancer: New Dimensions. *Cancer Discov.* **12**, 31–46 (2022).
11. Baghban, R. *et al.* Tumor microenvironment complexity and therapeutic implications at a glance. *Cell Commun. Signal.* **18**, 59 (2020).
12. Quail, D. F. & Joyce, J. A. Microenvironmental regulation of tumor progression and metastasis. *Nat. Med.* **19**, 1423–1437 (2013).

13. Hanahan, D. & Coussens, L. M. Accessories to the crime: functions of cells recruited to the tumor microenvironment. *Cancer Cell* **21**, 309–322 (2012).
14. Liu, T. *et al.* Cancer-associated fibroblasts: an emerging target of anti-cancer immunotherapy. *J. Hematol. Oncol.J Hematol Oncol* **12**, 86 (2019).
15. Chen, X. & Song, E. Turning foes to friends: targeting cancer-associated fibroblasts. *Nat. Rev. Drug Discov.* **18**, 99–115 (2019).
16. Duan, Z. & Luo, Y. Targeting macrophages in cancer immunotherapy. *Signal Transduct. Target. Ther.* **6**, 1–21 (2021).
17. Hu, G. *et al.* Nanoparticles Targeting Macrophages as Potential Clinical Therapeutic Agents Against Cancer and Inflammation. *Front. Immunol.* **10**, (2019).
18. Ponzoni, M., Pastorino, F., Di Paolo, D., Perri, P. & Brignole, C. Targeting Macrophages as a Potential Therapeutic Intervention: Impact on Inflammatory Diseases and Cancer. *Int. J. Mol. Sci.* **19**, 1953 (2018).
19. Bertolini, F., Shaked, Y., Mancuso, P. & Kerbel, R. S. The multifaceted circulating endothelial cell in cancer: towards marker and target identification. *Nat. Rev. Cancer* **6**, 835–845 (2006).
20. Klein, D. The Tumor Vascular Endothelium as Decision Maker in Cancer Therapy. *Front. Oncol.* **8**, (2018).
21. Binnewies, M. *et al.* Understanding the tumor immune microenvironment (TIME) for effective therapy. *Nat. Med.* **24**, 541–550 (2018).
22. Burnet, F. M. The concept of immunological surveillance. *Prog. Exp. Tumor Res.* **13**, 1–27 (1970).
23. Shankaran, V. *et al.* IFNγ and lymphocytes prevent primary tumour development and shape tumour immunogenicity. *Nature* **410**, 1107–1111 (2001).
24. Marusyk, A., Janiszewska, M. & Polyak, K. Intratumor Heterogeneity: The Rosetta Stone of Therapy Resistance. *Cancer Cell* **37**, 471–484 (2020).
25. Dunn, G. P., Bruce, A. T., Ikeda, H., Old, L. J. & Schreiber, R. D. Cancer immunoediting: from immunosurveillance to tumor escape. *Nat. Immunol.* **3**, 991–998 (2002).

26. O'Donnell, J. S., Teng, M. W. L. & Smyth, M. J. Cancer immunoediting and resistance to T cell-based immunotherapy. *Nat. Rev. Clin. Oncol.* **16**, 151–167 (2019).
27. Dunn, G. P., Old, L. J. & Schreiber, R. D. The immunobiology of cancer immunosurveillance and immunoediting. *Immunity* **21**, 137–148 (2004).
28. Chen, D. S. & Mellman, I. Oncology Meets Immunology: The Cancer-Immunity Cycle. *Immunity* **39**, 1–10 (2013).
29. Fu, C. & Jiang, A. Dendritic Cells and CD8 T Cell Immunity in Tumor Microenvironment. *Front. Immunol.* **9**, 3059 (2018).
30. Martínez-Lostao, L., Anel, A. & Pardo, J. How Do Cytotoxic Lymphocytes Kill Cancer Cells? *Clin. Cancer Res. Off. J. Am. Assoc. Cancer Res.* **21**, 5047–5056 (2015).
31. Muntjewerff, E. M., Meesters, L. D. & van den Bogaart, G. Antigen Cross-Presentation by Macrophages. *Front. Immunol.* **11**, (2020).
32. Quatromoni, J. G. & Eruslanov, E. Tumor-associated macrophages: function, phenotype, and link to prognosis in human lung cancer. *Am. J. Transl. Res.* **4**, 376–389 (2012).
33. Lin, Y., Xu, J. & Lan, H. Tumor-associated macrophages in tumor metastasis: biological roles and clinical therapeutic applications. *J. Hematol. Oncol.J Hematol Oncol* **12**, 76 (2019).
34. Pan, Y., Yu, Y., Wang, X. & Zhang, T. Tumor-Associated Macrophages in Tumor Immunity. *Front. Immunol.* **11**, (2020).
35. Boutilier, A. J. & Elsawa, S. F. Macrophage Polarization States in the Tumor Microenvironment. *Int. J. Mol. Sci.* **22**, 6995 (2021).
36. Schreiber, R. D., Old, L. J. & Smyth, M. J. Cancer immunoediting: integrating immunity's roles in cancer suppression and promotion. *Science* **331**, 1565–1570 (2011).
37. Vinay, D. S. *et al.* Immune evasion in cancer: Mechanistic basis and therapeutic strategies. *Semin. Cancer Biol.* **35 Suppl**, S185–S198 (2015).
38. Lee, J. B., Ha, S.-J. & Kim, H. R. Clinical Insights Into Novel Immune Checkpoint Inhibitors. *Front. Pharmacol.* **12**, (2021).

39. Zheng, Y., Fang, Y.-C. & Li, J. PD-L1 expression levels on tumor cells affect their immunosuppressive activity. *Oncol. Lett.* **18**, 5399–5407 (2019).
40. Yi, M., Niu, M., Xu, L., Luo, S. & Wu, K. Regulation of PD-L1 expression in the tumor microenvironment. *J. Hematol. Oncol.J Hematol Oncol* **14**, 10 (2021).
41. Wu, Y., Chen, W., Xu, Z. P. & Gu, W. PD-L1 Distribution and Perspective for Cancer Immunotherapy—Blockade, Knockdown, or Inhibition. *Front. Immunol.* **10**, (2019).
42. Jiang, X. *et al.* Role of the tumor microenvironment in PD-L1/PD-1-mediated tumor immune escape. *Mol. Cancer* **18**, 10 (2019).
43. Massagué, J. TGFbeta in Cancer. *Cell* **134**, 215–230 (2008).
44. Batlle, E. & Massagué, J. Transforming Growth Factor-β Signaling in Immunity and Cancer. *Immunity* **50**, 924–940 (2019).
45. Meireson, A., Devos, M. & Brochez, L. IDO Expression in Cancer: Different Compartment, Different Functionality? *Front. Immunol.* **11**, (2020).
46. Zaidi, M. R. The Interferon-Gamma Paradox in Cancer. *J. Interferon Cytokine Res.* **39**, 30–38 (2019).
47. Sucker, A. *et al.* Acquired IFNγ resistance impairs anti-tumor immunity and gives rise to T-cell-resistant melanoma lesions. *Nat. Commun.* **8**, 1–15 (2017).
48. Gao, J. *et al.* Loss of IFN-γ pathway genes in tumor cells as a mechanism of resistance to anti-CTLA-4 therapy. *Cell* **167**, 397-404.e9 (2016).
49. Wheelock, E. F. Interferon-Like Virus-Inhibitor Induced in Human Leukocytes by Phytohemagglutinin. *Science* **149**, 310–311 (1965).
50. Bach, E. A., Aguet, M. & Schreiber, R. D. The IFN gamma receptor: a paradigm for cytokine receptor signaling. *Annu. Rev. Immunol.* **15**, 563–591 (1997).
51. Boehm, U., Klamp, T., Groot, M. & Howard, J. C. CELLULAR RESPONSES TO INTERFERON-γ. *Annu. Rev. Immunol.* **15**, 749–795 (1997).
52. Kak, G., Raza, M. & Tiwari, B. K. Interferon-gamma (IFN-γ): Exploring its implications in infectious diseases. *Biomol. Concepts* **9**, 64–79 (2018).

53. Teixeira, L. K., Fonseca, B. P., Barboza, B. A. & Viola, J. P. The role of interferon-gamma on immune and allergic responses. *Mem. Inst. Oswaldo Cruz* **100**, 137–144 (2005).
54. Aqbi, H. F., Wallace, M., Sappal, S., Payne, K. K. & Manjili, M. H. IFN-γ orchestrates tumor elimination, tumor dormancy, tumor escape and progression. *J. Leukoc. Biol.* (2018) doi:10.1002/JLB.5MIR0917-351R.
55. Zhang, C. *et al.* Lack of interferon-γ receptor results in a microenvironment favorable for intestinal tumorigenesis. *Oncotarget* **7**, 42099–42109 (2016).
56. Ikeda, H., Old, L. J. & Schreiber, R. D. The roles of IFN gamma in protection against tumor development and cancer immunoediting. *Cytokine Growth Factor Rev.* **13**, 95–109 (2002).
57. Kaplan, D. H. *et al.* Demonstration of an interferon γ-dependent tumor surveillance system in immunocompetent mice. *Proc. Natl. Acad. Sci. U. S. A.* **95**, 7556–7561 (1998).
58. Farrar, M. A. & Schreiber, R. D. The molecular cell biology of interferon-gamma and its receptor. *Annu. Rev. Immunol.* **11**, 571–611 (1993).
59. Castro, F., Cardoso, A. P., Gonçalves, R. M., Serre, K. & Oliveira, M. J. Interferon-Gamma at the Crossroads of Tumor Immune Surveillance or Evasion. *Front. Immunol.* **9**, (2018).
60. Szabo, S. J., Sullivan, B. M., Peng, S. L. & Glimcher, L. H. Molecular mechanisms regulating Th1 immune responses. *Annu. Rev. Immunol.* **21**, 713–758 (2003).
61. Frucht, D. M. *et al.* IFN-gamma production by antigen-presenting cells: mechanisms emerge. *Trends Immunol.* **22**, 556–560 (2001).
62. Ealick, S. E. *et al.* Three-dimensional structure of recombinant human interferon-gamma. *Science* **252**, 698–702 (1991).
63. Three Molecular Weight Forms of Natural Human Interferon-Gamma Revealed by Immunoprecipitation With Monoclonal Antibody - PubMed. https://pubmed.ncbi.nlm.nih.gov/6423641/.
64. Tau, G. & Rothman, P. Biologic functions of the IFN-γ receptors. *Allergy* **54**, 1233–1251 (1999).

65. Bernabei, P. *et al.* Interferon-gamma receptor 2 expression as the deciding factor in human T, B, and myeloid cell proliferation or death. *J. Leukoc. Biol.* **70**, 950–960 (2001).
66. Schroder, K., Hertzog, P. J., Ravasi, T. & Hume, D. A. Interferon-γ: an overview of signals, mechanisms and functions. *J. Leukoc. Biol.* **75**, 163–189 (2004).
67. Levy, D. E. & Darnell, J. E. STATs: transcriptional control and biological impact. *Nat. Rev. Mol. Cell Biol.* **3**, 651–662 (2002).
68. Krause, C. D. *et al.* Preassembly and ligand-induced restructuring of the chains of the IFN-gamma receptor complex: the roles of Jak kinases, Stat1 and the receptor chains. *Cell Res.* **16**, 55–69 (2006).
69. Blouin, C. M. & Lamaze, C. Interferon Gamma Receptor: The Beginning of the Journey. *Front. Immunol.* **4**, (2013).
70. Pestka, S. *et al.* Interleukin-10 and Related Cytokines and Receptors. *Annu. Rev. Immunol.* **22**, 929–979 (2004).
71. Farrar, M. A., Campbell, J. D. & Schreiber, R. D. Identification of a functionally important sequence in the C terminus of the interferon-gamma receptor. *Proc. Natl. Acad. Sci. U. S. A.* **89**, 11706–11710 (1992).
72. Greenlund, A. C., Farrar, M. A., Viviano, B. L. & Schreiber, R. D. Ligand-induced IFN gamma receptor tyrosine phosphorylation couples the receptor to its signal transduction system (p91). *EMBO J.* **13**, 1591–1600 (1994).
73. Majoros, A. *et al.* Canonical and Non-Canonical Aspects of JAK–STAT Signaling: Lessons from Interferons for Cytokine Responses. *Front. Immunol.* **8**, (2017).
74. Stark, G. R., Kerr, I. M., Williams, B. R., Silverman, R. H. & Schreiber, R. D. How cells respond to interferons. *Annu. Rev. Biochem.* **67**, 227–264 (1998).
75. Shuai, K., Stark, G. R., Kerr, I. M. & Darnell, J. E. A single phosphotyrosine residue of Stat91 required for gene activation by interferon-gamma. *Science* **261**, 1744–1746 (1993).
76. Kotenko, S. V. & Pestka, S. Jak-Stat signal transduction pathway through the eyes of cytokine class II receptor complexes. *Oncogene* **19**, 2557–2565 (2000).

77. Decker, T., Lew, D. J., Mirkovitch, J. & Darnell, J. E. Cytoplasmic activation of GAF, an IFN-gamma-regulated DNA-binding factor. *EMBO J.* **10**, 927–932 (1991).
78. Aaronson, D. S. & Horvath, C. M. A road map for those who don't know JAK-STAT. *Science* **296**, 1653–1655 (2002).
79. Schoggins, J. W. Interferon-Stimulated Genes: What Do They All Do? *Annu. Rev. Virol.* **6**, 567–584 (2019).
80. Schoggins, J. W. & Rice, C. M. Interferon-stimulated genes and their antiviral effector functions. *Curr. Opin. Virol.* **1**, 519–525 (2011).
81. Samarajiwa, S. A., Forster, S., Auchettl, K. & Hertzog, P. J. INTERFEROME: the database of interferon regulated genes. *Nucleic Acids Res.* **37**, D852–D857 (2009).
82. Schneider, W. M., Chevillotte, M. D. & Rice, C. M. Interferon-Stimulated Genes: A Complex Web of Host Defenses. *Annu. Rev. Immunol.* **32**, 513–545 (2014).
83. Stark, G. R. & Darnell, J. E. The JAK-STAT Pathway at Twenty. *Immunity* **36**, 503–514 (2012).
84. Platanias, L. C. Mechanisms of type-I- and type-II-interferon-mediated signalling. *Nat. Rev. Immunol.* **5**, 375–386 (2005).
85. Kimura, T. *et al.* Involvement of the IRF-1 transcription factor in antiviral responses to interferons. *Science* **264**, 1921–1924 (1994).
86. Michalska, A., Blaszczyk, K., Wesoly, J. & Bluyssen, H. A. R. A Positive Feedback Amplifier Circuit That Regulates Interferon (IFN)-Stimulated Gene Expression and Controls Type I and Type II IFN Responses. *Front. Immunol.* **9**, (2018).
87. Liau, N. P. D. *et al.* The molecular basis of JAK/STAT inhibition by SOCS1. *Nat. Commun.* **9**, 1–14 (2018).
88. Celada, A. & Schreiber, R. D. Internalization and degradation of receptor-bound interferon-gamma by murine macrophages. Demonstration of receptor recycling. *J. Immunol.* **139**, 147–153 (1987).
89. Regis, G., Conti, L., Boselli, D. & Novelli, F. IFNgammaR2 trafficking tunes IFNgamma-STAT1 signaling in T lymphocytes. *Trends Immunol.* **27**, 96–101 (2006).
90. Johnson, H. M. & Ahmed, C. M. Noncanonical IFN Signaling: Mechanistic Linkage of Genetic and Epigenetic Events. *Mediators Inflamm.* **2016**, (2016).

91. Interferon Gamma - an overview | ScienceDirect Topics. https://www.sciencedirect.com/topics/immunology-and-microbiology/interferon-gamma.
92. Jorgovanovic, D., Song, M., Wang, L. & Zhang, Y. Roles of IFN-γ in tumor progression and regression: a review. *Biomark. Res.* **8**, 49 (2020).
93. Garcia-Diaz, A. *et al.* Interferon Receptor Signaling Pathways Regulating PD-L1 and PD-L2 Expression. *Cell Rep.* **19**, 1189–1201 (2017).
94. Lee, A. J. & Ashkar, A. A. The Dual Nature of Type I and Type II Interferons. *Front. Immunol.* **9**, (2018).
95. Devos, R. *et al.* Molecular cloning of human immune interferon cDNA and its expression in eukaryotic cells. *Nucleic Acids Res.* **10**, 2487 (1982).
96. Billiau, A. & Matthys, P. Interferon-gamma: a historical perspective. *Cytokine Growth Factor Rev.* **20**, 97–113 (2009).
97. Miller, C. H. T., Maher, S. G. & Young, H. A. Clinical Use of Interferon-γ. *Ann. N. Y. Acad. Sci.* **1182**, 69–79 (2009).
98. Alberts, D. S. *et al.* Randomized phase 3 trial of interferon gamma-1b plus standard carboplatin/paclitaxel versus carboplatin/paclitaxel alone for first-line treatment of advanced ovarian and primary peritoneal carcinomas: results from a prospectively designed analysis of progression-free survival. *Gynecol. Oncol.* **109**, 174–181 (2008).
99. Younes, H. M. & Amsden, B. G. Interferon-γ Therapy: Evaluation of Routes of Administration and Delivery Systems. *J. Pharm. Sci.* **91**, 2–17 (2002).
100. Seidelin, J. B., Jäättelä, M. & Nielsen, O. H. Continuous interferon-gamma or tumor necrosis factor-alpha exposure of enterocytes attenuates cell death responses. *Cytokine* **27**, 113–119 (2004).
101. Ni, L. & Lu, J. Interferon gamma in cancer immunotherapy. *Cancer Med.* **7**, 4509–4516 (2018).
102. Beatty, G. & Paterson, Y. IFN-gamma-dependent inhibition of tumor angiogenesis by tumor-infiltrating CD4+ T cells requires tumor responsiveness to IFN-gamma. *J. Immunol. Baltim. Md 1950* **166**, 2276–2282 (2001).

103. Skurkovich, S., Skurkovich, B. & Kelly, J. Anticytokine therapy, particularly anti-IFN-γ, in Th1-mediated autoimmune diseases. *Expert Rev. Clin. Immunol.* **1**, 11–25 (2005).
104. Curtsinger, J. M., Agarwal, P., Lins, D. C. & Mescher, M. F. Autocrine IFN-γ promotes naive CD8 T cell differentiation and synergizes with IFN-α to stimulate strong function. *J. Immunol. Baltim. Md 1950* **189**, 659–668 (2012).
105. Krummel, M. F. *et al.* Paracrine costimulation of IFN-γ signaling by integrins modulates CD8 T cell differentiation. *Proc. Natl. Acad. Sci.* **115**, 11585–11590 (2018).
106. Uhl, L. F. K. & Gérard, A. Modes of Communication between T Cells and Relevance for Immune Responses. *Int. J. Mol. Sci.* **21**, (2020).
107. Krummel, M. F. *et al.* Paracrine costimulation of IFN-γ signaling by integrins modulates CD8 T cell differentiation. *Proc. Natl. Acad. Sci. U. S. A.* **115**, 11585–11590 (2018).
108. Cantrell, D. Signaling in Lymphocyte Activation. *Cold Spring Harb. Perspect. Biol.* **7**, a018788 (2015).
109. Smith-Garvin, J. E., Koretzky, G. A. & Jordan, M. S. T cell activation. *Annu. Rev. Immunol.* **27**, 591–619 (2009).
110. Krogsgaard, M. & Davis, M. M. How T cells 'see' antigen. *Nat. Immunol.* **6**, 239–245 (2005).
111. Nikolich-Zugich, J., Slifka, M. K. & Messaoudi, I. The many important facets of T-cell repertoire diversity. *Nat. Rev. Immunol.* **4**, 123–132 (2004).
112. Germain, R. N. T-cell development and the CD4-CD8 lineage decision. *Nat. Rev. Immunol.* **2**, 309–322 (2002).
113. Wang, X. *et al.* TCR-dependent transformation of mature memory phenotype T cells in mice. *J. Clin. Invest.* **121**, 3834–3845 (2011).
114. Hwang, J.-R., Byeon, Y., Kim, D. & Park, S.-G. Recent insights of T cell receptor-mediated signaling pathways for T cell activation and development. *Exp. Mol. Med.* **52**, 750–761 (2020).

115. THAPA, P. & FARBER, D. L. THE ROLE OF THE THYMUS IN THE IMMUNE RESPONSE. *Thorac. Surg. Clin.* **29**, 123–131 (2019).
116. Haynes, B. F., Markert, M. L., Sempowski, G. D., Patel, D. D. & Hale, L. P. The role of the thymus in immune reconstitution in aging, bone marrow transplantation, and HIV-1 infection. *Annu. Rev. Immunol.* **18**, 529–560 (2000).
117. janeways-immunobiology-9th-ed_booksmedicos.org_.pdf.
118. Greenwald, R. J., Freeman, G. J. & Sharpe, A. H. The B7 family revisited. *Annu. Rev. Immunol.* **23**, 515–548 (2005).
119. Xiao, Z., Casey, K. A., Jameson, S. C., Curtsinger, J. M. & Mescher, M. F. Programming for CD8 T cell memory development requires IL-12 or Type I IFN. *J. Immunol. Baltim. Md 1950* **182**, 2786–2794 (2009).
120. Curtsinger, J. M. & Mescher, M. F. Inflammatory cytokines as a third signal for T cell activation. *Curr. Opin. Immunol.* **22**, 333–340 (2010).
121. Hamilton, S. E. & Jameson, S. C. The nature of the lymphopenic environment dictates protective function of homeostatic-memory CD8 $^{+}$ T cells. *Proc. Natl. Acad. Sci.* **105**, 18484–18489 (2008).
122. Mescher, M. F. *et al.* Signals required for programming effector and memory development by CD8+ T cells. *Immunol. Rev.* **211**, 81–92 (2006).
123. Kolumam, G. A., Thomas, S., Thompson, L. J., Sprent, J. & Murali-Krishna, K. Type I interferons act directly on CD8 T cells to allow clonal expansion and memory formation in response to viral infection. *J. Exp. Med.* **202**, 637–650 (2005).
124. Dustin, M. L. Coordination of T cell activation and migration through formation of the immunological synapse. *Ann. N. Y. Acad. Sci.* **987**, 51–59 (2003).
125. Tseng, S.-Y. & Dustin, M. L. T-cell activation: a multidimensional signaling network. *Curr. Opin. Cell Biol.* **14**, 575–580 (2002).
126. Bossi, G. *et al.* The secretory synapse: the secrets of a serial killer. *Immunol. Rev.* **189**, 152–160 (2002).
127. Trambas, C. M. & Griffiths, G. M. Delivering the kiss of death. *Nat. Immunol.* **4**, 399–403 (2003).

128. Philip, M. & Schietinger, A. CD8+ T cell differentiation and dysfunction in cancer. *Nat. Rev. Immunol.* **22**, 209–223 (2022).
129. Newick, K., O'Brien, S., Moon, E. & Albelda, S. M. CAR T Cell Therapy for Solid Tumors. *Annu. Rev. Med.* **68**, 139–152 (2017).
130. Im, S. J. *et al.* Defining CD8+ T cells that provide the proliferative burst after PD-1 therapy. *Nature* **537**, 417–421 (2016).
131. Tetramer - an overview | ScienceDirect Topics. https://www.sciencedirect.com/topics/pharmacology-toxicology-and-pharmaceutical-science/tetramer.
132. Im, S. J., Konieczny, B. T., Hudson, W. H., Masopust, D. & Ahmed, R. PD-1+ stemlike CD8 T cells are resident in lymphoid tissues during persistent LCMV infection. *Proc. Natl. Acad. Sci. U. S. A.* **117**, 4292–4299 (2020).
133. Hudson, W. H. *et al.* Proliferating Transitory T Cells with an Effector-like Transcriptional Signature Emerge from PD-1+ Stem-like CD8+ T Cells during Chronic Infection. *Immunity* **51**, 1043-1058.e4 (2019).
134. Chen, Z. *et al.* TCF-1-Centered Transcriptional Network Drives an Effector versus Exhausted CD8 T Cell-Fate Decision. *Immunity* **51**, 840-855.e5 (2019).
135. Nolz, J. C., Starbeck-Miller, G. R. & Harty, J. T. Naive, effector and memory CD8 T-cell trafficking: parallels and distinctions. *Immunotherapy* **3**, 1223–1233 (2011).
136. Gerlach, C. *et al.* One naive T cell, multiple fates in CD8+ T cell differentiation. *J. Exp. Med.* **207**, 1235–1246 (2010).
137. van den Broek, T., Borghans, J. A. M. & van Wijk, F. The full spectrum of human naive T cells. *Nat. Rev. Immunol.* **18**, 363–373 (2018).
138. De Rosa, S. C., Herzenberg, L. A., Herzenberg, L. A. & Roederer, M. 11-color, 13-parameter flow cytometry: Identification of human naive T cells by phenotype, function, and T-cell receptor diversity. *Nat. Med.* **7**, 245–248 (2001).
139. Willinger, T. *et al.* Human Naive CD8 T Cells Down-Regulate Expression of the WNT Pathway Transcription Factors Lymphoid Enhancer Binding Factor 1 and Transcription Factor 7 (T Cell Factor-1) following Antigen Encounter In Vitro and In Vivo1. *J. Immunol.* **176**, 1439–1446 (2006).

140. Zhao, X., Shan, Q. & Xue, H.-H. TCF1 in T cell immunity: a broadened frontier. *Nat. Rev. Immunol.* (2021) doi:10.1038/s41577-021-00563-6.
141. Escobar, G., Mangani, D. & Anderson, A. C. T cell factor 1: A master regulator of the T cell response in disease. *Sci. Immunol.* **5**, eabb9726 (2020).
142. Utzschneider, D. T. *et al.* Early precursor T cells establish and propagate T cell exhaustion in chronic infection. *Nat. Immunol.* **21**, 1256–1266 (2020).
143. Kahan, S. M., Wherry, E. J. & Zajac, A. J. T cell exhaustion during persistent viral infections. *Virology* **479–480**, 180–193 (2015).
144. Wherry, E. J. & Kurachi, M. Molecular and cellular insights into T cell exhaustion. *Nat. Rev. Immunol.* **15**, 486–499 (2015).
145. Gattinoni, L., Klebanoff, C. A. & Restifo, N. P. Paths to stemness: building the ultimate antitumour T cell. *Nat. Rev. Cancer* **12**, 671–684 (2012).
146. Dolina, J. S., Van Braeckel-Budimir, N., Thomas, G. D. & Salek-Ardakani, S. CD8+ T Cell Exhaustion in Cancer. *Front. Immunol.* **12**, (2021).
147. Jiang, W. *et al.* Exhausted CD8+T Cells in the Tumor Immune Microenvironment: New Pathways to Therapy. *Front. Immunol.* **11**, (2021).
148. Yi, L. & Yang, L. Stem-like T cells and niches: Implications in human health and disease. *Front. Immunol.* **13**, (2022).
149. He, R. *et al.* Follicular CXCR5- expressing CD8(+) T cells curtail chronic viral infection. *Nature* **537**, 412–428 (2016).
150. Utzschneider, D. T. *et al.* T Cell Factor 1-Expressing Memory-like CD8+ T Cells Sustain the Immune Response to Chronic Viral Infections. *Immunity* **45**, 415–427 (2016).
151. Leong, Y. A. *et al.* CXCR5(+) follicular cytotoxic T cells control viral infection in B cell follicles. *Nat. Immunol.* **17**, 1187–1196 (2016).
152. Wu, T. *et al.* The TCF1-Bcl6 axis counteracts type I interferon to repress exhaustion and maintain T cell stemness. *Sci. Immunol.* **1**, eaai8593 (2016).
153. Kanev, K. *et al.* Proliferation-competent Tcf1+ CD8 T cells in dysfunctional populations are CD4 T cell help independent. *Proc. Natl. Acad. Sci. U. S. A.* **116**, 20070–20076 (2019).

154. Zander, R. *et al.* CD4+ T Cell Help Is Required for the Formation of a Cytolytic CD8+ T Cell Subset that Protects against Chronic Infection and Cancer. *Immunity* **51**, 1028-1042.e4 (2019).
155. Hu, Y. *et al.* TGF-β regulates the stem-like state of PD-1+ TCF-1+ virus-specific CD8 T cells during chronic infection. *J. Exp. Med.* **219**, e20211574 (2022).
156. Pais Ferreira, D. *et al.* Central memory CD8+ T cells derive from stem-like Tcf7hi effector cells in the absence of cytotoxic differentiation. *Immunity* **53**, 985-1000.e11 (2020).
157. Petrovas, C. *et al.* Follicular CD8 T cells accumulate in HIV infection and can kill infected cells in vitro via bispecific antibodies. *Sci. Transl. Med.* **9**, eaag2285 (2017).
158. Miles, B. *et al.* Follicular Regulatory CD8 T Cells Impair the Germinal Center Response in SIV and Ex Vivo HIV Infection. *PLoS Pathog.* **12**, e1005924 (2016).
159. Gettinger, S. N. *et al.* A dormant TIL phenotype defines non-small cell lung carcinomas sensitive to immune checkpoint blockers. *Nat. Commun.* **9**, 3196 (2018).
160. Brummelman, J. *et al.* High-dimensional single cell analysis identifies stem-like cytotoxic CD8+ T cells infiltrating human tumors. *J. Exp. Med.* **215**, 2520–2535 (2018).
161. Connolly, K. A. *et al.* A reservoir of stem-like CD8+ T cells in the tumor-draining lymph node preserves the ongoing antitumor immune response. *Sci. Immunol.* **6**, eabg7836 (2021).
162. Sade-Feldman, M. *et al.* Defining T Cell States Associated with Response to Checkpoint Immunotherapy in Melanoma. *Cell* **175**, 998-1013.e20 (2018).
163. Siddiqui, I. *et al.* Intratumoral Tcf1+PD-1+CD8+ T Cells with Stem-like Properties Promote Tumor Control in Response to Vaccination and Checkpoint Blockade Immunotherapy. *Immunity* **50**, 195-211.e10 (2019).
164. Miller, B. C. *et al.* Subsets of exhausted CD8+ T cells differentially mediate tumor control and respond to checkpoint blockade. *Nat. Immunol.* **20**, 326–336 (2019).

165. Jansen, C. S. *et al.* An intra-tumoral niche maintains and differentiates stem-like CD8 T cells. *Nature* **576**, 465–470 (2019).
166. Gearty, S. V. *et al.* An autoimmune stem-like CD8 T cell population drives type 1 diabetes. *Nature* 1–6 (2021) doi:10.1038/s41586-021-04248-x.
167. Kallies, A., Zehn, D. & Utzschneider, D. T. Precursor exhausted T cells: key to successful immunotherapy? *Nat. Rev. Immunol.* **20**, 128–136 (2020).
168. Zheng, W. *et al.* Regnase-1 suppresses TCF-1+ precursor exhausted T-cell formation to limit CAR–T-cell responses against ALL. *Blood* **138**, 122–135 (2021).
169. Zhang, Y., Joe, G., Hexner, E., Zhu, J. & Emerson, S. G. Host-reactive CD8+ memory stem cells in graft-versus-host disease. *Nat. Med.* **11**, 1299–1305 (2005).
170. Wang, Y. *et al.* Stem cell-like memory T cells: The generation and application. *J. Leukoc. Biol.* **110**, 1209–1223 (2021).
171. Qi, Q. *et al.* Diversity and clonal selection in the human T-cell repertoire. *Proc. Natl. Acad. Sci.* **111**, 13139–13144 (2014).
172. Fagnoni, F. F. *et al.* Shortage of circulating naive CD8(+) T cells provides new insights on immunodeficiency in aging. *Blood* **95**, 2860–2868 (2000).
173. Rudd, B. D. *et al.* Nonrandom attrition of the naive CD8+ T-cell pool with aging governed by T-cell receptor:pMHC interactions. *Proc. Natl. Acad. Sci.* **108**, 13694–13699 (2011).
174. Fares, C. M., Van Allen, E. M., Drake, C. G., Allison, J. P. & Hu-Lieskovan, S. Mechanisms of Resistance to Immune Checkpoint Blockade: Why Does Checkpoint Inhibitor Immunotherapy Not Work for All Patients? *Am. Soc. Clin. Oncol. Educ. Book Am. Soc. Clin. Oncol. Annu. Meet.* **39**, 147–164 (2019).
175. Kalbasi, A. & Ribas, A. Tumour-intrinsic resistance to immune checkpoint blockade. *Nat. Rev. Immunol.* **20**, 25–39 (2020).
176. Haslam, A. & Prasad, V. Estimation of the Percentage of US Patients With Cancer Who Are Eligible for and Respond to Checkpoint Inhibitor Immunotherapy Drugs. *JAMA Netw. Open* **2**, e192535 (2019).
177. Schoenfeld, A. J. & Hellmann, M. D. Acquired Resistance to Immune Checkpoint Inhibitors. *Cancer Cell* **37**, 443–455 (2020).

178. Sharma, P., Hu-Lieskovan, S., Wargo, J. A. & Ribas, A. Primary, Adaptive, and Acquired Resistance to Cancer Immunotherapy. *Cell* **168**, 707–723 (2017).
179. Jenkins, R. W., Barbie, D. A. & Flaherty, K. T. Mechanisms of resistance to immune checkpoint inhibitors. *Br. J. Cancer* **118**, 9–16 (2018).
180. Philip, M. *et al.* Chromatin states define tumour-specific T cell dysfunction and reprogramming. *Nature* **545**, 452–456 (2017).
181. Pauken, K. E. *et al.* Epigenetic stability of exhausted T cells limits durability of reinvigoration by PD-1 blockade. *Science* **354**, 1160–1165 (2016).
182. Zehn, D., Thimme, R., Lugli, E., de Almeida, G. P. & Oxenius, A. 'Stem-like' precursors are the fount to sustain persistent CD8+ T cell responses. *Nat. Immunol.* **23**, 836–847 (2022).
183. Prokhnevska, N. *et al.* CD8+ T cell activation in cancer comprises an initial activation phase in lymph nodes followed by effector differentiation within the tumor. *Immunity* **0**, (2022).
184. Li, Z. *et al.* In vivo labeling reveals continuous trafficking of TCF-1+ T cells between tumor and lymphoid tissue. *J. Exp. Med.* **219**, e20210749 (2022).
185. Cabrita, R. *et al.* Tertiary lymphoid structures improve immunotherapy and survival in melanoma. *Nature* **577**, 561–565 (2020).
186. Im, S. J. & Ha, S.-J. Re-defining T-Cell Exhaustion: Subset, Function, and Regulation. *Immune Netw.* **20**, e2 (2020).
187. Yamazaki, C. *et al.* Critical roles of a dendritic cell subset expressing a chemokine receptor, XCR1. *J. Immunol. Baltim. Md 1950* **190**, 6071–6082 (2013).
188. Dorner, B. G. *et al.* Selective expression of the chemokine receptor XCR1 on cross-presenting dendritic cells determines cooperation with CD8+ T cells. *Immunity* **31**, 823–833 (2009).
189. Kroczek, R. A. & Henn, V. The Role of XCR1 and its Ligand XCL1 in Antigen Cross-Presentation by Murine and Human Dendritic Cells. *Front. Immunol.* **3**, 14 (2012).
190. Hua, Y. *et al.* Cancer immunotherapies transition endothelial cells into HEVs that generate TCF1+ T lymphocyte niches through a feed-forward loop. *Cancer Cell* **0**, (2022).

191. Hanna, B. S. *et al.* Interleukin-10 receptor signaling promotes the maintenance of a PD-1int TCF-1+ CD8+ T cell population that sustains anti-tumor immunity. *Immunity* **0**, (2021).
192. DuPage, M., Mazumdar, C., Schmidt, L. M., Cheung, A. F. & Jacks, T. Expression of tumour-specific antigens underlies cancer immunoediting. *Nature* **482**, 405–409 (2012).
193. Zitvogel, L., Tesniere, A. & Kroemer, G. Cancer despite immunosurveillance: immunoselection and immunosubversion. *Nat. Rev. Immunol.* **6**, 715–727 (2006).
194. Ni, L. & Dong, C. New checkpoints in cancer immunotherapy. *Immunol. Rev.* **276**, 52–65 (2017).
195. Iwai, Y., Hamanishi, J., Chamoto, K. & Honjo, T. Cancer immunotherapies targeting the PD-1 signaling pathway. *J. Biomed. Sci.* **24**, 26 (2017).
196. Sharma, P. & Allison, J. P. The future of immune checkpoint therapy. *Science* **348**, 56–61 (2015).
197. Robert, C. A decade of immune-checkpoint inhibitors in cancer therapy. *Nat. Commun.* **11**, 3801 (2020).
198. Hamid, O. *et al.* Safety and tumor responses with lambrolizumab (anti-PD-1) in melanoma. *N. Engl. J. Med.* **369**, 134–144 (2013).
199. Castro, F., Cardoso, A. P., Gonçalves, R. M., Serre, K. & Oliveira, M. J. Interferon-Gamma at the Crossroads of Tumor Immune Surveillance or Evasion. *Front. Immunol.* **9**, (2018).
200. Dighe, A. S., Richards, E., Old, L. J. & Schreiber, R. D. Enhanced in vivo growth and resistance to rejection of tumor cells expressing dominant negative IFN gamma receptors. *Immunity* **1**, 447–456 (1994).
201. Zaidi, M. R. & Merlino, G. The Two Faces of Interferon-γ in Cancer. *Clin. Cancer Res.* **17**, 6118–6124 (2011).
202. Mojic, M., Takeda, K. & Hayakawa, Y. The Dark Side of IFN-γ: Its Role in Promoting Cancer Immunoevasion. *Int. J. Mol. Sci.* **19**, (2017).

203. Mandai, M. *et al.* Dual Faces of IFNγ in Cancer Progression: A Role of PD-L1 Induction in the Determination of Pro- and Antitumor Immunity. *Clin. Cancer Res.* **22**, 2329–2334 (2016).
204. Gattinoni, L. *et al.* Wnt signaling arrests effector T cell differentiation and generates CD8+ memory stem cells. *Nat. Med.* **15**, 808–813 (2009).
205. Zhao, M. *et al.* Rapid in vitro generation of bona fide exhausted CD8+ T cells is accompanied by Tcf7 promotor methylation. *PLoS Pathog.* **16**, e1008555 (2020).
206. Zehn, D., Lee, S. Y. & Bevan, M. J. Complete but curtailed T-cell response to very low-affinity antigen. *Nature* **458**, 211–214 (2009).
207. Hao, Y. *et al.* Integrated analysis of multimodal single-cell data. *Cell* **184**, 3573-3587.e29 (2021).
208. Korsunsky, I. *et al.* Fast, sensitive and accurate integration of single-cell data with Harmony. *Nat. Methods* **16**, 1289–1296 (2019).
209. DeTomaso, D. *et al.* Functional interpretation of single cell similarity maps. *Nat. Commun.* **10**, 4376 (2019).
210. Andreatta, M. & Carmona, S. J. UCell: Robust and scalable single-cell gene signature scoring. *Comput. Struct. Biotechnol. J.* **19**, 3796–3798 (2021).
211. Qiu, X. *et al.* Reversed graph embedding resolves complex single-cell trajectories. *Nat. Methods* **14**, 979–982 (2017).
212. Borcherding, N., Bormann, N. L. & Kraus, G. scRepertoire: An R-based toolkit for single-cell immune receptor analysis. *F1000Research* **9**, 47 (2020).
213. Kaech, S. M. & Cui, W. Transcriptional control of effector and memory CD8+ T cell differentiation. *Nat. Rev. Immunol.* **12**, 749–761 (2012).
214. Zhang, N. & Bevan, M. J. CD8+ T Cells: Foot Soldiers of the Immune System. *Immunity* **35**, 161–168 (2011).
215. Alspach, E., Lussier, D. M. & Schreiber, R. D. Interferon γ and Its Important Roles in Promoting and Inhibiting Spontaneous and Therapeutic Cancer Immunity. *Cold Spring Harb. Perspect. Biol.* a028480 (2018) doi:10.1101/cshperspect.a028480.
216. de Araújo-Souza, P. S., Hanschke, S. C. H. & Viola, J. P. B. Epigenetic Control of Interferon-Gamma Expression in CD8 T Cells. *Journal of Immunology Research*

https://www.hindawi.com/journals/jir/2015/849573/ (2015) doi:10.1155/2015/849573.

217. Uhl, L. F. K. & Gérard, A. Modes of Communication between T Cells and Relevance for Immune Responses. *Int. J. Mol. Sci.* **21**, E2674 (2020).
218. Whitmire, J. K., Tan, J. T. & Whitton, J. L. Interferon-γ acts directly on CD8+ T cells to increase their abundance during virus infection. *J. Exp. Med.* **201**, 1053–1059 (2005).
219. Curtsinger, J. M., Agarwal, P., Lins, D. C. & Mescher, M. F. Autocrine IFN-γ Promotes Naive CD8 T Cell Differentiation and Synergizes with IFN-α To Stimulate Strong Function. *J. Immunol.* **189**, 659–668 (2012).
220. Badovinac, V. P., Tvinnereim, A. R. & Harty, J. T. Regulation of Antigen-Specific CD8+ T Cell Homeostasis by Perforin and Interferon-γ. *Science* **290**, 1354–1357 (2000).
221. Sercan, Ö., Stoycheva, D., Hämmerling, G. J., Arnold, B. & Schüler, T. IFN-γ Receptor Signaling Regulates Memory CD8+ T Cell Differentiation. *J. Immunol.* **184**, 2855–2862 (2010).
222. Whitmire, J. K., Eam, B., Benning, N. & Whitton, J. L. Direct Interferon-γ Signaling Dramatically Enhances CD4 + and CD8 + T Cell Memory . *J. Immunol.* **179**, 1190–1197 (2007).
223. Prabhu, N. *et al.* Gamma Interferon Regulates Contraction of the Influenza Virus-Specific CD8 T Cell Response and Limits the Size of the Memory Population. *J. Virol.* **87**, 12510–12522 (2013).
224. Badovinac, V. P., Porter, B. B. & Harty, J. T. CD8+ T cell contraction is controlled by early inflammation. *Nat. Immunol.* **5**, 809–817 (2004).
225. Tewari, K., Nakayama, Y. & Suresh, M. Role of Direct Effects of IFN-γ on T Cells in the Regulation of CD8 T Cell Homeostasis. *J. Immunol.* **179**, 2115–2125 (2007).
226. Ouyang, W., Beckett, O., Flavell, R. A. & Li, M. O. An Essential Role of the Forkhead-Box Transcription Factor Foxo1 in Control of T Cell Homeostasis and Tolerance. *Immunity* **30**, 358–371 (2009).

227. Qiang, L., Banks, A. S. & Accili, D. Uncoupling of Acetylation from Phosphorylation Regulates FoxO1 Function Independent of Its Subcellular Localization*. *J. Biol. Chem.* **285**, 27396–27401 (2010).
228. Rodriguez, F., Harkins, S., Slifka, M. K. & Whitton, J. L. Immunodominance in Virus-Induced CD8 + T-Cell Responses Is Dramatically Modified by DNA Immunization and Is Regulated by Gamma Interferon . *J. Virol.* **76**, 4251–4259 (2002).
229. Liu, F., Whitton, J. L. & Slifka, M. K. The Rapidity with Which Virus-Specific CD8 + T Cells Initiate IFN-γ Synthesis Increases Markedly over the Course of Infection and Correlates with Immunodominance . *J. Immunol.* **173**, 456–462 (2004).
230. Bhat, P., Leggatt, G., Waterhouse, N. & Frazer, I. H. Interferon-γ derived from cytotoxic lymphocytes directly enhances their motility and cytotoxicity. *Cell Death Dis.* **8**, e2836 (2017).
231. Kambayashi, T., Assarsson, E., Lukacher, A. E., Ljunggren, H.-G. & Jensen, P. E. Memory CD8+ T Cells Provide an Early Source of IFN-γ. *J. Immunol.* **170**, 2399–2408 (2003).
232. Pfizenmaier, K. *et al.* High affinity human IFN-gamma-binding capacity is encoded by a single receptor gene located in proximity to c-ros on human chromosome region 6q16 to 6q22. *J. Immunol.* **141**, 856–860 (1988).
233. Bach, E. A. *et al.* Ligand-Induced Autoregulation of IFN-γ Receptor β Chain Expression in T Helper Cell Subsets. *Science* **270**, 1215–1218 (1995).
234. Pernis, A. *et al.* Lack of interferon gamma receptor beta chain and the prevention of interferon gamma signaling in TH1 cells. *Science* **269**, 245–247 (1995).
235. Watson, R. A. *et al.* Immune checkpoint blockade sensitivity and progression-free survival associates with baseline CD8+ T cell clone size and cytotoxicity. *Sci. Immunol.* **6**, eabj8825 (2021).
236. Fairfax, B. P. *et al.* Peripheral CD8 + T cell characteristics associated with durable responses to immune checkpoint blockade in patients with metastatic melanoma. *Nat. Med.* **26**, 193–199 (2020).

237. Huang, S. *et al.* Immune response in mice that lack the interferon-gamma receptor. *Science* **259**, 1742–1745 (1993).
238. Muller, U. *et al.* Functional role of type I and type II interferons in antiviral defense. *Science* **264**, 1918–1921 (1994).
239. Tau, G. & Rothman, P. Biologic functions of the IFN-gamma receptors. *Allergy* **54**, 1233–1251 (1999).
240. Lohman, B. L. & Welsh, R. M. Apoptotic Regulation of T Cells and Absence of Immune Deficiency in Virus-Infected Gamma Interferon Receptor Knockout Mice. *J. Virol.* **72**, 7815–7821 (1998).
241. Bouloc, A., Cavani, A. & Katz, S. I. Contact hypersensitivity in MHC class II-deficient mice depends on CD8 T lymphocytes primed by immunostimulating Langerhans cells. *J. Invest. Dermatol.* **111**, 44–49 (1998).
242. Alimi, E., Huang, S., Brazillet, M. P. & Charreire, J. Experimental autoimmune thyroiditis (EAT) in mice lacking the IFN-gamma receptor gene. *Eur. J. Immunol.* **28**, 201–208 (1998).
243. Kageyama, Y. *et al.* Reduced Susceptibility to Collagen-Induced Arthritis in Mice Deficient in IFN-γ Receptor. *J. Immunol.* **161**, 1542–1548 (1998).
244. Wang, B. *et al.* Interferon-γ impacts at multiple points during the progression of autoimmune diabetes. *Proc. Natl. Acad. Sci.* **94**, 13844–13849 (1997).
245. Zhang, G. X. *et al.* Mice with IFN-gamma receptor deficiency are less susceptible to experimental autoimmune myasthenia gravis. *J. Immunol. Baltim. Md 1950* **162**, 3775–3781 (1999).
246. Maillard, I. *et al.* Immune response to mouse mammary tumor virus in mice lacking the alpha/beta interferon or the gamma interferon receptor. *J. Virol.* **72**, 2638–2646 (1998).
247. Schijns, V. E., Wierda, C. M., Hoeij, M. van & Horzinek, M. C. Exacerbated viral hepatitis in IFN-gamma receptor-deficient mice is not suppressed by IL-12. *J. Immunol.* **157**, 815–821 (1996).

248. Schijns, V. E. *et al.* IFN-gamma receptor-deficient mice generate antiviral Th1-characteristic cytokine profiles but altered antibody responses. *J. Immunol. Baltim. Md 1950* **153**, 2029–2037 (1994).
249. Sandberg, J. O., Benda, B., Lycke, N. & Korsgren, O. Xenograft rejection of porcine islet-like cell clusters in normal, interferon-gamma, and interferon-gamma receptor deficient mice. *Transplantation* **63**, 1446–1452 (1997).
250. Steiger, J. U., Nickerson, P. W., Hermle, M., Thiel, G. & Heim, M. H. Interferon-gamma receptor signaling is not required in the effector phase of the alloimmune response. *Transplantation* **65**, 1649–1652 (1998).
251. Lu, B. *et al.* Targeted disruption of the interferon-gamma receptor 2 gene results in severe immune defects in mice. *Proc. Natl. Acad. Sci. U. S. A.* **95**, 8233–8238 (1998).
252. Tau, G. Z., Cowan, S. N., Weisburg, J., Braunstein, N. S. & Rothman, P. B. Regulation of IFN-γ Signaling Is Essential for the Cytotoxic Activity of CD8+ T Cells. *J. Immunol.* **167**, 5574–5582 (2001).
253. Thompson, L. J., Kolumam, G. A., Thomas, S. & Murali-Krishna, K. Innate Inflammatory Signals Induced by Various Pathogens Differentially Dictate the IFN-I Dependence of CD8 T Cells for Clonal Expansion and Memory Formation. *J. Immunol.* **177**, 1746–1754 (2006).
254. Whitmire, J. K., Eam, B., Benning, N. & Whitton, J. L. Direct Interferon-γ Signaling Dramatically Enhances CD4+ and CD8+ T Cell Memory. *J. Immunol.* **179**, 1190–1197 (2007).
255. Prabhu, N. *et al.* Gamma Interferon Regulates Contraction of the Influenza Virus-Specific CD8 T Cell Response and Limits the Size of the Memory Population. *J. Virol.* **87**, 12510–12522 (2013).
256. Karachaliou, N. *et al.* Interferon gamma, an important marker of response to immune checkpoint blockade in non-small cell lung cancer and melanoma patients: *Ther. Adv. Med. Oncol.* (2018) doi:10.1177/1758834017749748.
257. Ji, H. *et al.* Construction of Interferon-Gamma-Related Gene Signature to Characterize the Immune-Inflamed Phenotype of Glioblastoma and Predict

Prognosis, Efficacy of Immunotherapy and Radiotherapy. *Front. Immunol.* **12**, (2021).

258. Hu, B. *et al.* Development of an IFNγ response-related signature for predicting the survival of cutaneous melanoma. *Cancer Med.* **9**, 8186–8201 (2020).
259. Espinosa, E. *et al.* Predictive factors of response to immunotherapy—a review from the Spanish Melanoma Group (GEM). *Ann. Transl. Med.* **5**, 389–389 (2017).
260. Chen, J. *et al.* Single-cell transcriptomics reveal the intratumoral landscape of infiltrated T-cell subpopulations in oral squamous cell carcinoma. *Mol. Oncol.* **15**, 866–886 (2021).
261. Yan, K., Lu, Y., Yan, Z. & Wang, Y. 9-Gene Signature Correlated With CD8+ T Cell Infiltration Activated by IFN-γ: A Biomarker of Immune Checkpoint Therapy Response in Melanoma. *Front. Immunol.* **12**, 622563 (2021).
262. Maekawa, Y. *et al.* Notch2 integrates signaling by the transcription factors RBP-J and CREB1 to promote T cell cytotoxicity. *Nat. Immunol.* **9**, 1140–1147 (2008).
263. Madisen, L. *et al.* A robust and high-throughput Cre reporting and characterization system for the whole mouse brain. *Nat. Neurosci.* **13**, 133–140 (2010).
264. Miyagawa, F., Gutermuth, J., Zhang, H. & Katz, S. I. The use of mouse models to better understand mechanisms of autoimmunity and tolerance. *J. Autoimmun.* **35**, 192–198 (2010).
265. Wilson, E. H. *et al.* Behavior of Parasite-Specific Effector CD8+ T Cells in the Brain and Visualization of a Kinesis-Associated System of Reticular Fibers. *Immunity* **30**, 300–311 (2009).
266. Pope, C. *et al.* Organ-Specific Regulation of the CD8 T Cell Response to Listeria monocytogenes Infection. *J. Immunol.* **166**, 3402–3409 (2001).
267. Krabbe, T. *et al.* Adoptive T Cell Therapy Is Complemented by Oncolytic Virotherapy with Fusogenic VSV-NDV in Combination Treatment of Murine Melanoma. *Cancers* **13**, 1044 (2021).
268. Boissonnas, A. *et al.* CD8+ Tumor-Infiltrating T Cells Are Trapped in the Tumor-Dendritic Cell Network. *Neoplasia N. Y. N* **15**, 85–94 (2013).

269. Menares, E. *et al.* Tissue-resident memory CD8 + T cells amplify anti-tumor immunity by triggering antigen spreading through dendritic cells. *Nat. Commun.* **10**, 4401 (2019).
270. Hopkins, F. G. On the separation of a pure albumin from egg-white. *J. Physiol.* **25**, 306–330 (1900).
271. Huntington, J. A. & Stein, P. E. Structure and properties of ovalbumin. **756**, 189–198 (2001).
272. Dombre, C. *et al.* Egg serpins: The chicken and/or the egg dilemma. *Semin. Cell Dev. Biol.* **62**, 120–132 (2017).
273. Bayne-Jones, S. EQUILIBRIA IN PRECIPITIN REACTIONS. *J. Exp. Med.* **25**, 837–853 (1917).
274. Tiselius, B. Y. A., D, P. & Kabat, E. A. AN ELECTROPHORETIC STUDY OF IMMUNE SERA AND PURIFIED ANTIBODY PREPARATIONS * t (From the Institute of Physical Chemistry , University of Upsala , Upsala , Sweden) Studies on the eleetrophoresis of serum have shown that besides the albumin normal sera po. 119–131 (1938).
275. HEIDELBERGER, M., PEDERSEN, K. A. I. O. & TISELIUS, A. Ultracentrifugal and Electrophoretic Studies on Antibodies. *Nature* **138**, 165 (1936).
276. Hooker, S. B. & Boyd, W. C. The Existence of Antigenic Determinants of Diverse Specificity in a Single Protein : III . Further Notes on Crystalline. (2021).
277. Boyd, W. C. & Bernard, H. Quantitative Changes in Antibodies and Globulin Fractions in Sera of Rabbits Injected with Several Antigens. *J. Immunol.* **33**, 111–122 (1937).
278. Hogquist, K. A. *et al.* T Cell Receptor Antagonist Peptides Induce Positive Selection. **76**, 17–27 (1994).
279. Boehmer, H. Von. Deciphering Thymic Development. *Front. Immunol.* **5**, 424 (2014).
280. Harty, J. T. & Badovinac, V. P. Shaping and reshaping CD8+ T-cell memory. *Nat. Rev. Immunol.* **8**, 107–119 (2008).

281. Etxeberria, I. *et al.* Intratumor Adoptive Transfer of IL-12 mRNA Transiently Engineered Antitumor CD8+ T Cells. *Cancer Cell* **36**, 613-629.e7 (2019).
282. Lau, D. *et al.* Intravital Imaging of Adoptive T-Cell Morphology, Mobility and Trafficking Following Immune Checkpoint Inhibition in a Mouse Melanoma Model. *Front. Immunol.* **11**, 1514 (2020).
283. van Grinsven, E., Prunier, C., Vrisekoop, N. & Ritsma, L. Two-Photon Intravital Microscopy Animal Preparation Protocol to Study Cellular Dynamics in Pathogenesis. in *Light Microscopy: Methods and Protocols* (eds. Markaki, Y. & Harz, H.) 51–71 (Springer, 2017). doi:10.1007/978-1-4939-6810-7_4.
284. Nakamura, K. *et al.* Characterization of mouse melanoma cell lines by their mortal malignancy using an experimental metastatic model. *Life Sci.* **70**, 791–798 (2002).
285. Potez, M. *et al.* Characterization of a B16-F10 melanoma model locally implanted into the ear pinnae of C57BL/6 mice. *PLoS ONE* **13**, (2018).
286. Overwijk, W. W. & Restifo, N. P. B16 as a Mouse Model for Human Melanoma. *Curr. Protoc. Immunol. Ed. John E Coligan Al* **CHAPTER**, Unit-20.1 (2001).
287. Burghoff, S. *et al.* Growth and metastasis of B16-F10 melanoma cells is not critically dependent on host CD73 expression in mice. *BMC Cancer* **14**, (2014).
288. Lechner, M. G. *et al.* Immunogenicity of murine solid tumor models as a defining feature of in vivo behavior and response to immunotherapy. *J. Immunother. Hagerstown Md 1997* **36**, 477–489 (2013).
289. Danciu, C. *et al.* Behaviour of four different B16 murine melanoma cell sublines: C57BL/6J skin. *Int. J. Exp. Pathol.* **96**, 73–80 (2015).
290. Hwang, S. H. *et al.* Suppression of metastasis of intravenously-inoculated B16/F10 melanoma cells by the novel ginseng-derived ingredient, gintonin: Involvement of autotaxin inhibition. *Int. J. Oncol.* **42**, 317–326 (2013).
291. Fraser, C. K. *et al.* Dasatinib alters the metastatic phenotype of B16-OVA melanoma in vivo. *Cancer Biol. Ther.* **10**, 715–727 (2010).
292. Corbett, T. H., Griswold, D. P., Roberts, B. J., Peckham, J. C. & Schabel, F. M. Tumor induction relationships in development of transplantable cancers of the

colon in mice for chemotherapy assays, with a note on carcinogen structure. *Cancer Res.* **35**, 2434–2439 (1975).

293. Woo, S.-R. *et al.* Immune Inhibitory Molecules LAG-3 and PD-1 Synergistically Regulate T-cell Function to Promote Tumoral Immune Escape. *Cancer Res.* **72**, 917–927 (2012).
294. Efremova, M. *et al.* Targeting immune checkpoints potentiates immunoediting and changes the dynamics of tumor evolution. *Nat. Commun.* **9**, 32 (2018).
295. Haring, J. S., Corbin, G. A. & Harty, J. T. Dynamic Regulation of IFN-γ Signaling in Antigen-Specific CD8+ T Cells Responding to Infection. *J. Immunol.* **174**, 6791–6802 (2005).
296. Prokhnevska, N. *et al.* CD8 T cell differentiation in cancer is comprised of two distinct phases. *J. Immunol.* **206**, 57.04-57.04 (2021).
297. Thompson, E. C. Focus issue: Structure and function of lymphoid tissues. *Trends Immunol.* **33**, 255 (2012).
298. Aoshi, T. *et al.* The cellular niche of Listeria monocytogenes infection changes rapidly in the spleen. *Eur. J. Immunol.* **39**, 417–425 (2009).
299. Aoshi, T. *et al.* Bacterial Entry to the Splenic White Pulp Initiates Antigen Presentation to CD8+ T Cells. *Immunity* **29**, 476–486 (2008).
300. Conlan, J. W. Y. 1996. Early pathogenesis of Listeria monocytogenes infection in the mouse spleen. *J. Med. Microbiol.* **44**, 295–302.
301. Waldman, A. D., Fritz, J. M. & Lenardo, M. J. A guide to cancer immunotherapy: from T cell basic science to clinical practice. *Nat. Rev. Immunol.* **20**, 651–668 (2020).
302. Saleh, J. Murine models of melanoma. *Pathol. Res. Pract.* **214**, 1235–1238 (2018).
303. Kuzu, O. F., Nguyen, F. D., Noory, M. A. & Sharma, A. Current State of Animal (Mouse) Modeling in Melanoma Research. *Cancer Growth Metastasis* **8**, 81–94 (2015).
304. Wang, J., Saffold, S., Cao, X., Krauss, J. & Chen, W. Eliciting T cell immunity against poorly immunogenic tumors by immunization with dendritic cell-tumor fusion vaccines. *J. Immunol. Baltim. Md 1950* **161**, 5516–5524 (1998).

305. Baird, J. R. *et al.* Immune-mediated regression of established B16F10 melanoma by intratumoral injection of attenuated Toxoplasma gondii protects against rechallenge. *J. Immunol. Baltim. Md 1950* **190**, 469–478 (2013).
306. B16-F10-OVA. *Biocytogen* https://biocytogen.com/products/other-cancer-cell-lines/b16-f10-ova/.
307. Lee, H.-M. *et al.* IFNγ signaling endows DCs with the capacity to control type I inflammation during parasitic infection through promoting T-bet+ regulatory T cells. *PLoS Pathog.* **11**, e1004635 (2015).
308. Villegas-Mendez, A. *et al.* Gamma Interferon Mediates Experimental Cerebral Malaria by Signaling within Both the Hematopoietic and Nonhematopoietic Compartments. *Infect. Immun.* **85**, e01035-16 (2017).
309. Langer, V. *et al.* IFN-**γ** drives inflammatory bowel disease pathogenesis through VE-cadherin–directed vascular barrier disruption. *J. Clin. Invest.* **129**, 4691–4707 (2019).
310. Oyler-Yaniv, J. *et al.* Catch and Release of Cytokines Mediated by Tumor Phosphatidylserine Converts Transient Exposure into Long-Lived Inflammation. *Mol. Cell* **66**, 635-647.e7 (2017).
311. Sackmann, E. & Tanaka, M. Critical role of lipid membranes in polarization and migration of cells: a biophysical view. *Biophys. Rev.* **13**, 123–138 (2021).
312. IL-2 Receptor - an overview | ScienceDirect Topics. https://www.sciencedirect.com/topics/neuroscience/il-2-receptor.
313. Bamford, R. N. *et al.* The interleukin (IL) 2 receptor beta chain is shared by IL-2 and a cytokine, provisionally designated IL-T, that stimulates T-cell proliferation and the induction of lymphokine-activated killer cells. *Proc. Natl. Acad. Sci.* **91**, 4940–4944 (1994).
314. Schroder, K., Hertzog, P. J., Ravasi, T. & Hume, D. A. Interferon-γ: an overview of signals, mechanisms and functions. *J. Leukoc. Biol.* **75**, 163–189 (2004).
315. Ahmed, C. M. I. & Johnson, H. M. IFN-γ and Its Receptor Subunit IFNGR1 Are Recruited to the IFN-γ-Activated Sequence Element at the Promoter Site of IFN-γ-

Activated Genes: Evidence of Transactivational Activity in IFNGR1. *J. Immunol.* **177**, 315–321 (2006).

316. STAT1 - an overview | ScienceDirect Topics. https://www.sciencedirect.com/topics/immunology-and-microbiology/stat1.
317. Subramaniam, P. S. & Johnson, H. M. Lipid Microdomains Are Required Sites for the Selective Endocytosis and Nuclear Translocation of IFN-γ, Its Receptor Chain IFN-γ Receptor-1, and the Phosphorylation and Nuclear Translocation of STAT1α. *J. Immunol.* **169**, 1959–1969 (2002).
318. Paul, S. & Lal, G. The Molecular Mechanism of Natural Killer Cells Function and Its Importance in Cancer Immunotherapy. *Front. Immunol.* **8**, (2017).
319. Williams, M. A. & Bevan, M. J. Effector and memory CTL differentiation. *Annu. Rev. Immunol.* **25**, 171–192 (2007).
320. Betts, M. R. & Koup, R. A. Detection of T-Cell Degranulation: CD107a and b. in *Methods in Cell Biology* vol. 75 497–512 (Academic Press, 2004).
321. Lord, S. J., Rajotte, R. V., Korbutt, G. S. & Bleackley, R. C. Granzyme B: a natural born killer. *Immunol. Rev.* **193**, 31–38 (2003).
322. Trapani, J. A. & Sutton, V. R. Granzyme B: pro-apoptotic, antiviral and antitumor functions. *Curr. Opin. Immunol.* **15**, 533–543 (2003).
323. Voskoboinik, I., Whisstock, J. C. & Trapani, J. A. Perforin and granzymes: function, dysfunction and human pathology. *Nat. Rev. Immunol.* **15**, 388–400 (2015).
324. Shalini, S., Dorstyn, L., Dawar, S. & Kumar, S. Old, new and emerging functions of caspases. *Cell Death Differ.* **22**, 526–539 (2015).
325. Ziegler, S. F., Ramsdell, F. & Alderson, M. R. The activation antigen CD69. *Stem Cells* **12**, 456–465 (1994).
326. Salmon, H., Remark, R., Gnjatic, S. & Merad, M. Host tissue determinants of tumour immunity. *Nat. Rev. Cancer* **19**, 215–227 (2019).
327. Pagès, F. *et al.* Immune infiltration in human tumors: a prognostic factor that should not be ignored. *Oncogene* **29**, 1093–1102 (2010).

328. van der Woude, L. L., Gorris, M. A. J., Halilovic, A., Figdor, C. G. & de Vries, I. J. M. Migrating into the Tumor: a Roadmap for T Cells. *Trends Cancer* **3**, 797–808 (2017).
329. Galon, J. & Bruni, D. Approaches to treat immune hot, altered and cold tumours with combination immunotherapies. *Nat. Rev. Drug Discov.* **18**, 197–218 (2019).
330. Lanitis, E., Dangaj, D., Irving, M. & Coukos, G. Mechanisms regulating T-cell infiltration and activity in solid tumors. *Ann. Oncol.* **28**, xii18–xii32 (2017).
331. Spranger, S., Bao, R. & Gajewski, T. F. Melanoma-intrinsic β-catenin signalling prevents anti-tumour immunity. *Nature* **523**, 231–235 (2015).
332. Herbst, R. S. *et al.* Predictive correlates of response to the anti-PD-L1 antibody MPDL3280A in cancer patients. *Nature* **515**, 563–567 (2014).
333. Hammerl, D. *et al.* Spatial immunophenotypes predict response to anti-PD1 treatment and capture distinct paths of T cell evasion in triple negative breast cancer. *Nat. Commun.* **12**, 5668 (2021).
334. Zhong, W. *et al.* Comparison of the molecular and cellular phenotypes of common mouse syngeneic models with human tumors. *BMC Genomics* **21**, 2 (2020).
335. Harlin, H. *et al.* Chemokine Expression in Melanoma Metastases Associated with CD8+ T-Cell Recruitment. *Cancer Res.* **69**, (2009).
336. González-Martín, A., Gómez, L., Lustgarten, J., Mira, E. & Mañes, S. Maximal T cell-mediated antitumor responses rely upon CCR5 expression in both CD4(+) and CD8(+) T cells. *Cancer Res.* **71**, 5455–5466 (2011).
337. Slaney, C. Y., Kershaw, M. H. & Darcy, P. K. Trafficking of T Cells into Tumors. *Cancer Res.* **74**, 7168–7174 (2014).
338. Donnadieu, E., Dupré, L., Pinho, L. G. & Cotta-de-Almeida, V. Surmounting the obstacles that impede effective CAR T cell trafficking to solid tumors. *J. Leukoc. Biol.* **108**, 1067–1079 (2020).
339. Fowell, D. J. & Kim, M. The spatio-temporal control of effector T cell migration. *Nat. Rev. Immunol.* **21**, 582–596 (2021).

340. Whitmire, J. K., Tan, J. T. & Whitton, J. L. Interferon-γ acts directly on CD8+ T cells to increase their abundance during virus infection. *J. Exp. Med.* **201**, 1053–1059 (2005).
341. Belnoue, E. *et al.* Control of pathogenic CD8+ T cell migration to the brain by IFN-gamma during experimental cerebral malaria. *Parasite Immunol.* **30**, 544–553 (2008).
342. Peng, W. *et al.* PD-1 blockade enhances T-cell migration to tumors by elevating IFN-γ inducible chemokines. *Cancer Res.* **72**, 5209–5218 (2012).
343. Hollenbaugh, J. A. & Dutton, R. W. IFN-γ Regulates Donor CD8 T Cell Expansion, Migration, and Leads to Apoptosis of Cells of a Solid Tumor. *J. Immunol.* **177**, 3004–3011 (2006).
344. Walling, B. L. & Kim, M. LFA-1 in T Cell Migration and Differentiation. *Front. Immunol.* **9**, (2018).
345. Verma, N. K. & Kelleher, D. Not Just an Adhesion Molecule: LFA-1 Contact Tunes the T Lymphocyte Program. *J. Immunol.* **199**, 1213–1221 (2017).
346. Metzemaekers, M., Vanheule, V., Janssens, R., Struyf, S. & Proost, P. Overview of the Mechanisms that May Contribute to the Non-Redundant Activities of Interferon-Inducible CXC Chemokine Receptor 3 Ligands. *Front. Immunol.* **8**, (2018).
347. Groom, J. R. & Luster, A. D. CXCR3 ligands: redundant, collaborative and antagonistic functions. *Immunol. Cell Biol.* **89**, 207–215 (2011).
348. Medoff, B. D. *et al.* CXCR3 and its ligands in a murine model of obliterative bronchiolitis: regulation and function. *J. Immunol. Baltim. Md 1950* **176**, 7087–7095 (2006).
349. Kim, C. H. Crawling of effector T cells on extracellular matrix: role of integrins in interstitial migration in inflamed tissues. *Cell. Mol. Immunol.* **11**, 1–4 (2014).
350. Sadjadi, Z., Zhao, R., Hoth, M., Qu, B. & Rieger, H. Migration of Cytotoxic T Lymphocytes in 3D Collagen Matrices. *Biophys. J.* **119**, 2141–2152 (2020).

351. Carman, C. V. & Martinelli, R. T Lymphocyte–Endothelial Interactions: Emerging Understanding of Trafficking and Antigen-Specific Immunity. *Front. Immunol.* **6**, 603 (2015).
352. Certo, M. *et al.* Endothelial cell and T-cell crosstalk: Targeting metabolism as a therapeutic approach in chronic inflammation. *Br. J. Pharmacol.* **178**, 2041–2059 (2021).
353. Lanitis, E., Irving, M. & Coukos, G. Targeting the tumor vasculature to enhance T cell activity. *Curr. Opin. Immunol.* **33**, 55–63 (2015).
354. Sakano, Y. *et al.* Tumor endothelial cell-induced CD8+ T-cell exhaustion via GPNMB in hepatocellular carcinoma. *Cancer Sci.* **113**, 1625–1638 (2022).
355. Yanguas, A. *et al.* ICAM-1-LFA-1 Dependent CD8+ T-Lymphocyte Aggregation in Tumor Tissue Prevents Recirculation to Draining Lymph Nodes. *Front. Immunol.* **0**, (2018).
356. Amersfoort, J., Eelen, G. & Carmeliet, P. Immunomodulation by endothelial cells — partnering up with the immune system? *Nat. Rev. Immunol.* **22**, 576–588 (2022).
357. Nassiri, F. *et al.* Endoglin (CD105): A Review of its Role in Angiogenesis and Tumor Diagnosis, Progression and Therapy. *Anticancer Res.* **31**, 2283–2290 (2011).
358. Kovacs, S. B., Oh, C., Aachoui, Y. & Miao, E. A. Evaluating cytokine production by flow cytometry using brefeldin A in mice. *STAR Protoc.* **2**, 100244 (2021).
359. Mazet, J. M., Chiodetti, A. L., Mahale, J. N. & Gérard, A. Imaging of In Situ Interferon Gamma Production in the Mouse Spleen following Listeria monocytogenes Infection. *J. Vis. Exp. JoVE* (2019) doi:10.3791/59819.
360. Suzuki, I., Martin, S., Boursalian, T. E., Beers, C. & Fink, P. J. Fas Ligand Costimulates the In Vivo Proliferation of CD8+ T Cells. *J. Immunol.* **165**, 5537–5543 (2000).
361. Suzuki, I. & Fink, P. J. The dual functions of Fas ligand in the regulation of peripheral $CD8^+$ and $CD4^+$ T cells. *Proc. Natl. Acad. Sci.* **97**, 1707–1712 (2000).

362. Lakins, M. A., Ghorani, E., Munir, H., Martins, C. P. & Shields, J. D. Cancer-associated fibroblasts induce antigen-specific deletion of CD8 + T Cells to protect tumour cells. *Nat. Commun.* **9**, 948 (2018).
363. Xie, Q., Ding, J. & Chen, Y. Role of CD8+ T lymphocyte cells: Interplay with stromal cells in tumor microenvironment. *Acta Pharm. Sin. B* **11**, 1365–1378 (2021).
364. Yajima, T. *et al.* Fas/FasL signaling is critical for the survival of exhausted antigen-specific CD8+ T cells during tumor immune response. *Mol. Immunol.* **107**, 97–105 (2019).
365. Gratiot-Deans, J., Merino, R., Nuñez, G. & Turka, L. A. Bcl-2 expression during T-cell development: early loss and late return occur at specific stages of commitment to differentiation and survival. *Proc. Natl. Acad. Sci.* **91**, 10685–10689 (1994).
366. Soares, A. *et al.* Novel application of Ki67 to quantify antigen-specific in vitro lymphoproliferation. *J. Immunol. Methods* **362**, 43–50 (2010).
367. Kretschmer, L. *et al.* Differential expansion of T central memory precursor and effector subsets is regulated by division speed. *Nat. Commun.* **11**, 113 (2020).
368. Maimela, N. R., Liu, S. & Zhang, Y. Fates of CD8+ T cells in Tumor Microenvironment. *Comput. Struct. Biotechnol. J.* **17**, 1–13 (2019).
369. Raskov, H., Orhan, A., Christensen, J. P. & Gögenur, I. Cytotoxic CD8+ T cells in cancer and cancer immunotherapy. *Br. J. Cancer* **124**, 359–367 (2021).
370. Shimizu, S. *et al.* Tumor-infiltrating CD8+ T-cell density is an independent prognostic marker for oral squamous cell carcinoma. *Cancer Med.* **8**, 80–93 (2019).
371. Steele, K. E. *et al.* Measuring multiple parameters of CD8+ tumor-infiltrating lymphocytes in human cancers by image analysis. *J. Immunother. Cancer* **6**, 20 (2018).
372. Melero, I., Rouzaut, A., Motz, G. T. & Coukos, G. T-Cell and NK-Cell Infiltration into Solid Tumors: A Key Limiting Factor for Efficacious Cancer Immunotherapy. *Cancer Discov.* **4**, 522–526 (2014).

373. Bellone, M. & Calcinotto, A. Ways to enhance lymphocyte trafficking into tumors and fitness of tumor infiltrating lymphocytes. *Front. Oncol.* **3**, 231 (2013).
374. Calzascia, T. *et al.* Homing phenotypes of tumor-specific CD8 T cells are predetermined at the tumor site by crosspresenting APCs. *Immunity* **22**, 175–184 (2005).
375. Kumar, S., Singh, S. K., Rana, B. & Rana, A. Tumor-infiltrating CD8+ T cell antitumor efficacy and exhaustion: molecular insights. *Drug Discov. Today* **26**, 951–967 (2021).
376. Zhang, J., Endres, S. & Kobold, S. Enhancing tumor T cell infiltration to enable cancer immunotherapy. *Immunotherapy* **11**, 201–213 (2019).
377. Peske, J. D., Woods, A. B. & Engelhard, V. H. Chapter Eight - Control of CD8 T-Cell Infiltration into Tumors by Vasculature and Microenvironment. in *Advances in Cancer Research* (eds. Wang, X.-Y. & Fisher, P. B.) vol. 128 263–307 (Academic Press, 2015).
378. Krummel, M. F., Bartumeus, F. & Gérard, A. T cell migration, search strategies and mechanisms. *Nat. Rev. Immunol.* **16**, 193–201 (2016).
379. Issekutz, T. B., Stoltz, J. M. & van der Meide, P. The recruitment of lymphocytes into the skin by T cell lymphokines: the role of gamma-interferon. *Clin. Exp. Immunol.* **73**, 70–75 (1988).
380. Gordon-Alonso, M., Hirsch, T., Wildmann, C. & van der Bruggen, P. Galectin-3 captures interferon-gamma in the tumor matrix reducing chemokine gradient production and T-cell tumor infiltration. *Nat. Commun.* **8**, 793 (2017).
381. Turner, M. D., Nedjai, B., Hurst, T. & Pennington, D. J. Cytokines and chemokines: At the crossroads of cell signalling and inflammatory disease. *Biochim. Biophys. Acta BBA - Mol. Cell Res.* **1843**, 2563–2582 (2014).
382. Franciszkiewicz, K., Boissonnas, A., Boutet, M., Combadière, C. & Mami-Chouaib, F. Role of Chemokines and Chemokine Receptors in Shaping the Effector Phase of the Antitumor Immune Response. *Cancer Res.* **72**, 6325–6332 (2012).

383. Mlecnik, B. *et al.* Biomolecular Network Reconstruction Identifies T-Cell Homing Factors Associated With Survival in Colorectal Cancer. *Gastroenterology* **138**, 1429–1440 (2010).
384. Maishi, N., Annan, D. A., Kikuchi, H., Hida, Y. & Hida, K. Tumor Endothelial Heterogeneity in Cancer Progression. *Cancers* **11**, 1511 (2019).
385. Dudley, A. C. Tumor Endothelial Cells. *Cold Spring Harb. Perspect. Med.* **2**, a006536 (2012).
386. Motz, G. T. *et al.* Tumor endothelium FasL establishes a selective immune barrier promoting tolerance in tumors. *Nat. Med.* **20**, 607–615 (2014).
387. Yu, J. S. *et al.* Intratumoral T cell subset ratios and Fas ligand expression on brain tumor endothelium. *J. Neurooncol.* **64**, 55–61 (2003).
388. Mazanet, M. M. & Hughes, C. C. W. B7-H1 Is Expressed by Human Endothelial Cells and Suppresses T Cell Cytokine Synthesis. *J. Immunol.* **169**, 3581–3588 (2002).
389. Rodig, N. *et al.* Endothelial expression of PD-L1 and PD-L2 down-regulates CD8+ T cell activation and cytolysis. *Eur. J. Immunol.* **33**, 3117–3126 (2003).
390. Huang, X. *et al.* Lymphoma endothelium preferentially expresses Tim-3 and facilitates the progression of lymphoma by mediating immune evasion. *J. Exp. Med.* **207**, 505–520 (2010).
391. Wu, F.-H. *et al.* Endothelial cell-expressed Tim-3 facilitates metastasis of melanoma cells by activating the NF-κB pathway. *Oncol. Rep.* **24**, 693–699 (2010).
392. Fonsatti, E. & Maio, M. Highlights on endoglin (CD105): from basic findings towards clinical applications in human cancer. *J. Transl. Med.* **2**, 18 (2004).
393. Stockmann, C., Schadendorf, D., Klose, R. & Helfrich, I. The Impact of the Immune System on Tumor: Angiogenesis and Vascular Remodeling. *Front. Oncol.* **4**, 69 (2014).
394. Park, H. S. *et al.* High endothelial venule is a surrogate biomarker for T-cell inflamed tumor microenvironment and prognosis in gastric cancer. *J. Immunother. Cancer* **9**, e003353 (2021).

395. Martinet, L. *et al.* Human Solid Tumors Contain High Endothelial Venules: Association with T- and B-Lymphocyte Infiltration and Favorable Prognosis in Breast Cancer. *Cancer Res.* **71**, 5678–5687 (2011).
396. Martinet, L. *et al.* High endothelial venules (HEVs) in human melanoma lesions. *OncoImmunology* **1**, 829–839 (2012).
397. Ager, A. & May, M. J. Understanding high endothelial venules: Lessons for cancer immunology. *OncoImmunology* **4**, e1008791 (2015).
398. Guo, B., Kumar, S., Li, C., Slevin, M. & Kumar, P. CD105 (Endoglin), Apoptosis, and Stroke. *Stroke* **35**, e94–e95 (2004).
399. Li, C. *et al.* CD105 prevents apoptosis in hypoxic endothelial cells. *J. Cell Sci.* **116**, 2677–2685 (2003).
400. Tomura, M. *et al.* Monitoring cellular movement in vivo with photoconvertible fluorescence protein "Kaede" transgenic mice. *Proc. Natl. Acad. Sci. U. S. A.* **105**, 10871–10876 (2008).
401. Torcellan, T. *et al.* In vivo photolabeling of tumor-infiltrating cells reveals highly regulated egress of T-cell subsets from tumors. *Proc. Natl. Acad. Sci. U. S. A.* **114**, 5677–5682 (2017).
402. Testa, I. *et al.* Spatial control of pa-GFP photoactivation in living cells. *J. Microsc.* **230**, 48–60 (2008).
403. Wang, Z. *et al.* Glycolysis and Oxidative Phosphorylation Play Critical Roles in Natural Killer Cell Receptor-Mediated Natural Killer Cell Functions. *Front. Immunol.* **11**, (2020).
404. Shiratori, R. *et al.* Glycolytic suppression dramatically changes the intracellular metabolic profile of multiple cancer cell lines in a mitochondrial metabolism-dependent manner. *Sci. Rep.* **9**, 18699 (2019).
405. Pendergrass, W., Wolf, N. & Poot, M. Efficacy of MitoTracker Green and CMXrosamine to measure changes in mitochondrial membrane potentials in living cells and tissues. *Cytom. Part J. Int. Soc. Anal. Cytol.* **61**, 162–169 (2004).
406. Yu, Y.-R. *et al.* Disturbed mitochondrial dynamics in CD8+ TILs reinforce T cell exhaustion. *Nat. Immunol.* **21**, 1540–1551 (2020).

407. Cuezva, J. M. *et al.* The bioenergetic signature of cancer: a marker of tumor progression. *Cancer Res.* **62**, 6674–6681 (2002).
408. Muz, B., de la Puente, P., Azab, F. & Azab, A. K. The role of hypoxia in cancer progression, angiogenesis, metastasis, and resistance to therapy. *Hypoxia* **3**, 83–92 (2015).
409. Blank, C. U. *et al.* Defining 'T cell exhaustion'. *Nat. Rev. Immunol.* **19**, 665–674 (2019).
410. Scharping, N. E. *et al.* The Tumor Microenvironment Represses T Cell Mitochondrial Biogenesis to Drive Intratumoral T Cell Metabolic Insufficiency and Dysfunction. *Immunity* **45**, 374–388 (2016).
411. Alberts, B. *et al.* An Overview of the Cell Cycle. *Mol. Biol. Cell 4th Ed.* (2002).
412. Wherry, E. J. & Kurachi, M. Molecular and cellular insights into T cell exhaustion. *Nat. Rev. Immunol.* **15**, 486–499 (2015).
413. Yi, J. S., Cox, M. A. & Zajac, A. J. T-cell exhaustion: characteristics, causes and conversion. *Immunology* **129**, 474–481 (2010).
414. Schillebeeckx, I. *et al.* T cell subtype profiling measures exhaustion and predicts anti-PD-1 response. *Sci. Rep.* **12**, 1342 (2022).
415. Chu, T. & Zehn, D. Charting the Roadmap of T Cell Exhaustion. *Immunity* **52**, 724–726 (2020).
416. Haring, J. S., Corbin, G. A. & Harty, J. T. Dynamic Regulation of IFN-γ Signaling in Antigen-Specific CD8+ T Cells Responding to Infection. *J. Immunol.* **174**, 6791–6802 (2005).
417. Monteiro, M., Evaristo, C., Legrand, A., Nicoletti, A. & Rocha, B. Cartography of gene expression in CD8 single cells: novel CCR7− subsets suggest differentiation independent of CD45RA expression. *Blood* **109**, 2863–2870 (2006).
418. Xiao, B., Deng, X., Zhou, W. & Tan, E.-K. Flow Cytometry-Based Assessment of Mitophagy Using MitoTracker. *Front. Cell. Neurosci.* **10**, (2016).
419. Garcia Fernandez, M. I., Ceccarelli, D. & Muscatello, U. Use of the fluorescent dye 10-N-nonyl acridine orange in quantitative and location assays of cardiolipin: a study on different experimental models. *Anal. Biochem.* **328**, 174–180 (2004).

420. van der Windt, G. J. W., Chang, C.-H. & Pearce, E. L. Measuring Bioenergetics in T Cells Using a Seahorse Extracellular Flux Analyzer. *Curr. Protoc. Immunol.* **113**, 3.16B.1-3.16B.14 (2016).
421. Argüello, R. J. *et al.* SCENITH: A Flow Cytometry-Based Method to Functionally Profile Energy Metabolism with Single-Cell Resolution. *Cell Metab.* **32**, 1063-1075.e7 (2020).
422. Huber, R. *et al.* Tumour hypoxia promotes melanoma growth and metastasis via High Mobility Group Box-1 and M2-like macrophages. *Sci. Rep.* **6**, 29914 (2016).
423. Im, S. J. *et al.* Defining CD8+ T cells that provide the proliferative burst after PD-1 therapy. *Nature* **537**, 417–421 (2016).
424. Siddiqui, I. *et al.* Intratumoral Tcf1+PD-1+CD8+ T Cells with Stem-like Properties Promote Tumor Control in Response to Vaccination and Checkpoint Blockade Immunotherapy. *Immunity* **50**, 195-211.e10 (2019).
425. Kurtulus, S. *et al.* Checkpoint Blockade Immunotherapy Induces Dynamic Changes in PD-1–CD8+ Tumor-Infiltrating T Cells. *Immunity* **50**, 181-194.e6 (2019).
426. Schenkel, J. M. *et al.* Conventional type I dendritic cells maintain a reservoir of proliferative tumor-antigen specific TCF-1+ CD8+ T cells in tumor-draining lymph nodes. *Immunity* **54**, 2338-2353.e6 (2021).
427. Ciecko, A. E. *et al.* Self-Renewing Islet TCF1+ CD8 T Cells Undergo IL-27-Controlled Differentiation to Become TCF1- Terminal Effectors during the Progression of Type 1 Diabetes. *J. Immunol. Baltim. Md 1950* **207**, 1990–2004 (2021).
428. Jorgovanovic, D., Song, M., Wang, L. & Zhang, Y. Roles of IFN-γ in tumor progression and regression: a review. *Biomark. Res.* **8**, 49 (2020).
429. Oliaro, J. *et al.* Asymmetric Cell Division of T Cells upon Antigen Presentation Uses Multiple Conserved Mechanisms. *J. Immunol.* **185**, 367–375 (2010).
430. Borsa, M. *et al.* Modulation of asymmetric cell division as a mechanism to boost CD8+ T cell memory. *Sci. Immunol.* **4**, eaav1730 (2019).
431. Ciocca, M. L., Barnett, B. E., Burkhardt, J. K., Chang, J. T. & Reiner, S. L. Asymmetric memory T cell division in response to re-challenge. *J. Immunol. Baltim. Md 1950* **188**, 4145–4148 (2012).

432. Shahriyari, L. & Komarova, N. L. Symmetric vs. Asymmetric Stem Cell Divisions: An Adaptation against Cancer? *PLoS ONE* **8**, e76195 (2013).
433. Gómez-López, S., Lerner, R. G. & Petritsch, C. Asymmetric cell division of stem and progenitor cells during homeostasis and cancer. *Cell. Mol. Life Sci.* **71**, 575–597 (2014).
434. Li, G. *et al.* TGF-β-dependent lymphoid tissue residency of stem-like T cells limits response to tumor vaccine. *Nat. Commun.* **13**, 6043 (2022).
435. de Bruin, A. M., Voermans, C. & Nolte, M. A. Impact of interferon-γ on hematopoiesis. *Blood* **124**, 2479–2486 (2014).
436. Morales-Mantilla, D. E. & King, K. Y. The Role of Interferon-Gamma in Hematopoietic Stem Cell Development, Homeostasis, and Disease. *Curr. Stem Cell Rep.* **4**, 264–271 (2018).
437. Liu, Y. *et al.* Blockade of IDO-kynurenine-AhR metabolic circuitry abrogates IFN-γ-induced immunologic dormancy of tumor-repopulating cells. *Nat. Commun.* **8**, 15207 (2017).
438. Ni, C. *et al.* IFN-γ selectively exerts pro-apoptotic effects on tumor-initiating label-retaining colon cancer cells. *Cancer Lett.* **336**, 174–184 (2013).
439. Martin-Hijano, L. & Sainz, B. The Interactions Between Cancer Stem Cells and the Innate Interferon Signaling Pathway. *Front. Immunol.* **11**, (2020).
440. Gattinoni, L. *et al.* Wnt signaling arrests effector T cell differentiation and generates CD8+ memory stem cells. *Nat. Med.* **15**, 808–813 (2009).
441. Lovatt, M. & Bijlmakers, M.-J. Stabilisation of β-Catenin Downstream of T Cell Receptor Signalling. *PLOS ONE* **5**, e12794 (2010).
442. Tang, Y. Y. *et al.* Effects of Glycogen Synthase Kinase-3β Inhibitor TWS119 on Proliferation and Cytokine Production of TILs From Human Lung Cancer. *J. Immunother. Hagerstown Md 1997* **41**, 319–328 (2018).
443. Lin, W.-H. W. *et al.* CD8+ T Lymphocyte Self-Renewal during Effector Cell Determination. *Cell Rep.* **17**, 1773–1782 (2016).
444. Driessens, G., Zheng, Y. & Gajewski, T. F. Beta-catenin does not regulate memory T cell phenotype. *Nat. Med.* **16**, 513–514; author reply 514-515 (2010).

445. Makkouk, A. & Weiner, G. J. Cancer immunotherapy and breaking immune tolerance: new approaches to an old challenge. *Cancer Res.* **75**, 5–10 (2015).
446. Ribas, A. & Wolchok, J. D. Cancer immunotherapy using checkpoint blockade. *Science* **359**, 1350–1355 (2018).
447. Yost, K. E. *et al.* Clonal replacement of tumor-specific T cells following PD-1 blockade. *Nat. Med.* **25**, 1251–1259 (2019).
448. Miller, B. C. *et al.* Subsets of exhausted CD8 + T cells differentially mediate tumor control and respond to checkpoint blockade. *Nat. Immunol.* **20**, 326 (2019).
449. Godfrey, D. I., Koay, H.-F., McCluskey, J. & Gherardin, N. A. The biology and functional importance of MAIT cells. *Nat. Immunol.* **20**, 1110–1128 (2019).
450. Wo, J. *et al.* The Role of Gamma-Delta T Cells in Diseases of the Central Nervous System. *Front. Immunol.* **11**, (2020).
451. Guo, X. *et al.* Global characterization of T cells in non-small-cell lung cancer by single-cell sequencing. *Nat. Med.* **24**, 978–985 (2018).
452. Duckworth, B. C. *et al.* Effector and stem-like memory cell fates are imprinted in distinct lymph node niches directed by CXCR3 ligands. *Nat. Immunol.* **22**, 434–448 (2021).
453. Prokhnevska, N. *et al.* CD8+ T cell activation in cancer comprises an initial activation phase in lymph nodes followed by effector differentiation within the tumor. *Immunity* (2022) doi:10.1016/j.immuni.2022.12.002.
454. You, R. *et al.* Active surveillance characterizes human intratumoral T cell exhaustion. *J. Clin. Invest.* **131**, (2021).
455. Sautès-Fridman, C., Petitprez, F., Calderaro, J. & Fridman, W. H. Tertiary lymphoid structures in the era of cancer immunotherapy. *Nat. Rev. Cancer* **19**, 307–325 (2019).
456. Schumacher, T. N. & Thommen, D. S. Tertiary lymphoid structures in cancer. *Science* **375**, eabf9419 (2022).
457. Trüb, M. & Zippelius, A. Tertiary Lymphoid Structures as a Predictive Biomarker of Response to Cancer Immunotherapies. *Front. Immunol.* **12**, (2021).